Natural Resources Canada Ressources naturelles Canada





Geological Survey of Canada
Scientific Presentation 81

Iron-oxide and alkali-calcic alteration ore systems and their polymetallic IOA, IOCG, skarn, albitite-hosted U±Au±Co, and affiliated deposits: a short-course series

Part 2: Overview of deposit types, distribution, ages, settings, alteration facies, and ore deposit models

L. Corriveau, E.G. Potter, J.-F. Montreuil[1,2], O. Blein[3], K. Ehrig[4], and A.F. De Toni[5,2]
[1]Red Pine Exploration; [2]formerly at INRS (Institut national de la Recherche scientifique); [3]BRGM; [4]BHP; [5]SOQUEM

2018

Celebrating 175 yrs

Canada

This short-course series updates courses given nationally and internationally in the last decade. Even if their titles are similar, the presentations in English and French may differ in their content and their format.

Permanent link: https://doi.org/10.4095/306560

This publication is available for free download through GEOSCAN (http://geoscan.nrcan.gc.ca/).

Recommended citation

Corriveau, L., Potter, E.G., Montreuil, J.-F., Blein, O., Ehrig, K., and De Toni, A.F., 2018. Iron-oxide and alkali-calcic alteration ore systems and their polymetallic IOA, IOCG, skarn, albitite-hosted U±Au±Co, and affiliated deposits: a short-course series. Part 2: Overview of deposit types, distribution, ages, settings, alteration facies, and ore deposit models; Geological Survey of Canada, Scientific Presentation 81, 154 p. https://doi.org/10.4095/306560

Publications in this series have not been edited; they are released as submitted by the author.

Acknowledgments

The course summarises research on the geology of iron-oxide and alkali-calcic alteration ore systems undertaken at the Geological Survey of Canada by the Targeted Geoscience Initiative and the Geomapping for Energy and Minerals programs in collaboration with territorial and provincial surveys, academia and private sector.

The author acknowledges Dr. Pedro Acosta-Góngora, Dr. Alain Plouffe and Mr. Roman Hanes for their review of this short course series.

We also acknowledge Dr. Sunil Gandhi, Dr. Robert Hildebrand and Dr. Hamid Mumin who pioneered IOCG research and mapping in Canada. We follow in their footsteps.

Additional acknowledgments can be found at slide 132.

Sunil S. Gandhi (1935 – 2017)

After working for the exploration industry in Quebec, Saskatchewan and Labrador (involved in discovery of the Michelin deposit), Sunil joined the GSC as research scientist (1977 – 1996) to carry out annual assessments of uranium resources in Canada.

His research focus was on Great Bear and East Arm regional metallogeny, particularly on “Olympic Dam type” deposits that would later become known as IOCG deposits. His research in 1980’s and 1990’s was instrumental in the discovery of the NICO deposit (1994). He was among the first to suggest linkages between IOA veins and IOCG systems.

After retiring from the GSC in 1996, Sunil consulted for exploration industry in Canada and abroad. He continued metallogenic research at the GSC as a Visiting Scientist and published his last synthesis map (southern Great Bear) in 2014.

Short course series contents

1. Introduction
2. **Overview of deposit types, distribution, ages, settings, examples, alteration facies and deposit model**
3. The Great Bear magmatic zone and other Canadian districts
4. Alteration facies, prograde metasomatic reaction paths and ore genesis
5. Na to Na-Ca-Fe facies
6. Skarns, HT Ca-Fe facies and IOA (iron oxide-apatite) deposits
7. High to low-temperature K-Fe facies, IOCG (iron oxide copper-gold) deposits, Co-Bi and K-skarn variants and albitite-hosted U or Au-U-Co deposits
8. Breccias
9. Geochemical footprints and element mobility across ore environments
10. Metasomatic facies as an exploration tool: Example from the NICO deposit
11. Footprints at granulite facies: Example from the Bondy gneiss complex

Table of contents

Abstract

Part 2 of the short course series reviews the deposit types, classification, distribution, ages, settings, alteration facies and ore deposit models of iron oxide and related alkali-calcic alteration ore systems. These systems include iron oxide copper-gold (IOCG) deposits and their Co- and Bi-rich variants, iron oxide–apatite (IOA) deposits and their rare-earth element-rich variants, some albitite-hosted U and Au-Co-U deposits, Mo-Re deposits and polymetallic skarn deposits. The course also discusses the continuum with epithermal systems and polymetallic vein deposits. Two main examples are used, the systems from the Great Bear magmatic zone in Canada and the Olympic Dam deposit in Australia.

The main references for this chapter include Hitzman et al. (1992), Hitzman (2000), Williams et al. (2005, 2010), Oliver et al. (2006), Corriveau (2007, 2017a, b), Corriveau and Mumin (2010), Corriveau et al. (2010a, b, 2016, 2017, in press a-h), Mumin et al. (2007, 2010), Porter (2010a, b), Rusk et al. (2010), Skirrow (2010), Williams (2010a, b), Montreuil et al. (2013, 2015, 2016a, b), Ehrig et al. (2012, 2017); Barton (2014) and Richards et al. (2017).

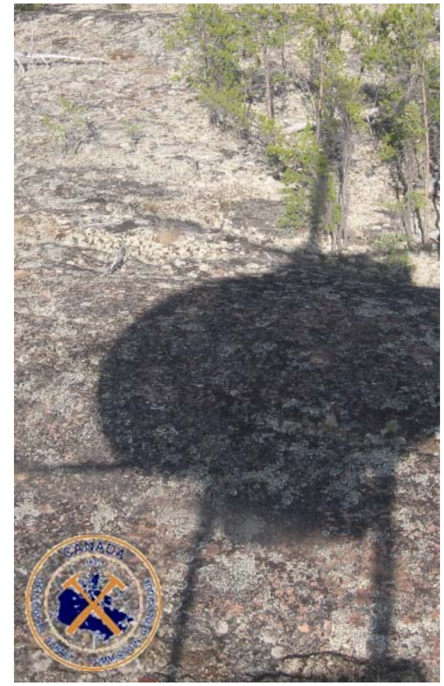

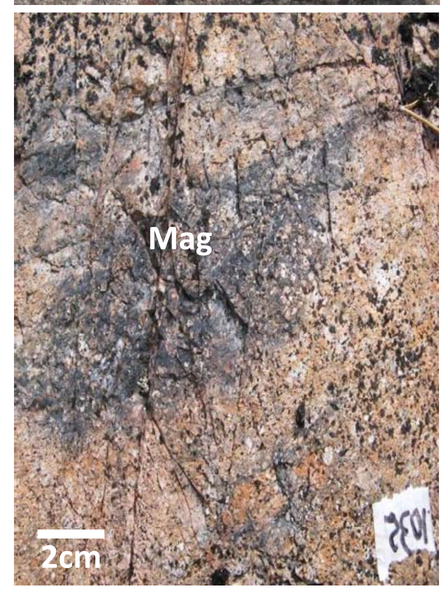

Notes

Previously published figures and photos included in this short course series are veiled by a figure caption referring to their source publication. This editorial choice is prompted by the importance of linking the abundant and more detailed illustration of the ore systems provided in this short course series with our published description and discussion of the systems.

In case of copyright issues with material presented in this short course series, please contact Dr. Louise Corriveau at Louise.Corriveau@canada.ca

Acronyms and abbreviations

IOCG-iron oxide copper-gold deposits; **IO±A-**iron oxide±apatite deposits
IOAA-iron oxide alkali-calcic alteration systems; **Grp-**group
HT-high temperature; **LT-**low(er) temperature
REE-rare-earth elements and Y; **PGE-**platinum-group elements
MLYRMB- Middle-Lower Yangtze River metallogenic belt
GSC-Geological Survey of Canada; **NTGS**-Northwest Territories Geological Survey; **GEM**-Geomapping for Energy and Minerals program
TGI-Targeted Geoscience Initiative

Minerals

Ab-albite, **Act**-actinote, **Amp**-amphibole, **Ap**-apatite, **Apy**-arsenopyrite, **Bn**-bornite, **Brt**-barite, **Bt**-biotite, **Cb**-carbonate, **Cc**-calcite, **Ccp**-chalcopyrite, **Cct**-chalcocite, **Cof**-coffinite, **Cpx**-clinopyroxene, **Cum**-cummingtonite, **Ep**-epidote, **Fl**-fluorite, **Gn**-galena, **Grt**-garnet, **Hbl**-hornblende, **Hem**-hematite, **Kfs**-K-feldspar, **Mag**-magnetite, **Mol**-molybdenite, **Pl**-plagioclase, **Py**-pyrite, **Rbk**-riebeckite, **Ru**-rutile, **Scp**-scapolite, **Sd**-siderite, **Ser**-white mica (sericite), **Sp**-sphalerite, **Sil**-sillimanite, **Sul**-sulphides, **Ttn**-titanite (Whitney and Evans 2010)

Iron oxide and alkali-calcic alteration ore systems

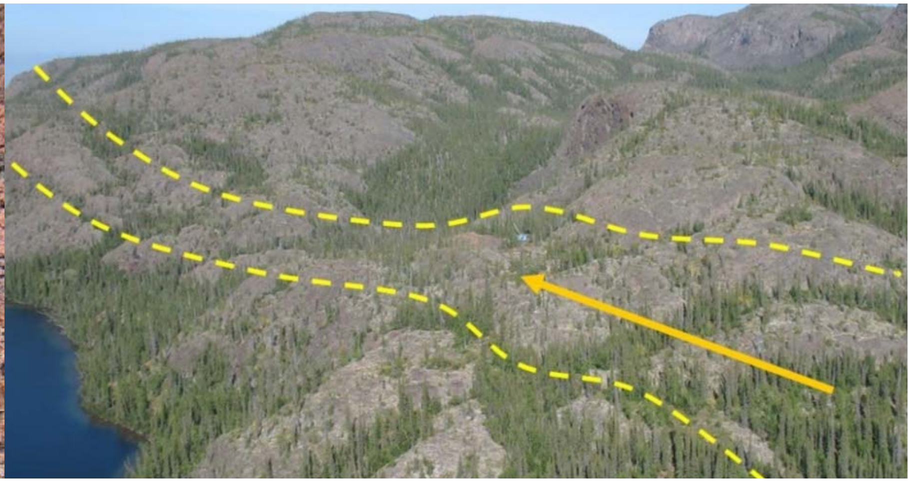

Iron oxide and alkali-calcic alteration ore systems

A series of fluid-rock reactions triggered by high salinity fluids across high geothermal gradients in tectonically active settings (800 to 250°C; spatial extent ~35x15x10 km)

Intense and pervasive Na, HT Ca-Fe, HT–LT K-Fe, LT Ca-Fe-Mg metasomatism leads to:

- **IOCG** – Iron oxide copper-gold deposits: polymetallic, base and precious-metal hydrothermal deposits with economic copper (± gold) (Williams et al. 2005; Groves et al. 2010; Porter 2010a, b; Williams 2010a, b; Skirrow 2010; Barton 2014)
- **IO±A** – Iron oxide±apatite±REE deposits: magnetite dominant, Ti-V< igneous Fe-Ti-V-P deposits (Hitzman et al. 1992; Porter 2010 a, b; Williams 2010a, b; Knipping et al. 2015; Tornos et al. 2016, 2017)
- Albitite-hosted U±Au ±Co; albitite-hosted 'orogenic' Au-U; some skarns, mantos, Mo-Re and alkaline intrusion-related iron oxide deposits (Porter 2010a; Wilde 2013; Corriveau et al. 2014, 2016; Montreuil et al. 2015)
- Epithermal polymetallic mineralisation (Mumin et al. 2010; Kreiner and Barton 2011)

Celebrating 175 yrs

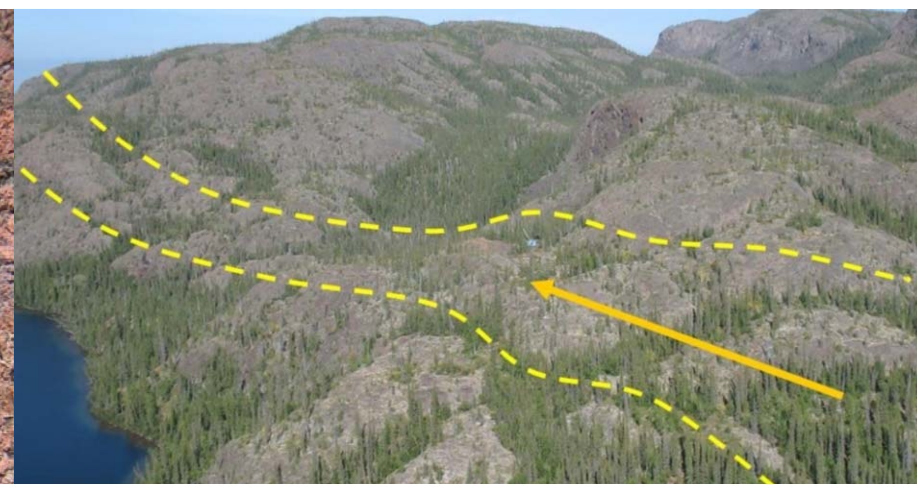

Deposits and prospects discussed in text

Sources of information at slide 50

Modified from Corriveau 2007; Porter 2010a

Canadian deposits and prospects

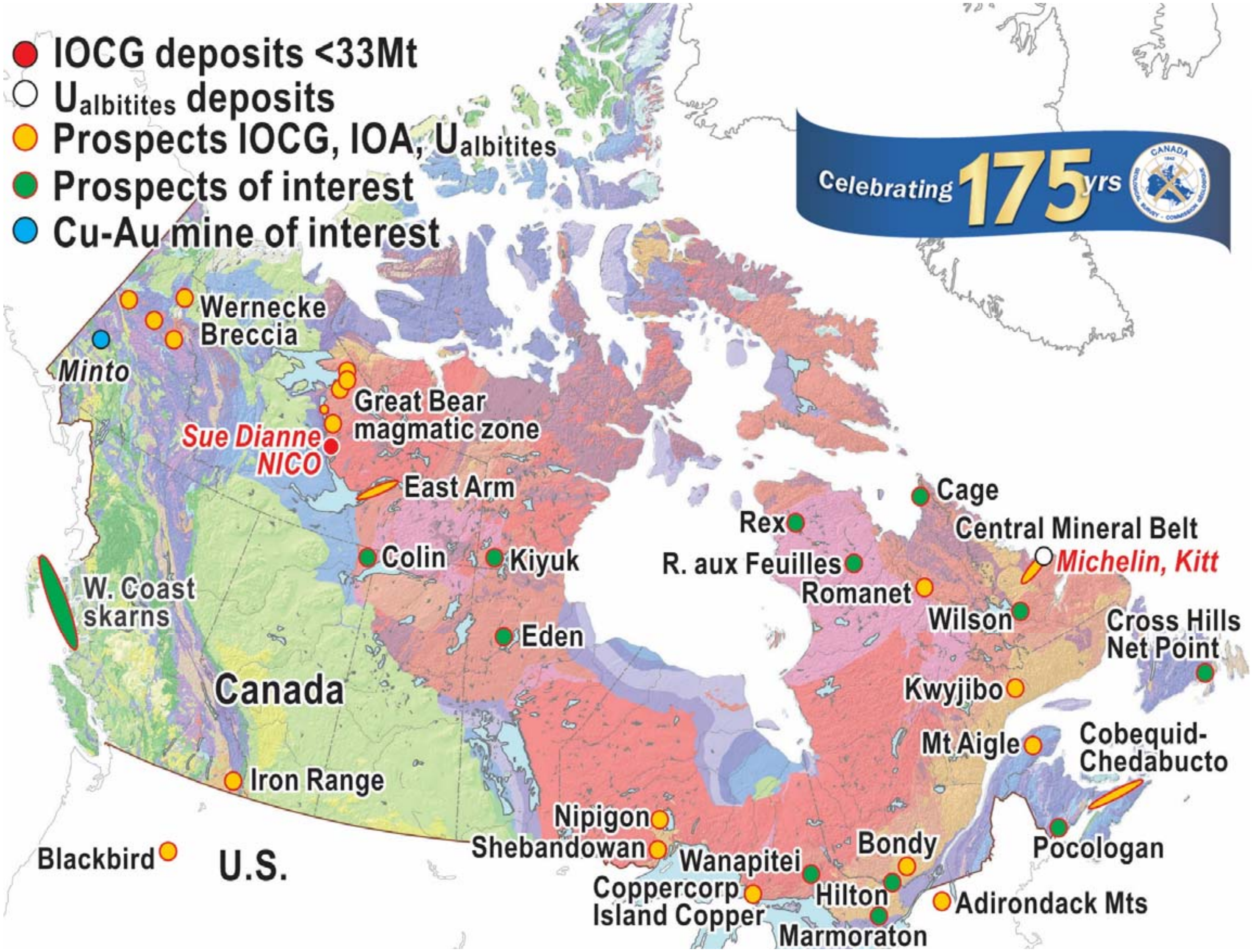

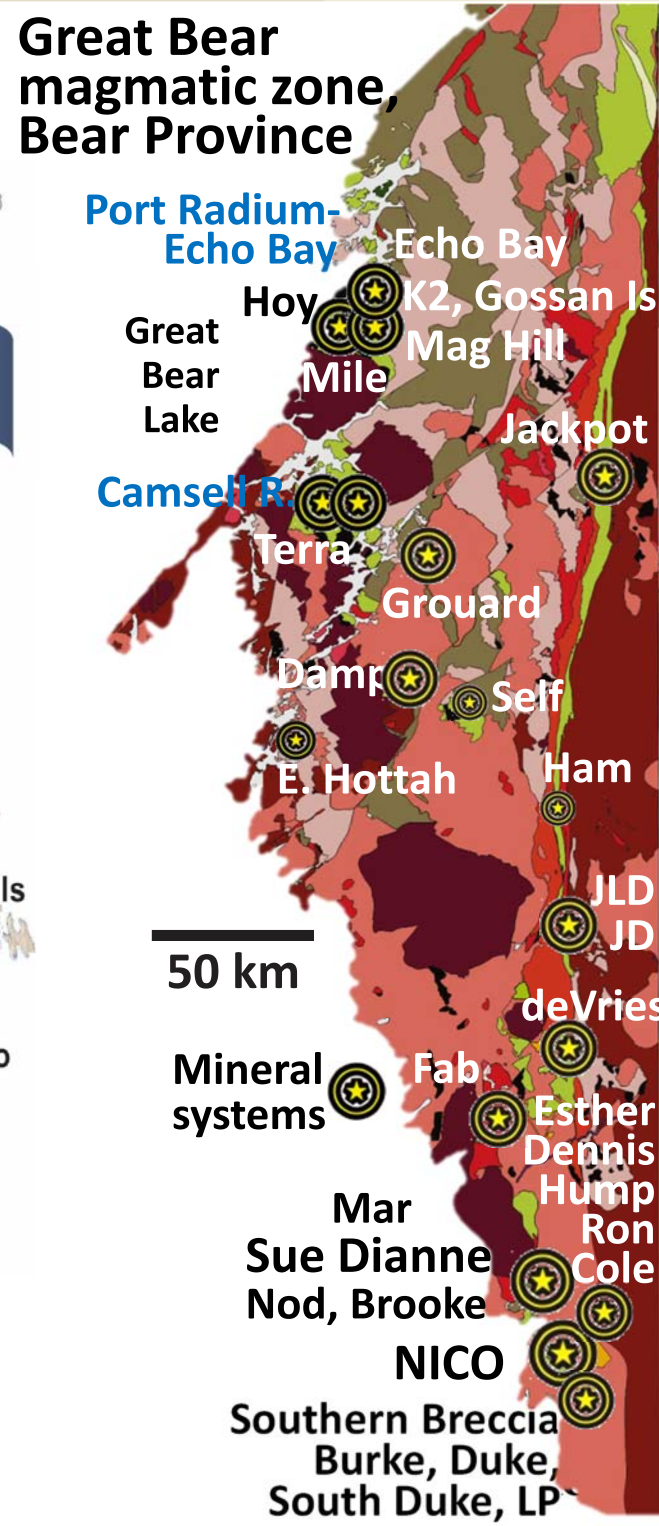

Sources of information at slide 50

Historic perspective

- 1975: Discovery of Olympic Dam defies existing ore deposit models. Deposit resources has increased steadily from 2000 Mt to current 10400 Mt
- 80s, early 90s: Discovery of Candelaria (Central Andes, Chile), Ernest Henry (Cloncurry district, Australia), and Sue Dianne and NICO (Great Bear, Canada)
- 1992: Hitzman et al. suggest the existence of a distinct class of “Proterozoic iron oxide (Cu-U-Au-REE) deposits” using three main case examples: Olympic Dam, Great Bear magmatic zone, Norbotten district (Sweden).
- 2000, 2002, 2010: Publication of “Hydrothermal iron oxide copper-gold and related deposits” volumes 1 to 4 (Porter 2000, 2002, 2010a, b)
- 2005: Publication of a discrete synthesis paper on IOCG and IOA deposits in the Economic Geology 100th Anniversary Volume (Williams et al. 2005)
- 2008+: Chemical discriminants (Benavides et al. 2008a, b; Montreuil et al. 2013)
- 2010: Publication of “ Exploring for iron oxide copper-gold deposits: Canada and global analogues” (Corriveau and Mumin 2010, > 660 copies sold) including empirical classifications of IOCG IOA and affiliated deposits (Williams 2010a, b)
- 2016: Economic Geology v. 111 on the Missouri and Great Bear districts

IOAA deposit continuum

Extraordinary range of polymetallic hydrothermal deposits

Can host most metals required for modern and future technology

- Base metals (Cu, Ni, Pb, Zn), Fe, precious metals (Ag, Au, Platinum-group)
- Rare earths, strategic metals (Bi, Co, Mo, V, F, Nb), nuclear metals (U, Th)
- Industrial material (magnetite, vermiculite, apatite, fluorite, albite)
- Anomalous concentration of nearly the entire periodic table within systems

Form new mines and districts worldwide with resources reaching 10,400 Mt total resources at the Olympic Dam (Australia) worth about

- **700** billion CAD$ Cu (order of magnitude in 2017)
- **185** billion CAD$ U (order of magnitude in 2017)
- **160** billion CAD$ Au (order of magnitude in 2017)
- **7** billion CAD$ Ag (order of magnitude in 2017)

U-Th-K: source of heat for geothermal energy

Deposit spectrum and continuum

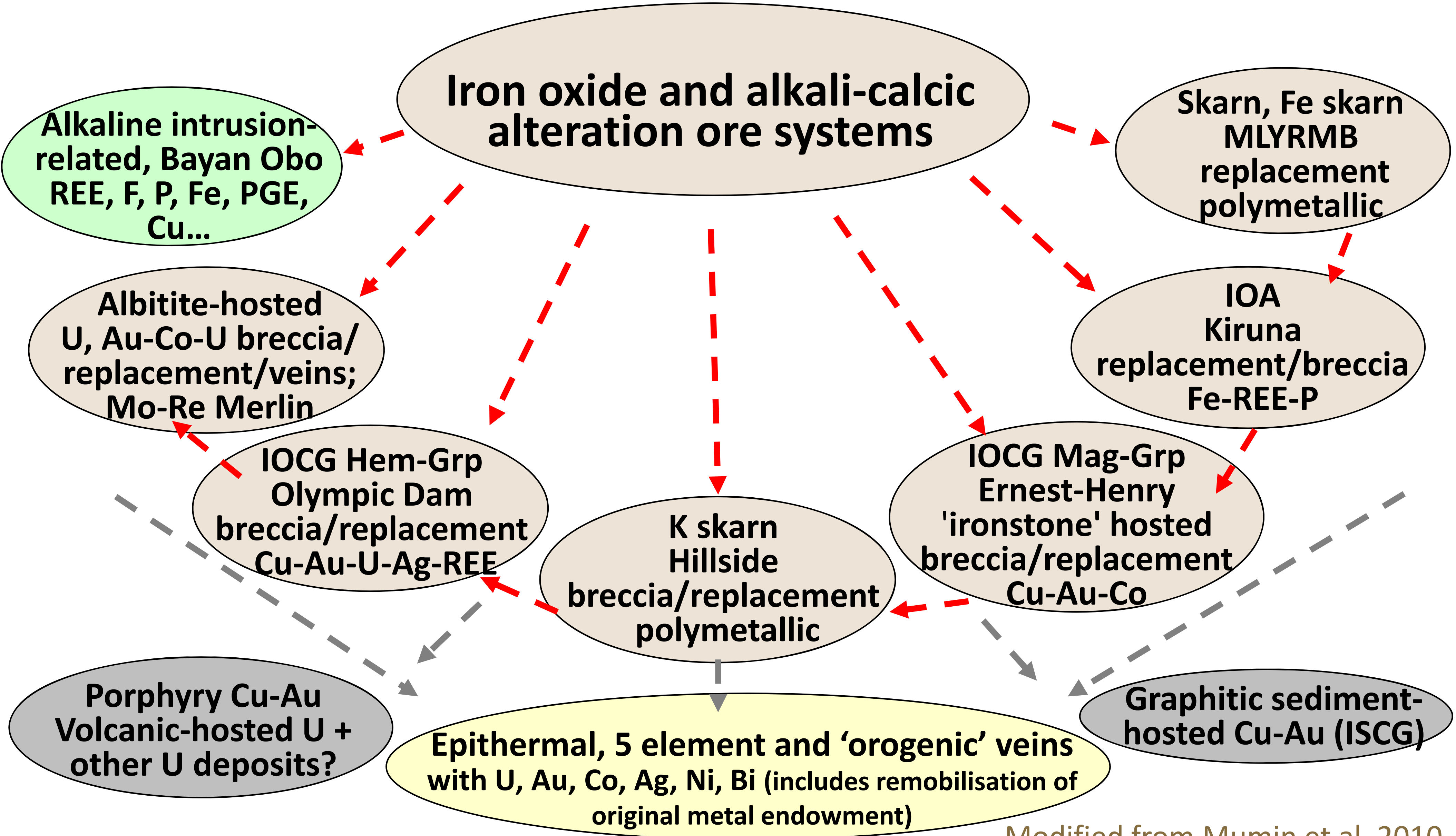

Modified from Mumin et al. 2010

See also Hitzman 2000; Corriveau et al. 2016; Porter 2010a; Day et al. 2016; Tornos et al. 2016, 2017; Zhao et al. 2017a

IOCG, IOA, affiliated deposits

- Definition, main characteristics
- Classification and continuum
- Location
- Ages

Ernest-Henry, Cloncurry district, Australia

IOCG deposits

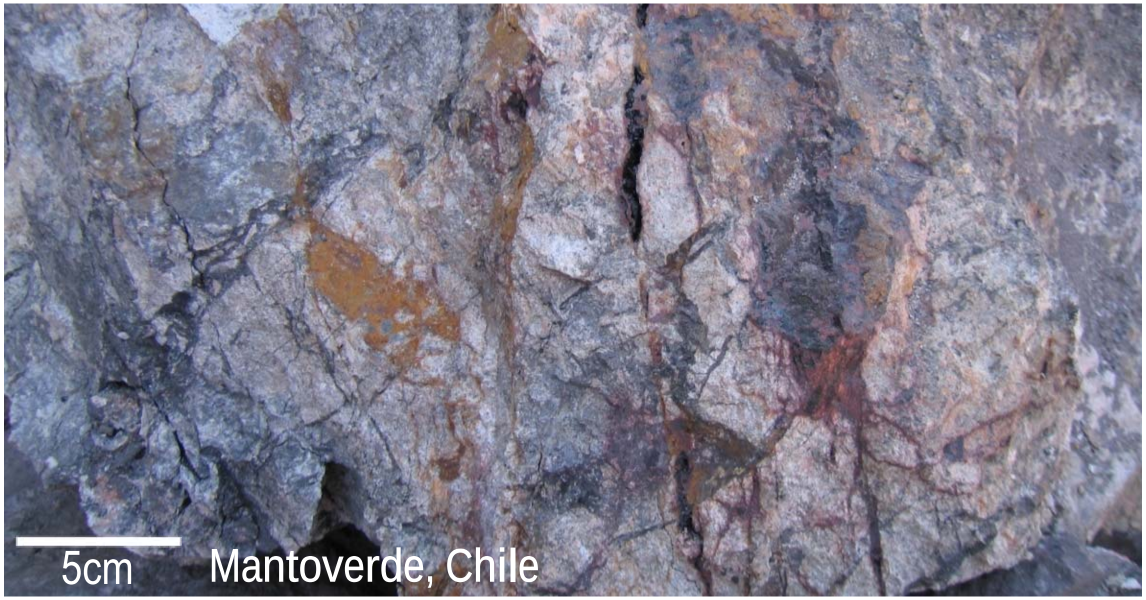

IOCG

Hydrothermal epigenetic mineralisation (breccia, vein, replacement)

Among >15-20% iron oxides (magnetite, hematite, Ti in oxides < in Fe-Ti-P deposits)

With copper ± gold resources

Local to lithospheric structural controls

Within highly diagnostic iron-oxide and alkali-calcic alteration systems coalescing across ≤ 35 x 15 x 10 km (length-width-depth)

Hitzman et al. 1992; Williams et al. 2005; Corriveau and Mumin 2010; Oliver et al. 2004, 2009; Rubenach 2012

Ore zones

- **Polymetallic**
- **< 6 x 1 x 2 km) (length-width-depth)**
- **Cu sulphides (chalcopyrite, bornite, chalcocite) content greater than Fe sulphides content in the ore** (but not throughout the entire system)
- **Fe oxides (magnetite, hematite, ±martite, ±mushketovite) content greater than Fe sulphides content (pyrrhotite-pyrite)**
- **Ni-, Pb-, Zn- sulphides, Ag-, Co-, Cu-, Ni-, U- arsenides, Ag-, Bi-, Co- tellurides, native Ag, Au, Bi and Cu, and electrum**
- **Little hydrothermal quartz but abundant syn-post mineralisation carbonate**

Hitzman et al. 1992; Hitzman 2000; Ray and Lefebure 2000; Williams et al. 2005; Corriveau and Mumin 2010; Ehrig et al. 2012, 2017; Corriveau et al. 2010b, 2016; Porter 2010a; Williams 2010a, b

Metal associations in ores

Host most metals required by society

- **Base metals (Cu, Ni, Pb, Zn) and iron**
- **Precious metals (Ag, Au, PGE)**
- **Rare earth elements (light to heavy REE)**
- **Specialty (strategic) metals (Bi, Co, Mo, V, F, Nb)**
- **Actinides (U at low grades, also Th)**
- **U-Th-K potential source of heat for geothermal energy**
- **+ P, Se, Te , Zr, As, B, Ba, Mn, W, …**

Olympic Dam, Australia
10,100 Mt at
0.78% **Cu**,
0.25kg/t **U_3O_8**,
0.33 g/t **Au**,
1.0 g/t **Ag**
(+ ~0.3% LREE, 0.01% HREE)
BHP 2017; REE numbers – personal comm.

Combine atypical metal associations

Fractionation and decoupling of elements that normally occur together

Potentially very large tonnage, intermediate to low grade

Hitzman et al. 1992; Hitzman 2000; Williams et al. 2005; Corriveau and Mumin 2010; Groves et al. 2010; Williams 2010a, b; Schofield 2012

Mineralisation styles and hosts

- Breccia, stockworks, veins
- Disseminations, replacement
- Mantos, skarn
- Stratabound, discordant
- In any host rocks
- At any stratigraphic levels
- Among units of different ages
- Within a single system, deposits can be hosted in volcanic, sedimentary, intrusive and metamorphic rocks
- Immediate host are intensely metasomatised at K-Fe alteration facies, i.e., HT K-Fe with Mag-Kfs-Bt parageneses and (or) LT K-Fe with Hem-Ser-Chl-Cb parageneses

A consequence of metasomatic growth of ore systems

Hitzman et al. 1992; Oliver and Bons 2001; Wang and Williams 2001; Williams et al. 2005; Oliver et al. 2006; Corriveau et al. 2010b, 2016; Porter 2010a; Williams 2010a, b

Reference IOCG deposits

Hematite-group IOCG deposits (Hem>>Mag; classification of Williams 2010a)

- Olympic Dam, Carrapateena, Prominent Hill (Gawler craton, Australia)
- Mina Justa (Central Andes, Peru)

Magnetite to hematite-group IOCG deposits (+low-Cu variants)

- Sue Dianne (Great Bear magmatic zone, Canada)
- Raul-Condestable (Central Andes, Peru)
- Mantoverde (Central Andes, Chile)

Magnetite-group IOCG deposits

- Ernest Henry (Cloncurry, Australia)
- Candelaria (Central Andes, Chile)
- Sossego, Salobo (Carajás, Brazil)
- Guelb Moghrein (Mauritania)
- Boss (SE Missouri, US)

IOCG-hosted skarn and K-skarn variants

- Hillside (Gawler, Australia)
- Hannukainen (Finland), Kaunisvaara (Sweden)

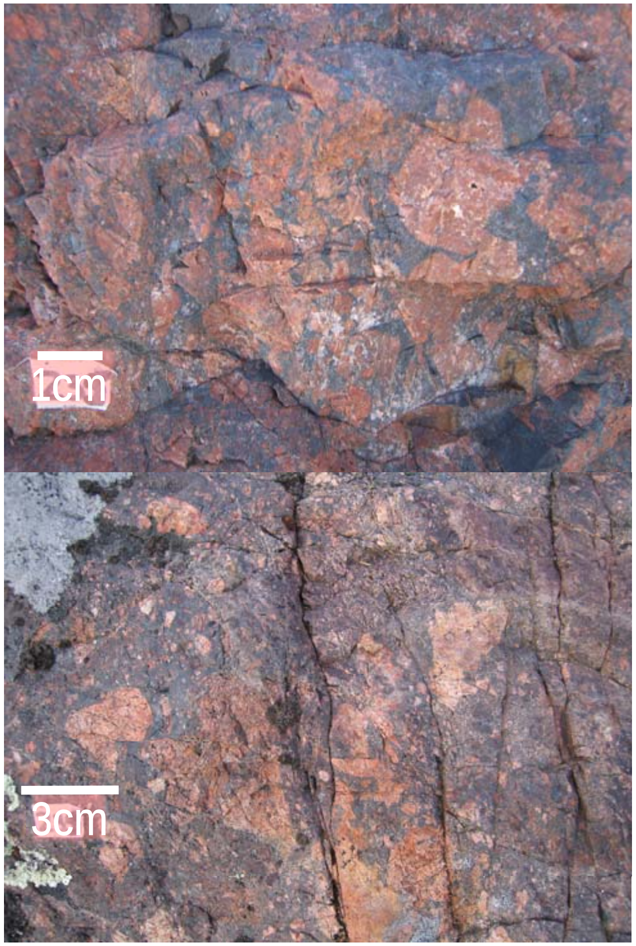

Williams et al. 2005; Porter 2010a; Williams 2010a,b; Chen 2013

Olympic Dam

Thousand tonnes U_3O_8

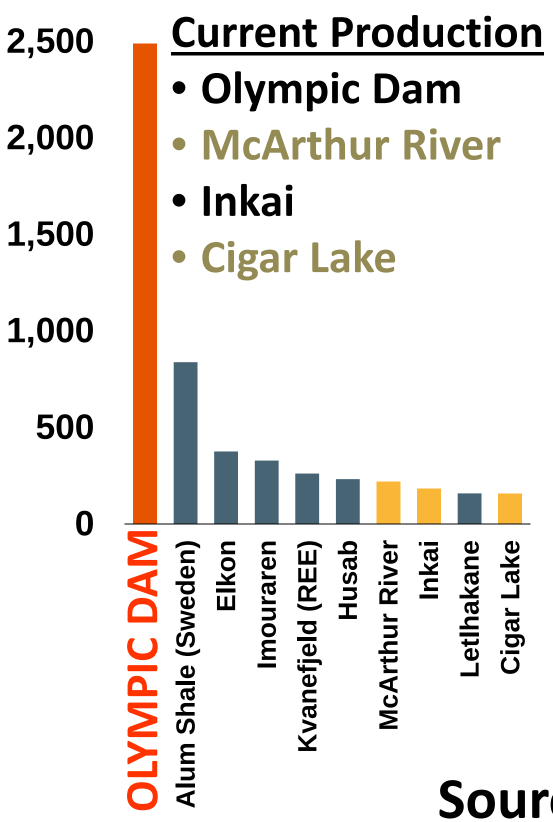

Million tonnes Copper

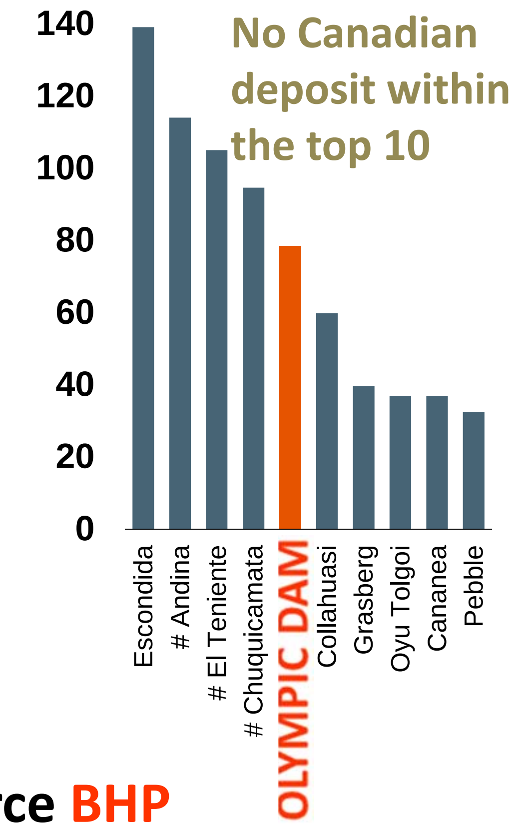

Million oz Gold

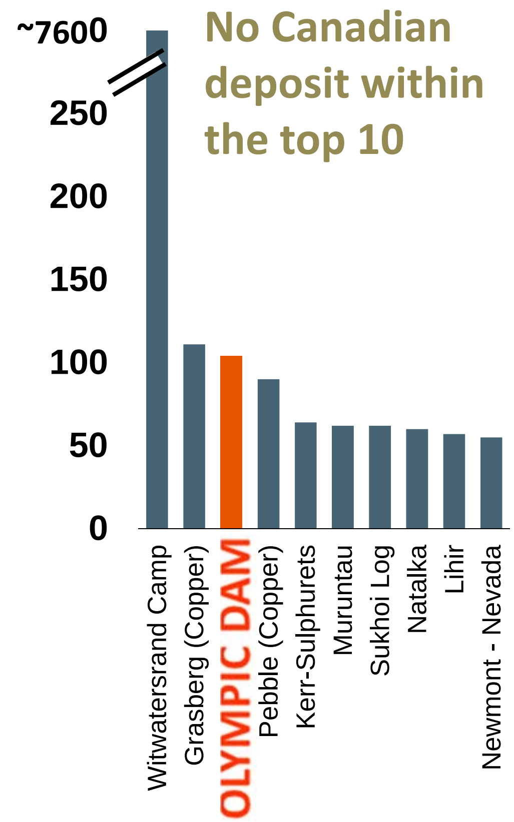

Source BHP

OD Total Resource 30 June 2017

10,100 Mt @ 0.78 % Cu, 250 ppm U_3O_8, 0.33 ppm Au, 1 ppm Ag

OD Total Metal Endowment

~80 Mt Cu
~2600 kt U_3O_8
~110 Moz Au,
~320 Moz Ag

Chart depicts contained metal. Sources: Company Annual Reports, press releases and International Atomic Energy Agency (BHPB figures as at 30 June 2015, all other figures as at Sep 2014). Witwatersrand figure is BHP Billiton estimate and is approximate only. # Based on Codelco reported figures at 0.2% Cu cut-off grade. BHP Billiton Mineral Resources for Olympic Dam and Escondida district (includes Pampa, Pinta Verde and Chimborazo) are on a 100% basis. The FY2015 Mineral Resource information for Olympic Dam and Escondida district on this slide is extracted from the report entitled BHP Billiton Annual Report 2015. The report can be viewed at www.bhpbilliton.com. The company confirms that it is not aware of any new information or data that materially affects the information included in the original market announcement and, in the case of estimates of Mineral Resources, that all material assumptions and technical parameters underpinning the estimates in the relevant market announcement continue to apply and have not materially changed. The company confirms that the form and context in which the Competent Person's findings are presented have not been materially modified from the original market announcement.

BHP Billiton 2015; BHP 2017

Co-rich IOCG variants

- **Idaho Co belt (US)**
- **Mt Cobalt ? (Cloncurry, Australia)**
- **NICO (Great Bear, Canada)**

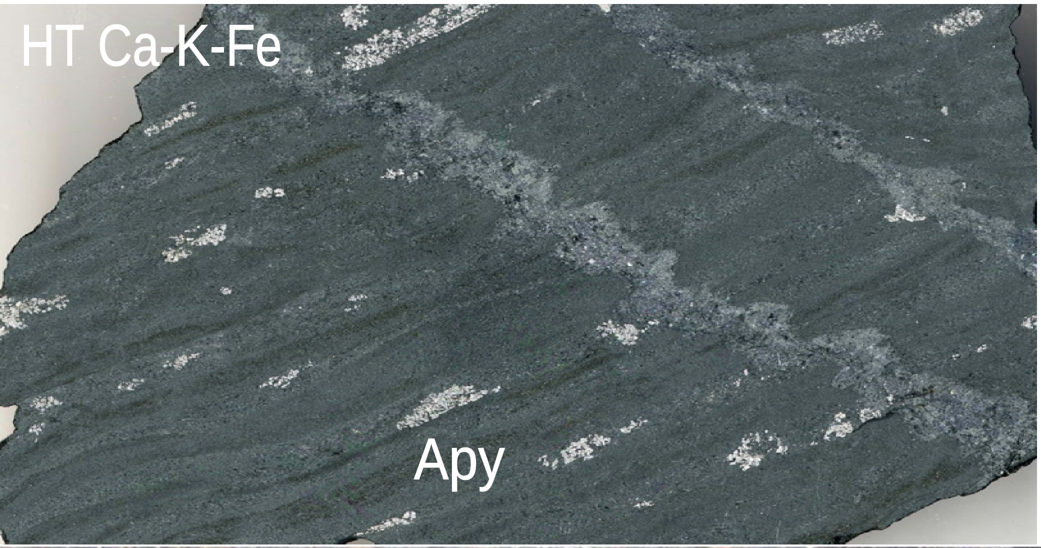

At the Au-Co-Bi-Cu NICO deposit and other Co-rich IOCG variants, HT Ca-K-Fe amphibole-magnetite-biotite alteration + HT K-Fe alteration + arsenopyrite, Au, Co, low Cu mineralisation cut and replace earlier Na or least-altered metasedimentary rocks

Goad et al. 2000; Corriveau et al. 2010b, 2016; Mumin et al. 2010; Slack 2013; Acosta-Góngora et al. 2015a, b; Montreuil et al. 2015, 2016b

See reference list at slide 50

What is NOT an IOCG deposit sensus stricto

but can be components of ore systems forming IOCG deposits

- Polymetallic deposits devoid of significant iron oxides (but siderite-rich breccia can be good targets for affiliated deposits)
- Iron oxide-apatite deposits ("Kiruna-type" / IOA) and other iron oxide bodies
- Polymetallic magmatic-hydrothermal iron deposits with Nb and REE as important economic commodities
- Albitite-hosted U and Au-Co-U and hematite-hosted U
- Skarn and porphyry deposits

Nomenclature used for IOCG deposits

- IOCG: Iron-Oxide Copper-Gold deposits
- Fe oxide Cu-Au±U
- Olympic Dam and Cloncurry types
- FeOx

See also Williams et al. (2005), Williams (2010a, b), Groves et al. (2010) for strict definitions of IOCG deposits.
Hitzman et al. (1992), Corriveau (2007), Porter (2010a) and Corriveau et al. (2010a, b, 2016, 2017) discuss the importance of an holistic system approach to exploring IOCG deposits in under explored terranes

Iron Oxide ± Apatite (IOA) deposits

Iron oxide-apatite (IOA) deposits

Iron oxide deposits (30-50% Fe) with or without rare-earth (REE) mineralisation

Also called Kiruna type (N.B. volcanic-hosted Fe and porphyrite Fe in Chinese literature)

- **Kiirunavaara (682 Mt, 47.5% Fe) in the IOA-IOCG Norbotten district, Sweden**
- **Oak Dam (~560 Mt , 41–56% Fe) (+ Cu, U, Au) in the IOCG-skarn Olympic Cu-Au province, Australia**
- **Marcona (~1940 Mt, 55.4% Fe) (+ Cu) in the IOA-IOCG central Andes province, Chile and Peru**
- **El Laco (734 Mt, 49% Fe) in the Andes**
- **Pea Ridge (161 Mt, ~ 54% Fe; 0.2Mt, 12% REE) in the IOA-IOCG SE Missouri district**
- **Bayan Obo (China) IOA(?) associated to carbonatites**
  - **1500 Mt @ 35% Fe**
  - **57 Mt @ 6% REE_2O_3**
  - **2 Mt @ 0.13% Nb_2O_5**

See reference list at slide 50

Ore and metasomatic facies

- **Same sets but different proportions of alteration facies as IOCG deposits** (i.e., Na, HT Na-Ca-Fe and HT Ca-Fe alteration facies at deposit to regional scale)
- **REE-rich variants replaced or spatially associated by Ca-K-Fe or K-Fe alteration**
- **Skarn (clinopyroxene, garnet) common among IOA ores**
- **HT Ca-Fe (Act, Amp-Mag) assemblages are distinct from and should not be included as skarns**
- **Poor in sulphides and U** unless overprinted by fertile HT Ca-K-Fe (Apy) and K-Fe alteration (Ccp, U)
- **Commonly fine grained**
- **Massive, vein, stockwork, breccia ores**

Badham and Morton, 1976; Hildebrand 1986; Hitzman et al. 1992; Williams et al. 2005; Corriveau et al. 2010a, b, 2016; Naranjo et al. 2010; Porter 2010a, b; Williams 2010a, b; Yu et al. 2011; Zhou et al. 2013; Knipping et al. 2015; Bilenker et al. 2016; Tornos et al. 2016, 2017; Zhao et al. 2016, 2017a

- Formed at depth within IOAA systems that evolved to IOCG mineralisation (Great Bear) or emplaced at or near surface (El Laco)
- High to very high temperatures (600-800°C)
- Conclusive field evidence of metasomatic attributes (replacement, breccia filling, fluidisation breccias)
- Alteration can preserve or destroy protolith textures
- Regularly associated with andesitic magmatism, commonly above the roof of intrusions
- Iron oxide melt inclusions in coeval andesites
- Highly saline magmatic-hydrothermal fluids stemming from coeval magmas and interacting with host rocks

See references in slides 27 and 29

Genesis

Are magmatic-hydrothermal fluids solely responsible of ore genesis?

Ore deposit models invoke:

- **Metasomatism, magmatic-hydrothermal alteration, highly saline fluids**
- **Iron oxide magmas (immiscible from silicate magmas); melt attributes include iron oxide melt inclusions in coeval andesites**
- **Iron oxide salt melt**
- **Fluidisation of hydrothermal precipitates**
- **Flotation of igneous magnetite**

Metasomatising agent(s) and Fe carrier(s) must also produce all other alteration facies

Magnetite in breccia matrix and replaces fragments

See: Hildebrand 1986; Hitzman et al. 1992; Williams et al. 2005; Corriveau et al. 2010a, b, 2016, unpublished; Porter 2010a, b; Williams 2010a, b; Chen 2013; Knipping et al. 2015; Li (W.) et al. 2015; Bilenker et al. 2016; Tornos et al. 2016, 2017; Zeng et al. 2016; Zhao et al. 2016, 2017a

Other deposits formed in IOAA systems

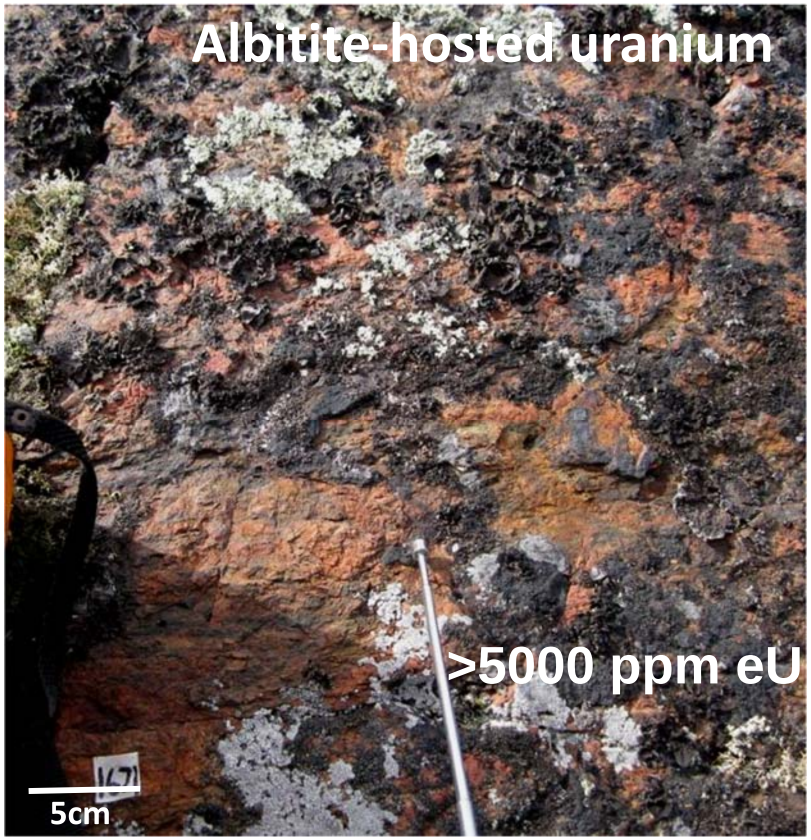

Affiliated deposits

Albitite-hosted U

- Valhalla (Mount Isa, Australia) 34.7 Mt at 830 ppm U_3O_8
- Lagoa Real (Brazil)
- Michelin (Canada) 37.5 Mt at 0.10 % U_3O_8
- Southern Breccia (prospect; Great Bear, Canada)

Albitite-hosted Au±Co±U

- Kuusamo (Finland) 3.8 Mt at 4.1 g/t Au, 9.1 Mt at 0.12% Co
- Larafella, Loraboué (Burkina Faso)
- Turamdih (India)
- Romanet Horst (prospects; Canada)

Alkaline intrusion-related

- Bayan Obo (China) here interpreted as an IOA
- Phalaborwa, Vergeneog (S. Africa)

Mo-Re deposit

- Merlin (Cloncurry, Australia) 6.4 Mt at 1.5% Mo, 26 g/t Re (reserves)

See reference list

Albitite-hosted U, Au±U±Co

- In regional-scale albitites associated with iron oxide alkali-calcic alteration mineral systems
  - Michelin, Kitt (Central Mineral Belt); Romanet Horst; Southern Breccia (Great Bear) (Canada)
  - Kuusamo (Finland)
  - Valhalla (Mount Isa, Australia)
  - Itatalia (NE Brazil)
- Occur in Cu districts of uncertain affinity with respect to iron oxide alkali-calcic alteration systems (e.g., Turamdih, Singhbhum Shear Zone, India)
- Spatial+temporal association between
  - albitite and U mineralisation
  - albitite and IOCG (e.g., Cloncurry)
- U precipitates AFTER albitisation
- Albitites: a structural, porous fluid corridor and a chemical (?) trap for U

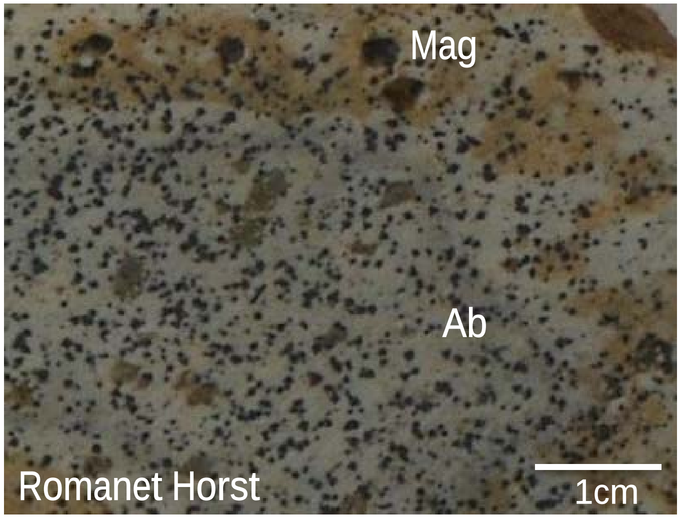

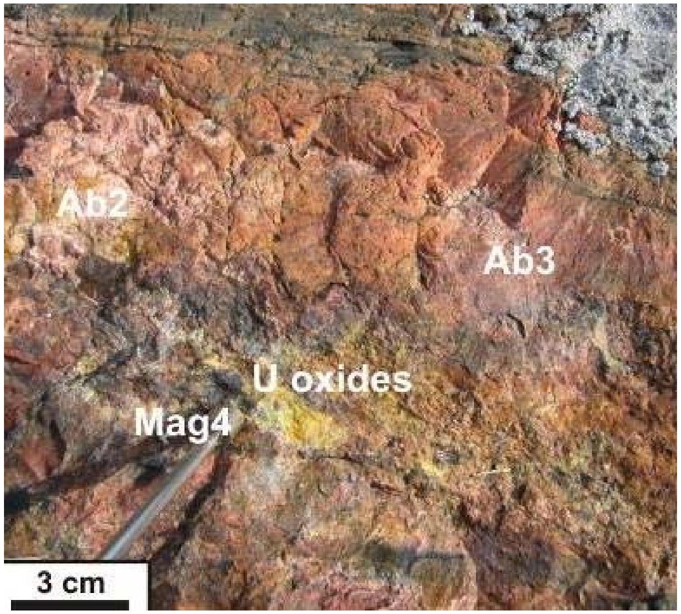

Gandhi 1978; Porto da Silveira et al. 1991; Béziat et al. 2008; Cuney and Kyser 2008; Kerr and Sparkes 2009; Skirrow et al. 2009; Williams 2010a; Corriveau et al. 2011; Cuney et al. 2012; Rubenach 2012; Wilde 2013; Dragon Mining 2014; Kontonikas-Charos et al. 2014; Montreuil et al. 2015, 2016b; Sparkes 2017

Albitite-hosted U, Au±U±Co

Also called
- Na-metasomatic U
- Metamorphic-metasomatic U
- Albitite-hosted Au±U±Co vein
- Orogenic Au-Co-U (e.g., Kuusamo in Finland; Laraboué, Larafella in Burkina Faso)

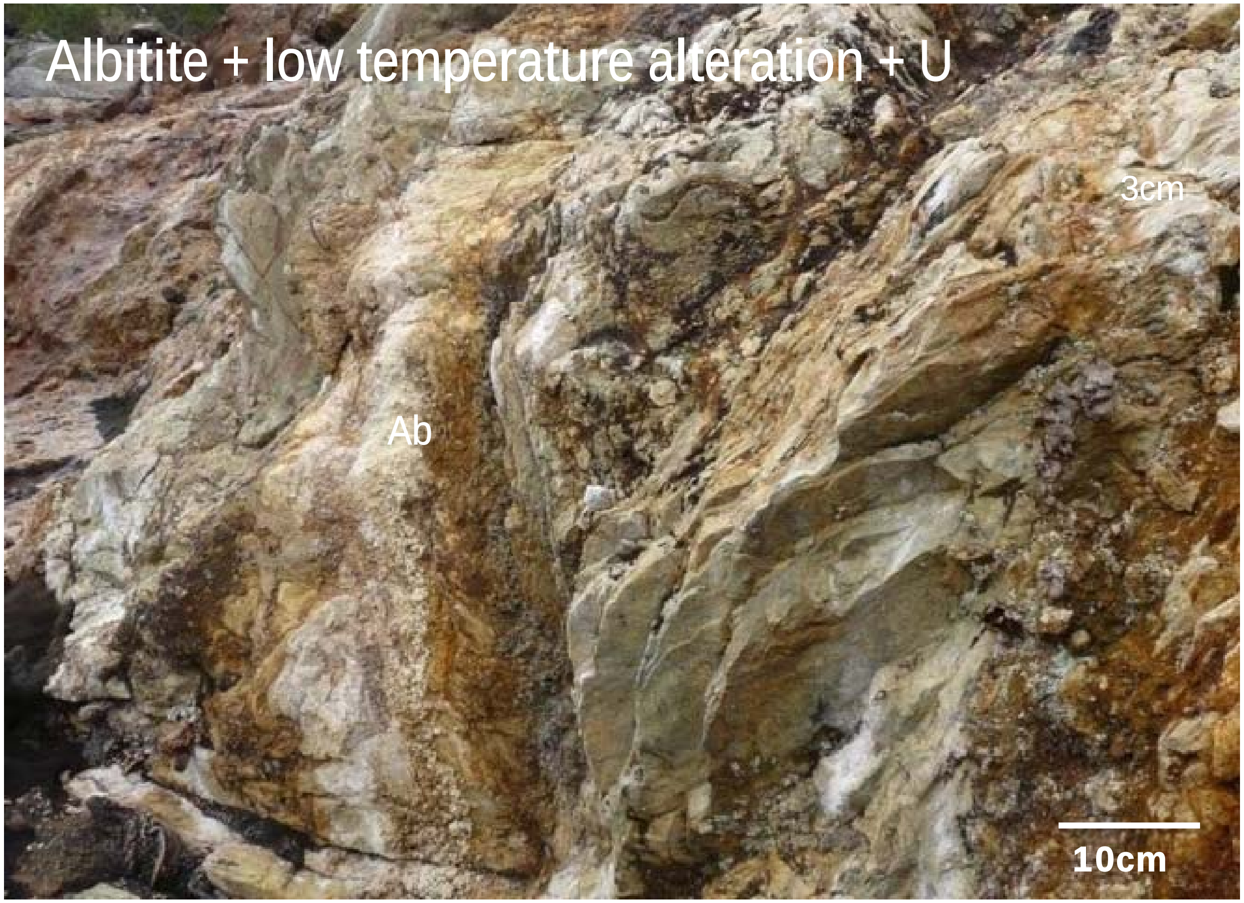

Multiple stages of
- Na (Ab ± Rbk, Na-Cpx),
- HT Ca–Fe (Amp, Cpx, Mag),
- K (Kfs),
- HT K-Fe (Bt) metasomatism

Commonly syn-deformation + LT Ca–Fe–Mg (Chl, Cb, Hem) overprints

Gandhi 1978; Porto da Silveira et al. 1991; Béziat et al. 2008; Cuney and Kyser 2008; Kerr and Sparkes, 2009; Skirrow et al. 2009; Williams 2010a; Corriveau et al. 2011; Cuney et al. 2012; Wilde 2013; Dragon Mining 2014; Kontonikas-Charos et al. 2014; Montreuil et al. 2015, 2016b; Sparkes 2017

Albitite-hosted U, Au±U±Co

Dominant U minerals

- Uraninite, Brannerite, Davidite, Coffinite
- Secondary hexavalent U mineral species

Elevated Zr, Nb, Ta, Sn in albitites

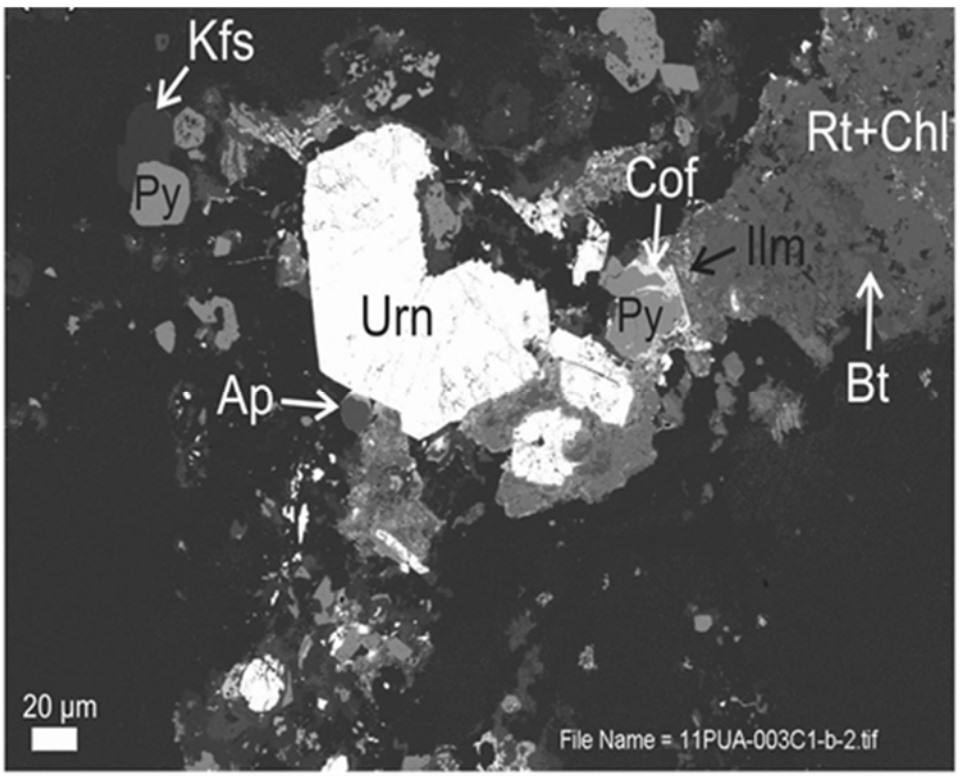

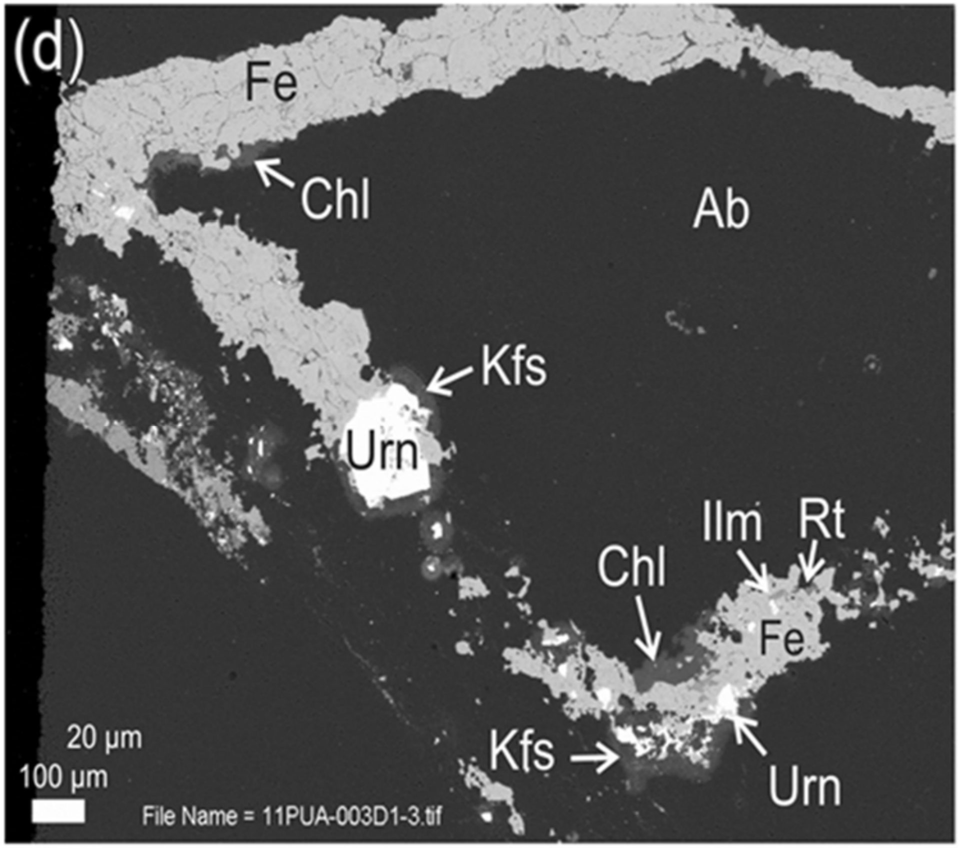

Epithermal, vein-type (U, Ag), five elements veins

- Prograde and retrograde epithermal alteration, veining and mineralisation
- LT remobilisation – quartz veining (Ray rock, Southern Breccia)
- LT remobilisation in hematite-lined fractures (various small showings)

Past-producing Ray Rock U mine, Great Bear, Canada

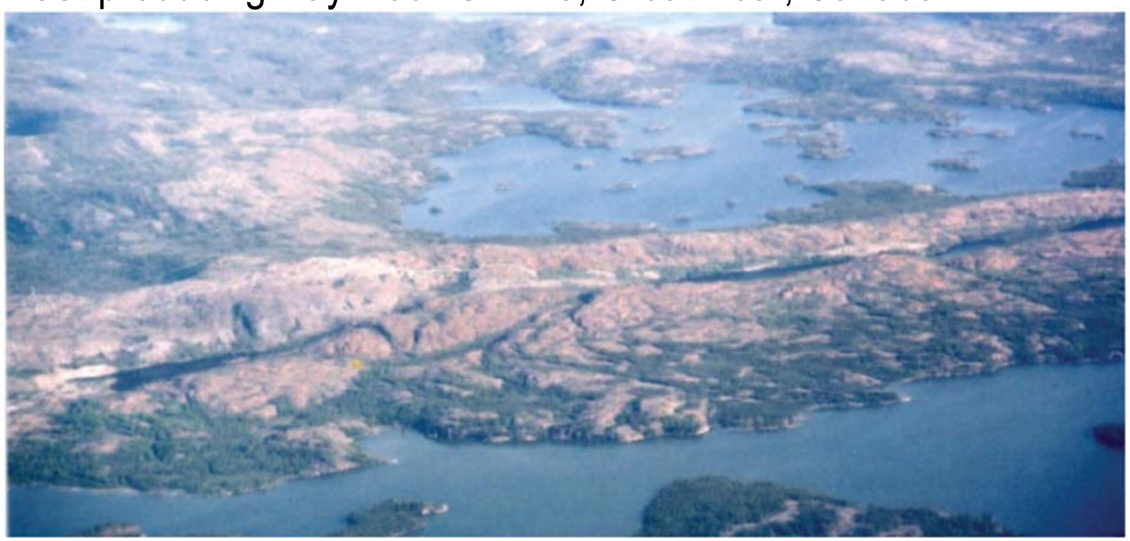

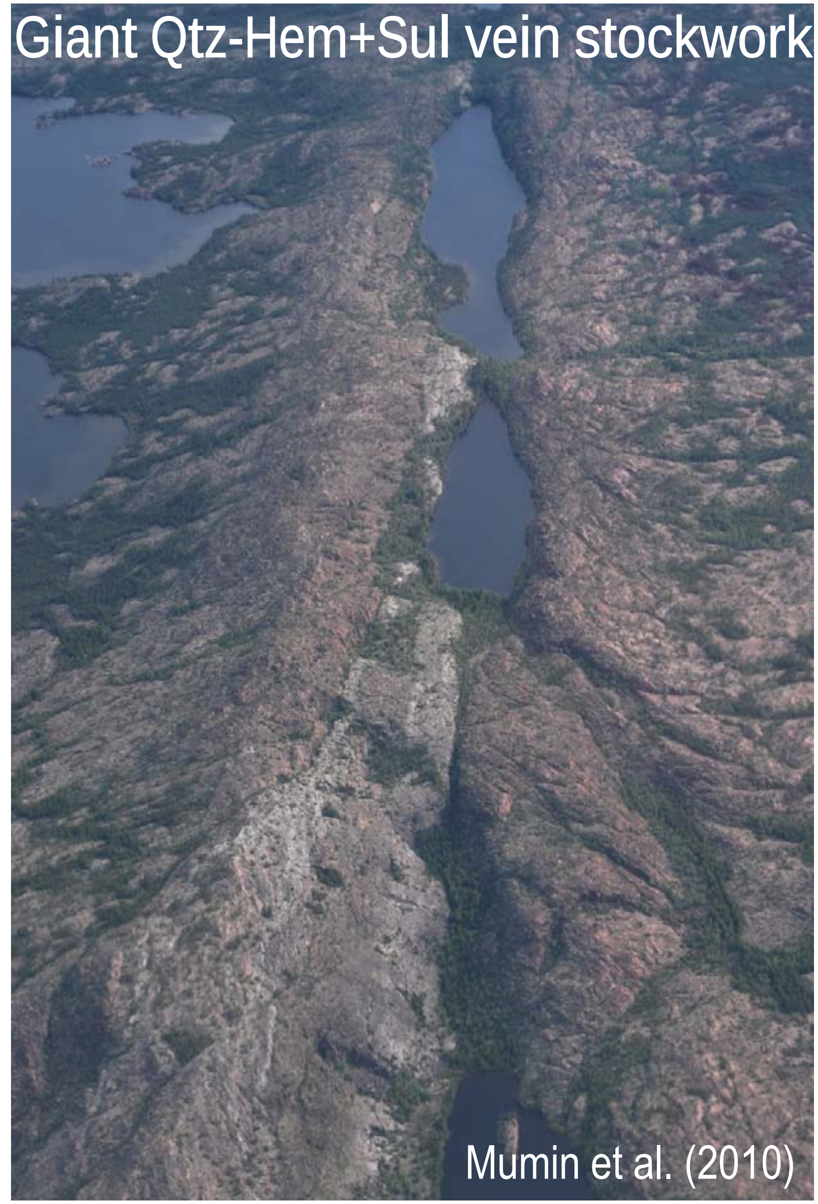

Continuum among IOCG and affiliated deposit types

Classification modified from Williams 2010a; Porter 2010a

Iron oxide and alkali-calcic alteration ore systems

Deposit type	Subtype	Examples
Albitite-hosted	Albitite-hosted U±Au-Co	Michelin, Turamdih, Valhalla, Cole, Southern Breccia
	Albitite-hosted 'orogenic' Au-Co ± U	Kuusamo, Mount Cobalt, *Romanet Horst*
Skarn-hosted + K skarn (± Fe oxides)	Pb, Zn, Au, Cu, Co, REE, U	Mile, Mt Elliott, Mary Kathleen, Bastnäs
IOCG Economic Cu ± Au, Ag, REE, U, etc.	Hematite group	Olympic Dam, Prominent Hill, Carapateena, Kitumba, Mina Justa
	Mag-Hem group	Starra, Sue-Dianne
	K-skarn	Hillside, Candelaria
	Magnetite group	Ernest-Henry, Candelaria, Sossego, Guelb Moghrein, Boss, Dahongshan, Lala
IOCG variants low Cu, Co, As, Bi, Au, Ag, U	Hem-Co-As-Ag-U-Cu	Echo Bay
	Mag-Au-Co-Bi-Cu	NICO, Echo Bay, *Romanet Horst*
Iron Oxide ± Apatite ± REE	Apatite-rich ± REE	Kiruna, Bayan Obo, Pea Ridge, Pilot Knob, *Bafq*, Port Radium, Mag Hill, K2, Kwyjibo
	Apatite-poor	*Cloncurry, Bear, MLYRMB*
Skarn	Skarn, Fe-skarn	Punt Hill, *Bear, Marmoraton, MLYRMB*

Canada

References at slide 50

Deposit spectrum and continuum

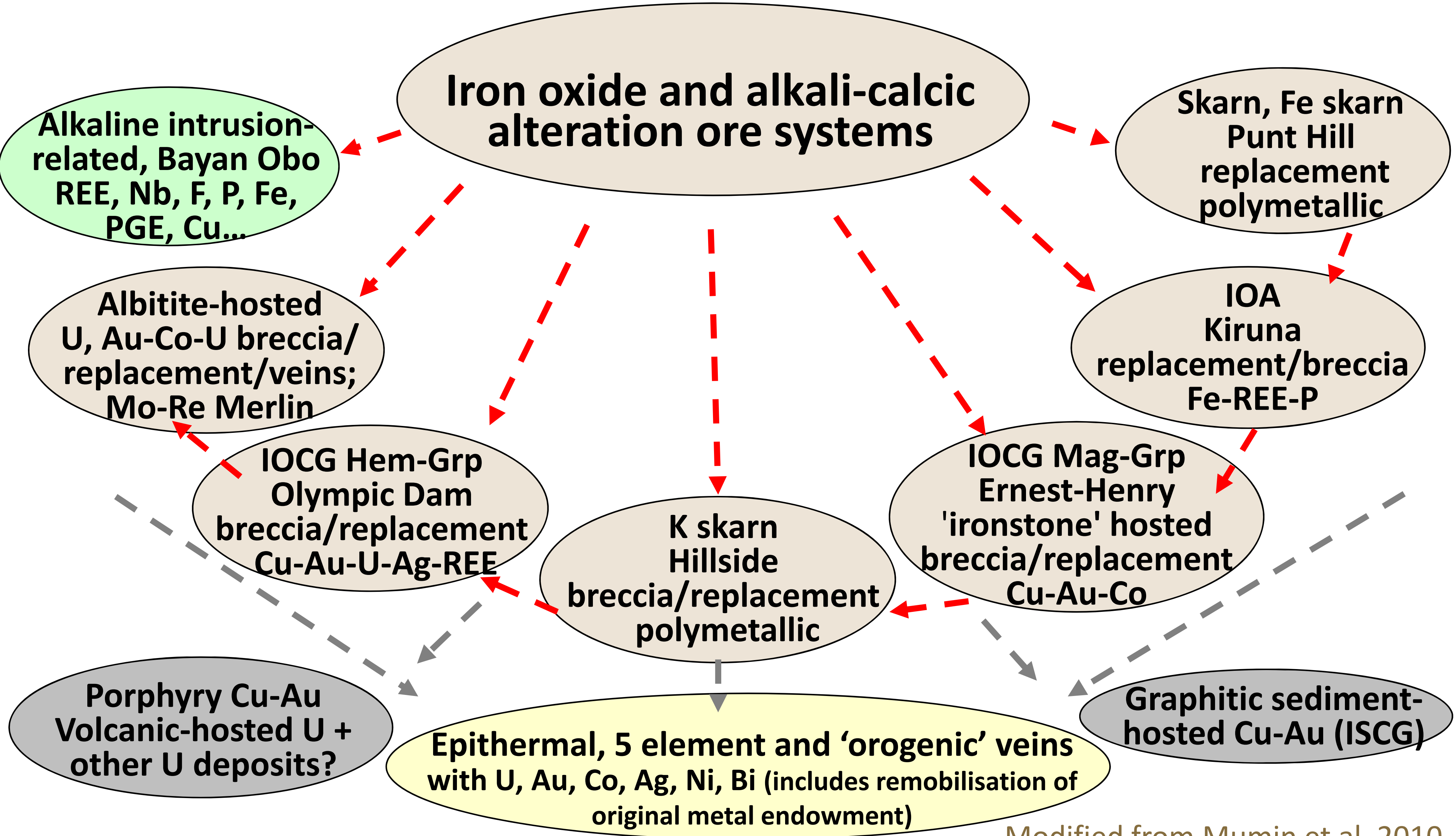

Modified from Mumin et al. 2010

See also Hitzman 2000; Corriveau et al. 2016; Porter 2010a; Day et al. 2016; Tornos et al. 2016, 2017; Zhao et al. 2017a

Metamorphosed continuum: To establish

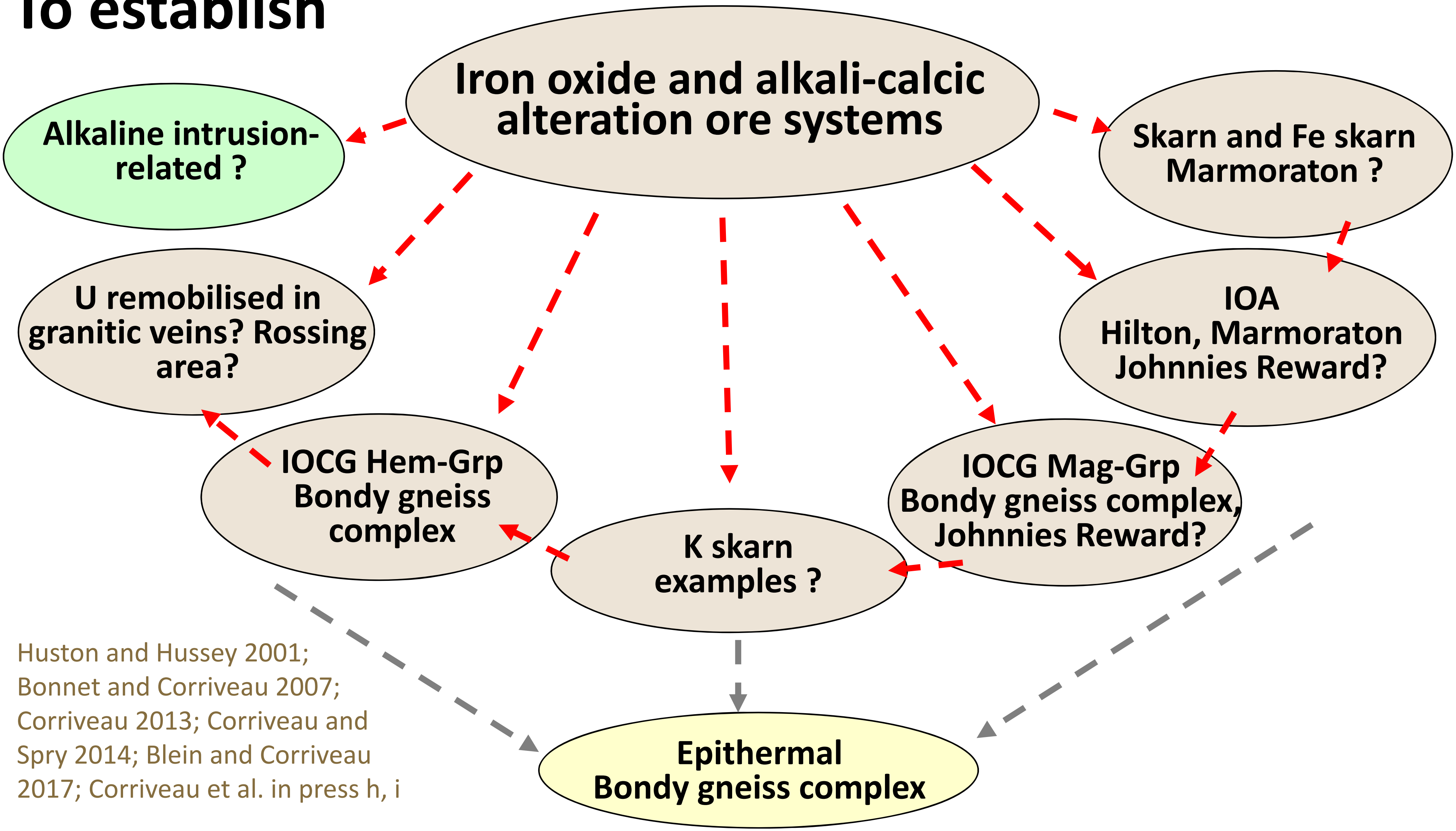

Huston and Hussey 2001; Bonnet and Corriveau 2007; Corriveau 2013; Corriveau and Spry 2014; Blein and Corriveau 2017; Corriveau et al. in press h, i

Resources within IOAA systems: Some examples

- Australia (Olympic Cu-Au Province, Cloncurry and other Mt Isa districts, Tennant Creek and Mt Painter districts)
- Brazil (Carajás)
- Chile and Peru (Central Andes, El Laco)
- Africa
- Asia
- Scandinavia
- Canada, US, Mexico

* Total resources listed unless indicated otherwise

Australia (discovery date, district)

Olympic Dam (1975, Olympic Cu-Au)
10,400 Mt at 0.77% Cu, 250ppm U_3O_8, 0.30g/t Au, 1.0g/t Ag (+ ~0.3% LREE, 0.01% HREE)

Prominent Hill (2001, Olympic Cu-Au)
178 Mt at 1.1% Cu, 0.7g/t Au, 2.7g/t Ag, 103ppm U

Carrapateena (2005, Olympic Cu-Au)
134 Mt at 1.5% Cu, 0.6g/t Au, 6.3g/t Ag (+U)

Hillside (2009, Olympic Cu-Au)
337 Mt at 0.6% Cu, 0.14g/t Au, 15.7% Fe

Khamsin (2012, Olympic Cu-Au)
202 Mt at 0.6% Cu, 0.1 g/t Au, 1.7 g/t Ag, 86ppm U

Oak Dam (1976, Olympic Cu-Au)
~560 Mt at 41–56% Fe, 0.2%Cu, 690ppm U

Rover 1 (Tennant Creek)
6.8 Mt at 1.73g/t Au, 1.20% Cu, 0.14% Bi, 0.06% Co

Peko (Tennant Creek) production
3 Mt at 4.1% Cu, 0.3% Bi, 3.5g/t Au, 14g/t Ag

Mt Gee (Mt Painter)
51 Mt at 0.11% Cu, 525ppm U

Ernest Henry (1990, Cloncurry)
167 Mt at 1.1% Cu, 0.5g/t Au (+ Co)

Mt Dore (Cloncurry)
111 Mt at 0.53% Cu, 0.09g/t Au, 0.06% Pb 0.31% Zn

Mt Elliot-Swan (1880-2013, Cloncurry)
353.7 Mt at 0.6%Cu, 0.35g/t Au

Merlin (2008, Cloncurry)
6.4 Mt at 1.5% Mo, 26 g/t Re (reserves)

Rocklands (2006, Cloncurry)
55.4 Mt at 0.64% Cu, 290ppm Co, 0.15ppm Au, 5.1% Mag + **227 Mt** at 16% Mag

Osborne (Cloncurry)
12 Mt at 1.4% Cu, 0.88g/t Au

Monakoff (Cloncurry)
2.4 Mt at 0.95% Cu, 0.3g/t Au (112ppm U_3O_8)

E1 (Cloncurry)
10 Mt at 0.7% Cu, 0.22g/t Au

Valhalla (Mt Isa)
34.7 Mt at 830ppm U_3O_8

Mary Kathleen, Elaine 1, Elaine-Dorothy
9.5 Mt at 1300ppm U_3O_8
0.83 Mt at 280ppm U_3O_8, 3200ppm TREE
26.1Mt at 0.56% Cu, 0.09g/t Au

See slide 50

Carajás district, Brazil

Salobo
789 Mt at 0.96% Cu, 0.52g/t Au, 55g/t Ag (+ 16-26ppm U)

Cristalino
500 Mt at 1.0% Cu, 0.3g/t Au

Igarapé Bahia/Alemão
219 Mt at 1.4% Cu, 0.86g/t Au + U, REE

Sossego
245 Mt at 1.1% Cu and 0.28g/t Au

Alemao
161 Mt at 1.3% Cu, 0.86g/t Au + U, REE

Gameleira
100 Mt at 0.7% Cu

Pedra Branca
2.4 Mt at 0.94% Cu, 0.27g/t Au

Alvo 118
170 Mt at 1.0% Cu, 0.3g/t Au

Andes, Chile, Peru

Candelaria and Ojos des Salado
501Mt at 0.54% Cu, 0.13g/t Au, 2.06g/t Ag

Cerro Negro Norte
377 Mt at 32.8% Fe

El Laco
734 Mt at 49.2% Fe

Los Colorados
943 Mt at 34.7% Fe

Mantoverde
400 Mt at 0.52% Cu, 0.11g/t Au

Marcona
~**1940 Mt** at 55.4% Fe, 0.12% Cu

Mina Justa
347 Mt at 0.71% Cu, 0.03g/t Au, 3.83g/t Ag

Romeral
454 Mt at 28.3% Fe

Santo Domingo and Iris
514 Mt at 0.31% Cu, 0.04g/t Au, 25.8% Fe

El Espino
123 Mt at 0.66% Cu, 0.24g/t Au

See slide 50

Africa

Phalaborwa, South Africa
~ 1200 Mt at 0.59 wt.% Cu

Kitumba, Zambia
38.8 Mt at 2.2% Cu, 222 ppm Co, 0.03g/t Au, 0.9g/t Ag, 27 ppm U

Guelb Moghrein (Akjoujt), Mauritania
31.3 Mt at 0.92% Cu, 0.69g/t Au (reserves)

Vergenoed, South Africa
122 Mt fluorine, 42% Fe (+REE)

Asia

Bayan Obo, China (reserves)
57.4 Mt at 6% REE_2O_3 ; **2.2 Mt** at 0.13% Nb_2O_5
1500 Mt at 35% Fe

Dahongshan, China
458.3 Mt at 41% Fe; **1.35 Mt** at 0.78% Cu + (16t Au, 141t Ag, 18,156t Co, 2.1t Pd+Pt)

Lala, China
163 Mt at 14% Fe, 1.02% Cu, 0.02% Mo, 0.17 g/t Au

Luodang, China, 73.5 Mt at 15% Fe, 0.8%Cu, 0.16g/t Au, 1.87g/t Ag, 0.02% Co, 0.02% Mo, 0.14% REE

Yinachang, China, 20 Mt at 41.9-44.5% Fe; **15 Mt** at 0.85-0.97% Cu + REE (~1127ppm)

Washan, MLYRMB, China, ~214 Mt at 50% Fe

Khetri belt, India, 140 Mt at 1.1-1.7% Cu, 0.5g/t Au

Sin Quyen, Vietnam, ~ 50 Mt at 0.9% Cu, 0.4g/t Au

Chador-Malu, Bafq district, Iran, 400 Mt at 55% Fe

Divriği, Turkey, 133.8 Mt at 56% Fe, 0.5% Cu

See slide 50

Scandinavia

Kiirunavaara (Kiruna district, Norrbotten)
682 Mt at 47.5% Fe

Malmberget (Kiruna district, Norrbotten)
271 Mt at 41.8% Fe

Kaunisvaara (Norbotten)
164.9 Mt at 32.7%

Grangesberg (Bergslagen district)
115.2 Mt at 40.2% Fe, 0.78% P (indicated)

Hangaslampi (Kuusamo deposit)
0.4 Mt at 0.06% Co, 5.1g/t Au, ≤260 ppm U

Juomasuo (Kuusamo deposit)
2.3 Mt at 0.13% Co, 4.6g/t Au, ≤260 ppm U

Hannukainen (Pajala district)
187 Mt at 30.0% Fe, 0.18% Cu, 0.11g/t Au

Kaunisvaara (reserves) (Pajala district)
164.9 Mt at 32.7% Fe

USA

Blackbird (Idaho Co belt)
16.8 Mt at 1.04 g/t Au, 0.73% Co, 0.14% Cu

Boss (SE Missouri)
40 Mt at 0.83% Cu, 0.035% Co (historic)

Pea Ridge (SE Missouri)
160.6 Mt at ~ 53-55% Fe + 0.2Mt at 12%TREE

Coles Hill (Virginia; indicated resources)
119 Mt at 0.056% U_3O_8

Mexico

Peña Colorada
300 Mt at 50-60% Fe

See reference list in slide 50

Canada

Great Bear magmatic zone (NWT)

NICO (reserves)
33 Mt at 1.02g/t Au, 0.12% Co, 0.14% Bi, 0.04% Cu

Sue Dianne
8.4 Mt at 0.80% Cu, 0.07 g/t Au, 3.2g/t Ag

Central Mineral Belt (Labrador)

Michelin
37.5 Mt at 0.10 % U_3O_8

Upper C, Moran Lake
6.92 Mt at 0.29 % U (indicated) +
2.84 Mt at 0.20% U (inferred)

Grenville Province

Marmoraton (Ontario)
28 Mt at 42% Fe

Kwyjibo (Quebec)
HREE

See slide 50

Distribution
Ages
Geodynamic settings

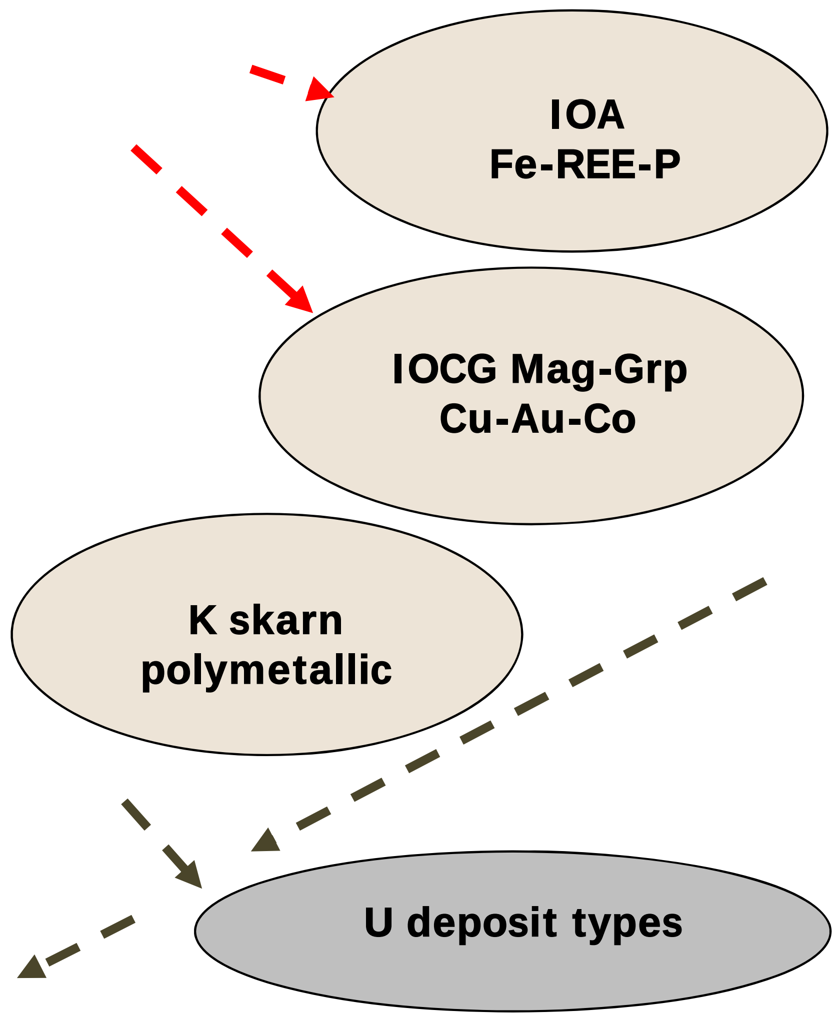

Distribution

Continental geodynamic settings (magmatic arcs, inverted back-arc, rifts)
Precambrian geodynamic settings remain uncertain or controversial

References at slide 50

Modified from Corriveau 2007; Porter 2010a

Celebrating 175 yrs

Canadian deposits and areas of interest

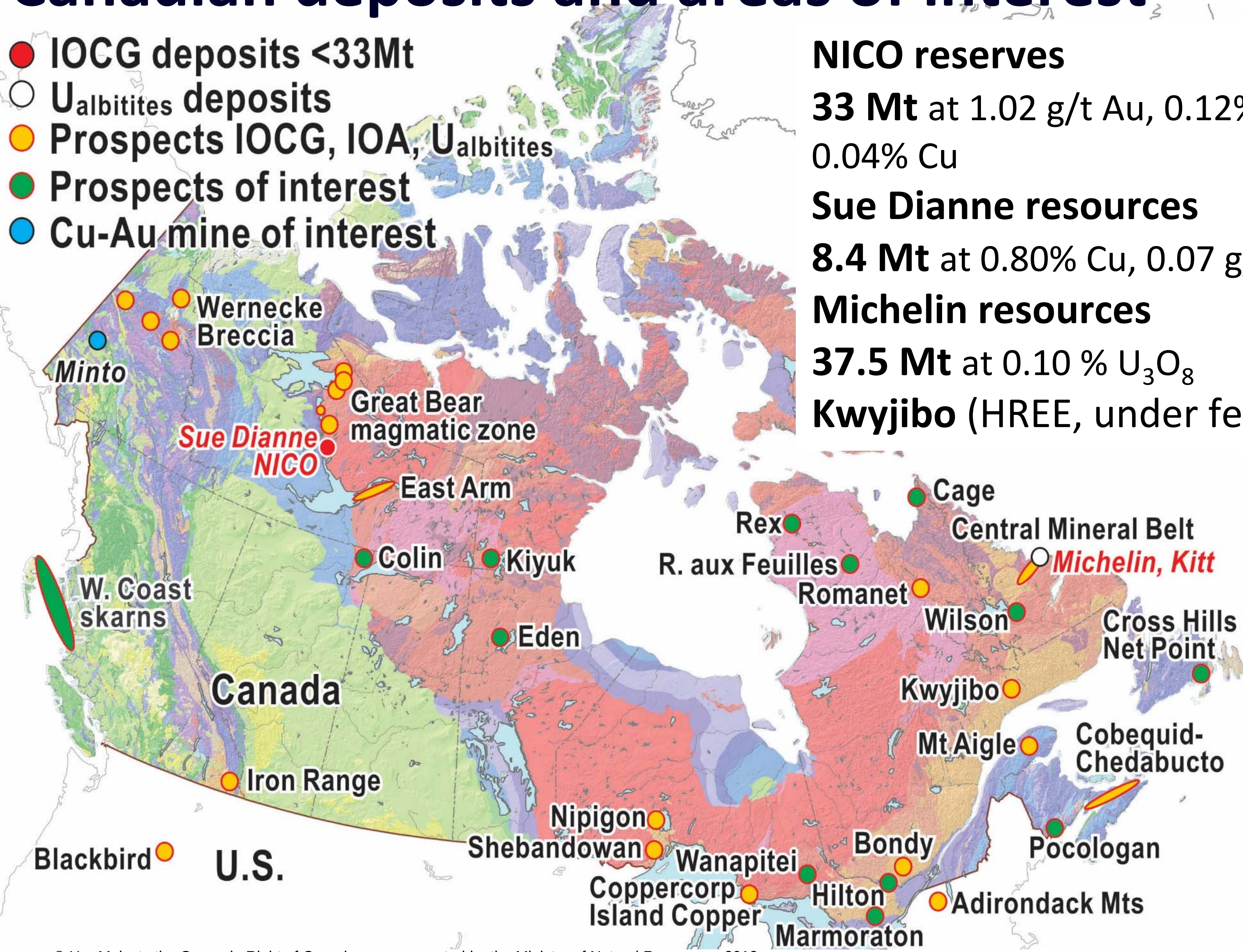

NICO reserves

33 Mt at 1.02 g/t Au, 0.12% Co, 0.14% Bi, 0.04% Cu

Sue Dianne resources

8.4 Mt at 0.80% Cu, 0.07 g/t Au, 3.2g/t Ag

Michelin resources

37.5 Mt at 0.10 % U_3O_8

Kwyjibo (HREE, under feasibility study)

References at slide 50

Celebrating 175 yrs

References for location, deposit types and resources of deposits

Jones 1974; N9GBYBGMR 1983 (in Chinese cited by Zhao et al. 2017b); Lyons 1988; Porto da Silveira et al. 1991; Skirrow 2000, 2010; Vanhanen 2001; Wang and Williams 2001; Knight et al. 2002; Oyarzun et al. 2003; Hitzman and Valenta 2005; Williams et al. 2005; Belperio et al. 2007; Benavides et al. 2007; Davidson et al. 2007; Doebrich et al. 2007; Béziat et al. 2008; Hennessey and Puritch 2008; Wu 2008; Polito et al. 2009; Chen et al. 2010; Chinalco 2010, 2012a, b; Clark et al. 2010; Daliran et al. 2010; Groves et al. 2010; Kuşcu et al. 2010; Lobo-Guerrero 2010; Porter 2010a, b; Rieger et al. 2010; Williams 2010a, b; Baker et al. 2011, 2014; Zulinski and Osmani 2011; Corona-Esquivel et al. 2011; Chen and Zhou 2012; Dragon Mining 2012, 2014; Puritch et al. 2012a, b; Sangster et al. 2012; Turner 2012; CAP 2013; Chen 2013; Decrée et al. 2013; First Quantum Minerals 2013; LKAB 2013; Nold et al. 2013, 2014; Oz Minerals 2013, 2014a, b, 2017; Potter et al. 2013; Slack 2013; Barton 2014; Burgess et al. 2014; Capstone Mining Corp 2014; Chinova Resources 2014, 2017; Corriveau et al. 2014; Couture et al. 2014; Desrochers 2014; Duncan et al. 2014; Evans 2014; Intrepid Mines 2014; Ismail et al. 2014; Lopez et al. 2014; Waller et al. 2014; Yılmazer et al. 2014; BHP Billiton 2015; Fan et al. 2015; Graupner et al. 2015; GTK 2015; Li (X.) et al. 2015; Montreuil et al. 2015, 2016a, b, c; Paladin Energy 2015a, b; Perreault and Lafrance 2015; Rex Minerals 2015; Seo et al. 2015; Woolrych et al. 2015; Day et al. 2016; Martinsson et al. 2016; Metal X 2016; Veríssimo et al. 2016; Babo et al. 2017; BHP 2017; Camprubí and González-Partida 2017; Cudeco 2017; Zhao et al. 2017a, b; Zhu et al. 2017

Ages of deposits and districts

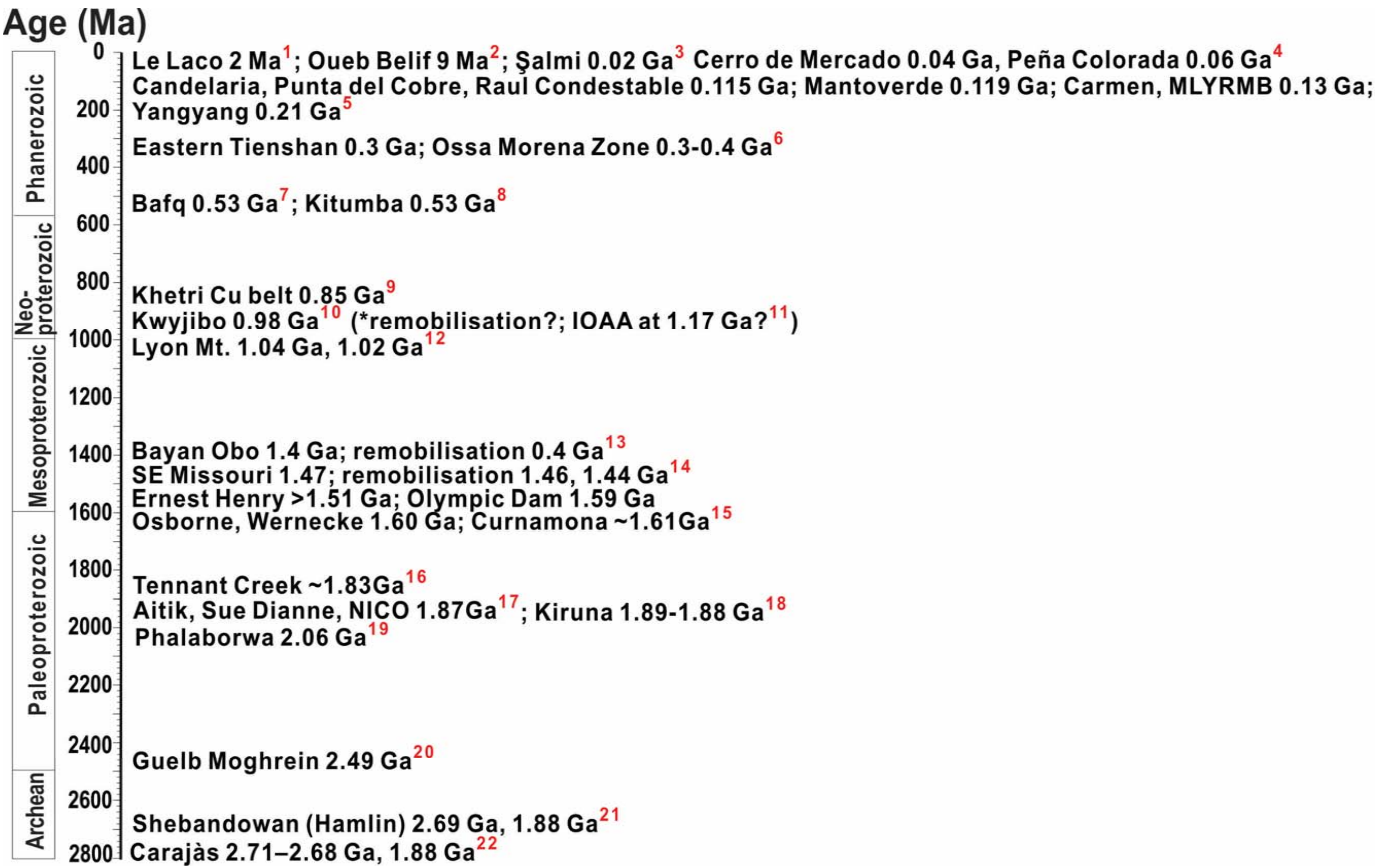

Ages of deposits and districts

1 - Nyström and Henríquez 1994
2 - Decrée et al. 2013
3 - Yılmazer et al. 2014
4 - Corona-Esquivel et al. 2011
5 - Mathur et al. 2002; Sillitoe 2003; Gelcich et al. 2005; Mao et al. 2011; Zhou et al. 2013; Seo et al. 2015
6 - Carriedo and Tornos 2010; Huang et al. 2013
7 - Torab and Lehmann 2007; Stosch et al. 2011
8 - Porter 2010a
9 - Knight et al. 2002
10 - Gauthier et al. 2004; Clark et al. 2005, 2010
11 - Corriveau et al. 2007
12 - Selleck et al. 2004; Valley et al. 2009, 2011
13 - Fan et al. 2014, 2015
14 - Aleinikoff et al. 2016; Neymark et al. 2016; Day et al. 2017
15 - Mark et al. 2000; Williams and Skirrow 2000; Gauthier et al. 2001; Thorkelson et al. 2001
16 - Skirrow 2000
17 - Gandhi et al. 2001; Wanhainen et al. 2003; Montreuil et al. 2016a
18 - Romer et al. 1994
19 - Reischmann 1995
20 - Kolb et al. 2010
21 - Tallarico et al. 2004; Moreto et al. 2015
22 - Forslund 2012

Ore system main characteristics

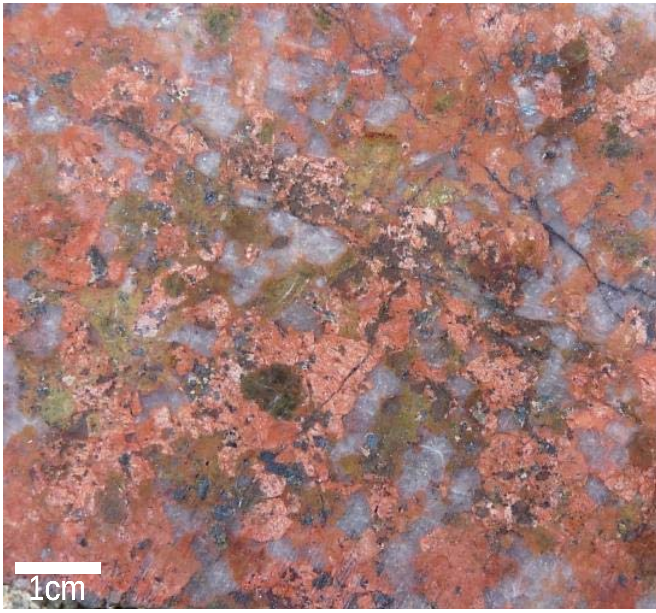

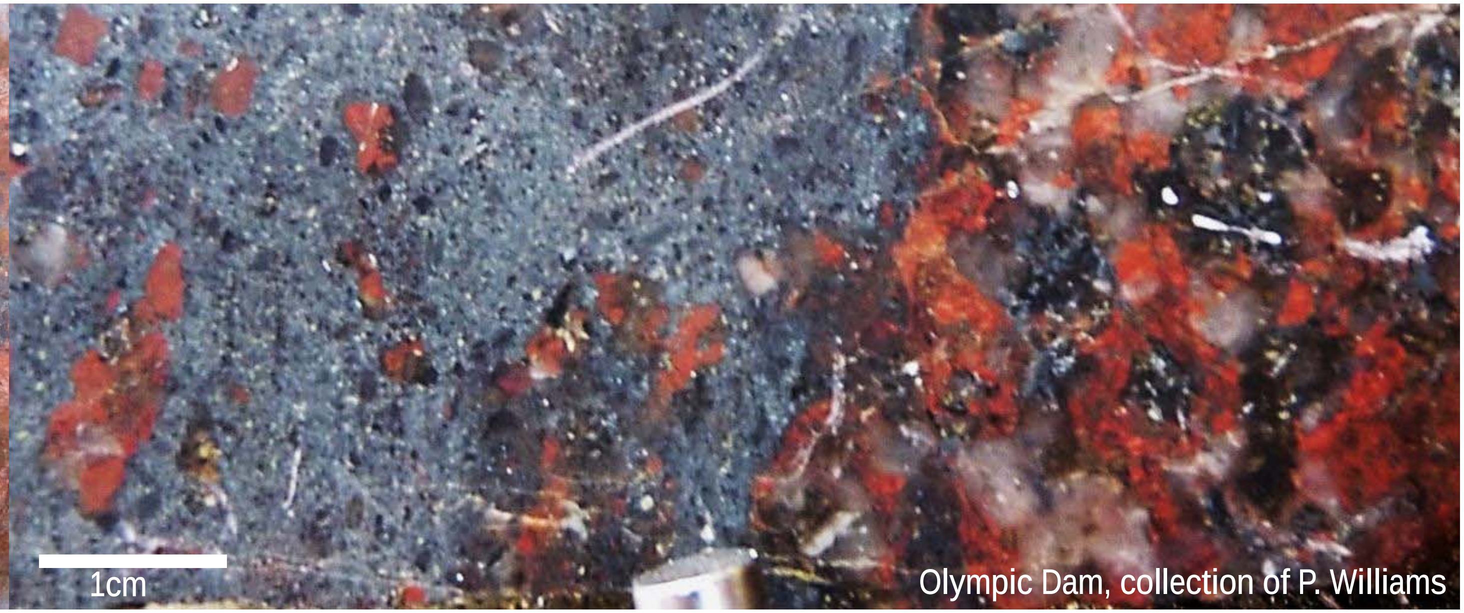

Metasomatic and structural controls lead to breccias, veins and replacement zones

Strong links to large-scale magmatism ultimately evolving to A-type magmas

No single causative intrusion (cf. porphyry deposits) but intrusions can serve as nuclei for regional-scale systems and be proximal

Local to lithosphere-scale faults and discontinuities serve as preferential pathways for fluids and magmas

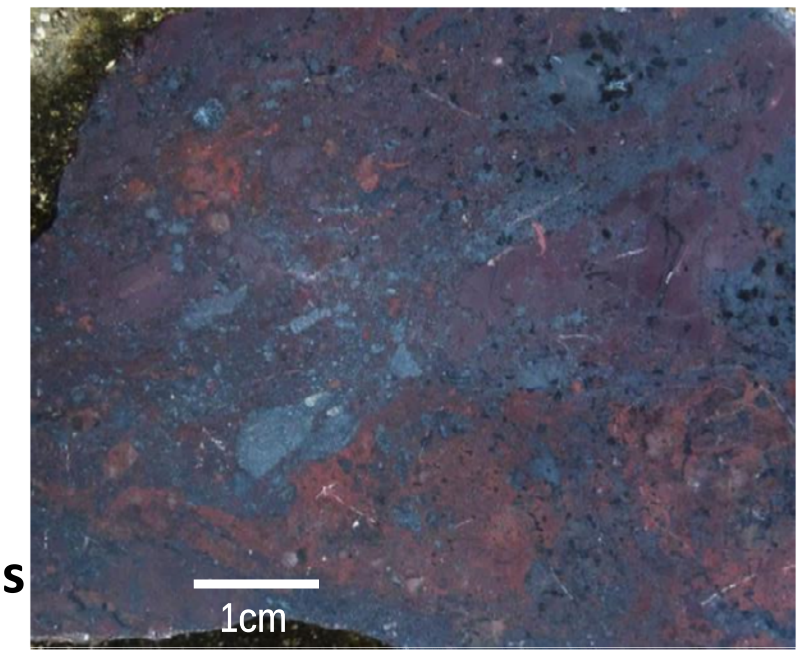

Ore system footprints

- Metasomatic in origin
- Intense Na, skarn, HT Ca-Fe, HT–LT K-Fe, K, K-skarn and LT Ca-Fe-Mg alteration
- Hydrothermal cells coalesce across ≤ 35 x 15 x 10 km (length-width-depth)
- Deposits clusters into districts 30 to 50 km apart that line up along metallogenic provinces 200 to 1500 km long
- High geothermal gradients (800-150°C) most commonly induced by magma chambers at high temperatures
- In tectonically active settings

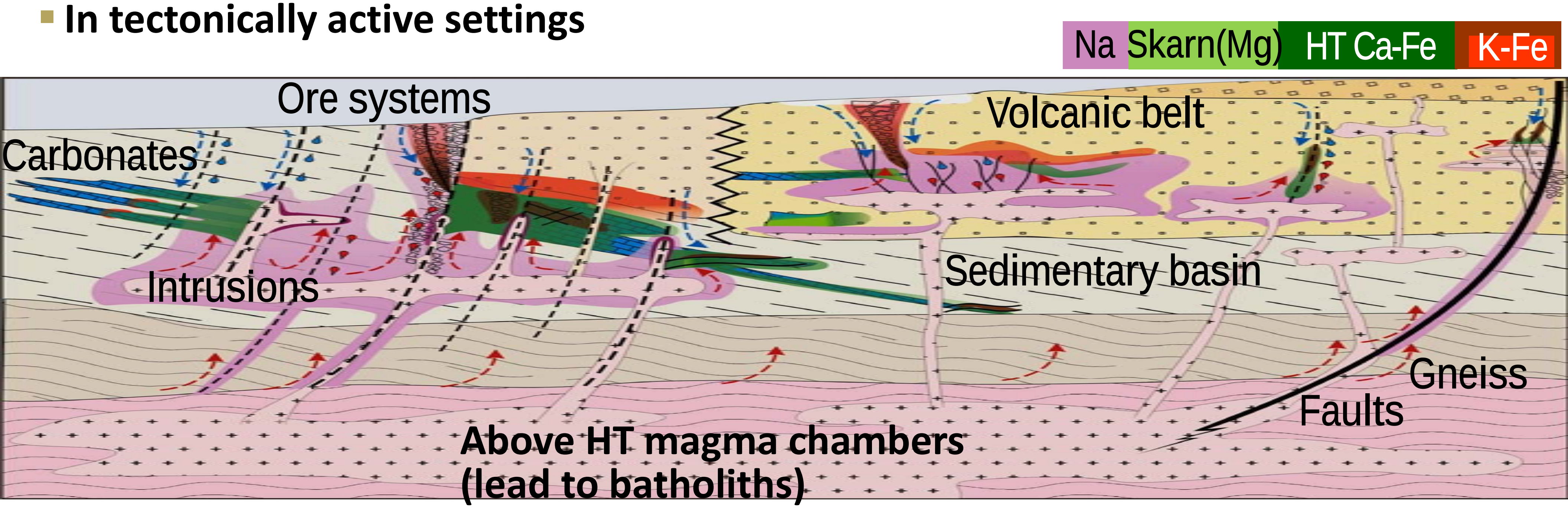

Mafic magmas as heat sources

Geodynamic settings: continental!

- Continental intra-arc to back-arc, basin inversion, collisional and intracontinental rift settings that can acquire a very high geothermal gradient including through ponding of mafic magmas at the base of the crust
- Many districts at the margin of Archean cratons (successor contienental arcs adjacent to an Archean craton appear particularly fertile)
- Above major discontinuities extending from the mantle to the upper crust
- Large-scale/domain-bounding extensional structures proximal or distal to, but active during magmatism; extension can occur in an overall compressional settings
- In oxidised volcanic and plutonic environments and along pre-existing ironstones, unconformities, permeable/reactive units, and faults zones
- At the local scale, system will developed over any host rocks

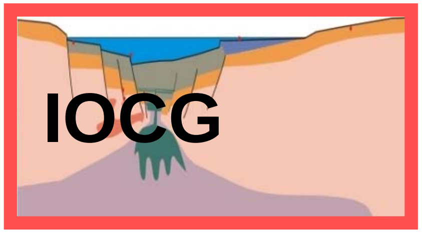

Hitzman et al. 1992; Hitzman 2000; Williams et al. 2005; Skirrow 2010; Groves et al. 2010; Porter 2010a, b; Chen et al. 2013; Richards et al. 2017

Celebrating 175 yrs

Lithosphere architecture
Mantle to surface discontinuities

Ore systems (NICO, Sue Dianne)
Extensive albitite corridors
Lamprophyre (Echo Bay)
Extensive and intense metasomatism

Minor to no metasomatism

Wopmay fault: vertical, abuts against Slave cratonic root
Extensive albitite corridors
Local IOA mineralisation

Under sedimentary cover; non explored (see anomalies in Hayward et al. 2013)

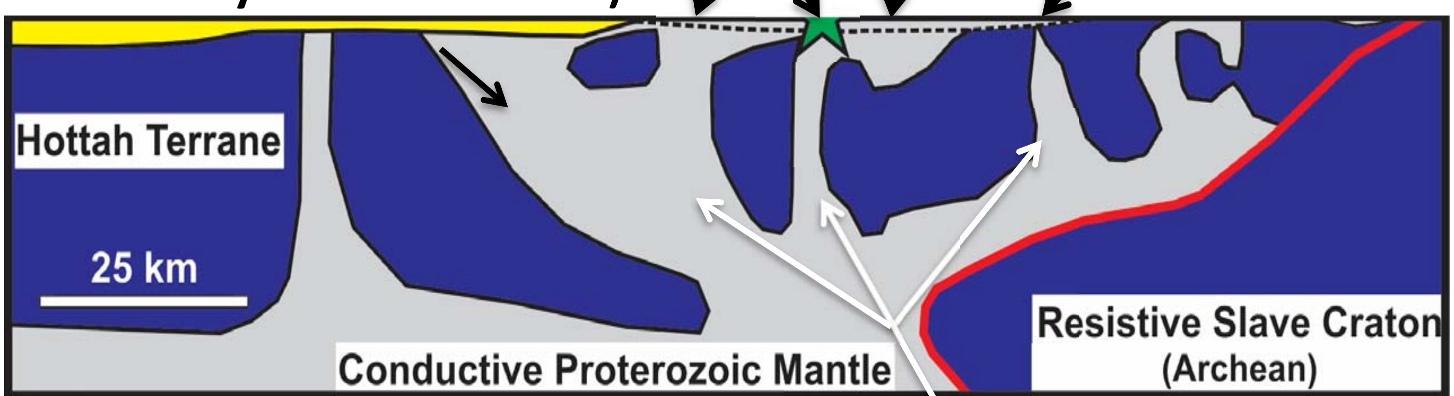

Trans lithosphere discontinuities

See magnetotelluric image in Spratt et al. 2009

Legend

- Conductive zone
- Resistive zone
- Sedimentary platform
- -------- GBMZ approximate boundary

In large igneous felsic province

- **Large volumes of plutonic and volcanic rocks, calc-alkaline to shoshonitic, intermediate to felsic, I to A types, oxidised, HT; mafic magmas ponding at the base of crust but minor volume towards surface**
- **Andesite commonly associated with IOA deposits; within IOCG deposits, andesite can be present but are commonly K-altered and interpreted as rhyolite**
- **Batholiths can form coevally or subsequently to metasomatic ore systems**
- **Melting of metasomatised sub-continental lithosphere**

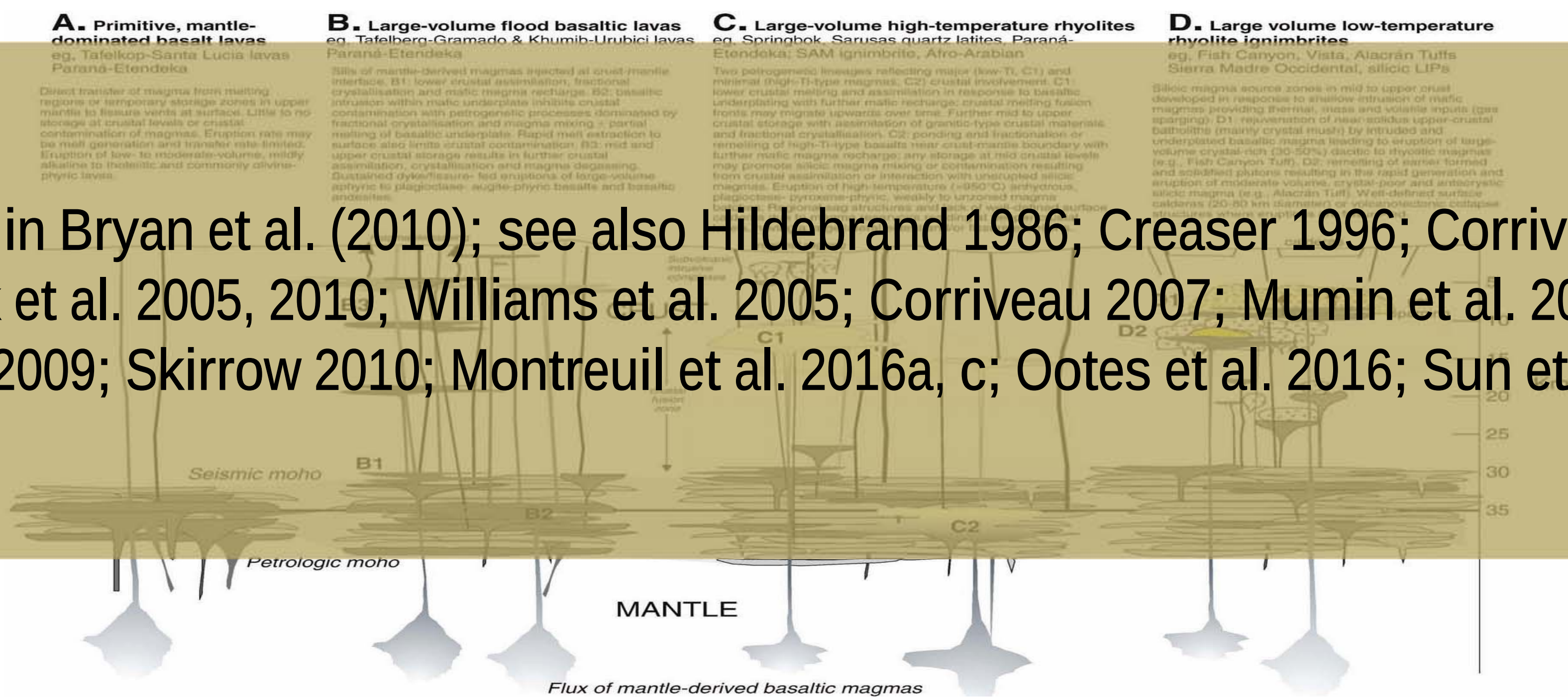

See figure in Bryan et al. (2010); see also Hildebrand 1986; Creaser 1996; Corriveau et al. 2007; Clark et al. 2005, 2010; Williams et al. 2005; Corriveau 2007; Mumin et al. 2007, 2010; Lafrance 2009; Skirrow 2010; Montreuil et al. 2016a, c; Ootes et al. 2016; Sun et al. 2017

Coeval emplacement of mafic or alkaline magmas

A clue to a mantle connection and extraneous heat and metal sources

Celebrating 175 yrs

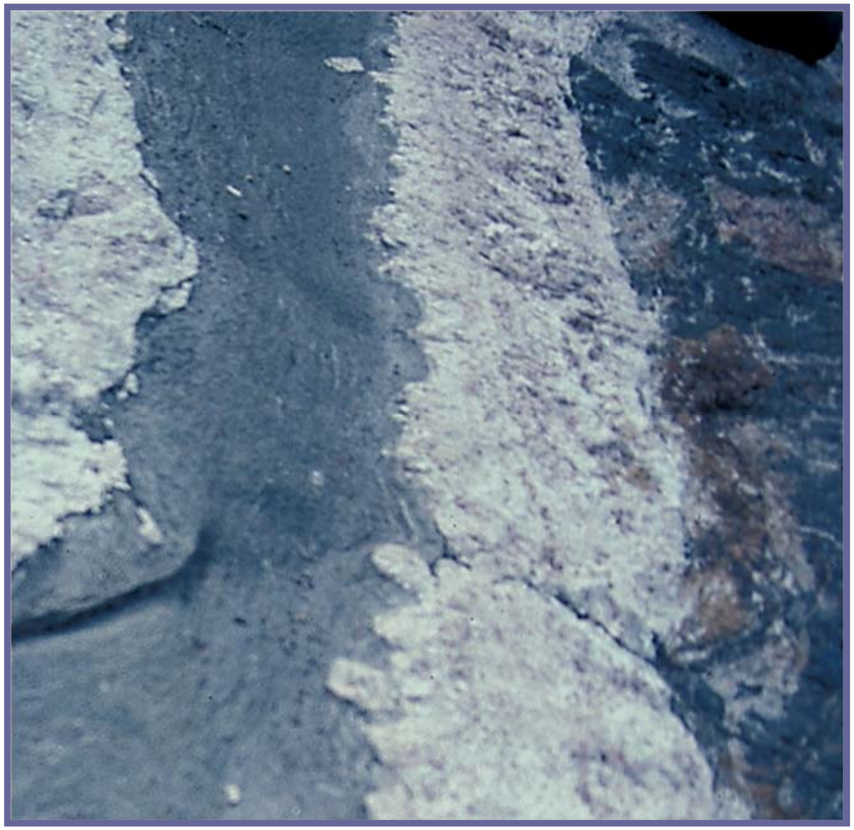

Mafic-felsic dyke typical of 1.16 Ga magmatism cutting a magnetite breccia within a 1.16 Ga granitoid at Kwyjibo (Quebec)

Carbonatites, syenites and fenites, Eden Lake (Manitoba)

Creaser 1996; Mumin and Corriveau 2004; Corriveau et al. 2007; Clark et al. 2005, 2010

Precambrian settings

The types of continental settings commonly remain uncertain in Precambrian terranes. For examples many conflicting models exist for Olympic Dam region:

Anorogenic rift (Allen and McPhie 2002)

Subduction-related continental back-arc (Betts and Giles 2006; Wade et al. 2006; Kositcin 2010)

Subduction evolving towards a mantle plume (Betts et al. 2009)

Lithospheric delamination (Creaser 1996; Skirrow 2010)

Mantle plume + fusion of sub-continental lithospheric mantle (Groves et al. 2010; Thiel and Heinson 2013)

Post-collisional setting (Verbaas et al. 2018)

Geological footprints of metasomatism: Alteration facies and metal associations

Natural Resources Canada
Ressources naturelles Canada
Canada

Iron oxide and alkali-calcic alteration ore systems

IOA, IOCG and affiliated deposits form as a consequence of

- a regular series of fluid-rock reactions triggered by high salinity fluids
- across high geothermal gradients
- in tectonically active settings

Metasomatic footprints include

- Regional-scale albitite corridors along fault zones and above sub-volcanic intrusions, many extensively brecciated, replaced by fertile alteration and mineralised
- Regional to deposit-scale, stratabound, HT Ca-Fe and HT Ca-K-Fe alteration facies
- Deposit-scale breccias with HT to LT K-Fe, K, K-skarn and LT Ca-Fe-Mg facies

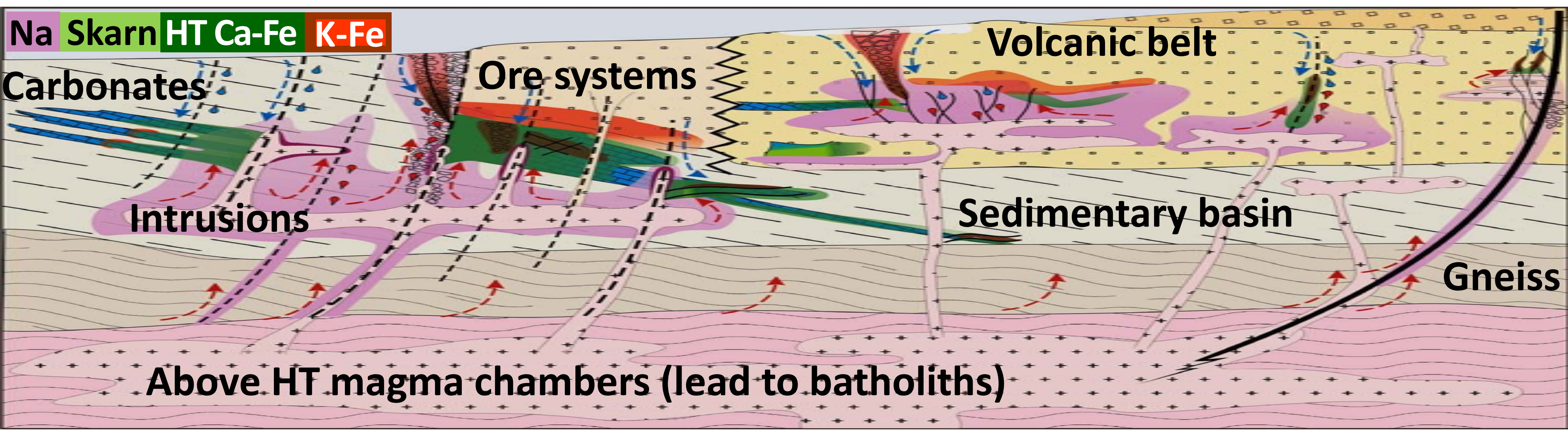

Mafic magmas as heat sources

Alteration attributes

Replace any host rocks, at any stratigraphic levels and among units of different ages

Within a single system, mineralisation can be hosted in volcanic, sedimentary, intrusive and metamorphic rocks

Parageneses and whole-rock composition largely independent of protolith where alteration is intense

Mineralisation in or close to fertile K-Fe alteration

Regional progradation of alteration, brecciation and mineralisation + local telescoping, permutation, cycling of alteration types: serve as predictive mapping and exploration tool, and vectors to ore

Rock physical properties are distinct for each alteration facies where replacement is intense and pervasive but can overlap where alteration is less intense or polyphase

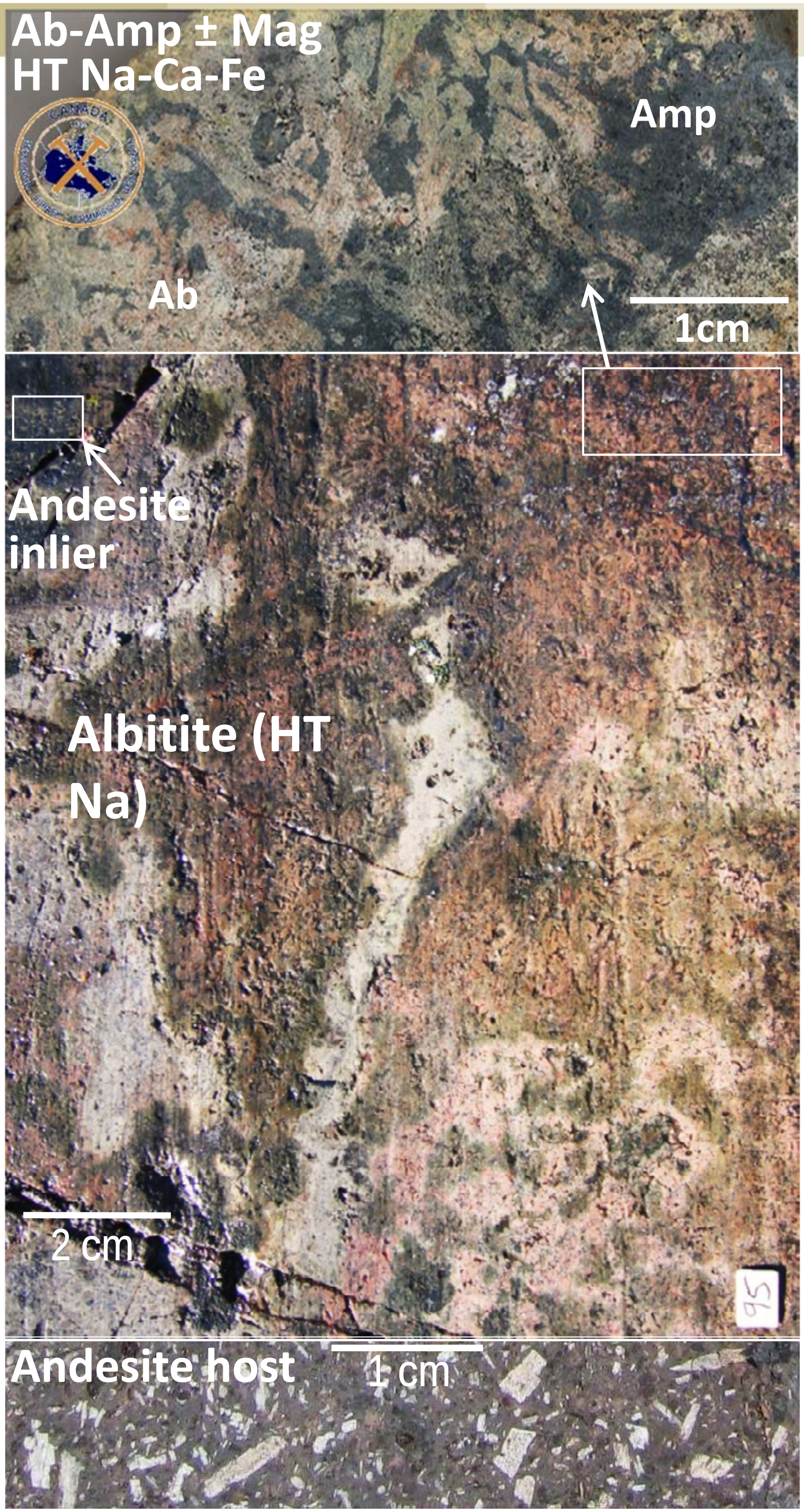

Corriveau et al. 2010a, b, 2016, 2017; Enkin et al. 2016

Selective metasomatism: protolith texture preserved

(*making it difficult to fully appreciate epigenetic origin of alteration*)

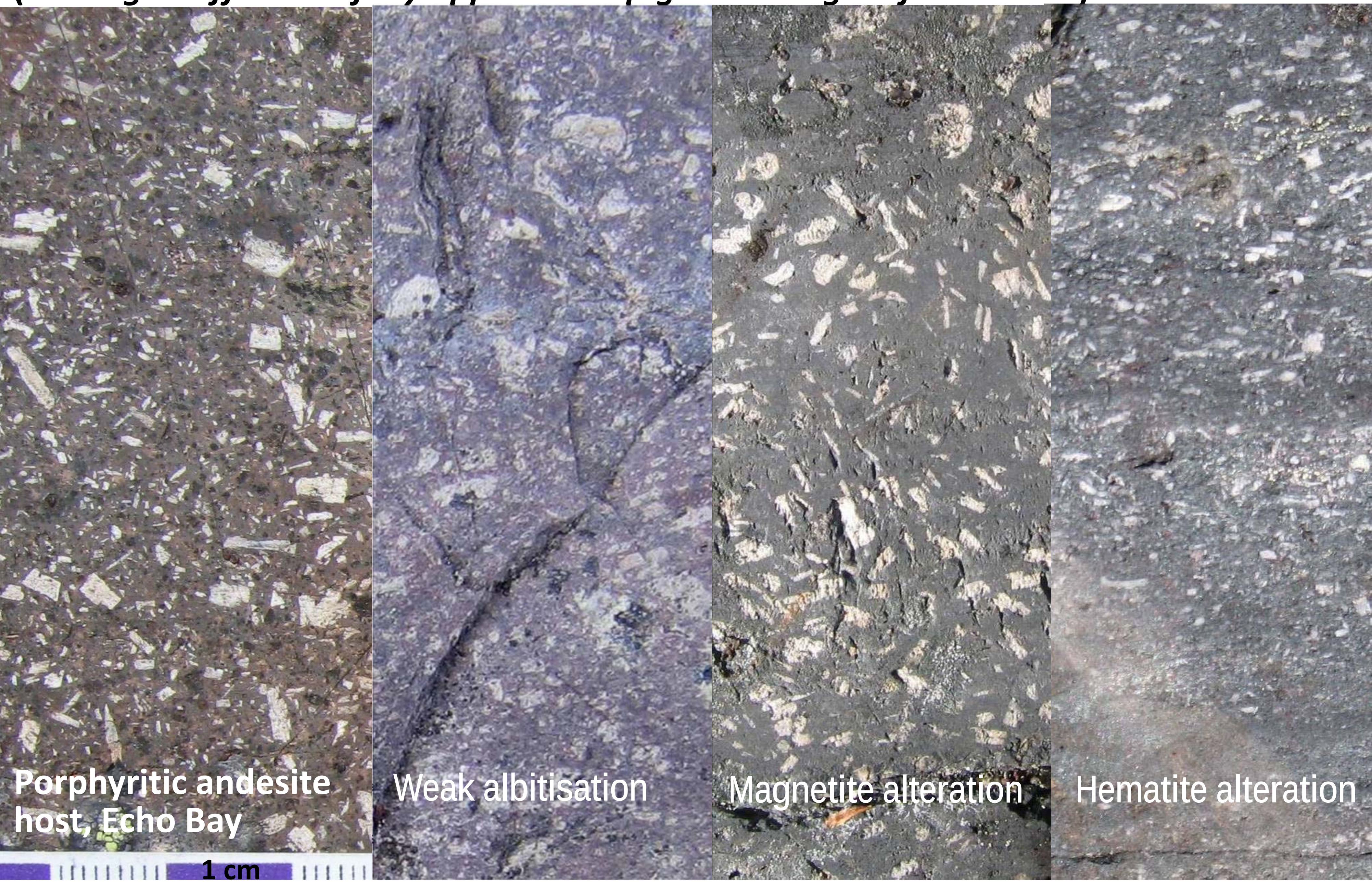

Metasomatism—Pervasive! (Globally independent of protoliths)

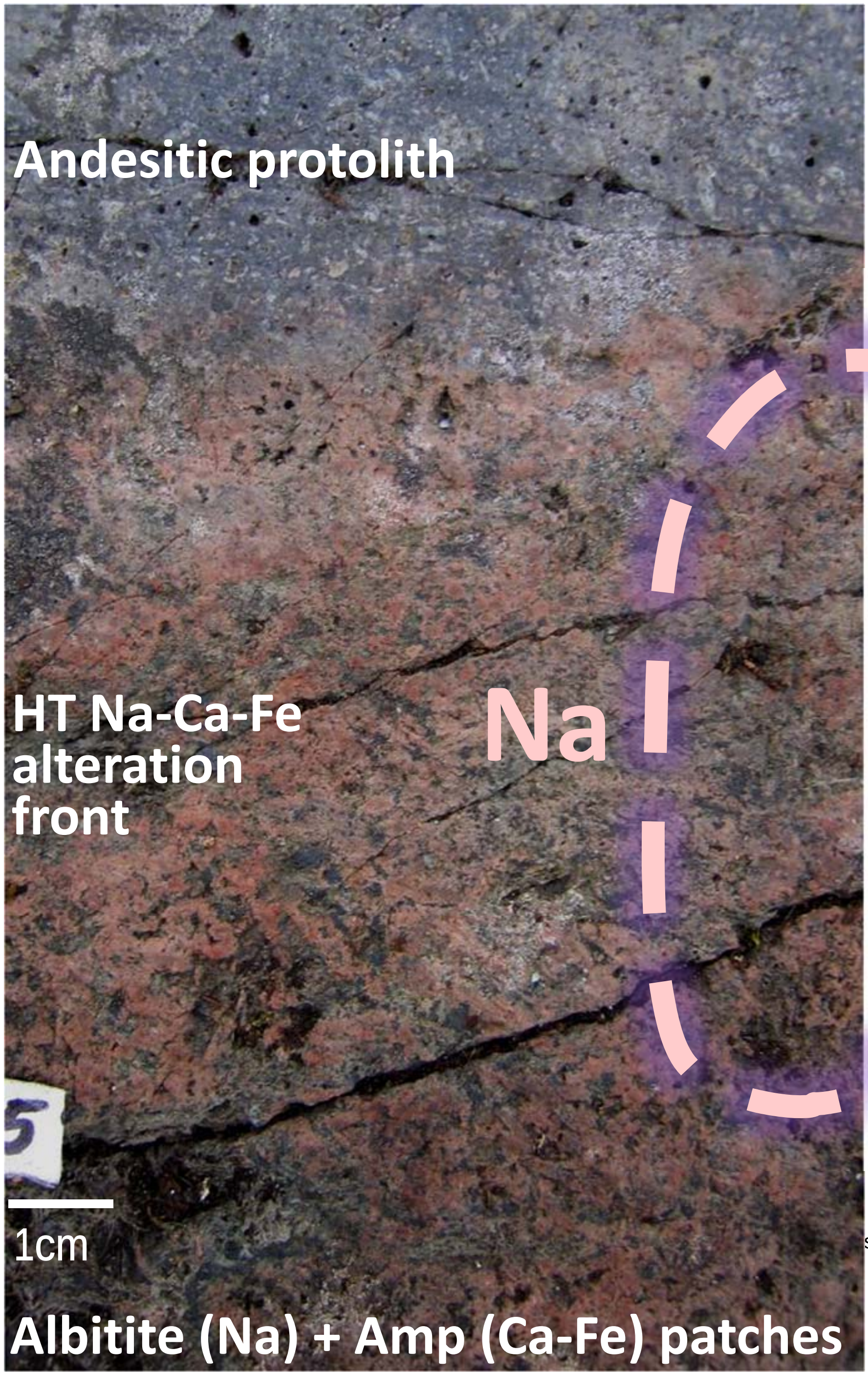

Significant grain coarsening at high temperature

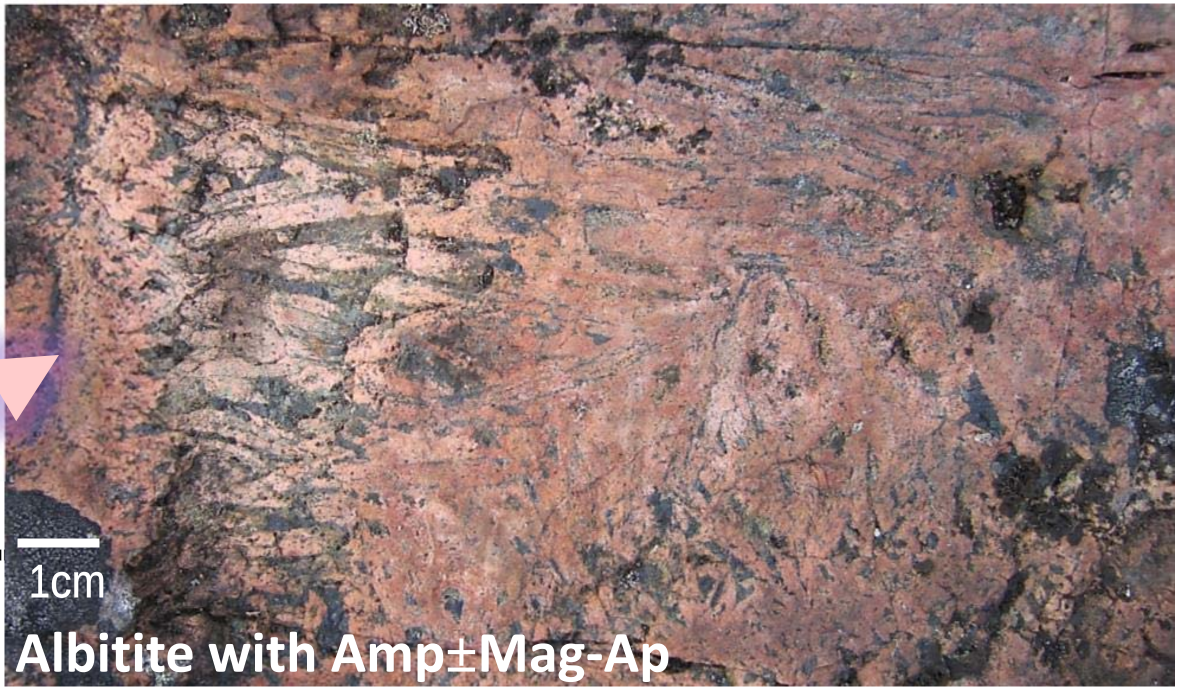

K-Fe metasomatism induces brecciation

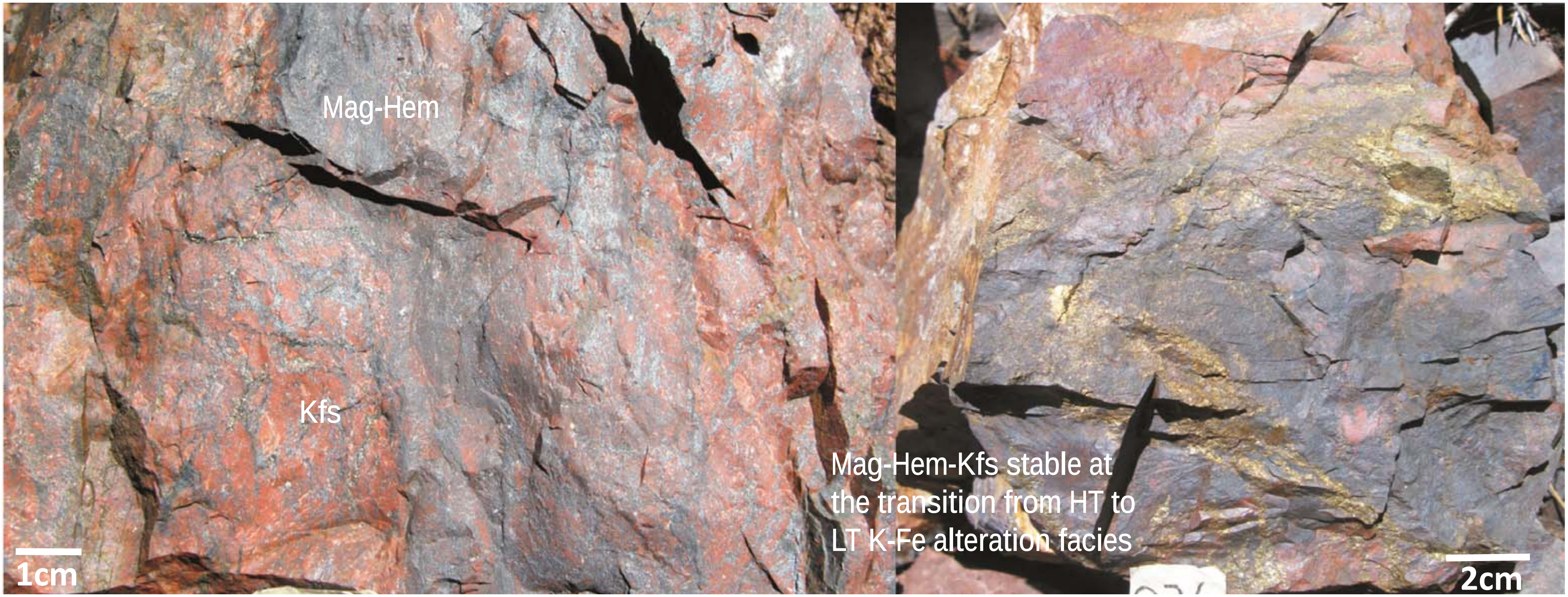

Intense Kfs replacement of fragments, brecciation and Cu-sulphides mineralisation

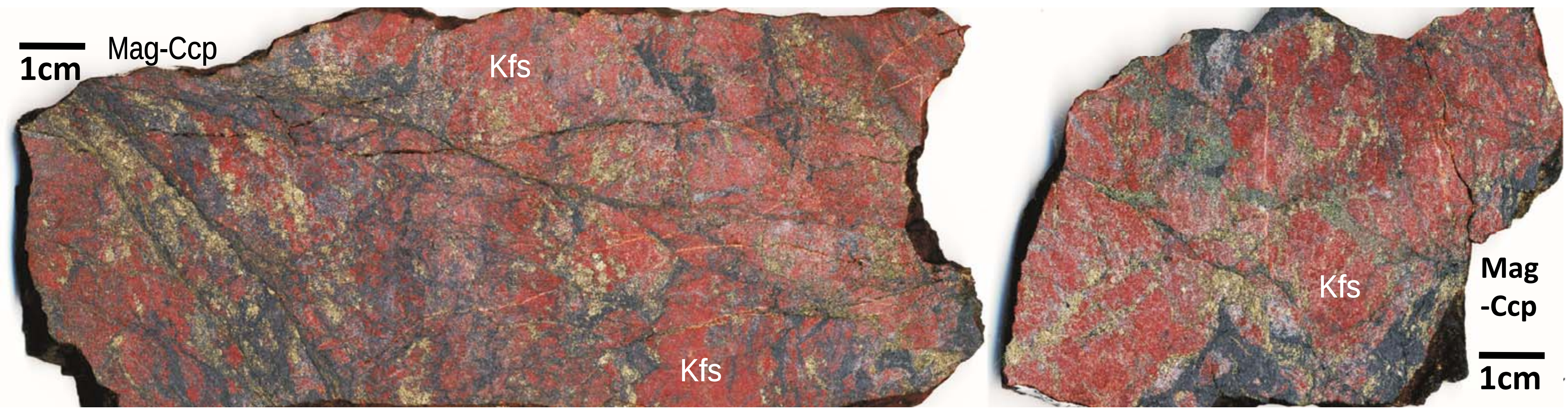

Alteration footprints

- **A great array of mineral assemblages**, grain size, textures, intensity of alteration, density of vein networks and types of breccias across ≤35 x 15 x15 km^3 (length, width, depth)
- Mapping and interpretation of systems complex without appropriate tools

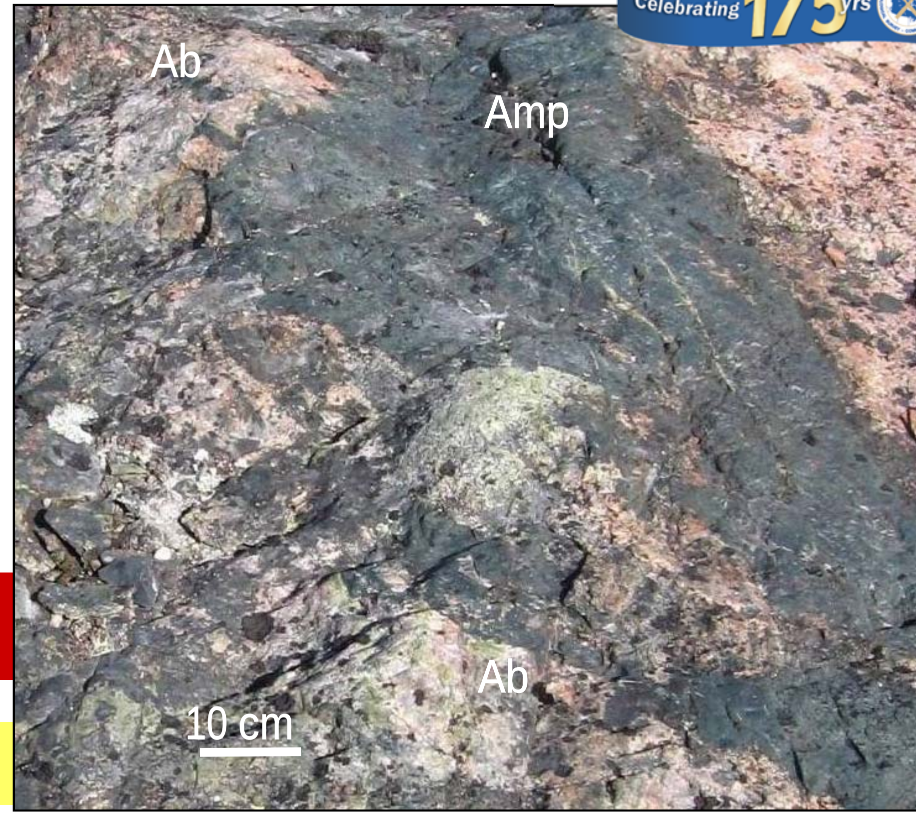

Kfs -Mag
Ab -Amp-Mag -Ap
Kfs -Bt -Mag
Amp -Mag -Bt
Chl-Hem-Kfs-Cb-Ser
Chl-Cb-Hem
Chlorite
Qz vein
Cpx - Kfs
Silicification
Ab - Amp
Kfs
Propyllitic
Cpx-Grt-Kfs
Hem
Ab -Amp-Ap
Chl -Hem
Amp-Mag -Bt -Kfs
Ep -Mag
Ser-Hem
Kfs -Hem
Tourmaline
Amp -Mag
Cpx
Amp
Ab -Amp-Mag
Bt
Ab
Ep -Hem - Qz -Cb
Cpx - Amp-Mag
Jasper
Mag
Acid
Ser
Ep-Qz -Cb
Phyllic / sericitic
Ep
Amp -Mag -Kfs
Ep -Hem -Qz
Amp-Mag -Ap
Bt -Mag
Ep -Hem
Carbonate
Hem-Kfs-Ser

Hydrothermal alteration zoning

Case example from the Sue Diane deposit, Great Bear

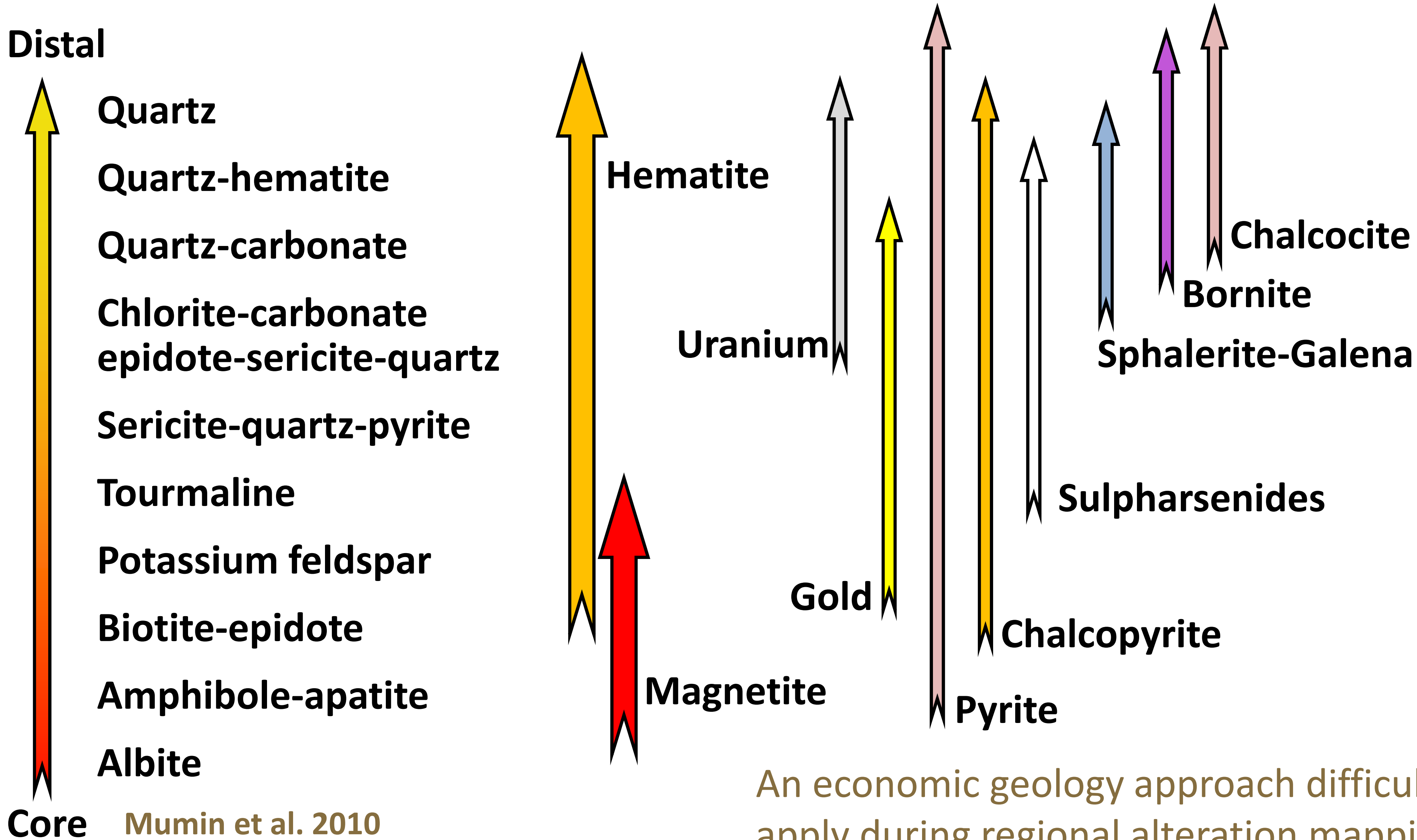

Mumin et al. 2010

An economic geology approach difficult to apply during regional alteration mapping

TGI and GEM geoscience framework

TGI ore deposit models, and exploration and mapping tools

GEM alteration facies maps, and geological and geochemical databases

Efficient for:

- Alteration discrimination, characterisation, mapping, baseline geology information
- Geological and geochemical exploration ; baseline geochemical characterisation
- Mineral potential assessment
- Ore deposit and geo-environmental models

See Part 4 presentation for details on the approach

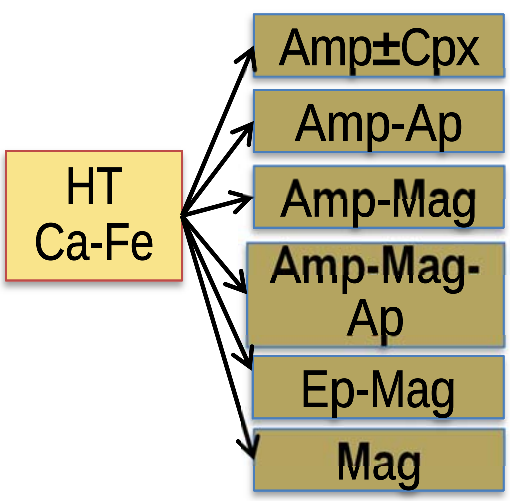

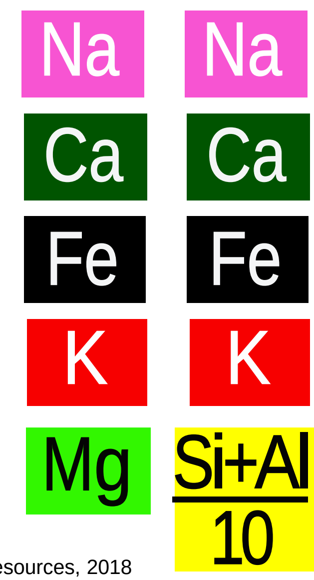

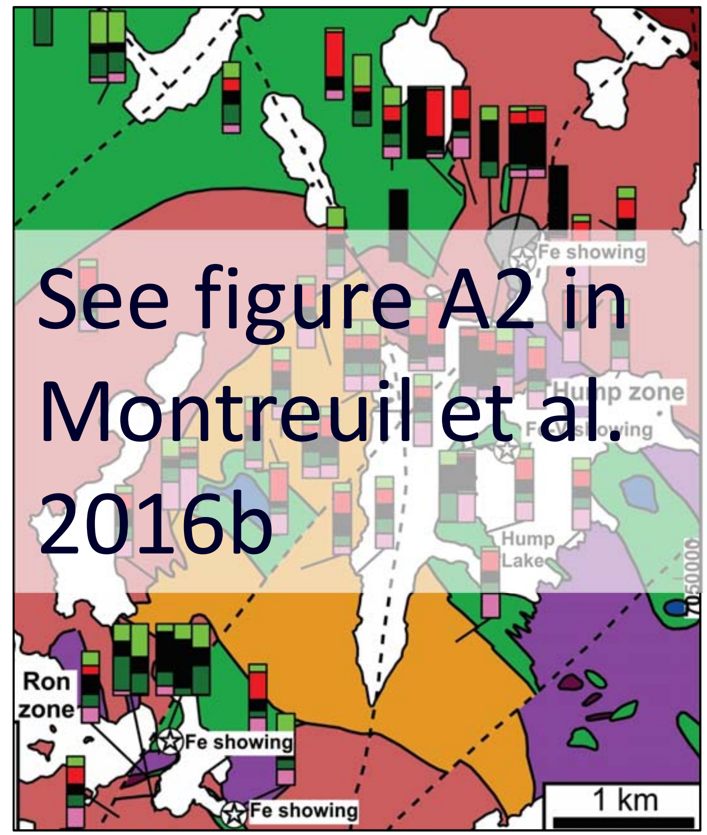

Alteration facies

Regrouping mineral assemblages into alteration facies provides an effective mean to characterise, map and explore iron oxide and alkali-calcic alteration systems
(see Part 4 for definition, classification, nomenclature, mapping protocol, examples)

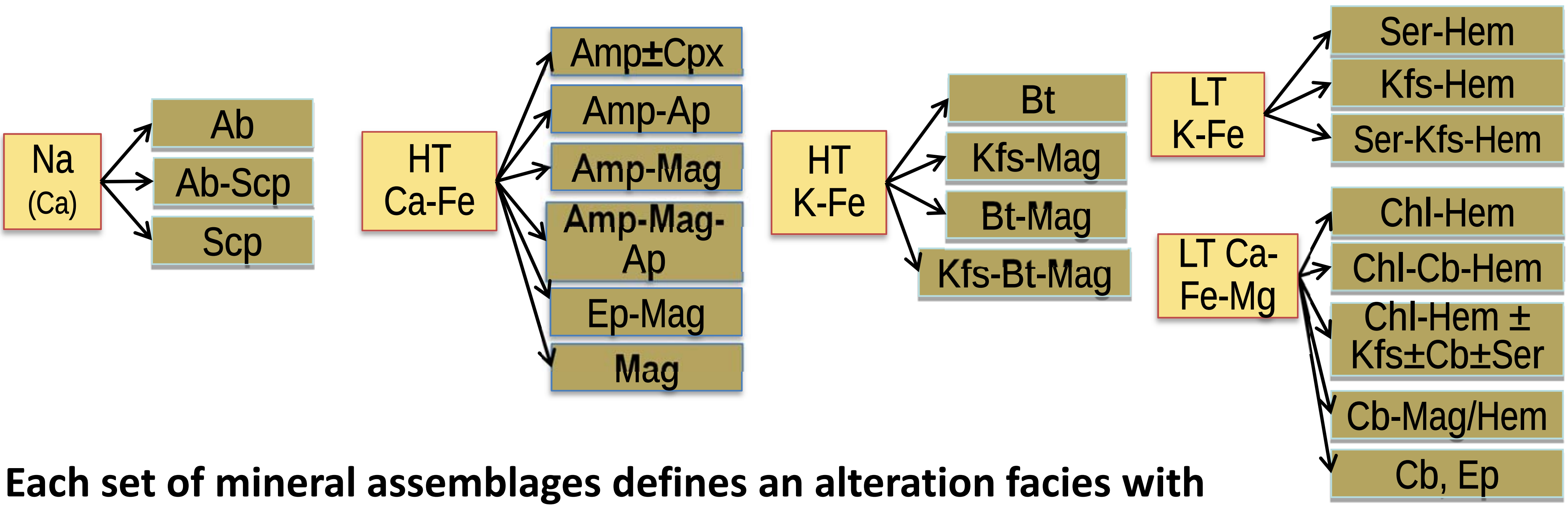

Each set of mineral assemblages defines an alteration facies with its own set of chemical signatures

Corriveau et al. 2010b, 2016, 2017, in prep a-h
Montreuil et al. 2013, 2016a, b, c; De Toni 2016

Prograde metasomatic reactions paths

In siliceous protoliths (including skarns)

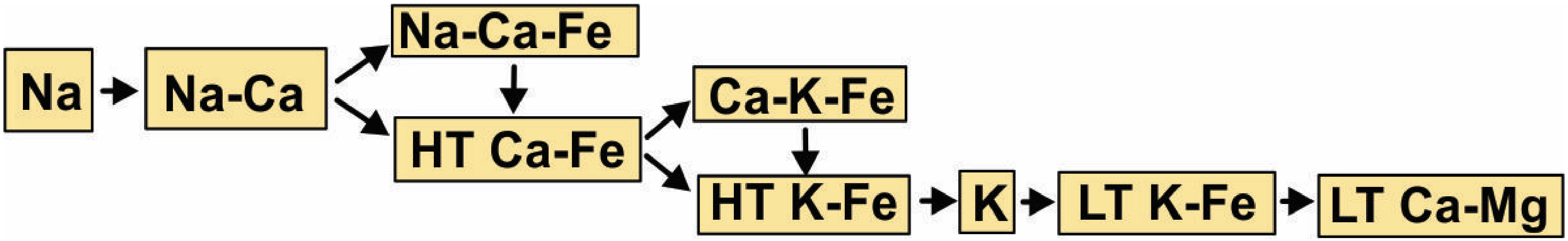

In carbonate protoliths

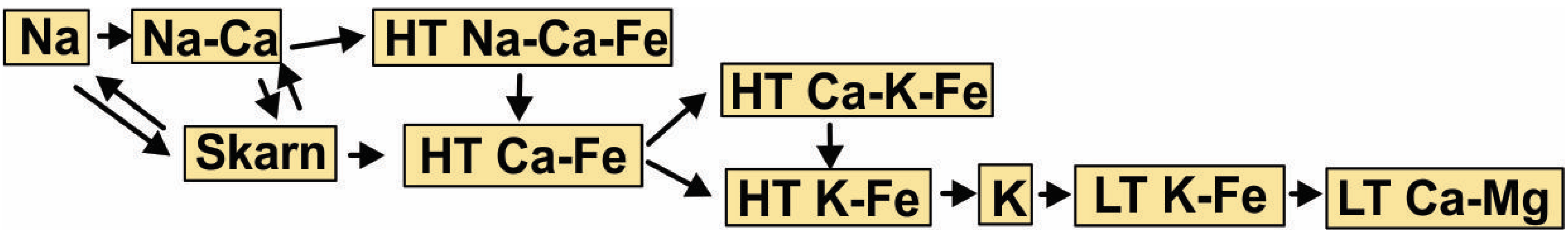

Where carbonates start precipitating at magnetite to hematite transition followed by heat ingress and development of K skarn

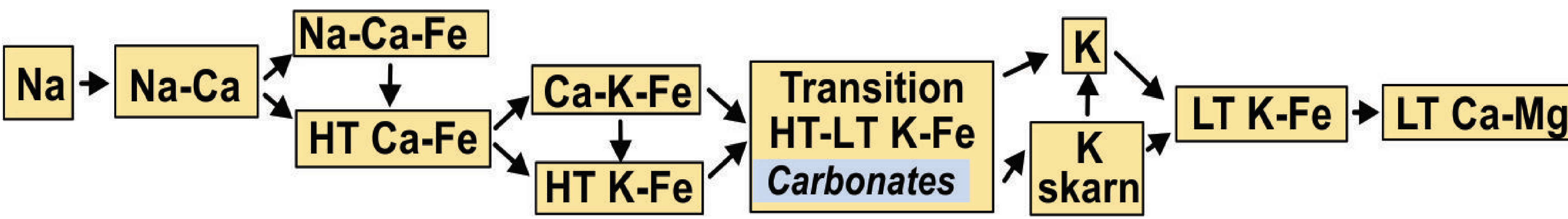

Celebrating 175 yrs

Alteration facies in known deposits

Distal
Lower Temp.
Shallow <1km
Later

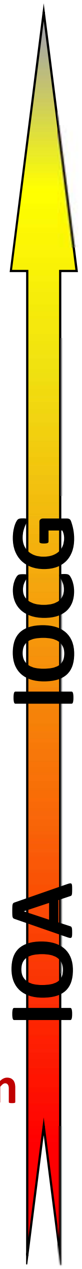

6 LT Si, K, Al, Ba	**Epithermal cap** *Central Andes, Olympic Dam, Great Bear*
5 LT K-Fe (Ca, Mg, H^+-CO_2) hematite-K-feldspar /sericite-carbonate-chlorite-sulphides	**Immediate host to Hem-group IOCG deposits** **Component of Mag–Hem-group IOCG deposits** *Olympic Dam, Prominent Hill, Carrapateena, Great Bear*
4 K-felsite K-feldspar **K-skarn** clinopyroxene-garnet-K feldspar-sulphides	**Immediate host to Hem-toMag and Mag-group + K skarn IOCG** *Candelaria, Mt Elliott (Cloncurry), Hillside (Gawler), Great Bear*
3 HT K-Fe magnetite-biotite/ K feldspar-sulphides	**Immediate host to Mag-group IOCG** *Ernest Henry, Salobo, Candelaria, Great Bear*
2-3 HT Ca-K-Fe	**Immediate host to Co-IOCG and REE-IOA variants** *NICO, Idaho Co belt*
2 HT Ca-Fe amphibole-magnetite ± apatite	**Wallrocks of Mag-Ap (IOA) Fe±REE deposits** *Kiruna, Central Andes, El Laco, Great Bear, MLYRMB*
1-2 skarn if carbonate host **1-2 HT Na-Ca± Fe**	**Outer zones of IOCG deposits** *Ernest Henry, Starra, Central Andes, Great Bear*
1 Na albite, albitite	**Regional scale, barren, preferential host for albitite-hosted U + some IOCG** *Cloncurry + Mt Isa, Gawler, Chilean Iron Belt, El Laco, Kiruna, Great Bear, MLYRMB*

Thermal core
High Temp.
Deeper 3-10km
Earlier

Modified from Corriveau et al. 2010b, 2016

Metasomatic system

HT K-Fe forms at 1-2 km depth
Diameter: **< 400 m** (found in Canada)
> 6x2x3 km (Olympic Dam)

Biotite
K-feldspar
Magnetite
Cu sulphides

HT Ca-Fe forms at 2-8 km depth
Extent: **1-10 km**
Width: **<1km**

Amphibole
Magnetite
Apatite

Na forms at 3-10 km depth
Extent: **1->10 km**
Width: **≤1km**
Depth: **> 1km**

Albite
Scapolite

Protolith

Quartz
Feldspar
Biotite,
Magnetite

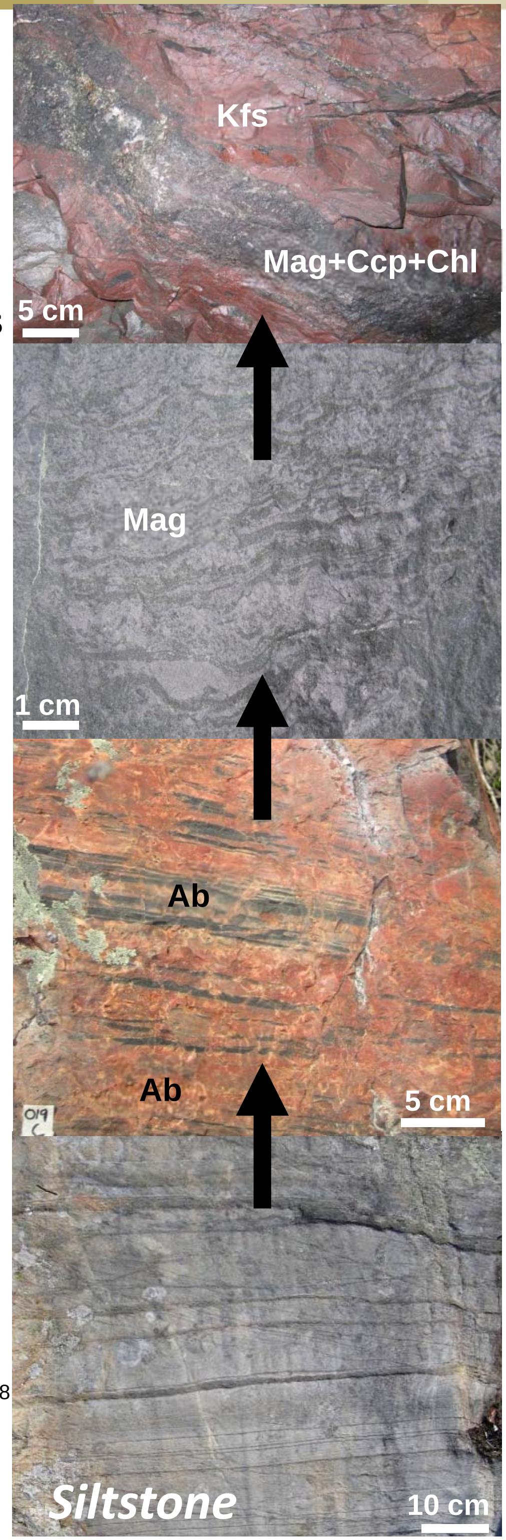

3. Fluids recharged in metals; reacts with hosts to form Ca-Fe and K-Fe alteration facies

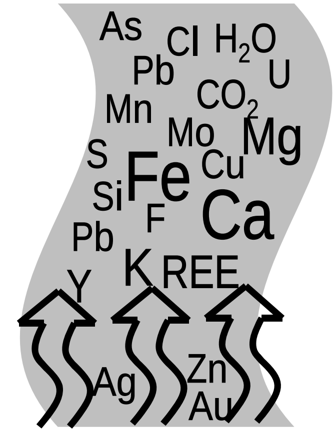

2. Na precipitates; most other elements leached

1. Reaction of highly saline fluids with host

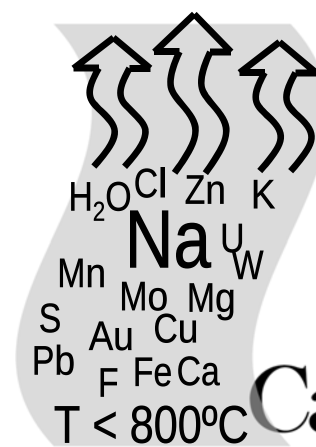

Ascent of highly saline fluids

Temperature ranges of fluids in alteration facies

- **Albitites (300–600°C)**
- **HT Ca-Fe alteration facies metasomatites and IOA deposits (500–800°C)**
- **HT K-Fe facies (350–400°C)**
- **LT K-Fe facies (~250°C)** (based on fluid inclusions and mineral parageneses)

Hypothesis:

- HT highly saline fluid column warms up host rocks at regional scale
- HT fluids cool as albitisation proceeds
- Renewed magma emplacement increases fluid T, salinity decreases leading to HT Ca-Fe alteration
- Fluid column rises and fluids cool as metasomatism proceeds or as column mixes with LT fluids leading to HT K-Fe facies (350–400°C) and to LT K-Fe facies (~250°C)

Kish and Cuney 1981; Bardina and Popov 1992; Sidder et al. 1993; Mark et al. 2000, 2006; Harlov et al. 2002; Marschik et al. 2003; Requia et al. 2003; Bastrakov and Skirrow 2007; Monteiro et al. 2008; Polito et al. 2009; Xavier et al. 2010; Chen et al. 2011; Somarin and Mumin 2014; Li (W.) et al. 2015; Bilenker et al. 2016

Deformation, veining and brecciation

Conditions		Alteration facies	Attributes
Distal Low Temp. Shallow Lateral Later	≤250ºC	6 LT Si-Al-K epithermal	Veins, breccias Brittle deformation
	≤350ºC	5 LT K-Fe–LT Ca-Fe-Mg metasomatites 4 K-skarn (if carbonates) Kfs-felsite breccias	Hydrothermal breccias formed regularly Brittle deformation dominant Brittle-ductile deformation and fluidisation can occur in shear zones
Steep thermal gradient	≤450ºC	3 HT K-Fe metasomatites	
Thermal core High Temp. Deeper	≤800ºC	2 HT Ca-Fe metasomatites Skarn in carbonate hosts	Confined ductile deformation Abundant veins (± haloes) Local brecciation (± fluidisation)
Earlier	≤600ºC	1 Na Albitites	Post-albitite structural breccias Haloes along fractures, fronts

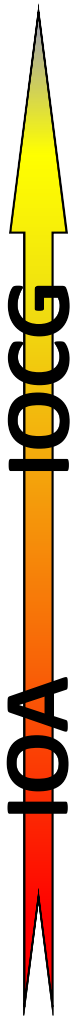

Domingos 2009
Corriveau et al. 2010b, 2016, in preparation
Montreuil et al. 2015, 2016a, b

Breciation and alteration

Sue Dianne, Great Bear magmatic zone

(photos A.H. Mumin)

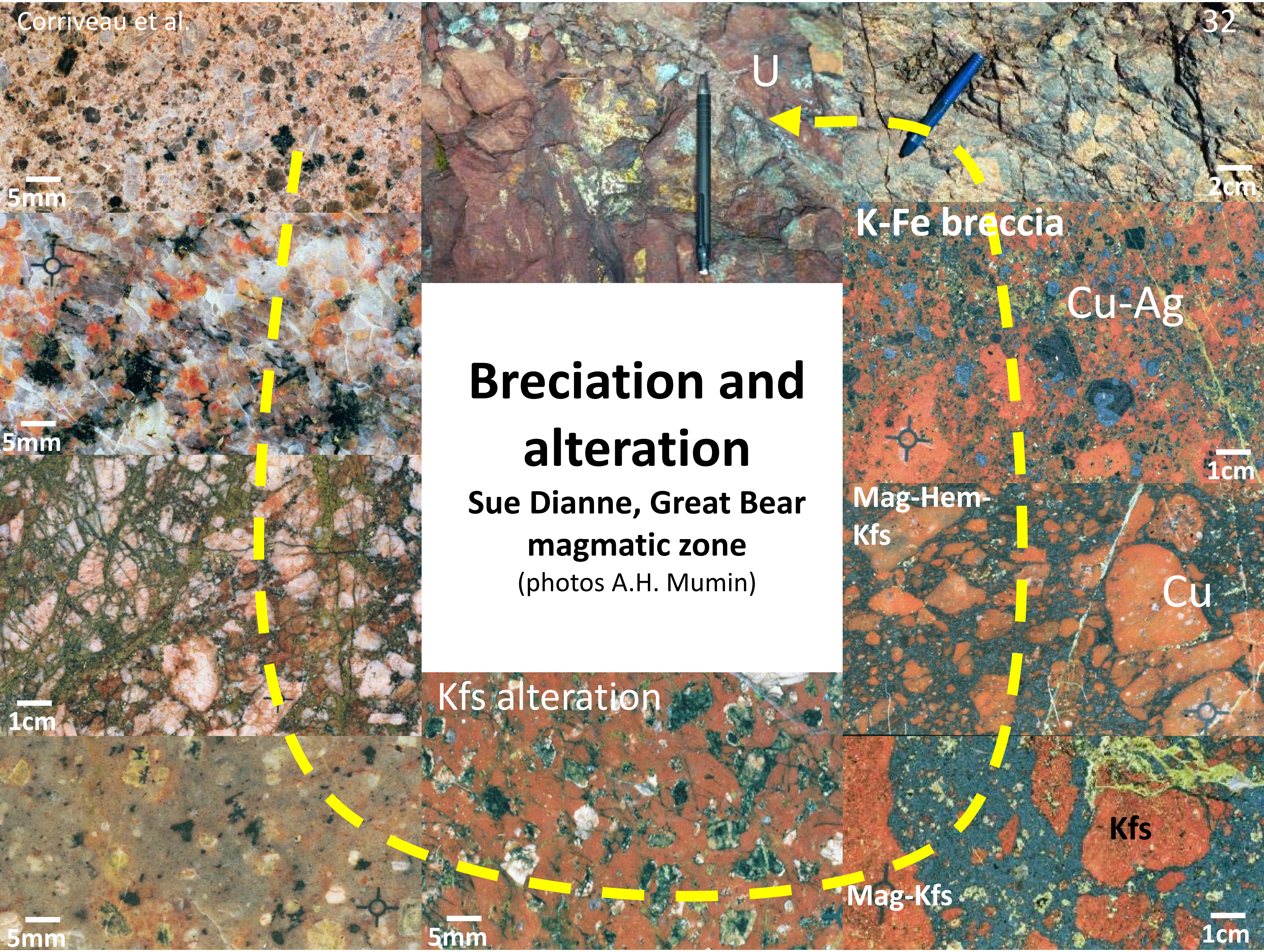

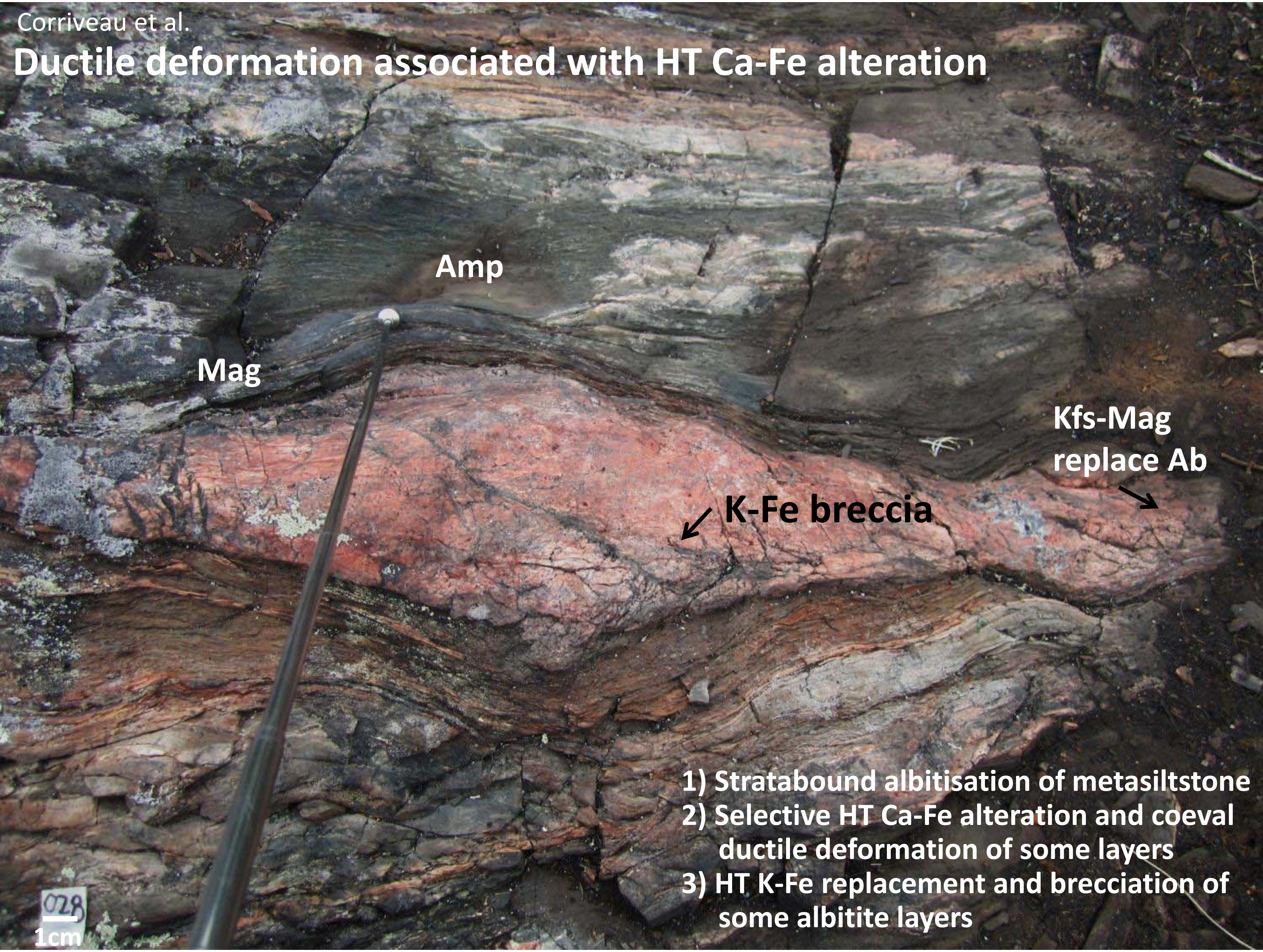
Corriveau et al.
Ductile deformation associated with HT Ca-Fe alteration
Amp
Mag
Kfs-Mag
replace Ab
K-Fe breccia
1) Stratabound albitisation of metasiltstone
2) Selective HT Ca-Fe alteration and coeval ductile deformation of some layers
3) HT K-Fe replacement and brecciation of some albitite layers
028
1cm

Lithogeochemical footprints of metasomatism:

Tools and examples

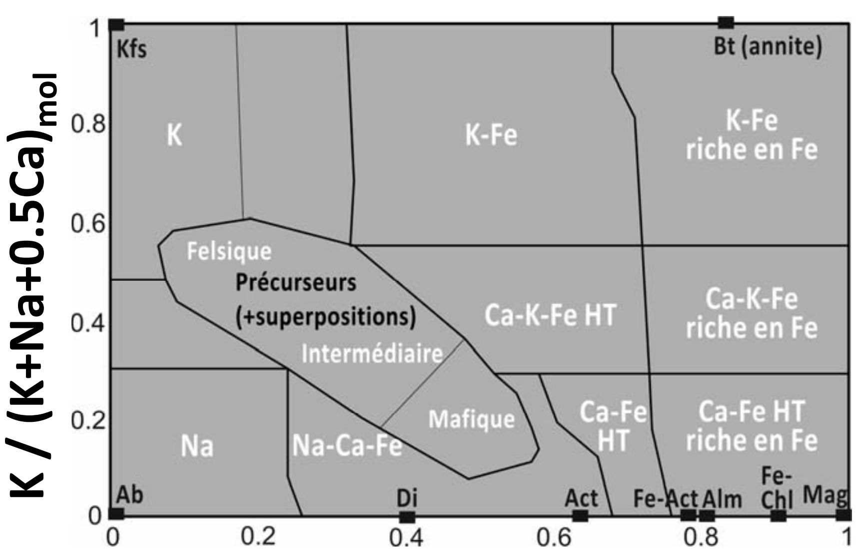

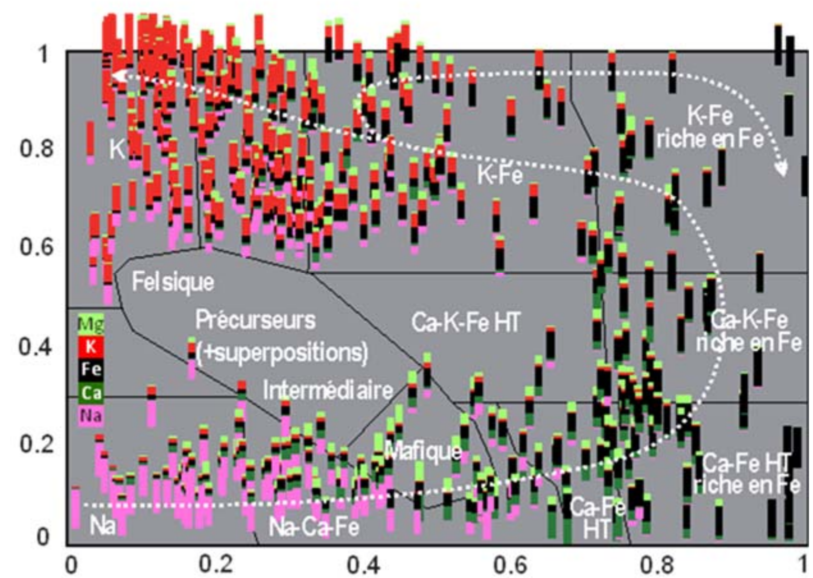

$$\frac{(2Ca+5Fe+2Mn)_{mol}}{(2Ca+5Fe+2Mn+Mg+Si)_{mol}}$$

Chemical discrimination: Alteration index and box plots

Each alteration facies has a distinct geochemical signature

Geochemical data refine the major-element mobility interpreted megascopically

Benavides et al. (2008a, b) index

- Detect IOCG alteration but difficult to apply widely as it requires CO_2 analyses
- Characterise intensity but not designed to discriminate facies

Montreuil et al. (2013) indices

- Based on molar concentration
- A-IOCG1 discriminates Na from K and Ca-Fe from K-Fe alteration
- A-IOCG2 discriminates alkali (Na-K) from Ca-Fe, K-Fe and Fe alteration

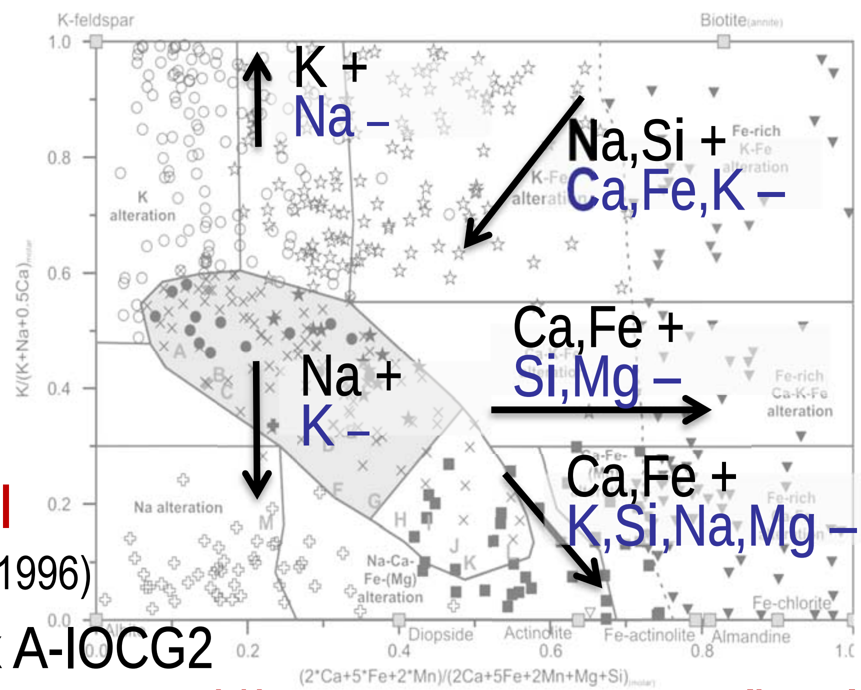

Index A-IOCG1

K/(K+Na+0.5Ca)mol

Modified from Madeisky (1996)

Index A-IOCG2

(2Ca+5Fe+2Mn)/(2Ca+5Fe+2Mn+Mg+Si)mol

Chemical discrimination: Cationic bar codes

- Cations are proxies for the distinctive minerals of the main alteration facies
  - Na — Na in light pink for albite
  - Ca — Ca in green for amphibole
  - Fe — Fe in black for iron oxides
  - K — K in red for K-feldspar
  - Mg — Mg in light green for chlorite
- Coloured bar codes are derived from molar cationic proportion from whole-rock geochemical analyses: Na Ca Fe K Mg
- The set of chemical signatures is diagnostic for each alteration facies and consists of cation bar code with 1, 2 or 3 dominant cations
- Bar codes of least-altered host rocks are distinct in having generally 3 to 5 dominant cations

Common rocks

Alteration facies

Corriveau et al. 2016, 2017; Blein and Corriveau 2017

Prograde metasomatic reaction path

- Chemistry and metal endowment of fluids evolve as fluid column rises, reacts with host rocks, leaches and precipitates metals
- Mineral stability induces precipitation of chemical components from fluids
- Mineral instability leads to dissolution of chemical components subsequently entrained by fluids
- Mineral assemblages change as physico-chemical conditions of rising fluid column change
- Distinct chemical footprints are induced by mineral stability during metasomatic fluid-rock reactions

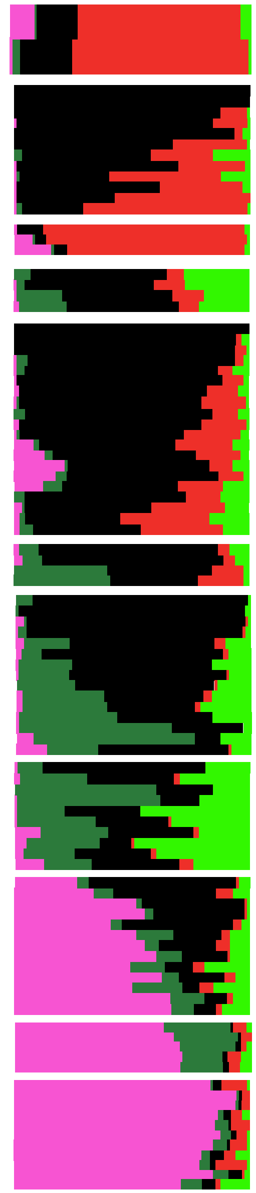

Argillic, advanced argillic, phyllic

LT K-Fe Hem-Kfs/Ser-Cb-Chl-Ccp

K-felsite Kfs

K-skarn Cpx-Grt-Kfs-Sul(Sp)

HT K-Fe Mag-Bt/ Kfs-Sul (Ccp)

HT Ca-K-Fe Amp-Mag-Bt/Kfs-Apy

HT Ca-Fe Amp-Mag± Ap

Skarn Cpx-Grt

HT Na-Ca-Fe Ab-Amp-Mag±Ap

HT Na-Ca Ab-Cpx-Amp±Scp

Na Ab, albitite

Geochemical data in Corriveau et al. 2015

Chemical maps

Southern Breccia

Albitite-hosted U (± Cu-Mo)

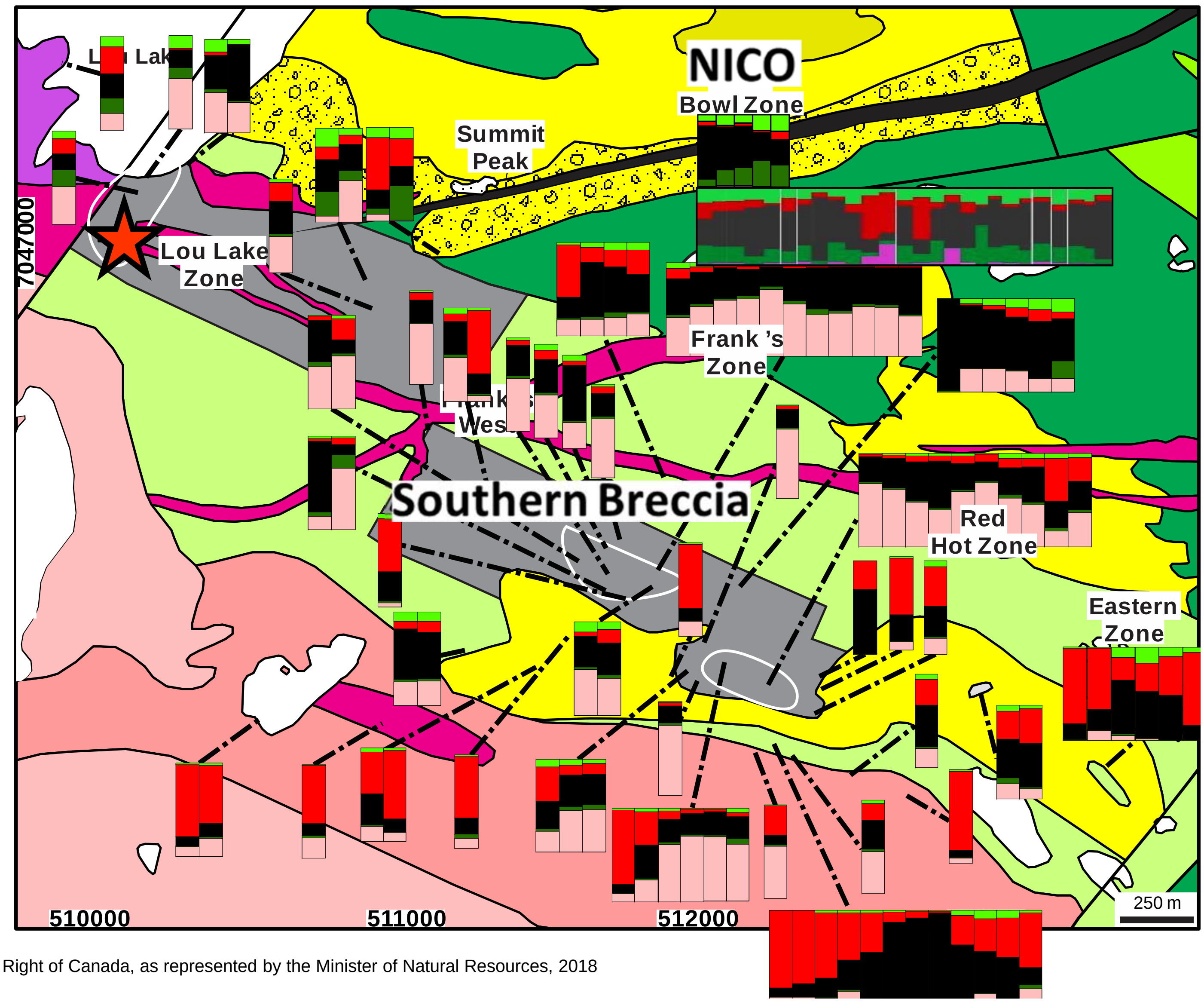

NICO Au-Co-Bi-Cu HT Ca-K-Fe

Modified from Montreuil et al. 2016b

Metal associations

Port Radium–Echo Bay

Transition IOA to IOCG

Metal X 100 ppm

Cu	Zn	Ni	Pb
0 - 2	0 - 2	0 - 0.5	0 - 2
2 - 5	2 - 5	0.5 - 1.5	2 - 5
5 - 10	5 - 20	1.5 - 3	5 - 20
10 - 20	20 - 50	3 - 5	20 - 50
20 - 100	50 - 200	5 - 10	50 - 200

Ce	V
0 - 0.6	0 - 0.5
0.6 - 1	0.5 - 1
1 - 2	1 - 3
2 - 3	3 - 8
3 - 10	8 - 20

Na Ca Fe K Si/3

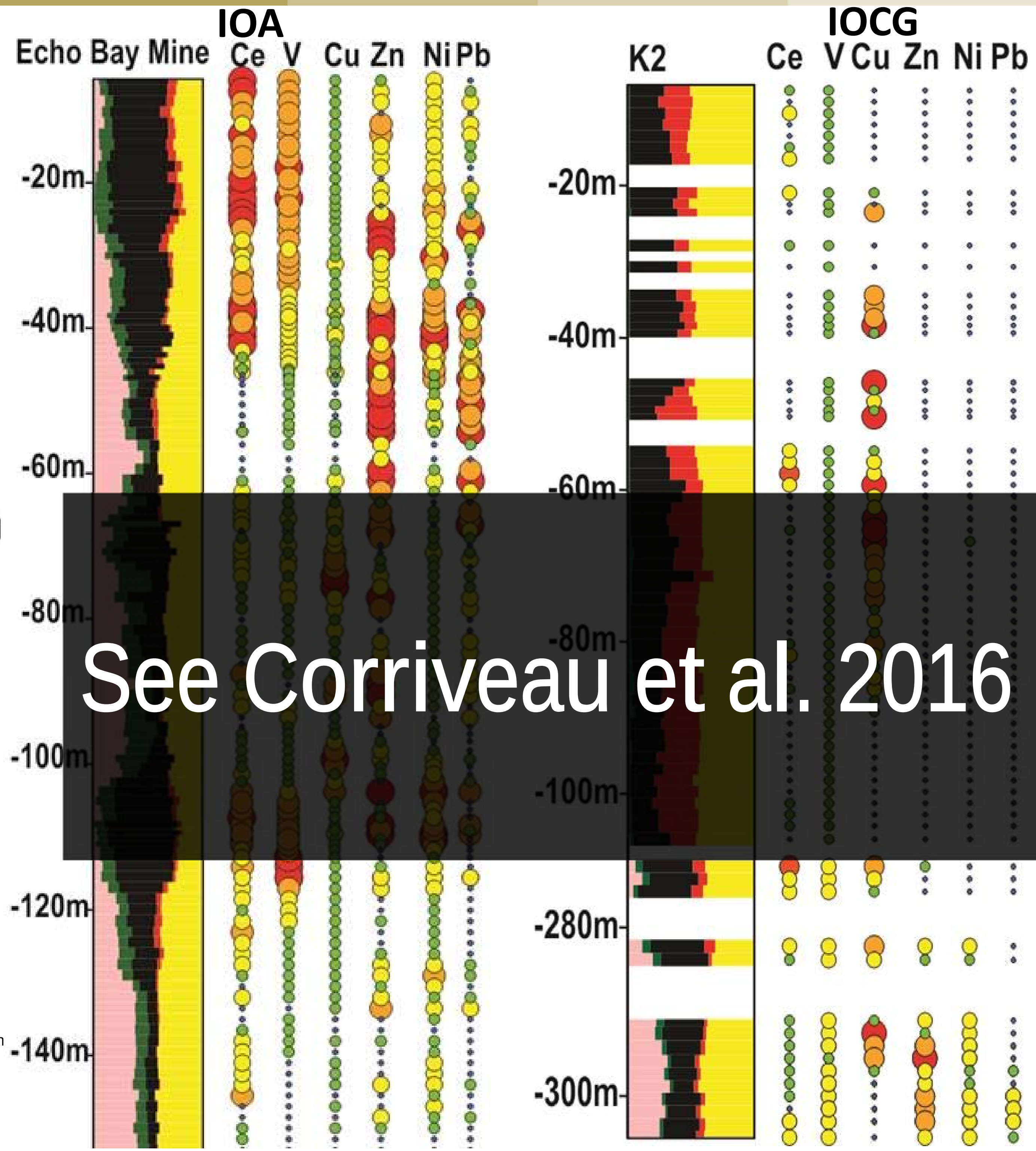

Alteration facies chemical footprint

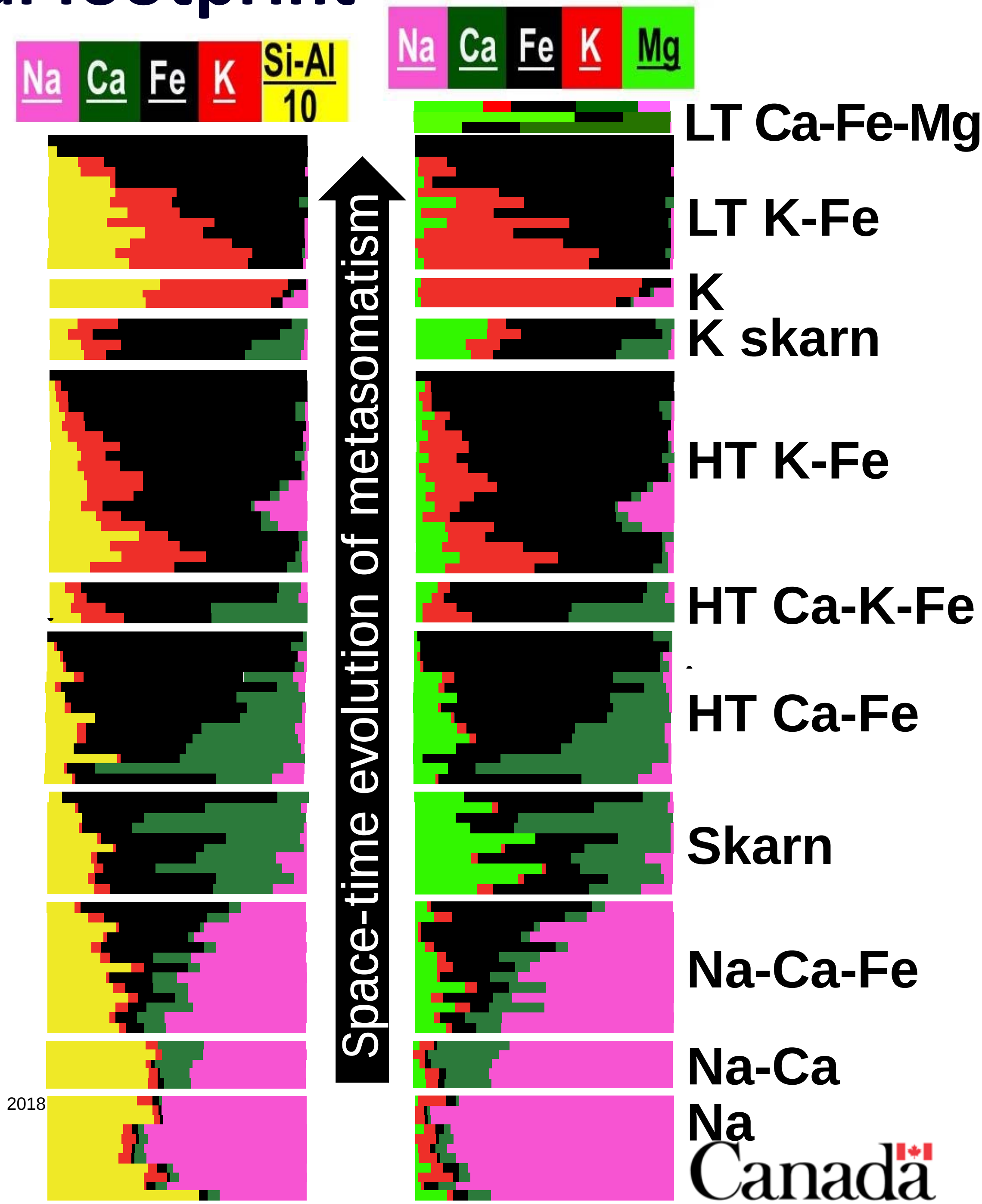

Prograde metasomatism

= changes in alteration facies

= changes in rock composition

= changes in fluid composition and precipitation conditions

= changes in metal associations

= continuum in deposit types formed

Common sedimentary, felsic to mafic igneous and metamorphic rocks

Corriveau et al. 2016, 2017

Deposit chemical footprint

IOA-REE
at HT Ca-Fe to Ca-K-Fe

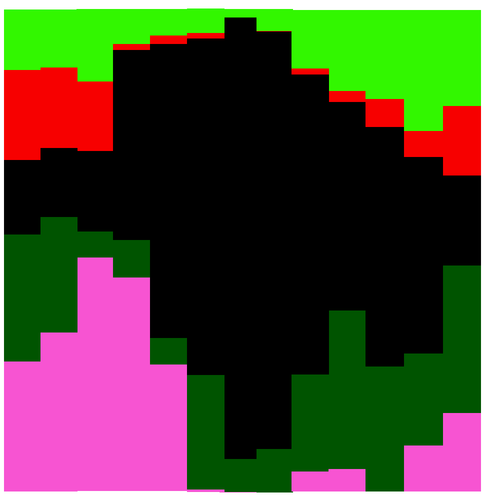

IOA + REE

Au-Co-Bi variant of
Mag-group IOCG at
HT Ca-K-Fe

Co-variant
IOCG

Cu-Ag-Au
Mag to Hem-group IOCG
at HT K-Fe

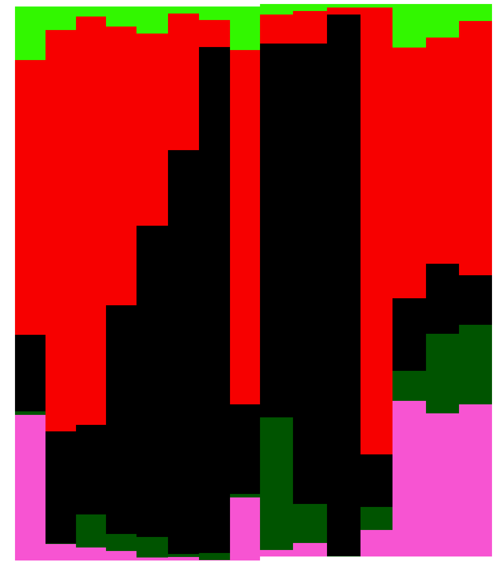

IOCG

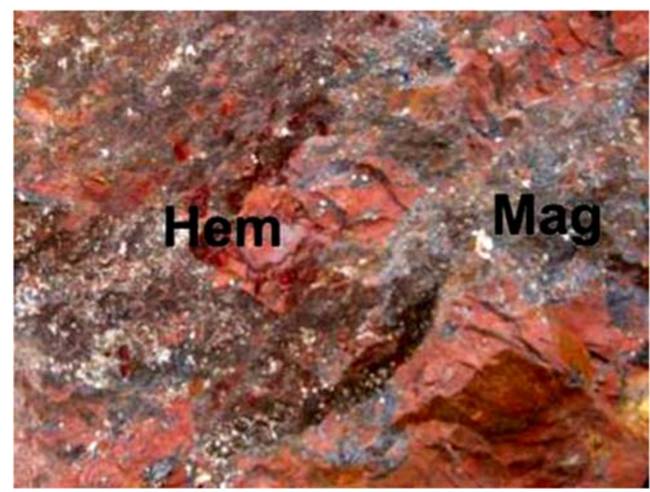

Corriveau et al. 2015, 2016

Mineral system chemical footprint

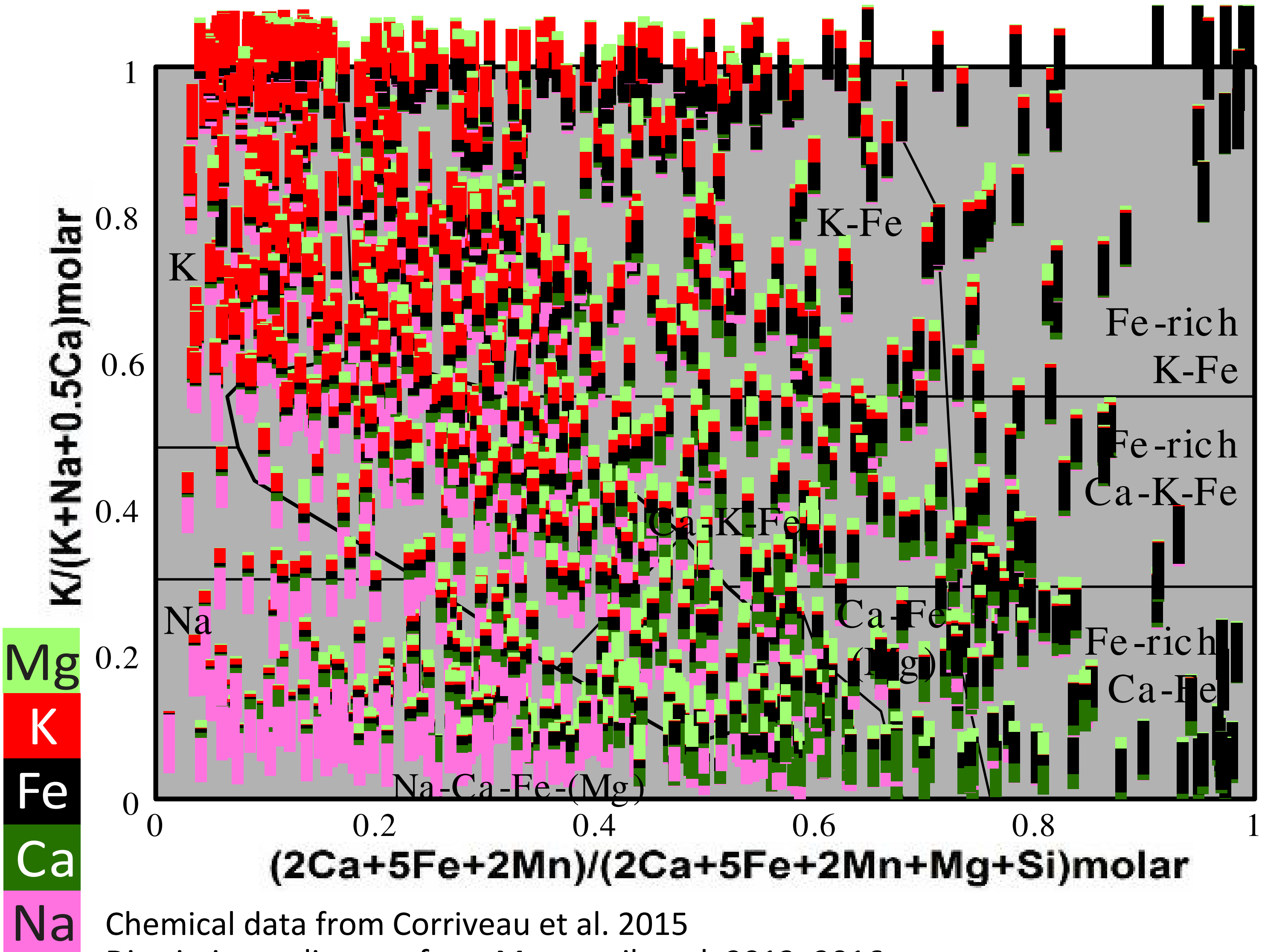

Chemical data from Corriveau et al. 2015
Discriminant diagram from Montreuil et al. 2013, 2016a

Bulk rock chemical footprint of Great Bear ore systems without discrimination of least-altered rocks and prograde and retrograde metasomatic rocks

Least-altered chemical footprint

Least-altered igneous, sedimentary and metamorphic host rocks, Great Bear

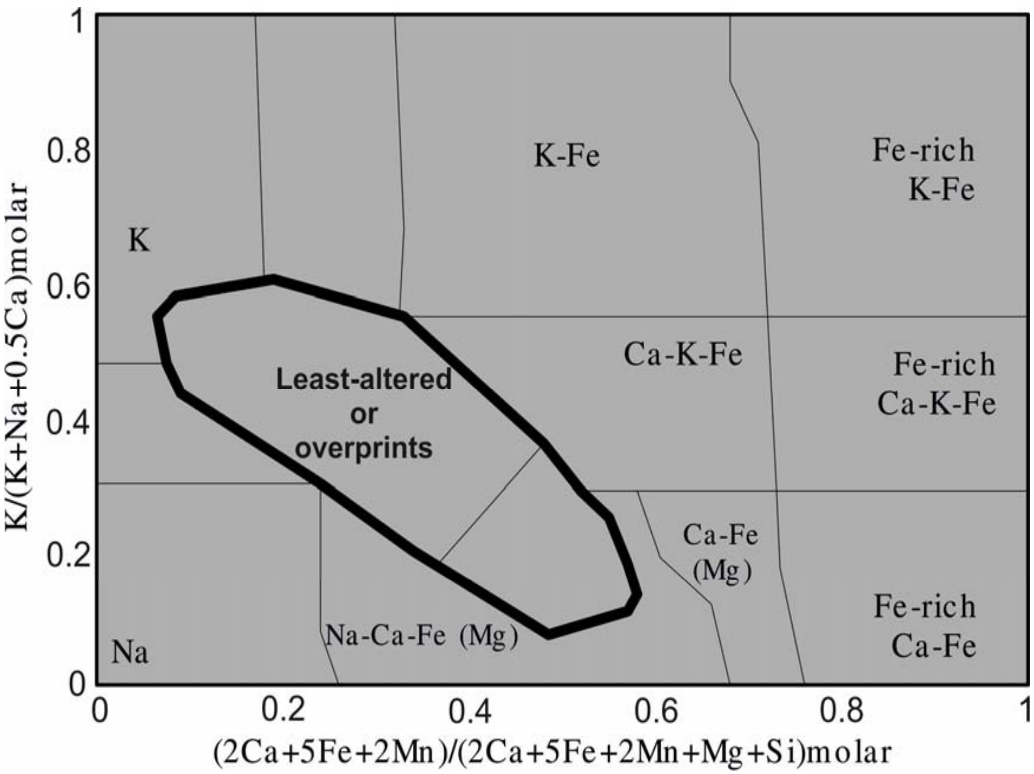

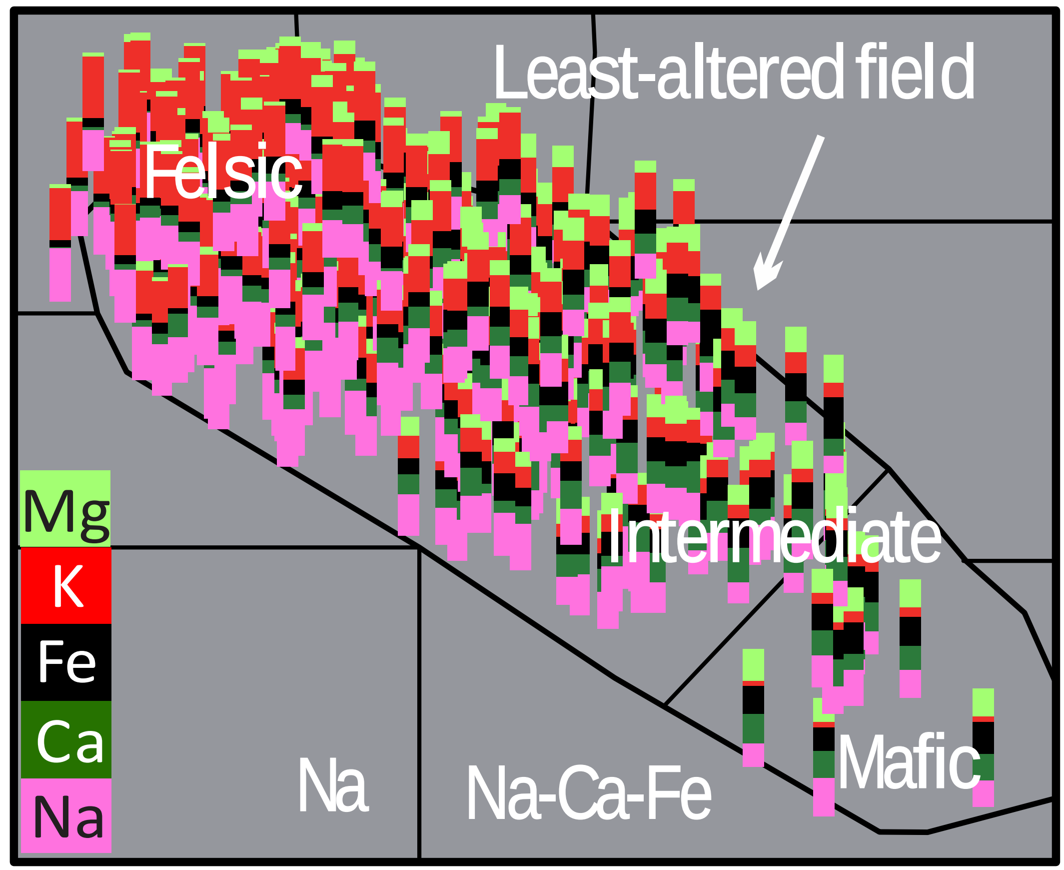

Samples combine a lack of field evidence for alteration and low Ishikawa alteration index

Modified from Corriveau et al. 2017
Chemical data from Corriveau et al. 2015
Discriminant diagram from Montreuil et al. 2013, 2016a

Footprint of common igneous rocks

Most high-K calc-alkaline igneous rocks fall slightly below the least-altered field of Montreuil et al. (2016a) derived from Great Bear data but fall largely within the global least-altered field of Montreuil et al. (2013); shoshonitic suites fall within the Great Bear field of least-altered rocks

Data points at the base of the Na-Ca-Fe-K-Mg bar codes

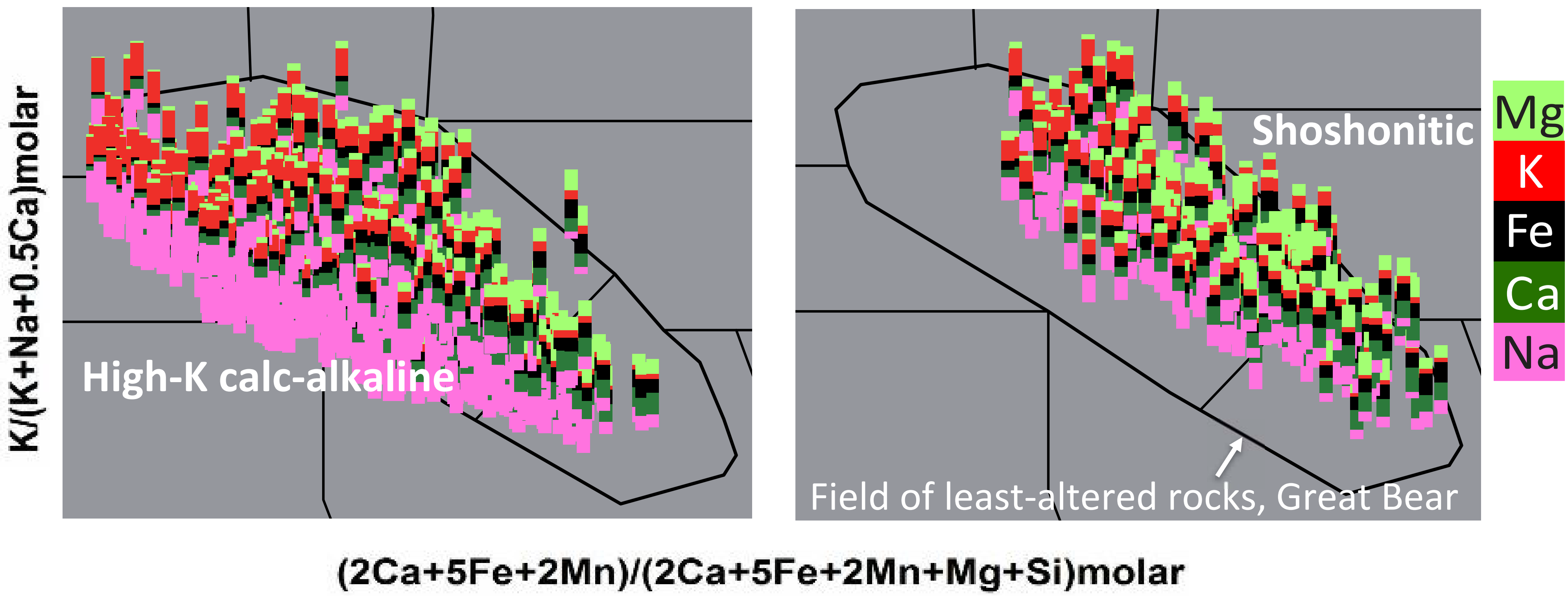

Discriminant diagram: Montreuil et al. 2013, 2016a

Footprint of prograde metasomatism, Great Bear

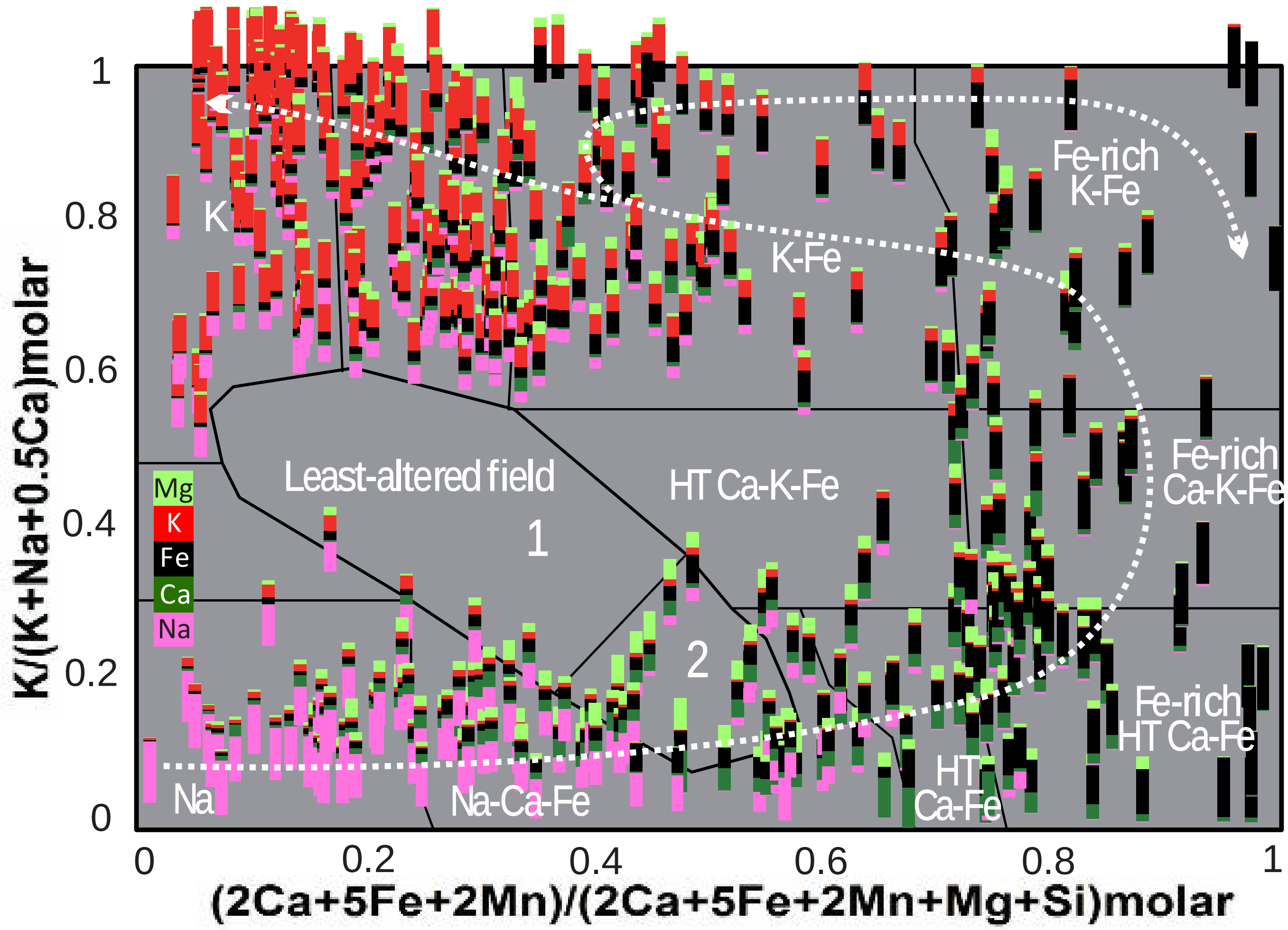

Footprint of prograde metasomatic reaction path (from Na to HT Ca-Fe, HT K-Fe, LT K-Fe and epithermal alteration facies) is highlighted by selecting whole-rock analyses of metasomatic rocks with a single dominant and intense alteration facies

Modified from Corriveau et al. 2017
Chemical data from Corriveau et al. 2015
Discriminant diagram from Montreuil et al. 2013, 2016a

Footprint of prograde metasomatism, Great Bear

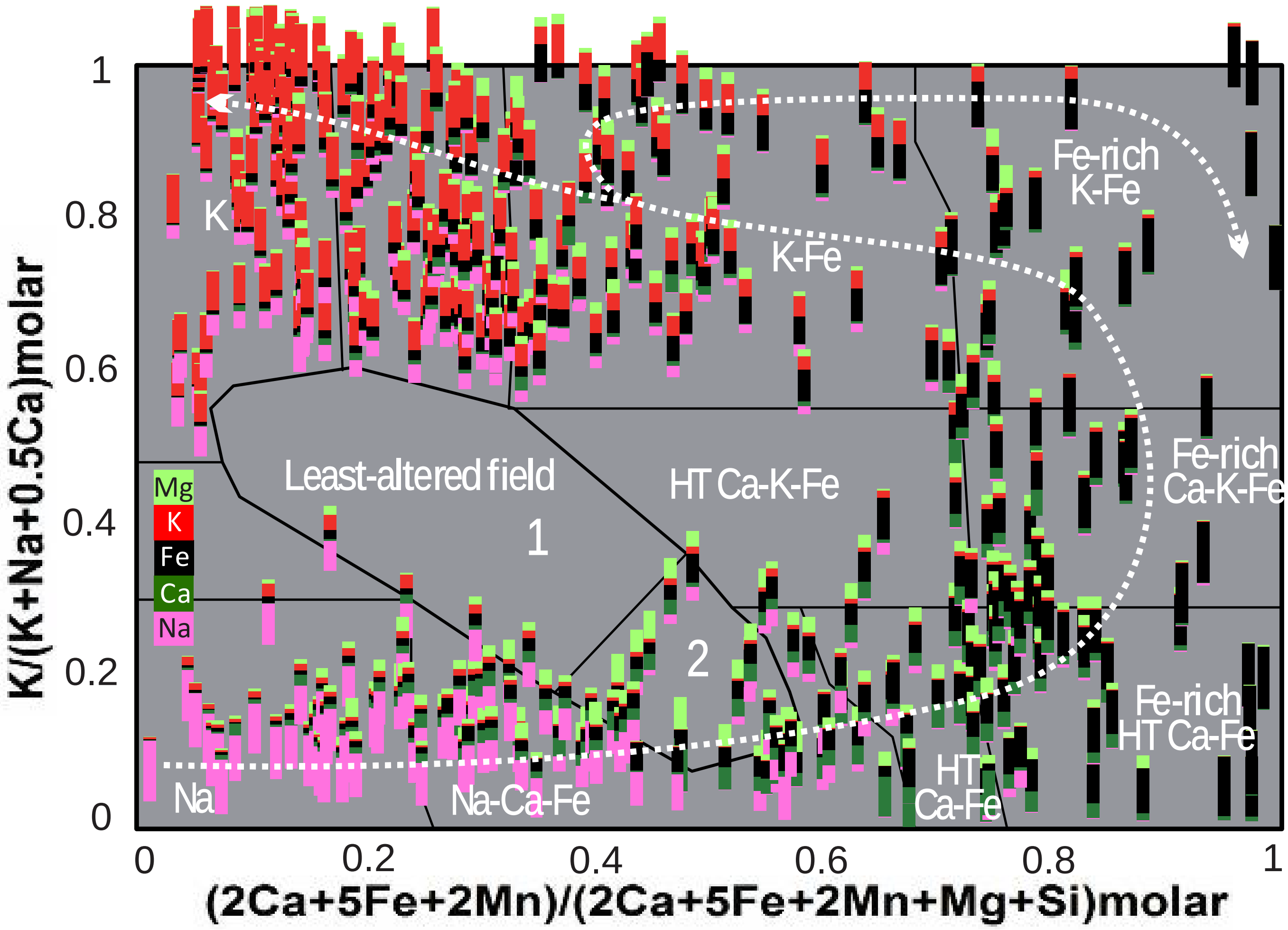

Metasomatic rocks with a dominant intense alteration facies

Modified from Corriveau et al. 2017
Chemical data from Corriveau et al. 2015
Discriminant diagram from Montreuil et al. 2013, 2016a

At the K-Fe facies, rocks can become highly enriched in Fe and then be carbonate altered with a trend toward Fe-rich Ca-K-Fe. Alternatively the K component increases more than Fe. Both trends can evolve to K-rich epithermal alteration

Albitites pervasively altered to K-feldspar conserve some Na and may have signatures similar to rhyolites
(Data points at the base of the bar codes)

Celebrating 175 yrs

Discriminating prograde and retrograde paths

Element bar codes highlight telescoped and/or retrograde metasomatic paths

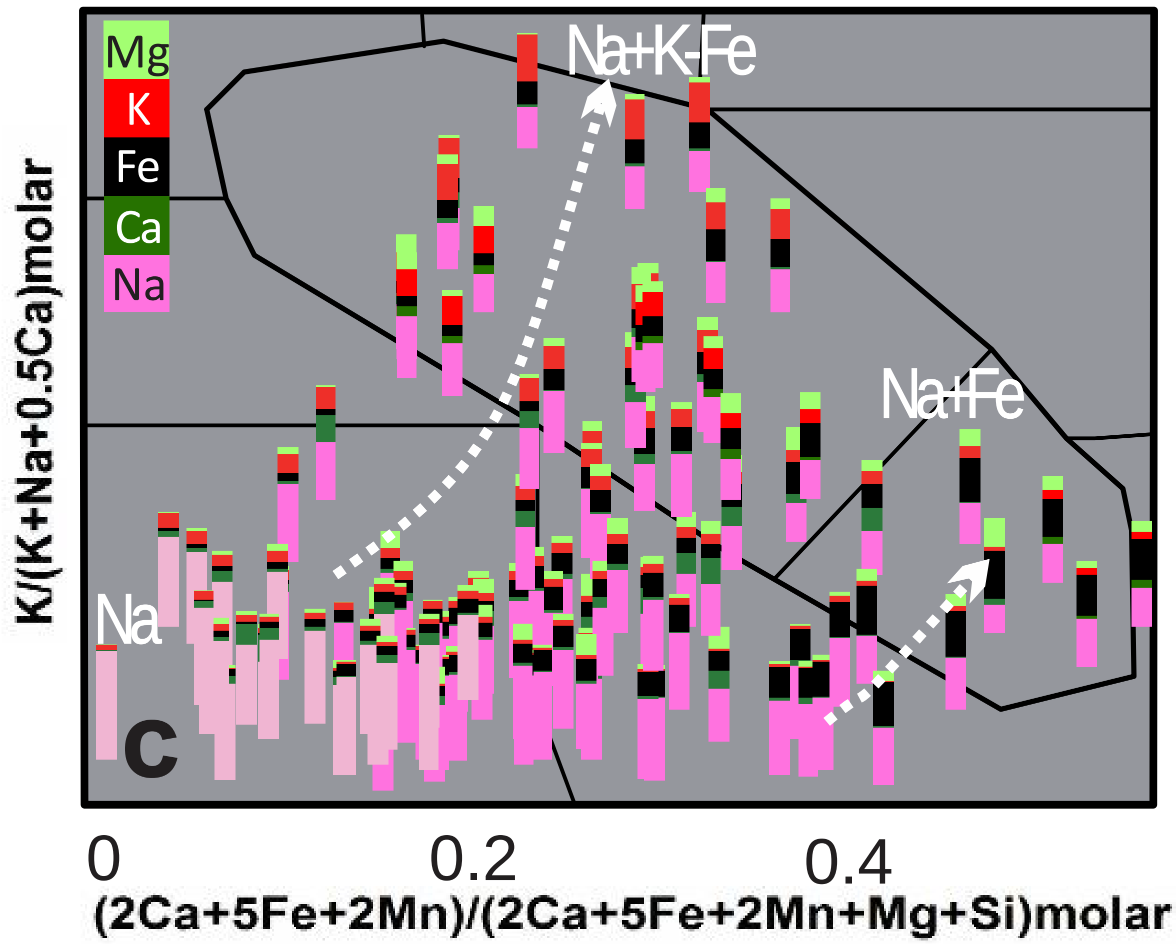

Albites telescoped to HT or LT K-Fe, LT K-Fe and Ca-Fe-Mg or to HT or LT Ca-Fe metasomatism occupy the least-altered field but their bar charts are commonly distinct from those of the least-altered rocks

N.B. bar codes with a light pink colour for Na are those of albitites with least overprints

Modified from Corriveau et al. 2017
Chemical data from Corriveau et al. 2015
Discriminant diagram from Montreuil et al. 2013, 2016a

Altered albitites and varied intensity of albitisation

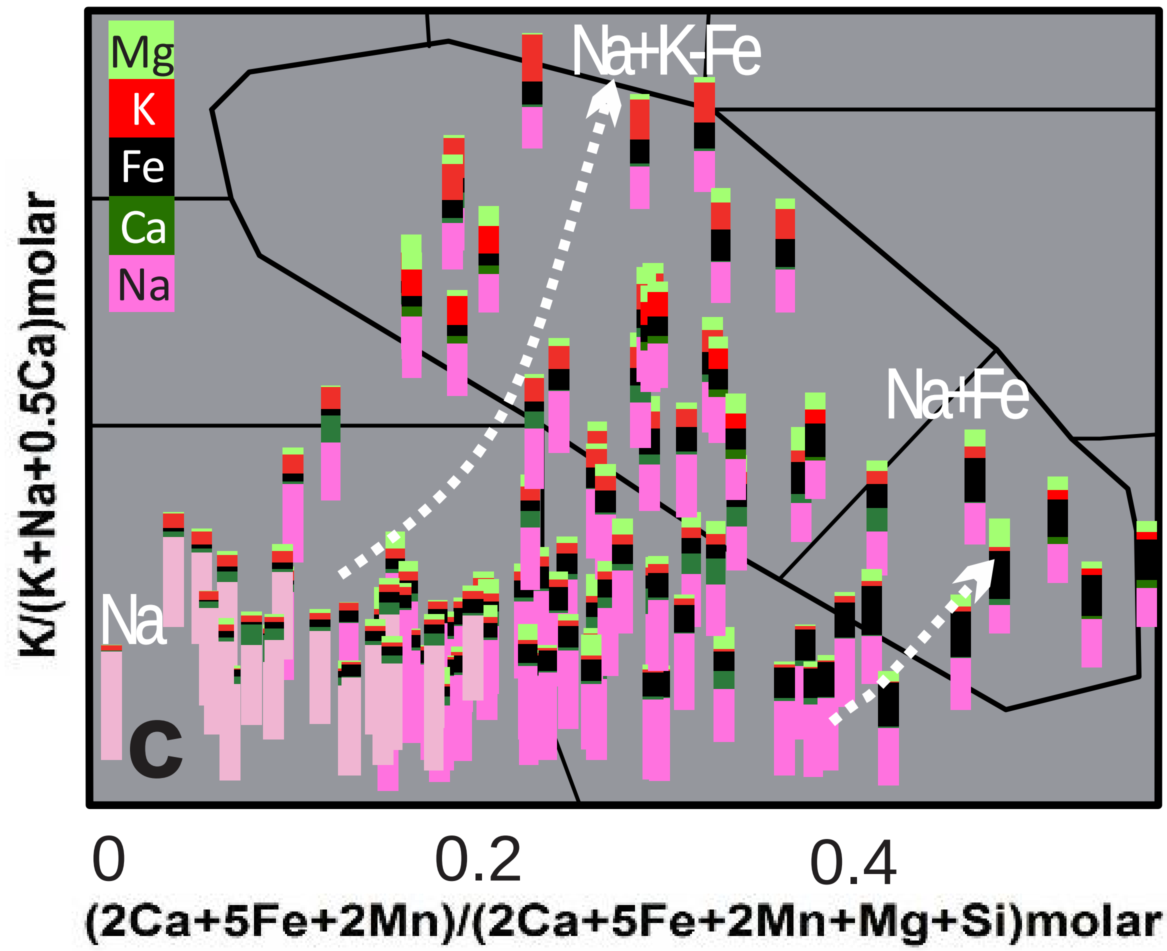

Modified from Corriveau et al. 2017
Chemical data from Corriveau et al. 2015
Discriminant diagram from Montreuil et al. 2013, 2016a

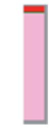

Albitites (Na in pale pink) can conserve some Ca, K and Fe.

Albitites (Na in darker pink) can be replaced by magnetite (Na+Fe trend).

Intensity of albitisation can vary from mild to moderate with the code bars preserving Ca-Fe-K-Mg

Albitites can be telescoped into the field of K-Fe alteration (Na+K-Fe trend)

As systems cooled, albitites are replaced by carbonates, chlorite, K-feldspar or sericite leading to a variety of Na+K-Fe-Ca-Mg trends

(Data points at the base of the bar codes)

K alteration of HT Na-Ca-Fe and Ca-Fe alteration

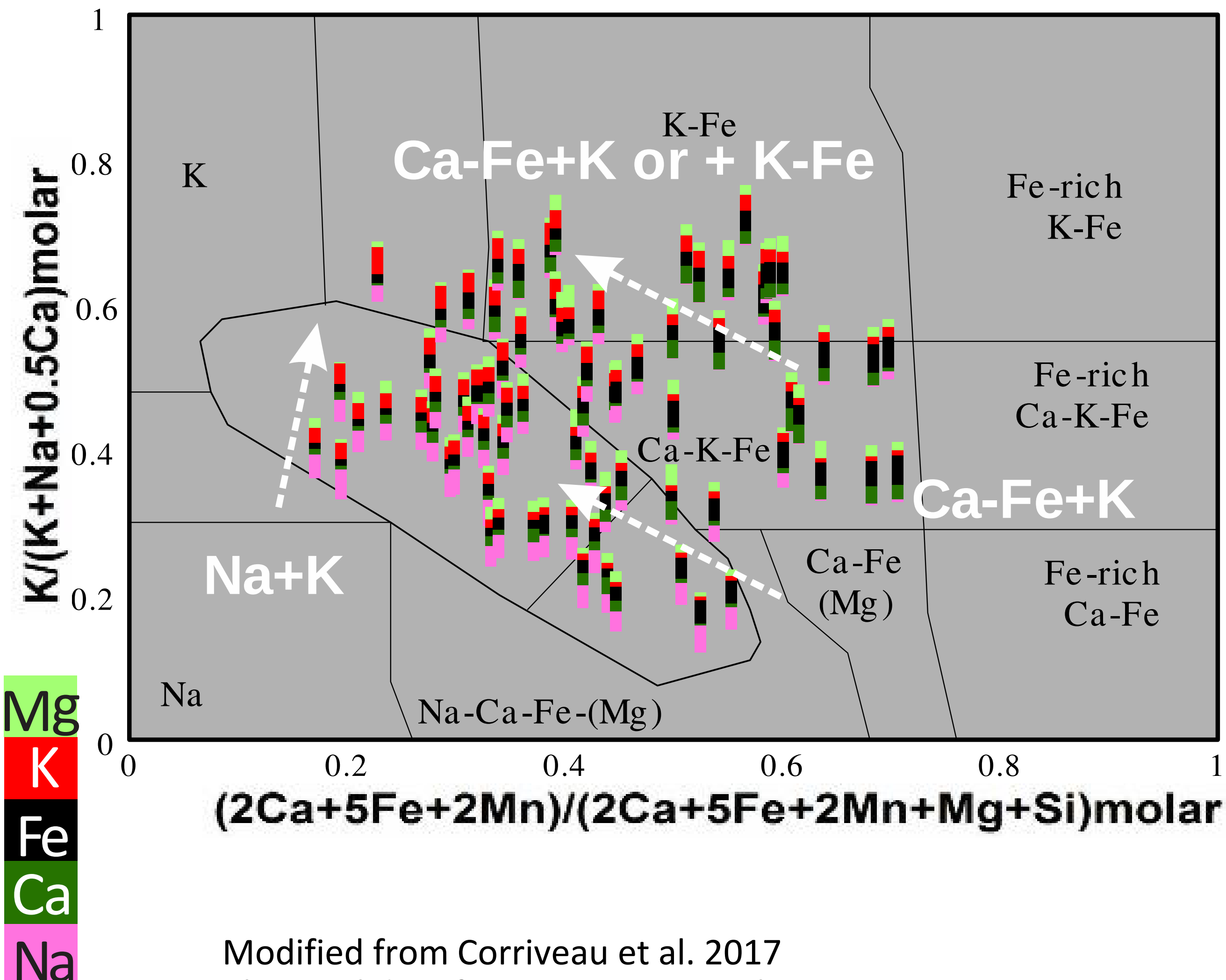

Prograde Na-Ca-Fe and HT Ca-Fe metasomatic rocks can be K altered. Bulk composition shifts to higher K/(K+Na+0.5Ca)molar index values, in the field of the least-altered rocks.

Modified from Corriveau et al. 2017
Chemical data from Corriveau et al. 2015
Discriminant diagram from Montreuil et al. 2013, 2016a

Prograde and telescoped evolution of alteration facies and deposit types

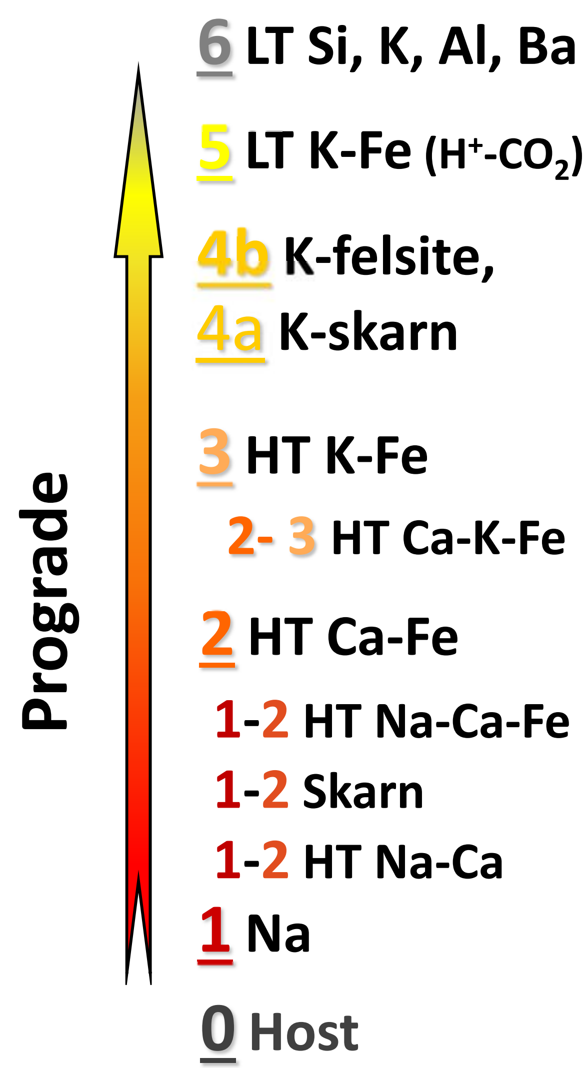

Each metasomatic reaction path and alteration facies lead to their own deposit type

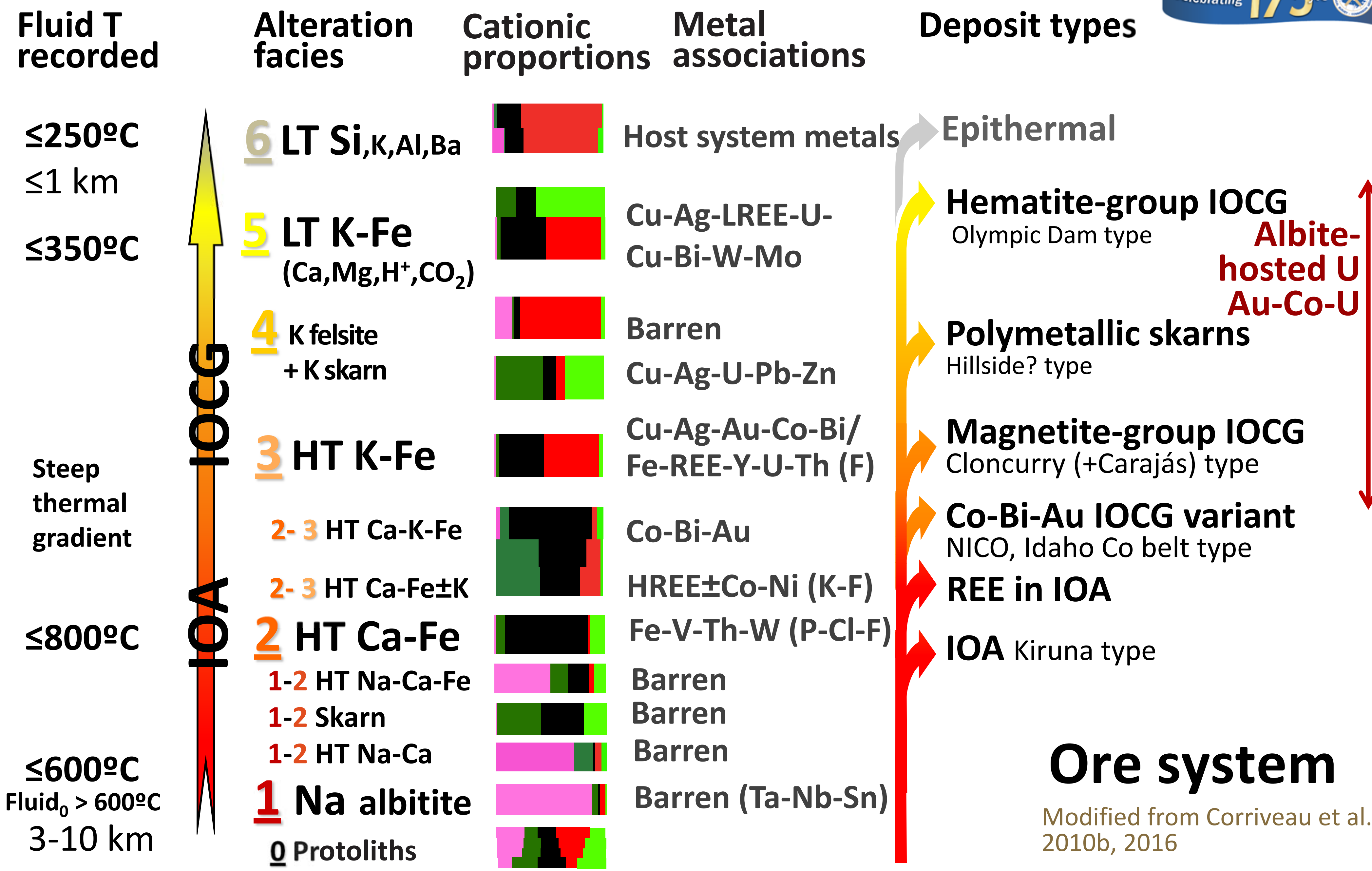
Fluid T recorded
Alteration facies
Cationic proportions
Metal associations
Deposit types
≤250ºC
≤1 km
≤350ºC
Steep thermal gradient
≤800ºC
≤600ºC
Fluid$_0$ > 600ºC
3-10 km
IOCG
IOA
6 LT Si,K,Al,Ba
5 LT K-Fe (Ca,Mg,H$^+$,CO$_2$)
4 K felsite + K skarn
3 HT K-Fe
2- 3 HT Ca-K-Fe
2- 3 HT Ca-Fe±K
2 HT Ca-Fe
1-2 HT Na-Ca-Fe
1-2 Skarn
1-2 HT Na-Ca
1 Na albitite
0 Protoliths
Host system metals
Cu-Ag-LREE-U-
Cu-Bi-W-Mo
Barren
Cu-Ag-U-Pb-Zn
Cu-Ag-Au-Co-Bi/
Fe-REE-Y-U-Th (F)
Co-Bi-Au
HREE±Co-Ni (K-F)
Fe-V-Th-W (P-Cl-F)
Barren
Barren
Barren
Barren (Ta-Nb-Sn)
Epithermal
Hematite-group IOCG
Olympic Dam type
Albite-hosted U
Au-Co-U
Polymetallic skarns
Hillside? type
Magnetite-group IOCG
Cloncurry (+Carajás) type
Co-Bi-Au IOCG variant
NICO, Idaho Co belt type
REE in IOA
IOA Kiruna type
Ore system
Modified from Corriveau et al. 2010b, 2016

Metasomatic reaction paths: IOA

Steep thermal gradient induced by high-temperature fluid columns and repeated magma emplacement

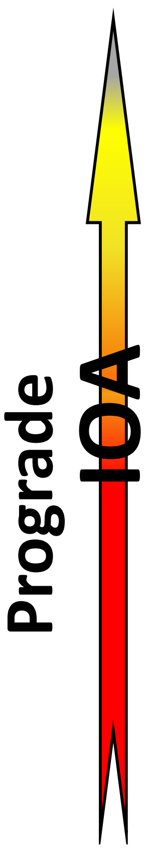

6 LT Si, K, Al, Ba

5 LT Ca-Fe-Mg
(H^+-CO_2)

2 HT Ca-Fe

1-2 HT Na-Ca-Fe

1-2 Skarn

1-2 HT Na-Ca

1 Na

0 Host

±Fe skarn

Sustained heat ingress through intrusion of diorites and rapid cooling at the HT Ca-Fe alteration facies after Na(± skarn facies)
(e.g., northern Great Bear; Hildebrand 1986; Mumin et al. 2007, 2010; Corriveau et al. 2010b, 2016)

IOA-REE
at HT Ca-Fe to Ca-K-Fe

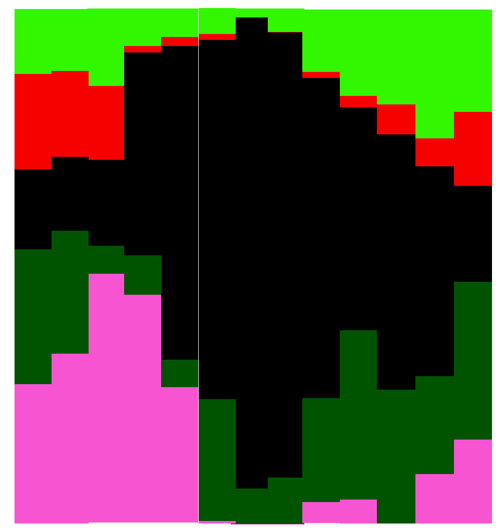

IOA + REE

See also examples in China and the Andes (Yu et al. 2011; Chen 2013; Tornos et al. 2016; Zhao et al. 2017a)

Modified from Corriveau et al. (2010b, 2016)

Celebrating 175 yrs

REE-rich IOA variants

Precipitation and remobilisation of REE; HREE abundant at that stage

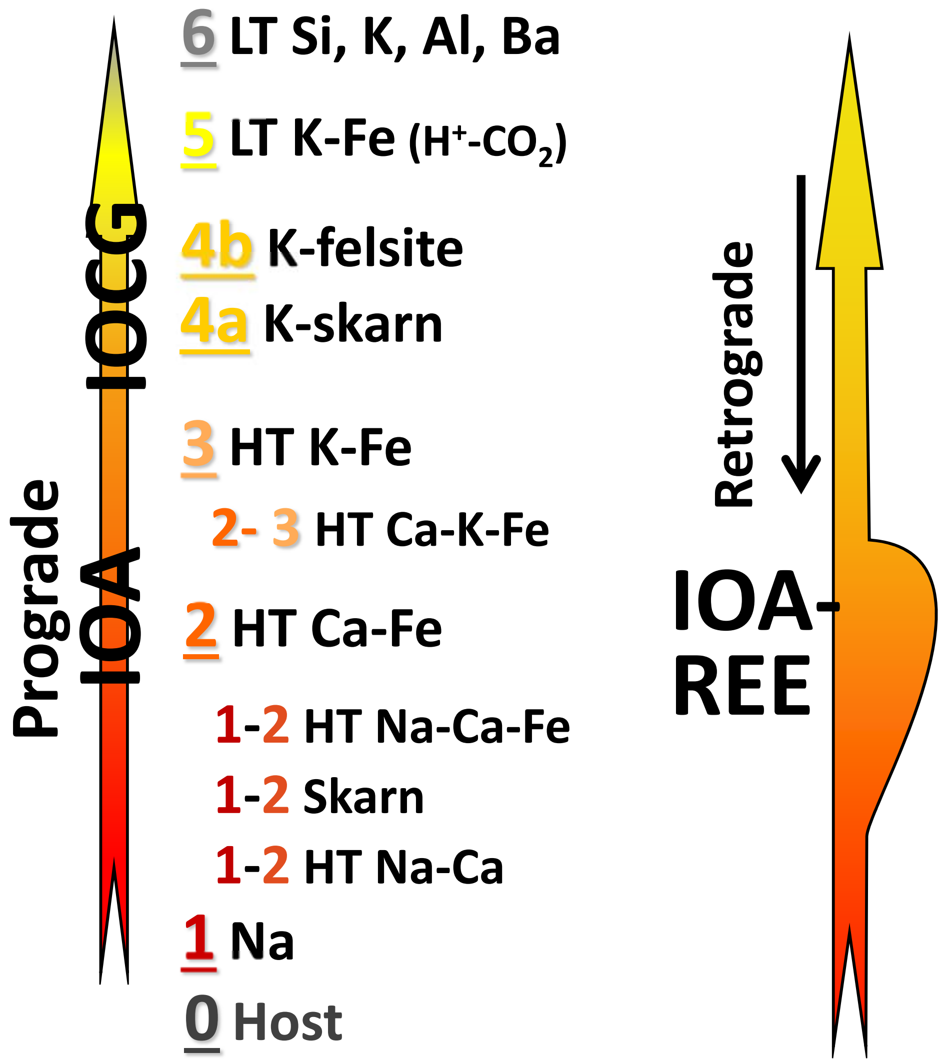

1. Systems that prograde to K-Fe facies crystallise REE-rich apatite at the HT Ca-Fe±K facies within IOA deposits
2. Retrograde or renewed fluid circulation within IOA and HT Ca-Fe metasomatites lead to recrystallization of original apatite and remobilisation of REE
3. Crystallisation of REE-bearing minerals (monazite, xenotime, etc.)
4. REE patterns of mineralisation zones commonly remain parallel to 'least-altered' IOA host supporting remobilisation without the need for additional REE from alkaline magmatism

Corriveau et al. 2016; De Toni 2016; Harlov et al. 2016; Montreuil et al. 2016b, c (cf. Perreault and Lafrance 2015; Hofstra et al. 2017)

Celebrating 175 yrs

Fluidised IOA ?

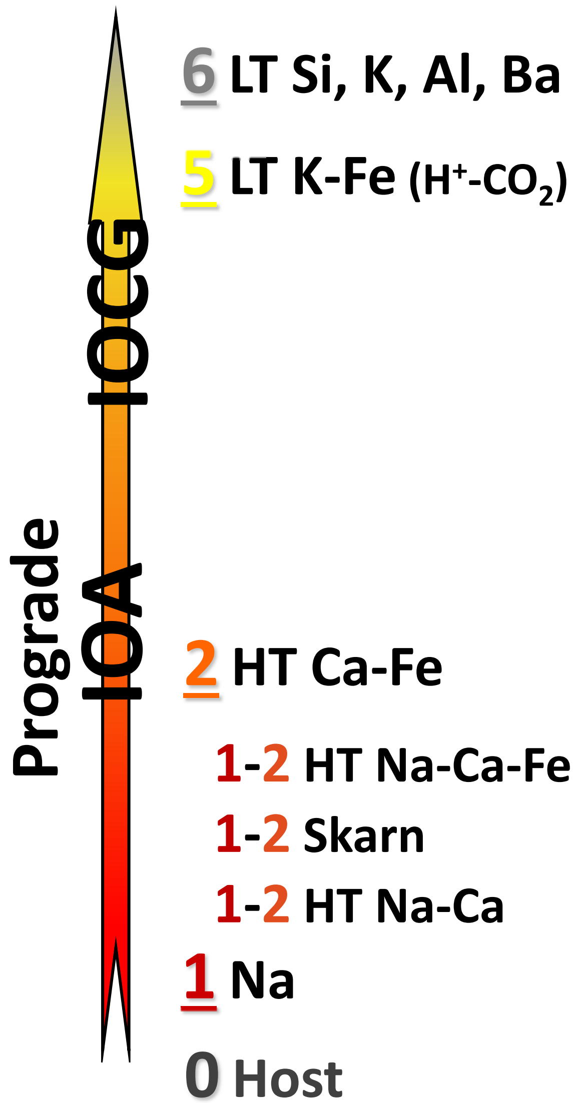

IOA ascending as fluidised breccias

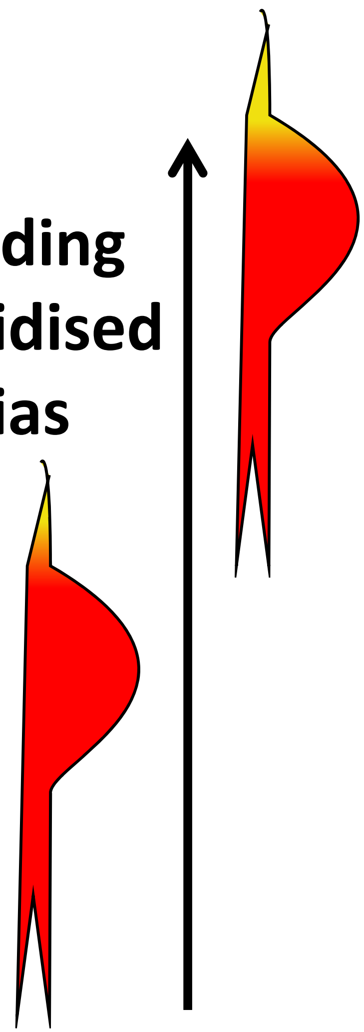

IOA fluidised breccias can ascend above original HT Ca-Fe alteration facies (e.g., Terra mine, Great Bear; Corriveau et al. unpublished data)

Is this mechanism involved in getting some IOA deposits near, or at surface ?

Modified from Corriveau et al. (2010b, 2016)

IOA deposits—Metal endowment

- **Kiirunavaara** (682 Mt, 47.5% Fe), **Malmberget** (271 Mt, 41.8%), **Kaunisvaara** (164.9Mt, 32.7%), **Grangesberg (Sweden)**
- **Oak Dam** (~560 Mt , 41–56%) **(+ Cu, U, Au)**, **Lightning Creek, Acropolis (Australia)**
- **Marcona** (~1940 Mt, 55.4%) (+ Cu), **Cerro Negro Norte** (377 Mt, 33%), **El Laco** (734 Mt, 49%), **Los Colorados** (943 Mt, 35%), **Romeral** (454 Mt, 28%) **(Andes)**
- **Bayan Obo (IOA?)** (1500 Mt, 35%) (+57 Mt, **6% REE_2O_3**; 2 Mt, **0.13% Nb_2O_5**), **Yinachang** (20 Mt, 42-44%) (+ Cu, REE), **Washan** (~214 Mt, 50% Fe), **(China)**
- **Cerro del Mercado, Peña Colorada** (300 Mt, 50-60%) **(Mexico)**
- **Pea Ridge** (160.6 Mt reserves, ~ 53-55%) + (0.2Mt, **12%TREE**), **Pilot Knob (US)**
- **Chador-Malu** (400 Mt, 55%), **Esfordi (Iran)**
- **Marmoraton** (28 Mt, 43%) **Kwyjibo** (REE) **(Canada)**

Alteration facies within systems help prognosticate the varied metal associations of IOA deposits

List of references for resources at slide 50

Stratabound high-Co IOCG variant

Prograde path + sustained fluid ingress at high to mid temperatures

Across metasedimentary sequences

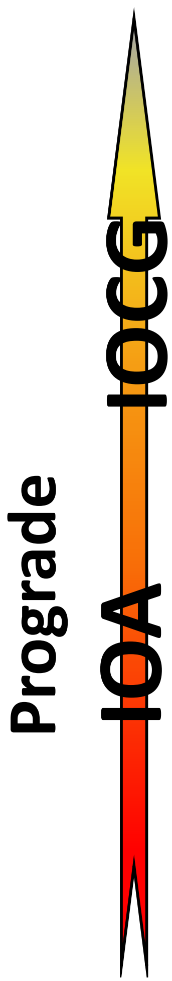

6 LT Si, K, Al, Ba

5 LT K-Fe (H^+-CO_2)

4 K-felsite + K-skarn breccias

3 HT K-Fe

2- 3 HT Ca-K-Fe

2 HT Ca-Fe

1-2 HT Na-Ca-Fe

1-2 Skarn

1-2 HT Na-Ca

1 Na

Low Cu, Au-Co-Bi variants of magnetite-group IOCG

Repeated ingress of Ca+Fe+Au+Co+Bi
Amp-Bt-Mag
Minor Kfs

Au-Co-Bi-Cu NICO
Great Bear, Canada
Corriveau et al. 2016

Goad et al. 2000; Corriveau et al. 2010b, 2016; Mumin et al. 2010; Acosta-Góngora et al. 2015a, b; Montreuil et al. 2015, 2016b

Stratabound magnetite-group IOCG

Prograde path associated with sustained fluid ingress at high to mid temperatures

Across metasedimentary sequences

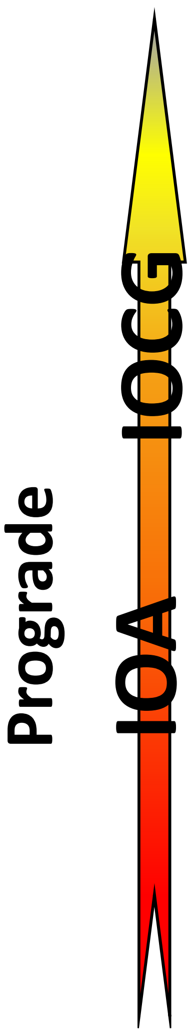

- **6** LT Si, K, Al, Ba
- **5** LT K-Fe (H^+-CO_2)
- **4** K-felsite + K-skarn breccias
- **3** HT K-Fe
  - **2- 3** HT Ca-K-Fe
- **2** HT Ca-Fe
  - **1-2** HT Na-Ca-Fe
  - **1-2** Skarn
  - **1-2** HT Na-Ca
- **1** Na

Amp-Bt-Mag evolves to Bt-Mag
Minor Kfs
Stratabound replacement
Amp-Grt-Bt forms if deformed and recrystallised as metasomatism proceeds

Dahongshan, China
Zhao et al. 2017b

Modified from Corriveau et al. 2010b, 2016

Breccia-hosted magnetite-group IOCG

Reaches intense HT K-Fe alteration with abundant Kfs in any host rocks

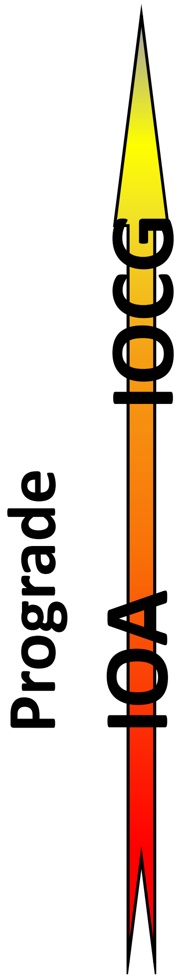

- 6 LT Si, K, Al, Ba
- 5 LT K-Fe/Ca-Fe-Mg (H^+-CO_2)
- 4 K-felsite + K-skarn breccias
- 3 HT K-Fe (Kfs-Mag)
- 3 HT K-Fe (Bt-Mag)
- 2- 3 HT Ca-K-Fe
- 2 HT Ca-Fe
- 1-2 HT Na-Ca-Fe
- 1-2 Skarn
- 1-2 HT Na-Ca
- 1 Na

Repeated ingress of Kfs-Mag, Bt-Mag
Then goes to LT Cc-Mag

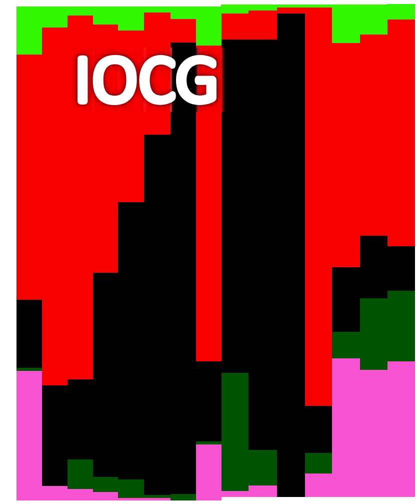

Ernest Henry
Australia

Prograde path +
Sustained fluid ingress at high to mid temperatures

Modified from Corriveau et al. 2010b, 2016

Metasomatic reaction paths

Prograde path with sustained fluid ingress at mid to low temperature

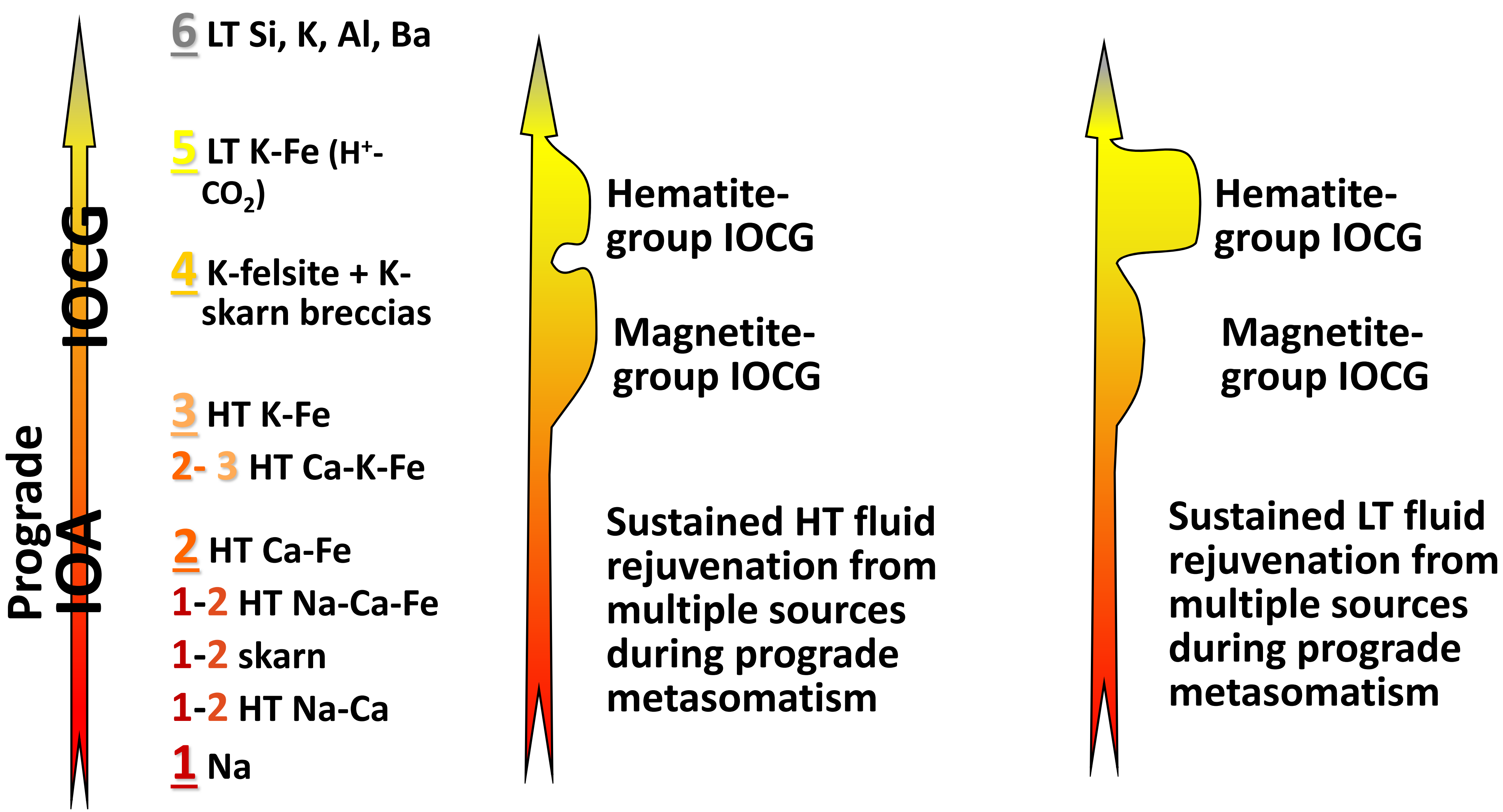

Modified from Corriveau et al. 2010b, 2016

Metasomatic reaction paths for albitite-hosted U

Differential exhumation during telescoping of alteration facies

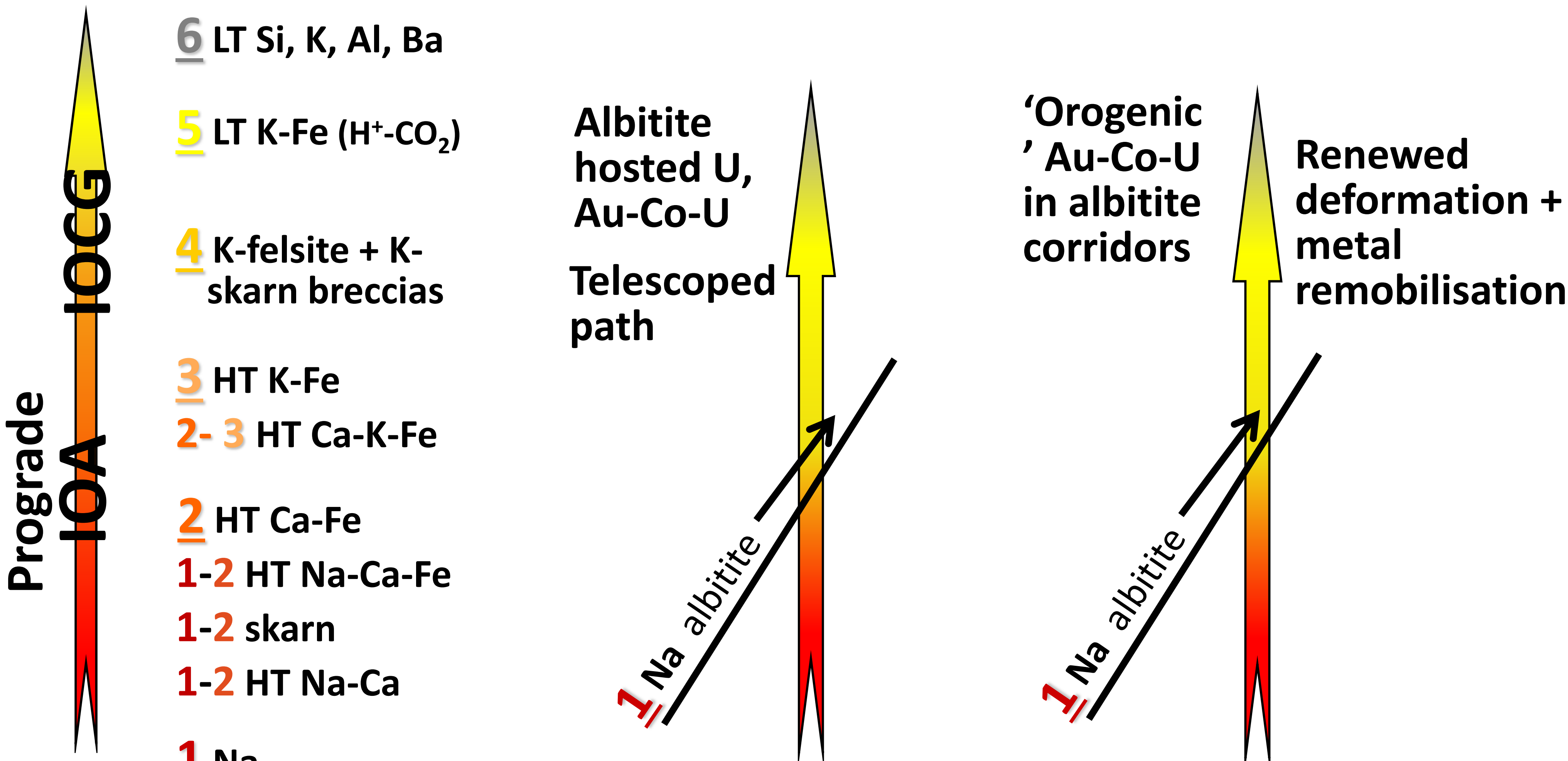

Modified from Corriveau et al. 2010b, 2016, 2017; Wilde 2013; Montreuil et al. 2015, 2016b, c; Hayward et al. 2016

Metasomatic facies

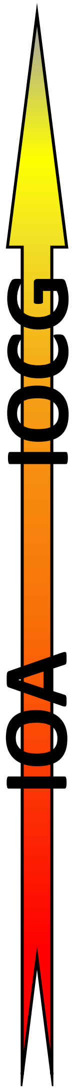

6 LT Si, K, Al, Ba

5 LT K-Fe (H^+-CO_2)

4a K-felsite

4b K-skarn

3 HT K-Fe

2- 3 HT Ca-K-Fe

2 HT Ca-Fe

1-2 HT Na-Ca-Fe

1-2 Skarn

1-2 HT Na-Ca

1 Na

0 Host

Prograde

Retrograde

Cyclical

Telescoped

- A petrological mapping tool
- A geological exploration tool
- A mean to unify ore systems with varied, even disparate, metal associations and deposit types and develop coherent exploration strategies

Olympic Dam

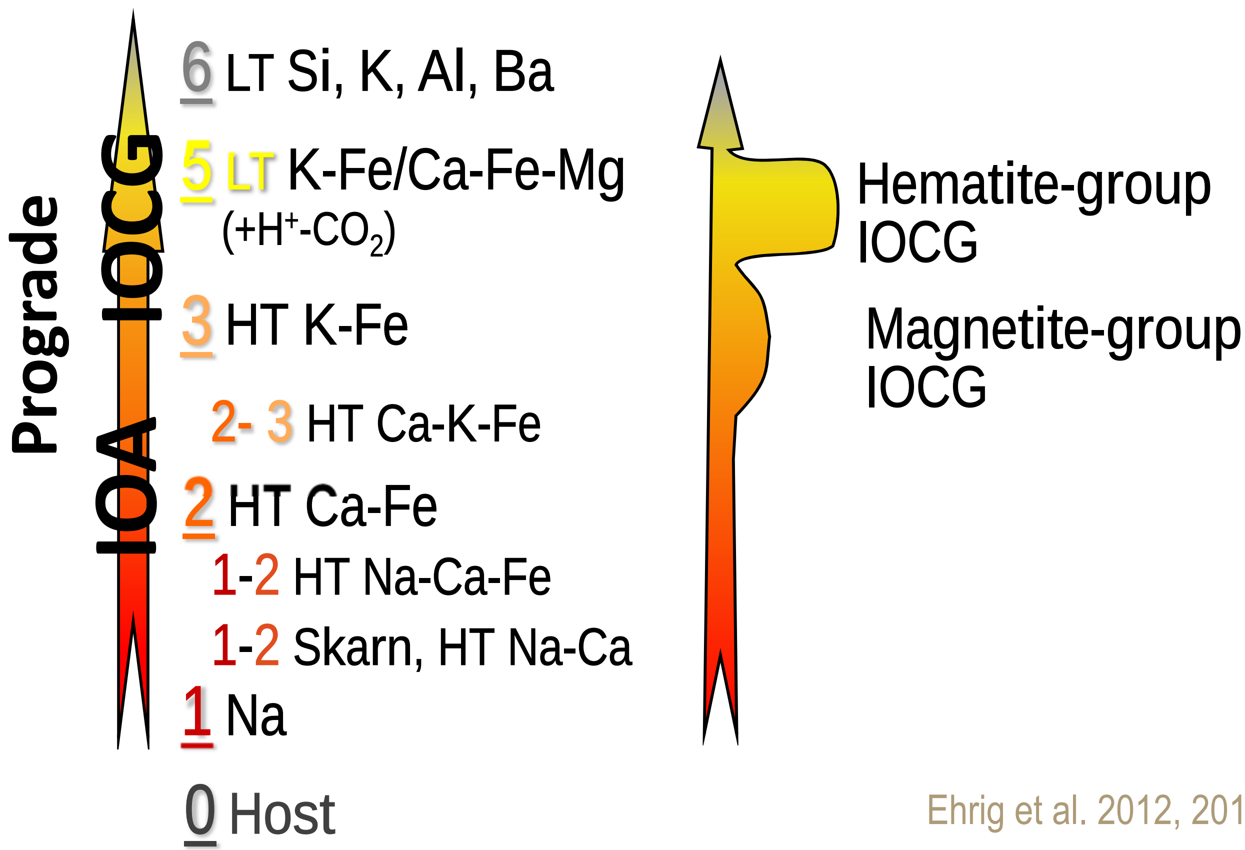

+ Episodic metal remobilisation (ex., U) through renewed fluid circulation after the development of host IOAA system

Ehrig et al. 2012, 2017; Macmillan et al. 2016; Cherry et al. 2017

Olympic Cu-Au Province
Gawler craton

Large igneous felsic, silicic province extending along 700 km

I-type + A-type magmatism with juvenile components

Plutonic and volcanic components

A-type granites
- **Evidence of high temperature magmas** (>900ºC; see Creaser 1996)
- **No evidence of anorogenic rift**

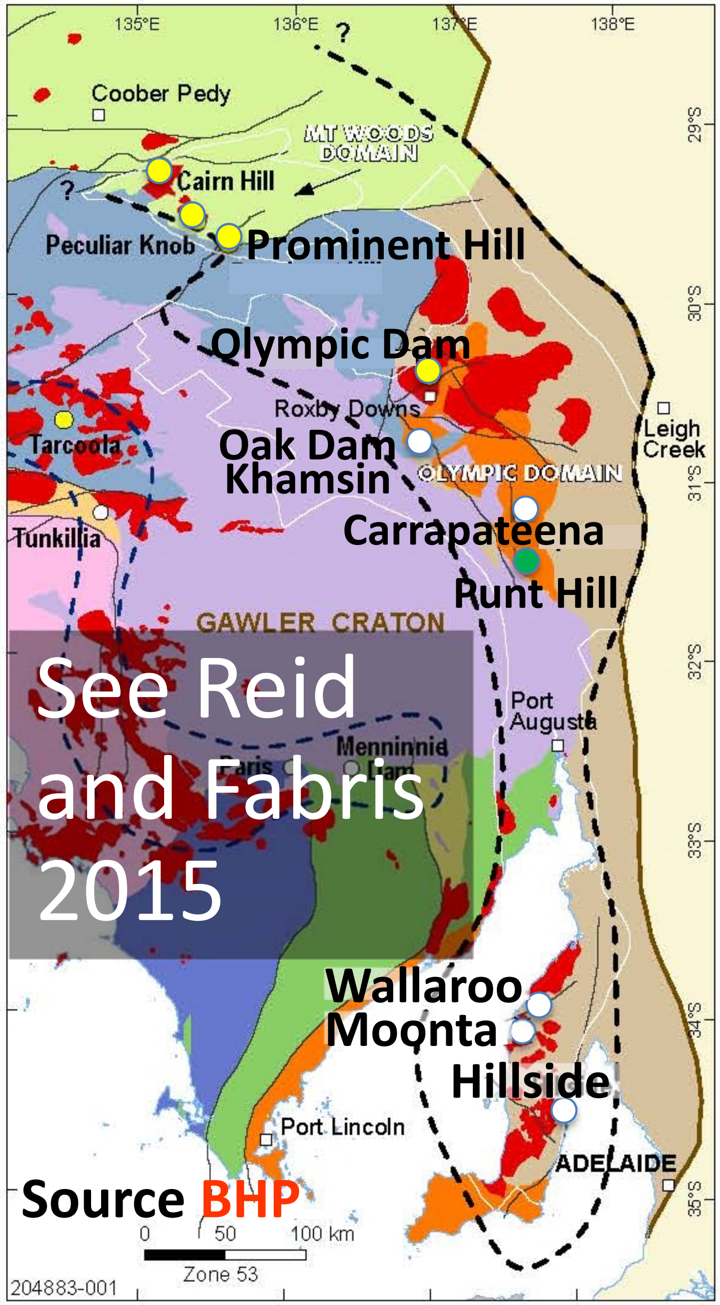

- Major mines
- Deposits (IOAA)
- Skarn
- X Historical mining districts
- Olympic Cu-Au Province
- Central Gawler Au Province

Geology
- Gawler Range volcanic, 1.59 Ga
- Hiltaba granite, 1.59 Ga
- 1.62 Ga volcano-plutonic suite
- 1.69-1.67 Ga plutonic suite
- 1.75 Ga supracrustal rocks
- 1.79-1.74 Ga metamorphic rocks
- 2-1.74 Ga metamorphic rocks
- 1.85 Ga granites
- 2.55-2.41 Ga complex
- 2.53-2.41 Ga, gneiss
- 3.2-3.15 Ga granite, gneiss
- Major shear zones

Haynes et al. 1995; Hayward and Skirrow 2010; Skirrow 2010; Ehrig et al. 2012, 2017; Reid et al. 2017

Celebrating 175 yrs

Key elements for metal endowment

Hayward and Skirrow (2010)

"… reworked lithosphere with **older** [> ~1590 Ma] metasomatised SCLM…"

"…high frequency of trans-lithospheric shear zones…"

"…oxidised A-type plutons…"

"…juvenile magmatic input manifest in mafic-ultramafic intrusions and basalts…"

"…abundance of mafic volcanics in the lower Gawler Range Volcanics"

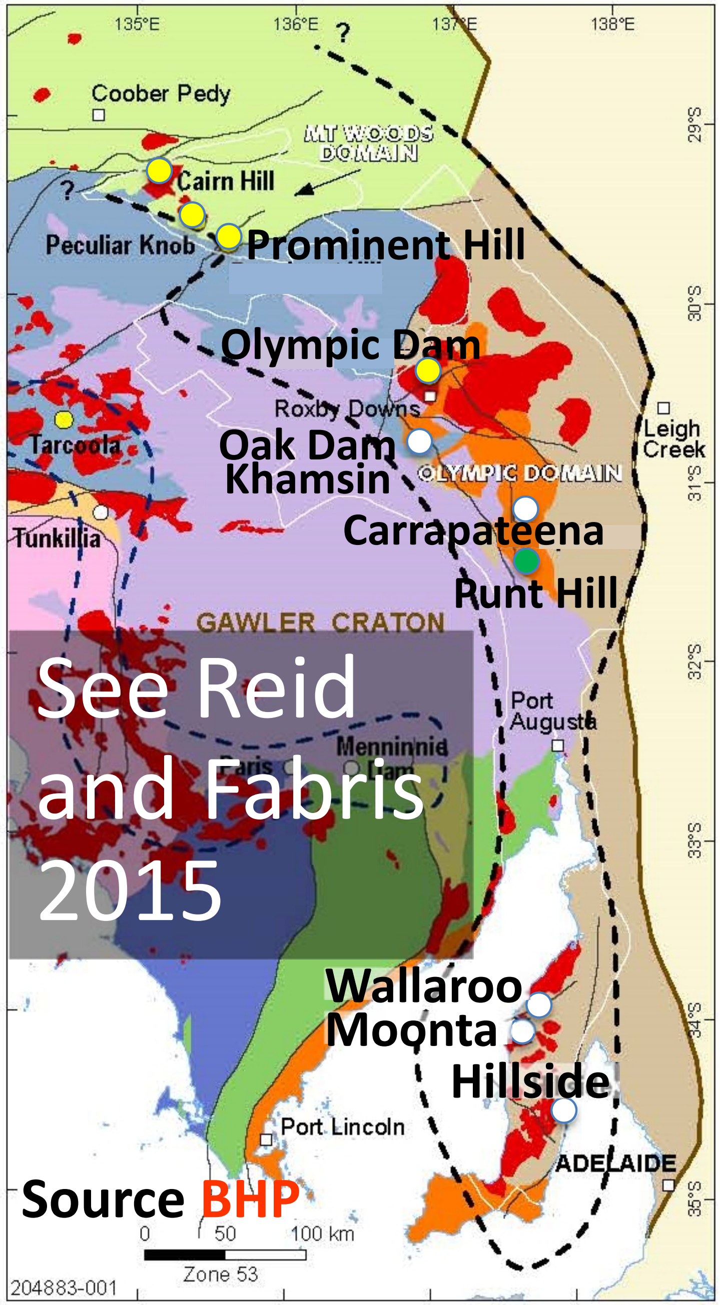

See also Haynes et al. 1995; Hitzman and Valenta 2005; Groves et al. 2010; Skirrow 2010; Ehrig et al. 2012, 2017; Kontonikas-Charos et al. 2017

- Major mines
- Deposits (IOAA)
- Skarn
- X Historical mining districts
- Olympic Cu-Au Province
- Central Gawler Au Province

Geology

- Gawler Range volcanic, 1.59 Ga
- Hiltaba granite, 1.59 Ga
- 1.62 Ga volcano-plutonic suite
- 1.69-1.67 Ga plutonic suite
- 1.75 Ga supracrustal rocks
- 1.79-1.74 Ga metamorphic rocks
- 2-1.74 Ga metamorphic rocks
- 1.85 Ga granites
- 2.55-2.41 Ga complex
- 2.53-2.41 Ga, gneiss
- 3.2-3.15 Ga granite, gneiss
- Major shear zones

Olympic Dam

- Fe-oxide Cu-U-Au-Ag deposit
- Under ~350m of unaltered 'cover sequence'
- Hosted in a tectonic–magmatic-hydrothermal (metasomatic) breccia *Olympic Dam Breccia Complex ~50 km²*
- Within ~1594 Ma Roxby Downs Granite
- Deposit footprint ~6 km x 3 km x 800 m
- Fe increases from edge to centre

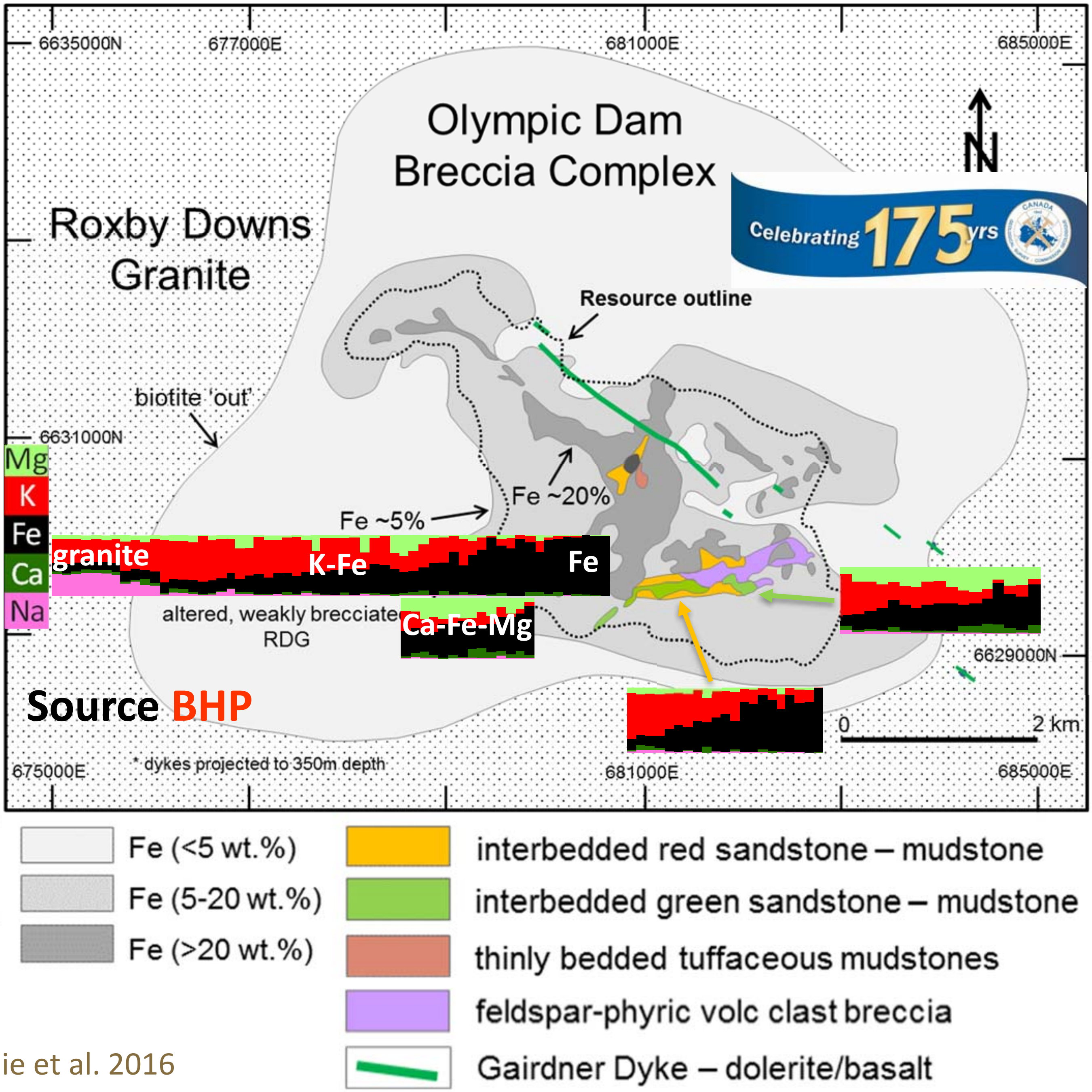

Figure modified from Ehrig et al. 2012
Geochemical data: Ehrig et al. 2012; McPhie et al. 2016

Olympic Dam

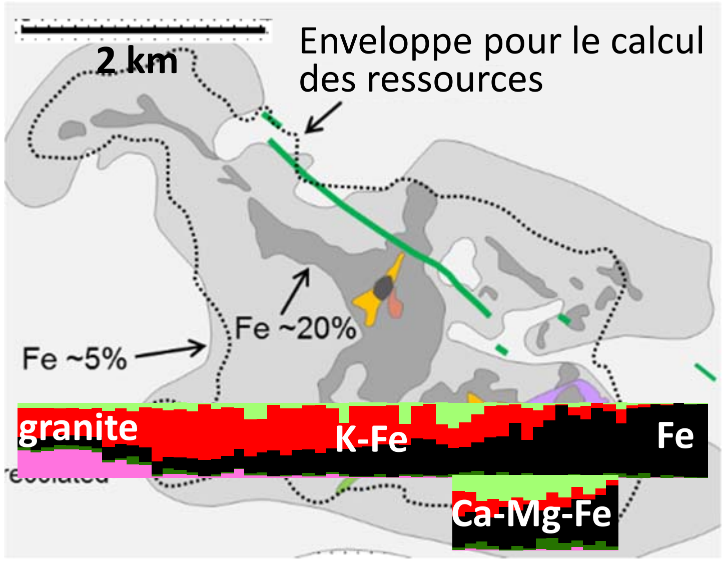

K-Fe and K-Fe+Ca-Fe-Mg alteration of granite

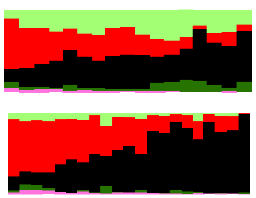

Green sandstone and wacke

Red sandstone and wacke

Typical composition of K-Fe and LT Ca-Fe-Mg alteration facies

Alteration:

- **Na** (Ab)
- **HT Ca-Fe** (Mag-Ap + Sd-Chl-Qz)
- **LT K-Fe** (Hem-Kfs-Ser-Fl\Hem-Ser-Fl\Hem-Qz-Brt)
- **LT Fe** (Hem-Qz-Brt)
- **Sulphide minerals** (Sp\Gn\Py\Ccp\Bn\Cct)
- **LT Ca-Fe-Ba-C-F-S** (Sd\Fl\Brt)
- **Advanced argillic** (Ser-Qz ± Al-OH)

Positive correlation of Fe vs Ag, As, Au, Ba, Bi, Cd, Co, CO_2, Cr, Cu, F, Fe, In, Mo, Nb, Ni, P, Pb, S, Sb, Se, Sn, Sr, Te, U, V, W, Y, Zn, REE

Figure modified from Ehrig et al. 2012

See Haynes et al. 1995; Hitzman and Valenta 2005; Skirrow 2010; Ehrig et al. 2012, 2017; Kontonikas-Charos et al. 2016, 2017

Olympic Dam alteration and mineralisation

- Fe-oxide (Fe^{+2} → Fe^{+3})
- Magnetite+apatite+chlorite → hematite+K-feldspar-sericite+siderite
- Siderite → fluorite → barite
- Hypogene: Py → Ccp → Bn → Cct → Cu/Au
- Polymetallic Zn-Pb-Ag and Mo-Sn-W associations
- Uraninite - coffinite - brannerite
- Two styles of gold mineralisation (sulphide and non-sulphide)

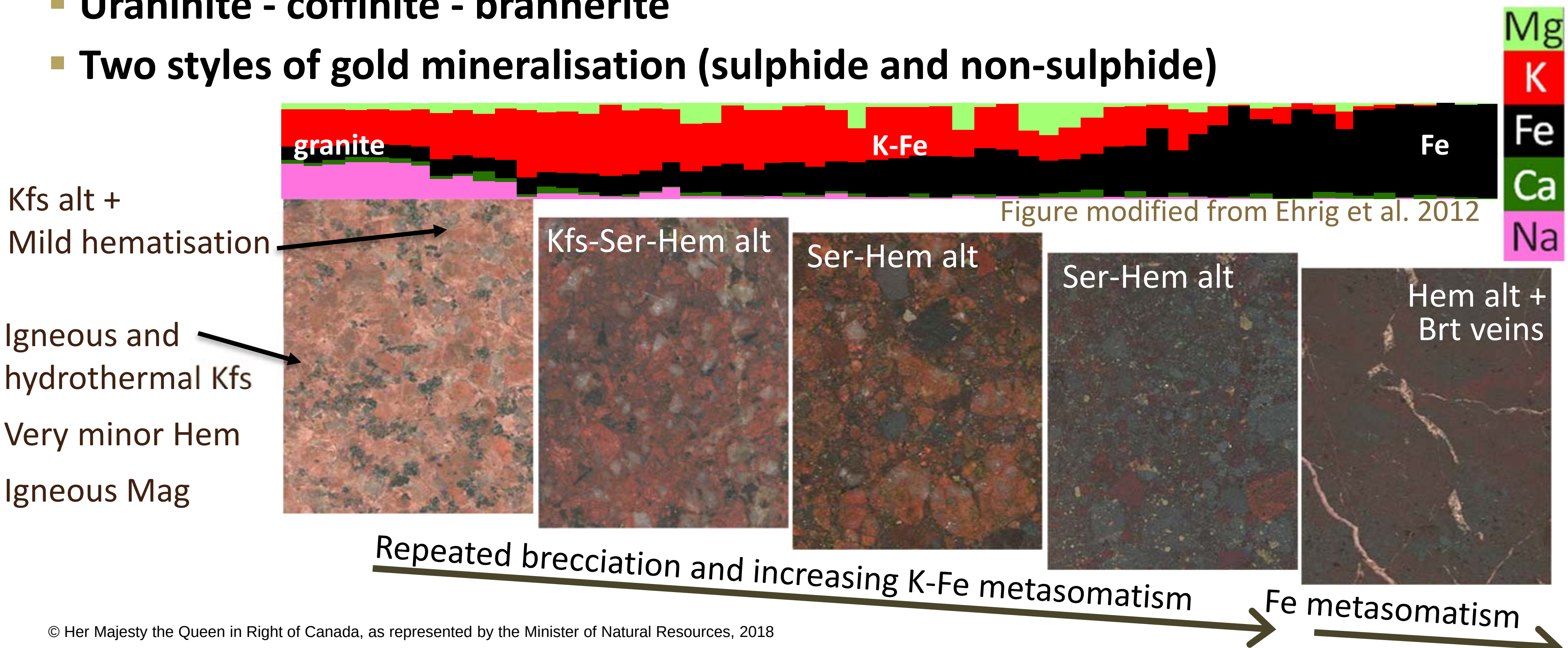

Source BHP

Olympic Dam breccias

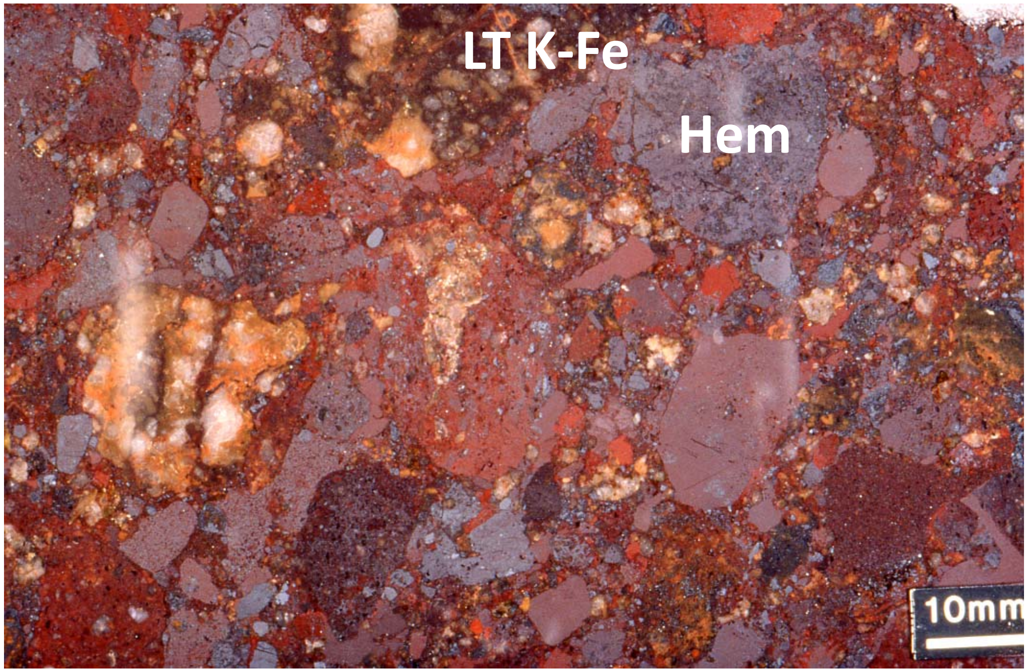

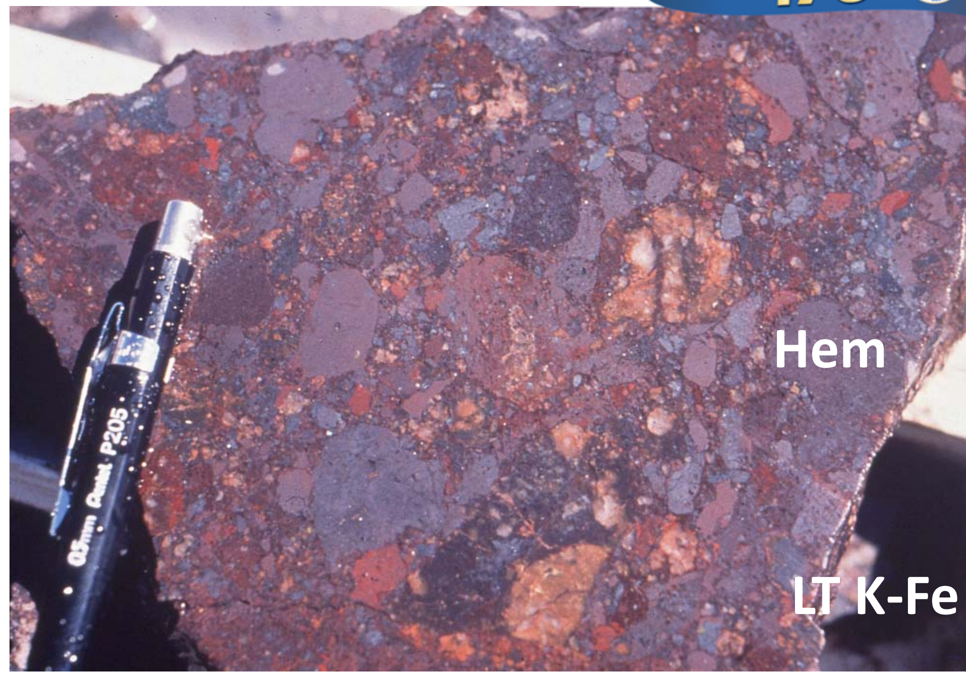

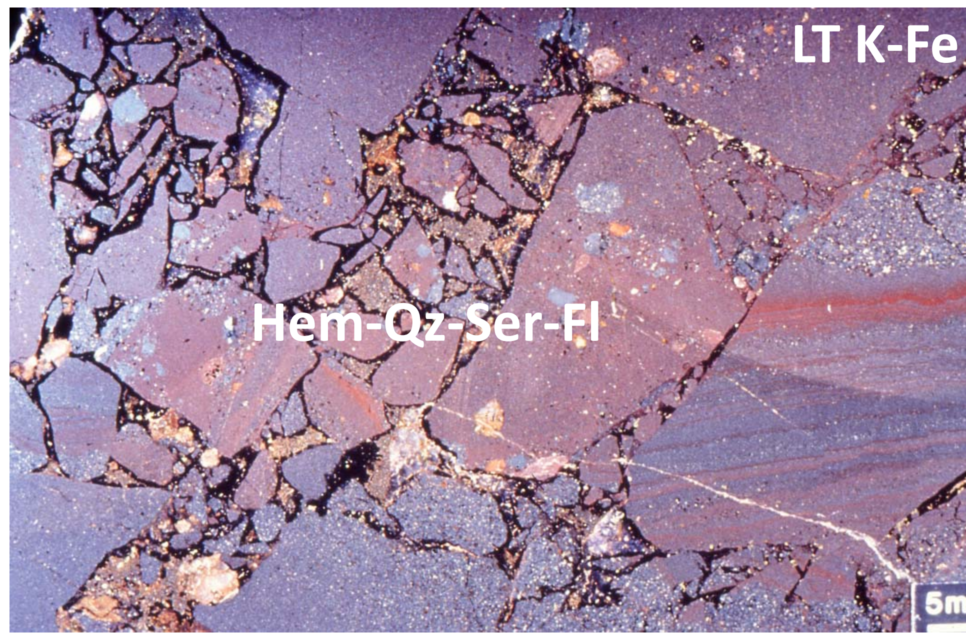

Source BHP

Olympic Dam, Gawler craton, Australia

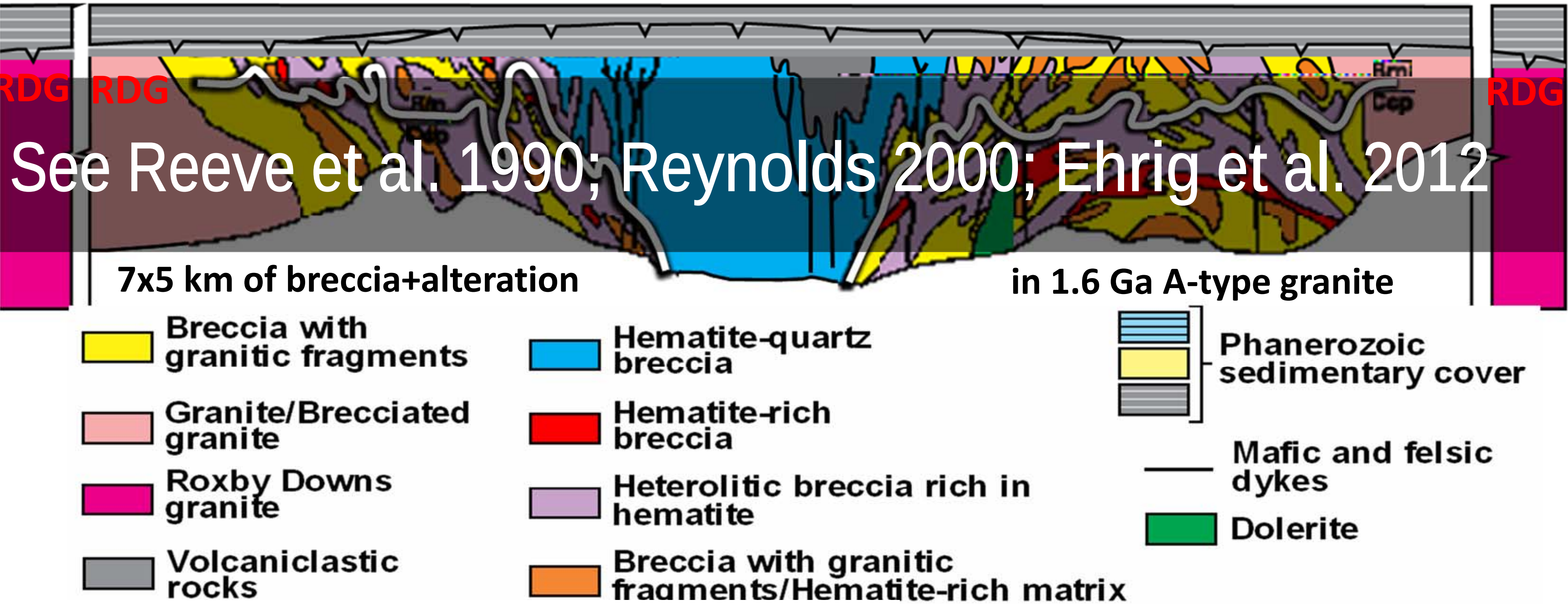

Alteration

- **Na, HT Ca-Fe** (Mag-Ap+Sd-Chl-Qz)
- **LT K-Fe** (Hem-Ser-Fl\Hem-Qz-Brt)
- **LT Fe-Ba-F** (Sd\Fl\Brt)
- **Ore** (Sp\Gn\Py\Ccp\Bn\Cct)
- **LT Fe** (Hem-Qz-Brt)
- **Advanced argillic alteration** (Ser-Qz± Al-OH)

RDG: Roxby Down granite, host of the Olympic Dam deposit

Fe-Cu sulphides, U, REE minerals

Olympic Dam chemical variations

Kfs-Ser altered granite cut by a bornite vein
(RD 2737, 593m)

Typical signature of epithermal alteration

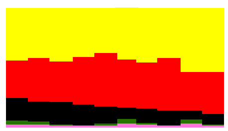

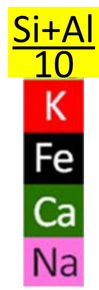

Typical signature of prograding IOCG mineralisation from K-Fe to Fe

Signature of HT Ca-K-Fe or K-Fe replaced by carbonates

Signature of Fe + Qz veins

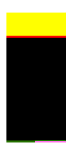

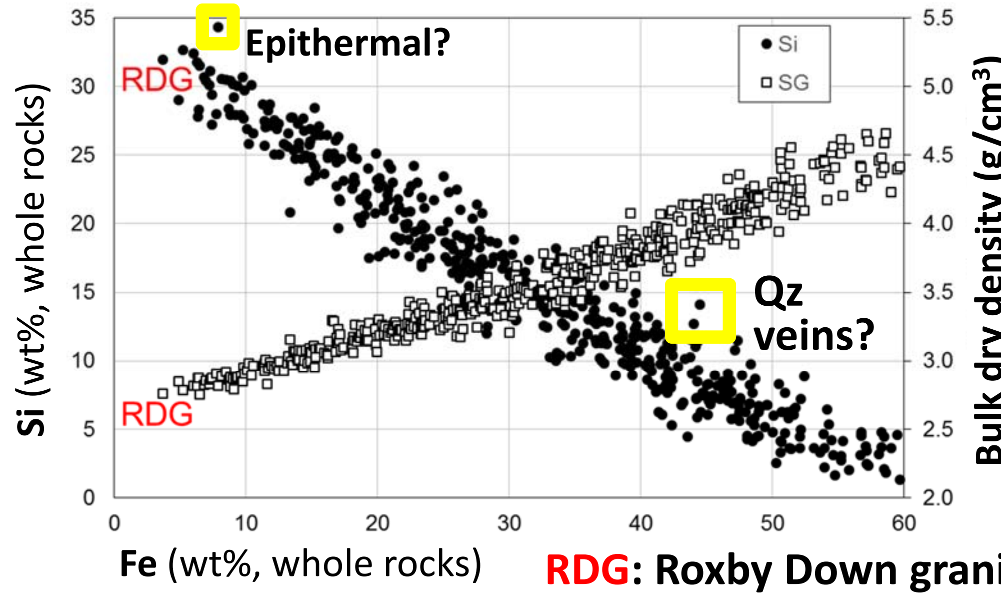

RDG: **Roxby Down granite**

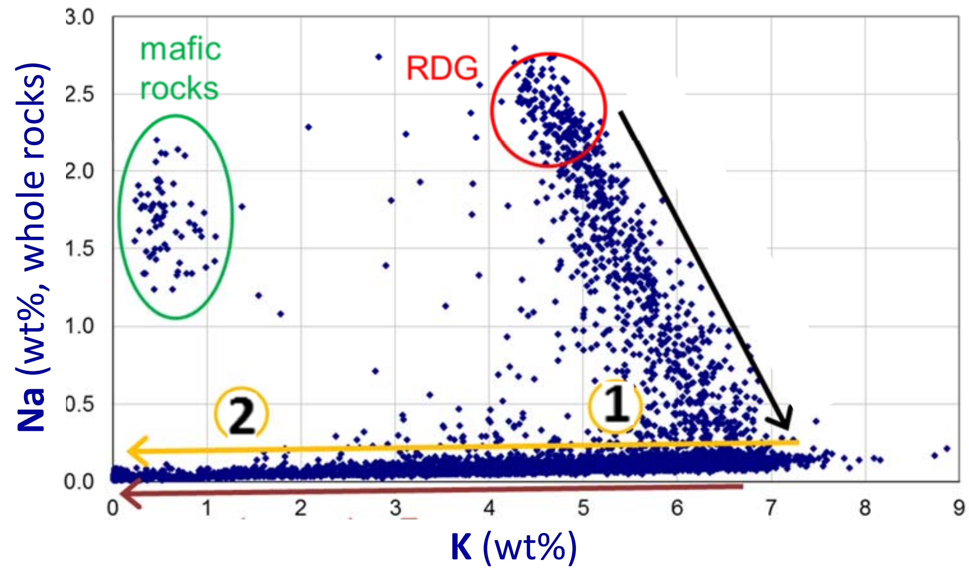

1- Transition Kfs-Hem to Ms (Ser)-Hem
2- Hem replace Ms (Ser)

Olympic Dam chemical trend

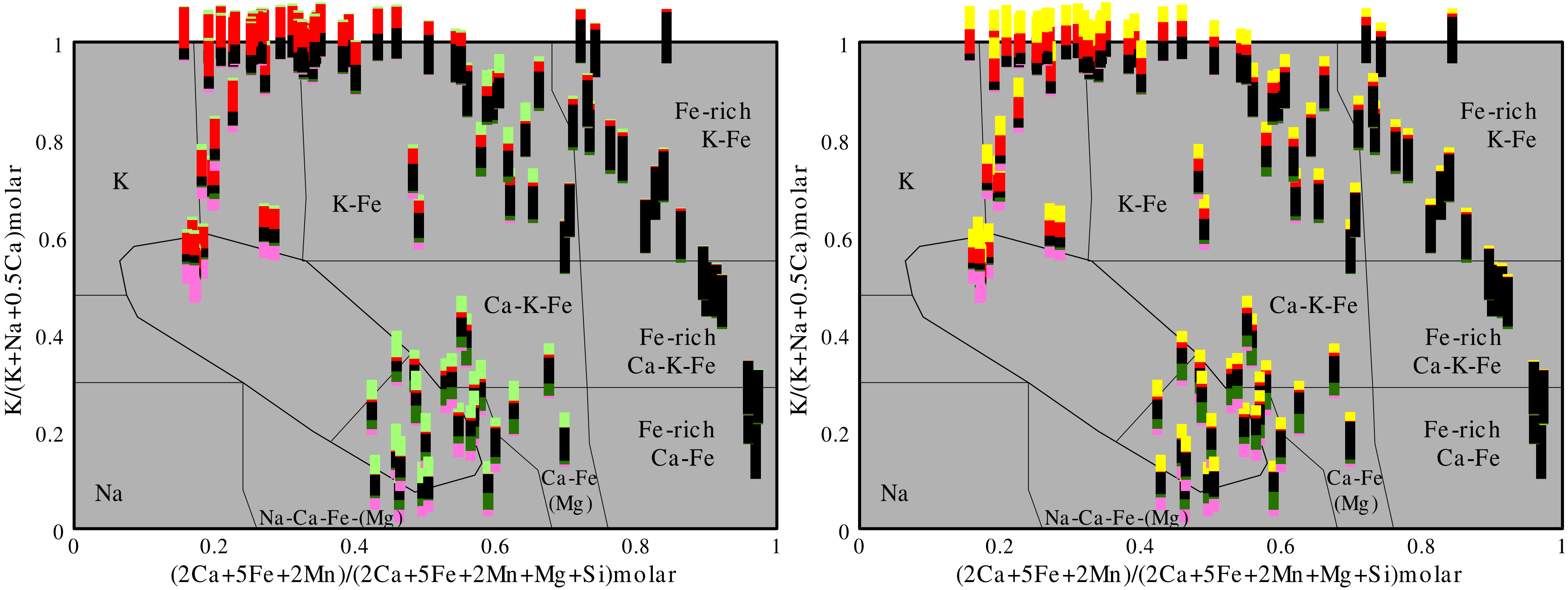

Element bar charts on the IOCG discriminant diagram record the evolution of the metasomatism across the Roxby Downs Granite host to Olympic Dam. The granitoid is progressively altered along a clock wise trend from the least-altered field to the K-Fe and then the Fe-rich alteration and finally into the Fe-rich Ca-Fe due to carbonate alteration. Another trend records the impact of low temperature chlorite-sericite metasomatism.

Data: Ehrig et al. 2012; McPhie et al. 2016; Huang et al. 2016; Discriminant diagram: Montreuil et al. 2016a

Quantitative Hematite – K-feldspar – Sericite

(-400mRL)

Distribution of K-feldspar and hematite (below 20%) defines a Kfs-rich LT K-Fe alteration facies

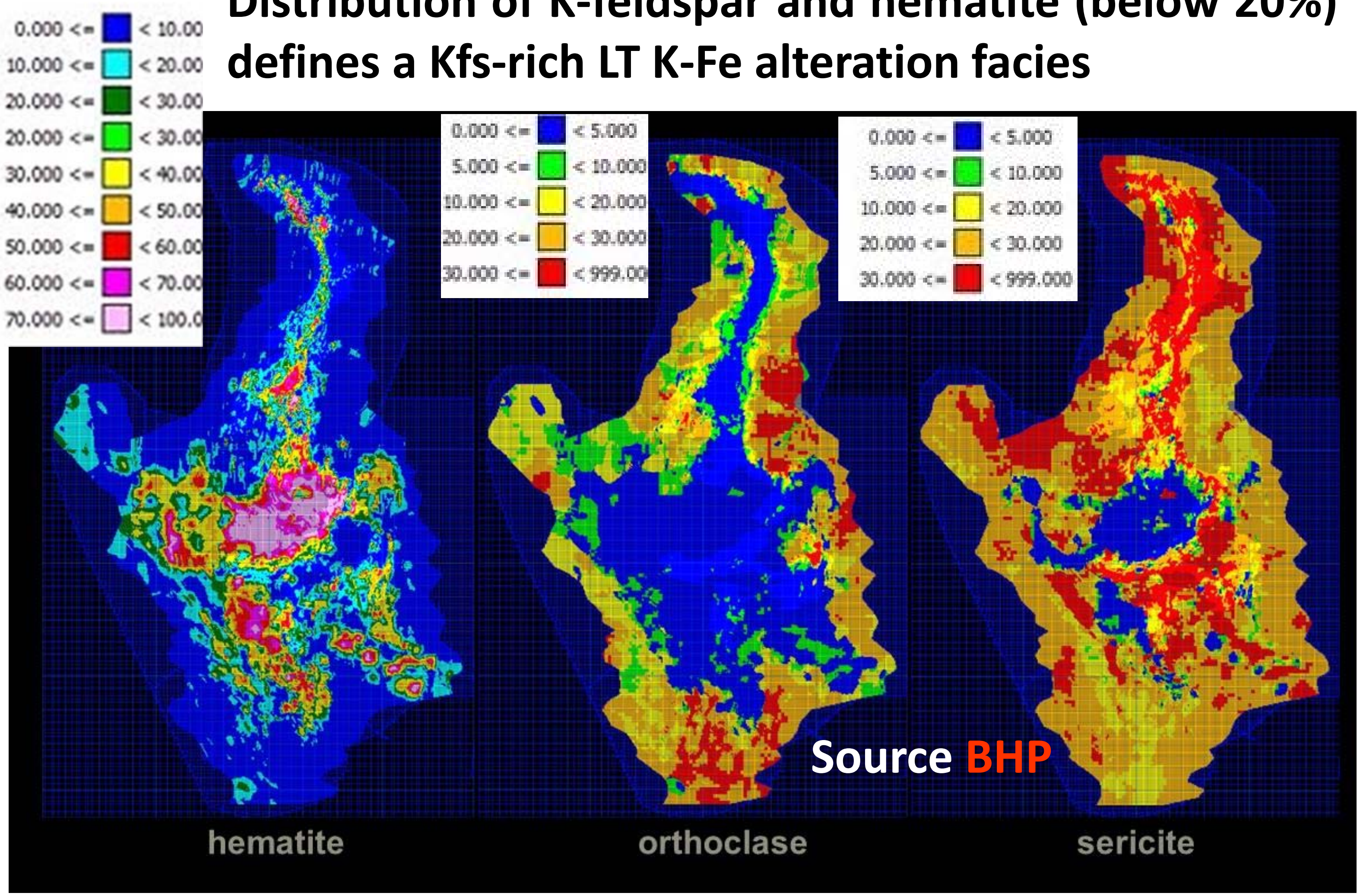

Quantitative Siderite-Fluorite-Barite

(-400mRL)

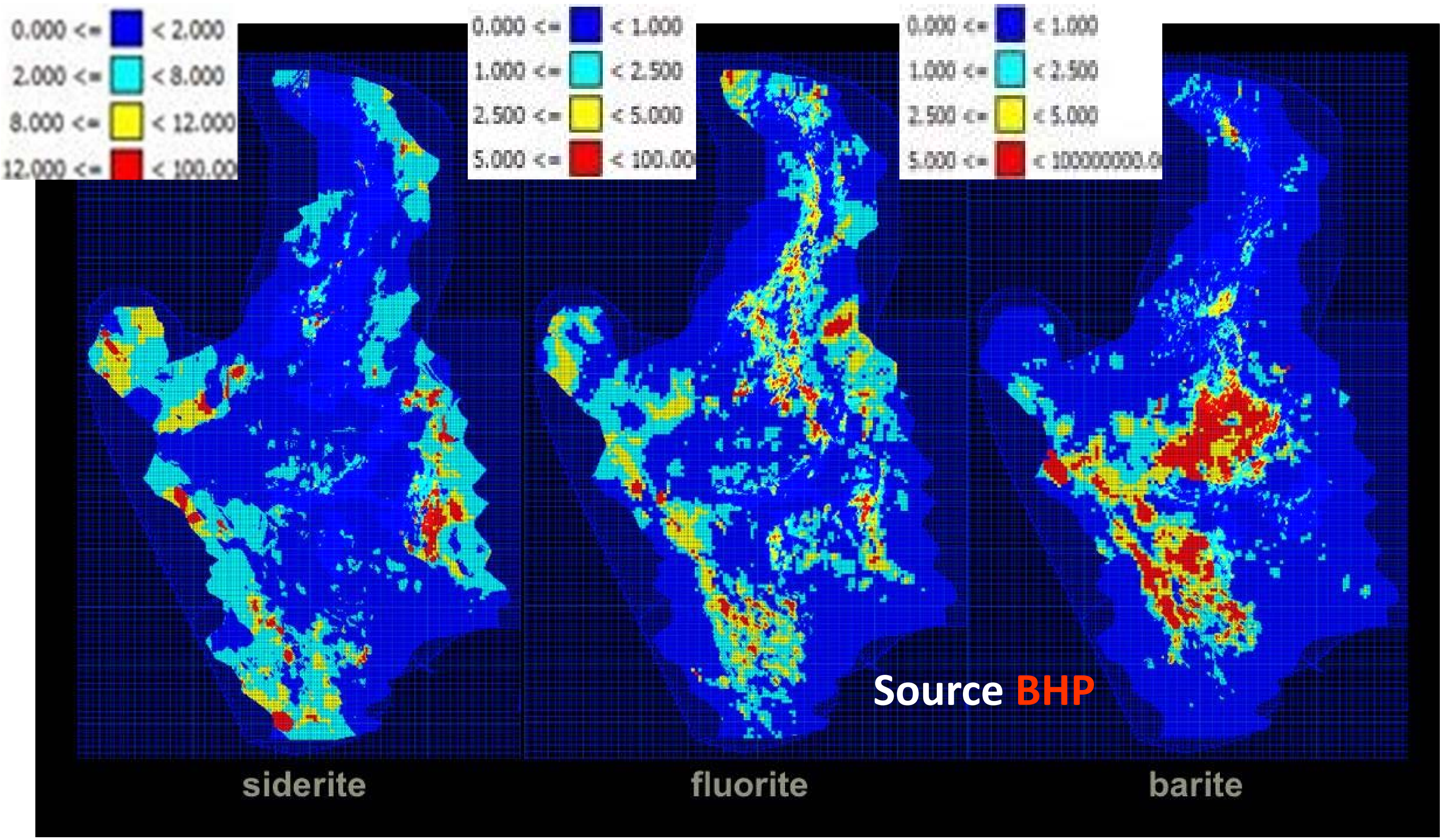

Celebrating 175 yrs

Cu-U_3O_8Pb distribution at ~400m below surface

Cu

Cu: within LT K-Fe alteration facies

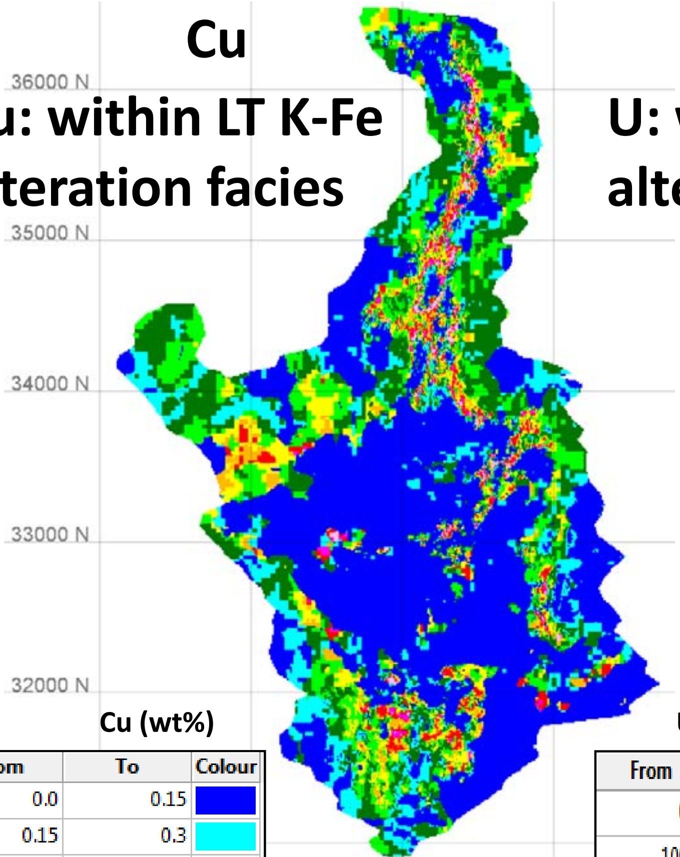

Cu (wt%)

From	To	Colour
0.0	0.15	blue
0.15	0.3	cyan
0.3	0.6	dark green
0.6	1.0	green
1.0	1.5	yellow
1.5	2.0	orange
2.0	3.0	red
3.0	4.0	magenta
4.0		pink

U_3O_8

U: within LT K-Fe alteration facies

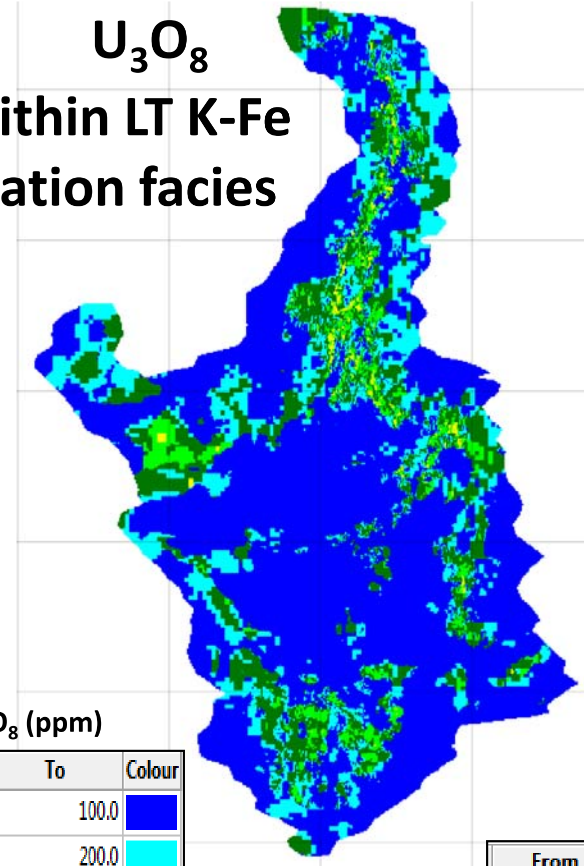

U_3O_8 (ppm)

From	To	Colour
0.0	100.0	blue
100.0	200.0	cyan
200.0	500.0	dark green
500.0	1000.0	green
1000.0	10000.0	yellow
10000.0	40000.0	orange
40000.0		red

Pb

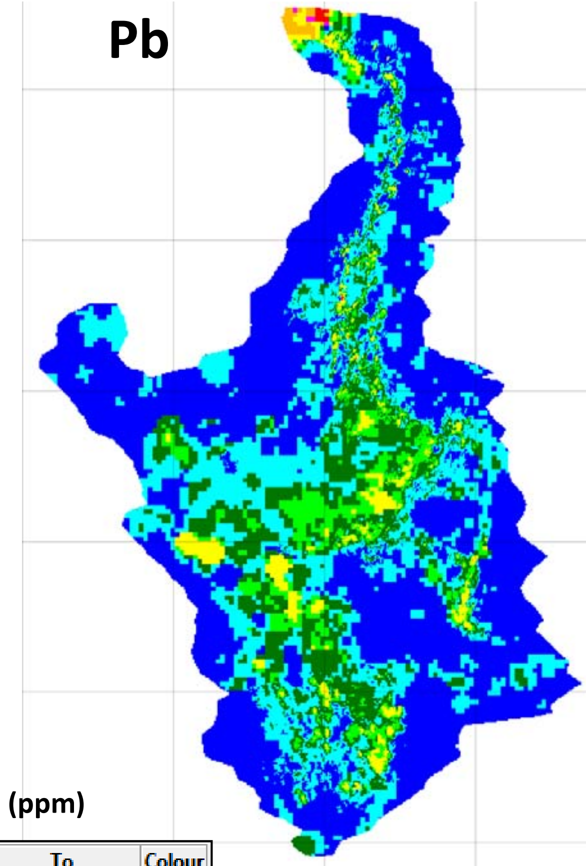

Pb (ppm)

From	To	Colour
0.0	25.0	blue
25.0	50.0	cyan
50.0	75.0	dark green
75.0	100.0	green
100.0	300.0	yellow
300.0	500.0	orange
500.0	1000.0	red
1000.0		magenta

Source BHP

Olympic Dam alteration facies

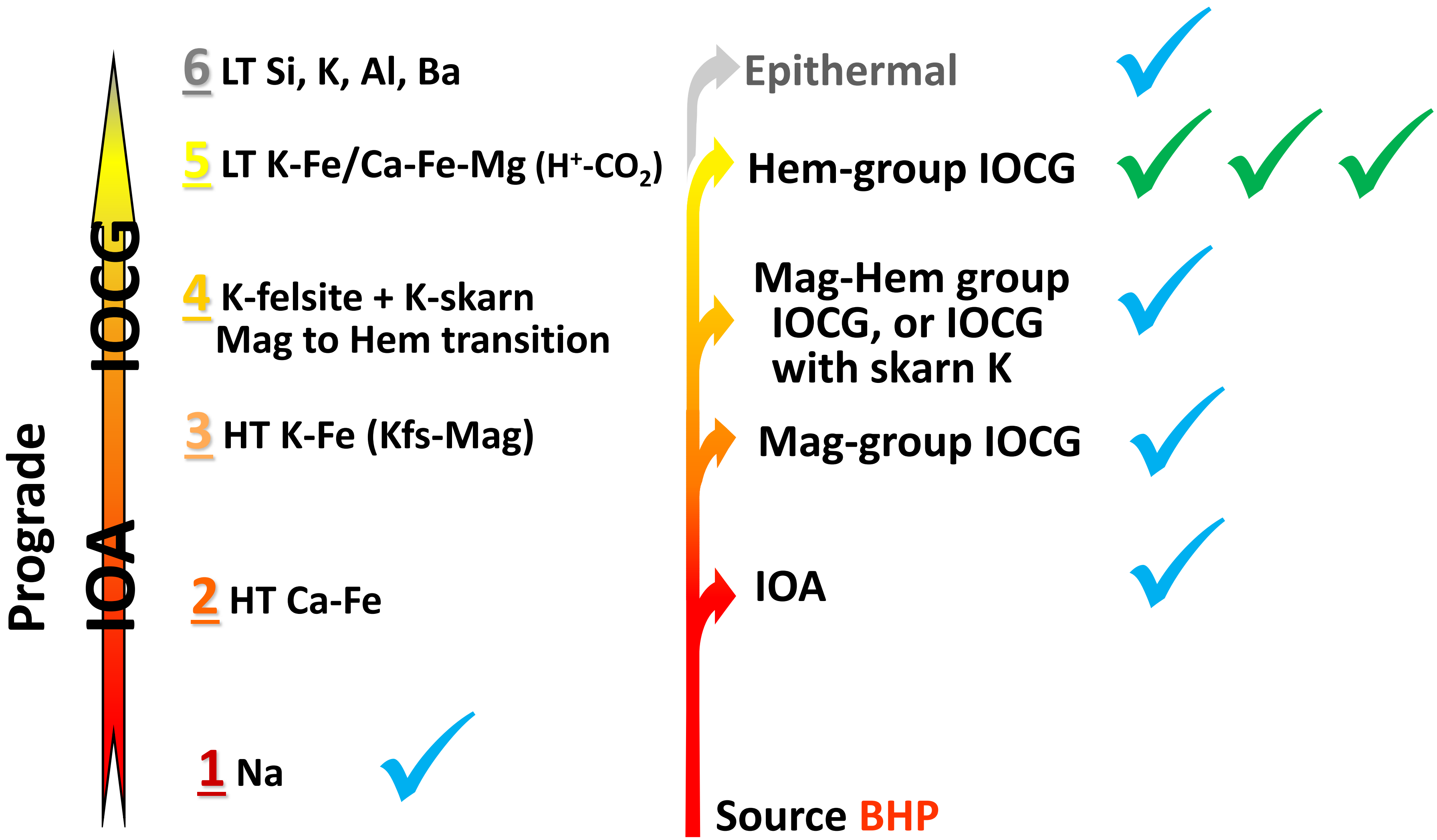

Modified from Corriveau et al. 2016

Crustal architecture of the Olympic Dam region

- **Fold-thrust belt + Doubly-vergent orogen: original interpretation of Drummond et al. (2006) being revised following reprocessing of seismic line (see Wise et al. 2016)**
- **Reflective crustal-scale ramp (thrusts)**
- **Abrupt decrease in Moho and lower crust reflectivity**
- **Along an Archean craton margin**
- **Melting of metasomatised sub-continental lithosphere**
- **Shear zones active at 1.59 Ga, some faults are magnetite altered**
- **Faults interpreted as first order conduits for the IOCG systems**
- **Vertical zones of reduced reflectivity across the upper crust below some of the main mineral systems (magma pathways, hydrothermal alteration such as albitite corridors?)**
- **Iron alteration leading to series of reflectors that extend across a 300 m wide to ~3 km depth**

See figures in Drummond et al. (2006), Hayward and Skirrow (2010) and Wise et al. (2016); see also Corriveau (2007), Griffin et al. (2013) and Thiel et al. (2016) for the importance of mantle to crust pathways for magmas, metals and fluids, including in IOCG ore systems.

Olympic Domain
Falcon Gravity and TMI (RTP 1VD)

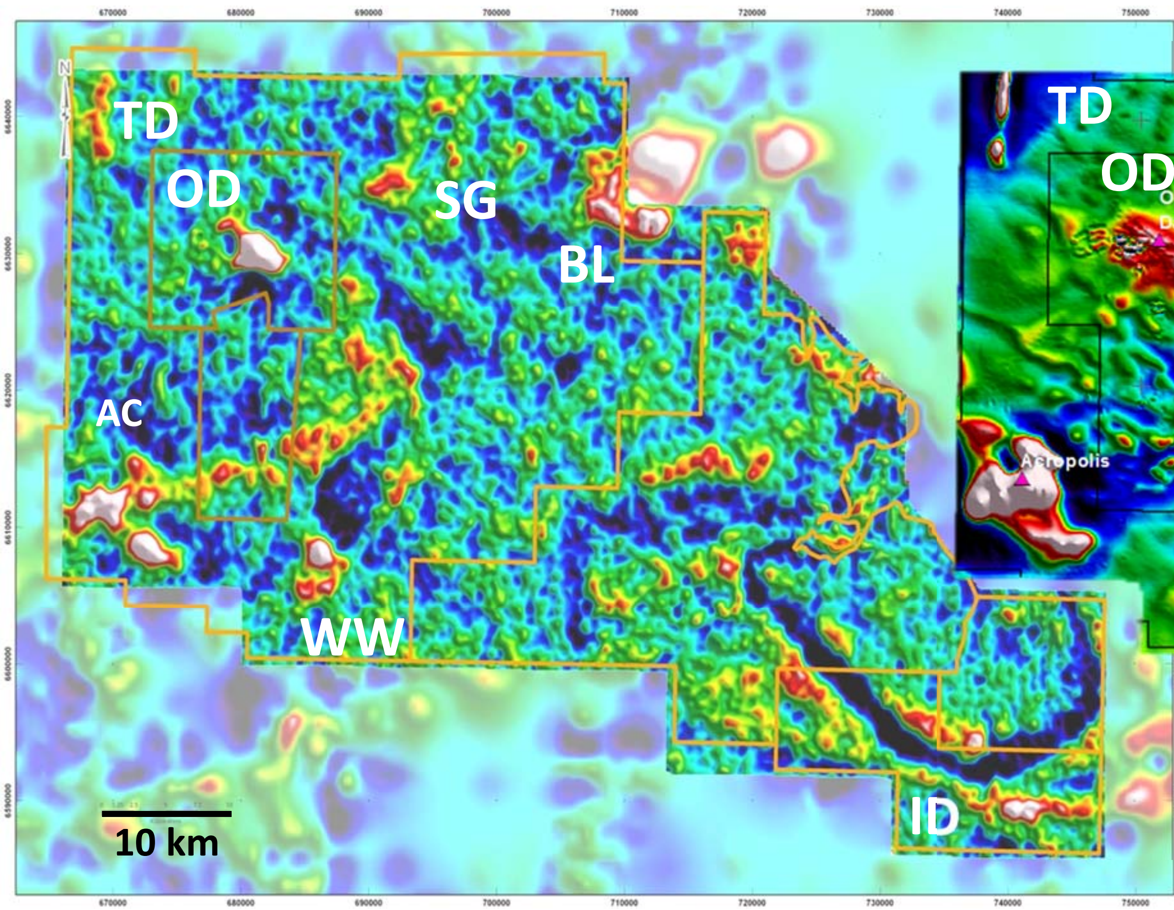

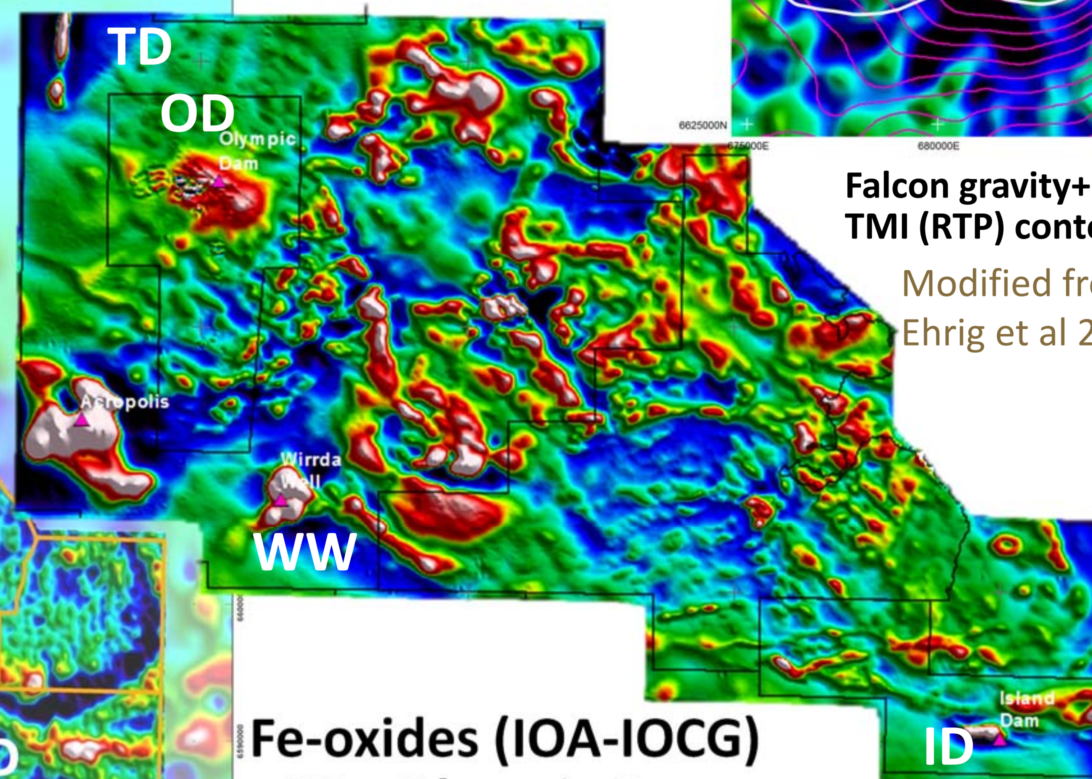

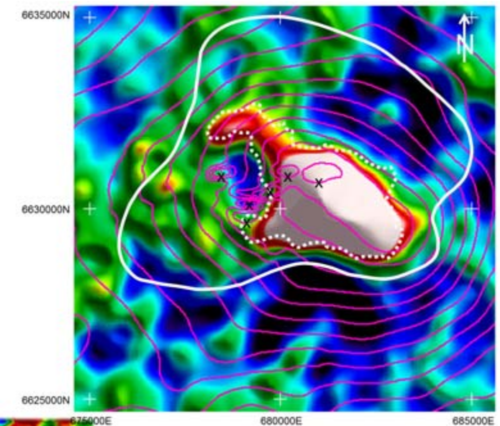

Falcon gravity+ TMI (RTP) contours

Modified from Ehrig et al 2012

Fe-oxides (IOA-IOCG)

- OD- Olympic Dam
- WW- Wirrda Well
- AC- Acropolis
- SG- Snake Gully
- BL- Bill's Lookout
- ID- Island Dam
- TD- Todd Dam

Source BHP

Acropolis and Wirrda Well
Alteration indices

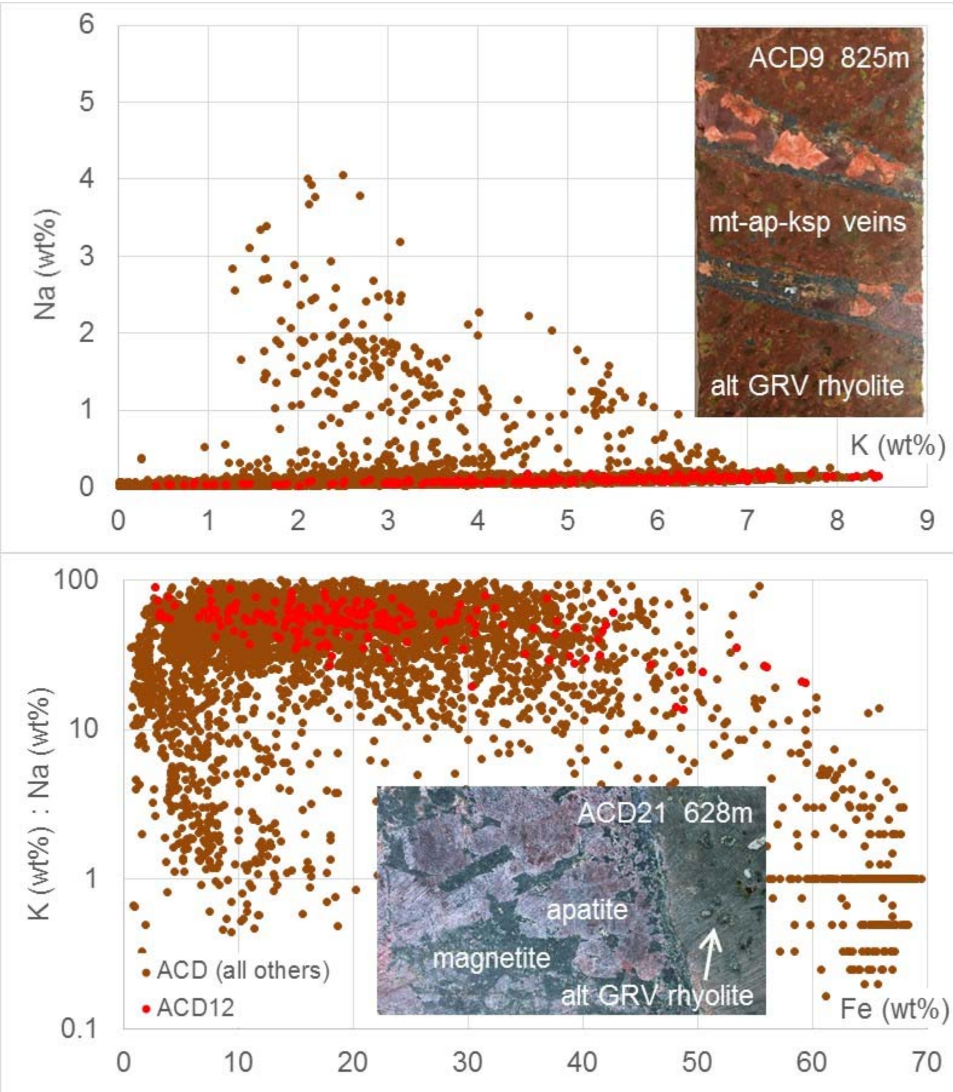

Modified from Krneta et al. 2017

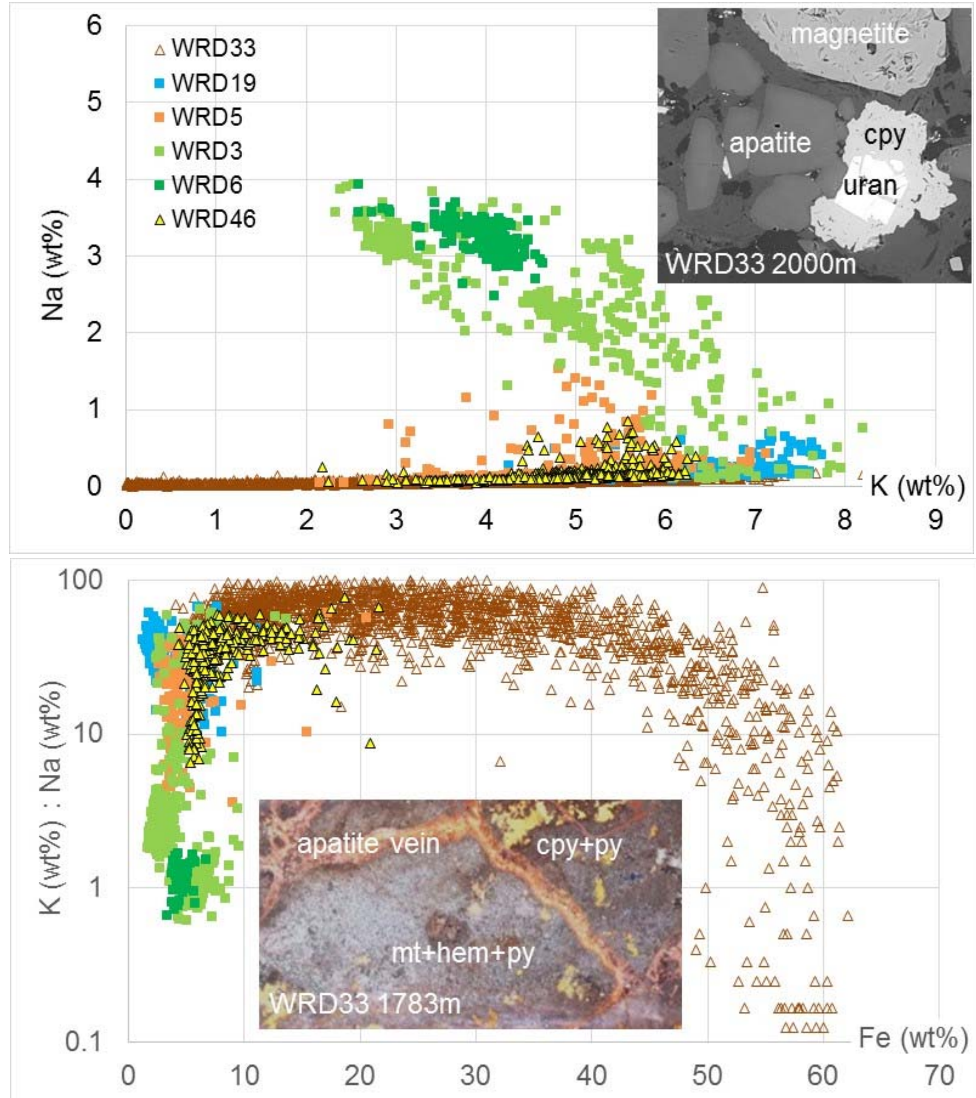

Source BHP

Olympic Dam and surrounding prospects

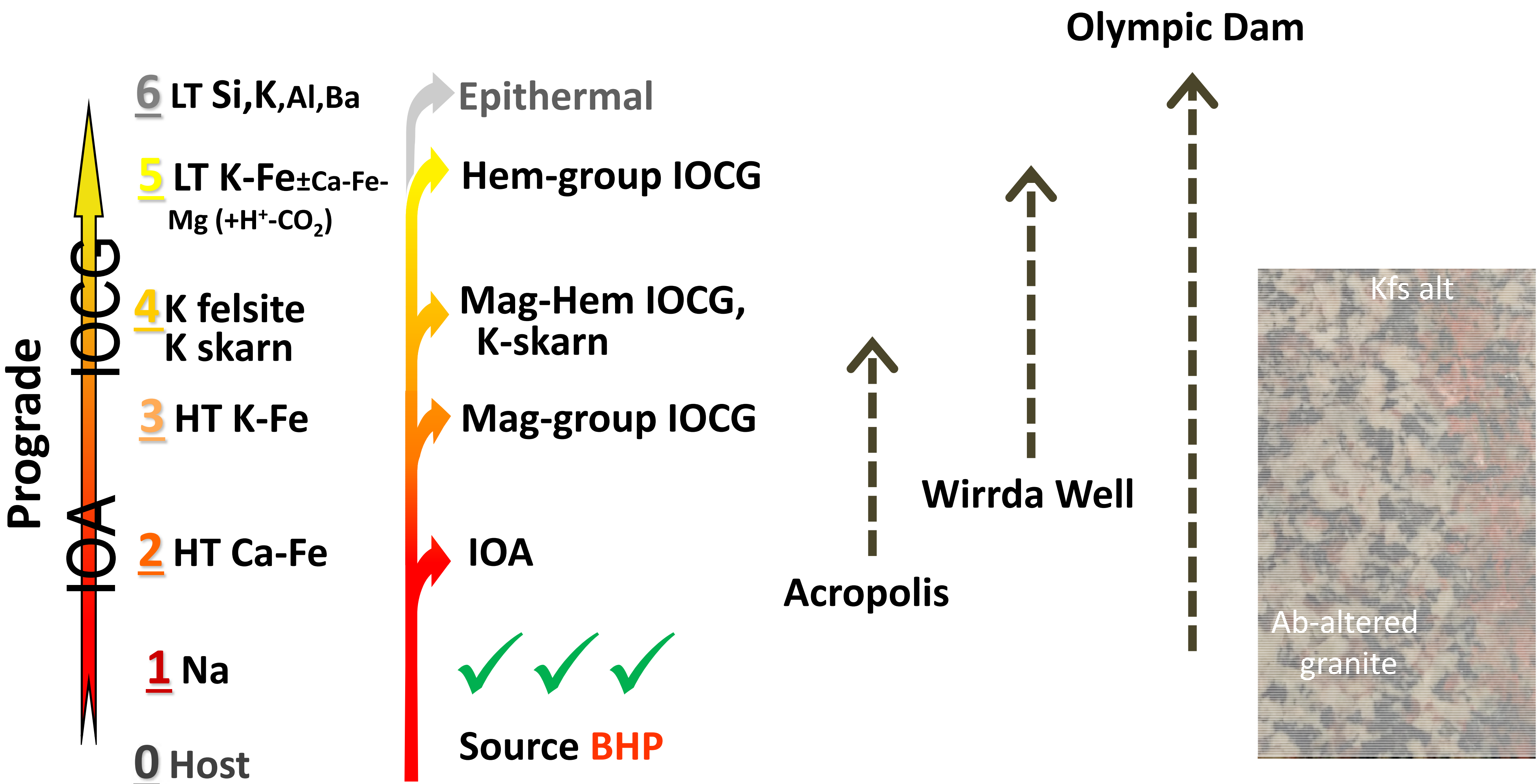

Modified from Corriveau et al. 2010b, 2016; Krneta et al. 2017

Celebrating 175 yrs

State of knowledge and impacts

Criterias for IOCG-U potential

Ore deposit and geoenvironmental models

Impact on renewing Canadian resources

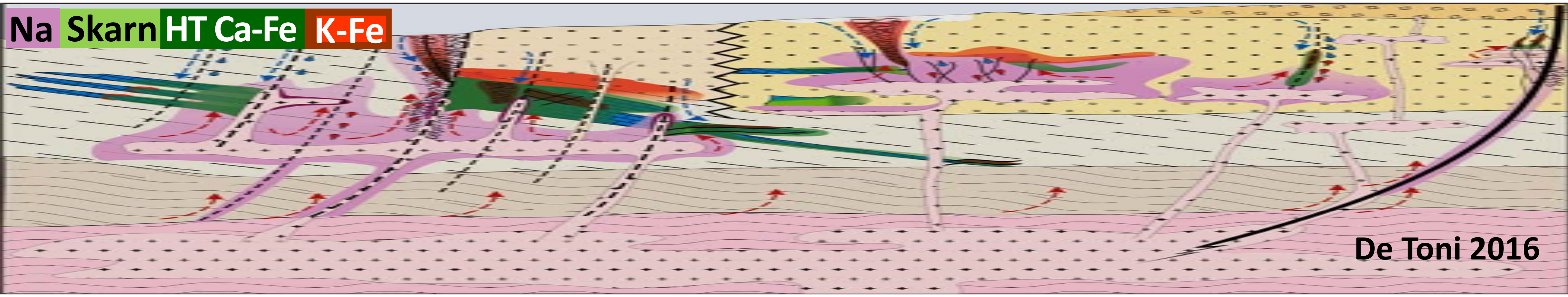

Criteria for high IOCG-U potential

- Continental settings
- Far-field continental backarc, Andean-type arc, intracontinental
- Extensive and ultimately voluminous mafic to felsic magmatism
- Subvolcanic to epithermal settings preserved
- Pre-IOCG sedimentary basins
- Crustal-scale structural pathways for magmas and fluids
- Mafic/ultramafic intrusions → thermal anomaly
- U-rich felsic subaerial volcanics and high-level intrusions (A-type)
- Compression → extension during magmatism
- Syn- to post-compressional magnetite-bearing (HT Ca-Fe) alteration; ductile behaviour of high temperature Ca-Fe metasomatites
- Tectonic exhumation + fluid mixing (e.g., with oxidised caldera fluids) + telescoping of alteration facies
- Fluid flow through U-rich hosts to sites of upflow
- Hematite-rich alteration facies formed above magnetite-bearing (HT Ca-Fe and HT K-Fe) alteration facies but commonly faulted subsequently

Modified from Skirrow 2010

Ore deposit model

Many ore deposit type models are strongly linked to specific geodynamic settings

Many geodynamic settings of Precambrian IOA and IOCG deposits remain uncertain despite abundant literature on the subject

Proposed settings for IOA and IOCG deposits greatly vary but all are continental and most ultimately generate A-type (high-temperature) magmas

Most IOA and IOCG deposits where regional settings are exposed or drilled at sufficiently large scale are shown to be hosted among a regular series of diagnostic alteration facies with distinctive extent, intensity and pervasiveness

High temperature saline fluids are required to trigger the regional-scale metasomatic systems but their sources can vary between and within systems

Metasomatic footprints are a result of, and record ore-forming processes

In high-grade metamorphic terranes (e.g., many Precambrian shields), geological evidence of repeated sub-volcanic intrusions, porphyritic dyke swarms, calderas and exhumation can be amalgamated as undifferentiated gneiss complexes and remain unnoticed

Iron oxide and alkali-calcic alteration ore systems

IOA, IOCG and affiliated deposits form as a consequence of

- a regular series of fluid-rock reactions triggered by high salinity fluids
- across high geothermal gradients
- in tectonically active settings

Celebrating 175 yrs

Metasomatic footprints include

- Regional albitite corridors along fault zones and above sub-volcanic intrusions, many extensively brecciated, replaced by fertile alteration and mineralised
- Regional to deposit-scale, stratabound, HT Ca-Fe and HT Ca-K-Fe alteration facies
- Deposit-scale breccias with HT to LT K-Fe, K, K-skarn and LT Ca-Fe-Mg alteration facies

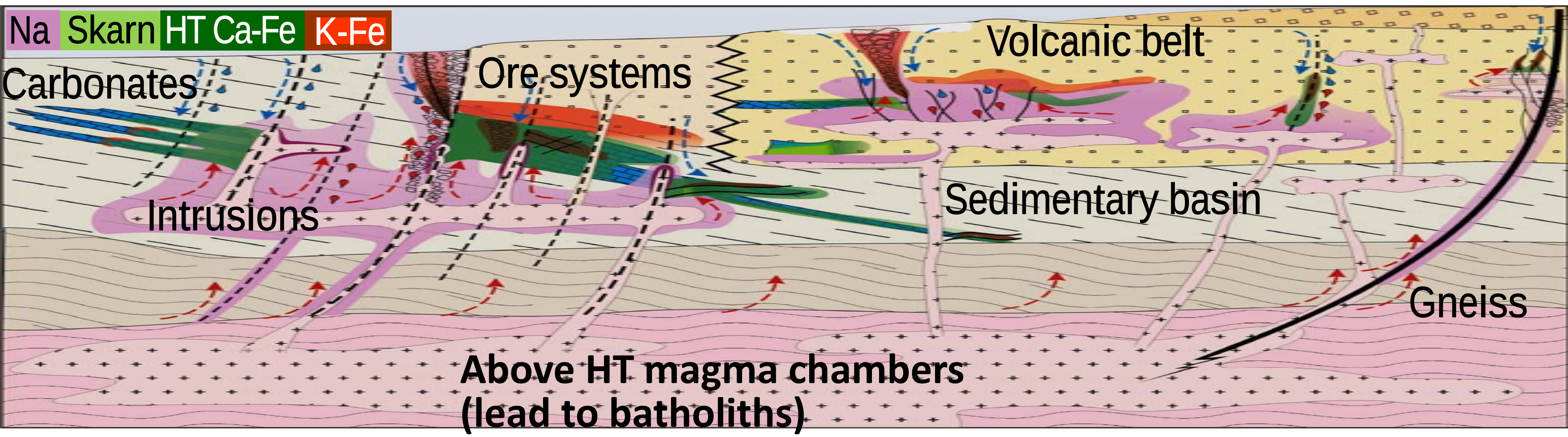

Mafic magmas as heat sources

Celebrating 175 yrs

Refining the classic model of Hitzman et al. 1992

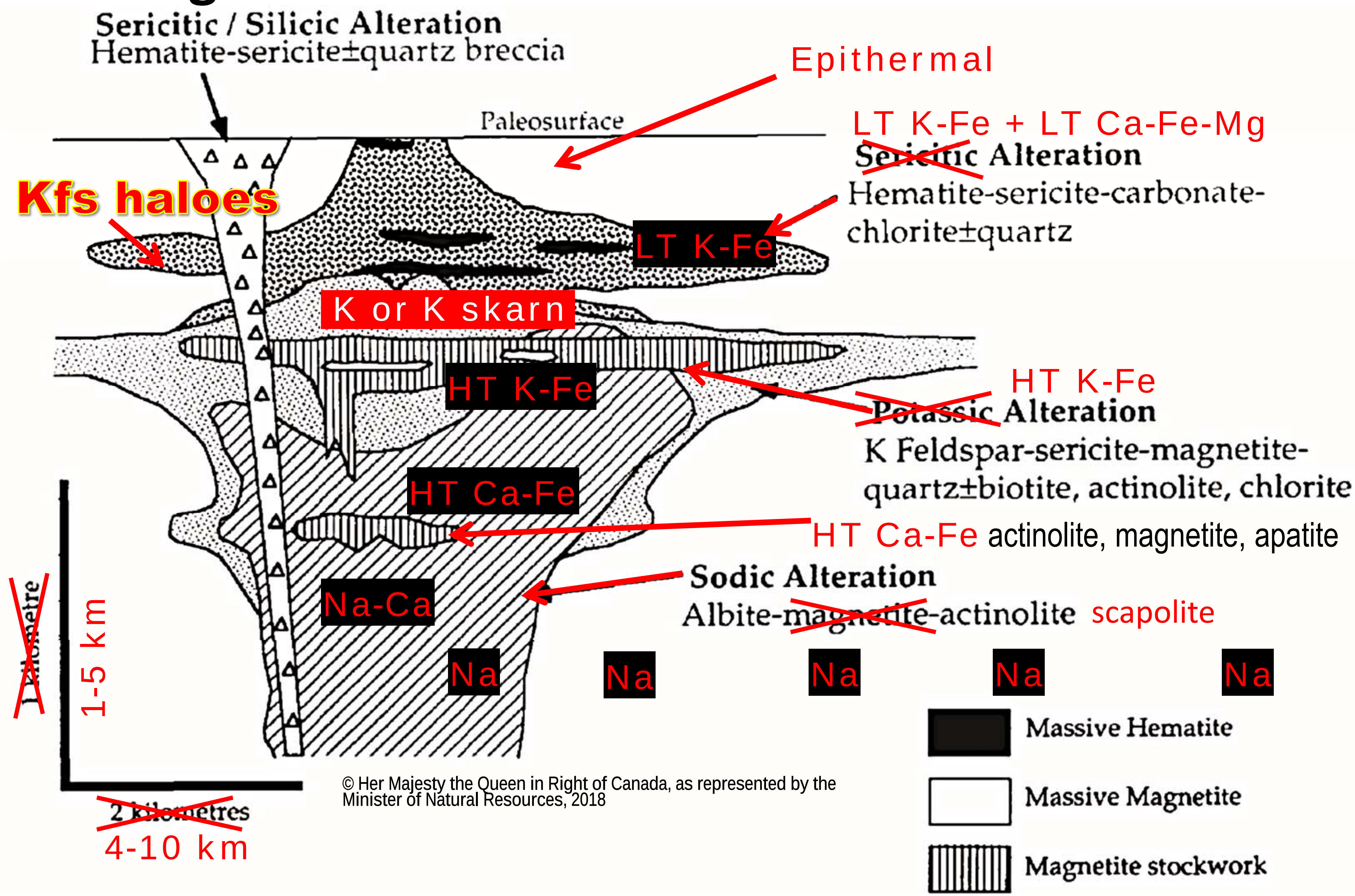

Ore genetic models

Better understanding of:

- Lateral, longitudinal and depth extent, types, evolution, intensity, parageneses, geochemical signatures and rock physical properties of alteration facies
- Metal associations and deposit types as a function of alteration facies (prograde, retrograde, cyclical and telescoped metasomatic paths)
- Role of metasomatic fluid-rock reactions (coupled dissolution-reprecipitation) on evolving fluid composition and acquisition of mixed fluid and metal source signatures from continuous fluid recharge and discharge across the ore environment (i.e., the upper crust)
- Distinctive features with respect to other deposit types (but depths can be of the same order as that of porphyry, compare with Reed et al. 2013)
- Bias in fluid inclusions information due to their more common preservation in low temperature minerals (e.g., quartz, carbonate)

Still have a fair way to go to predict metal endowment of IOAA systems

IOCG: Resources for future generations

Public geoscience

- Mapping and research
- Economic geology
- Environmental studies
- Management decisions
- Policy

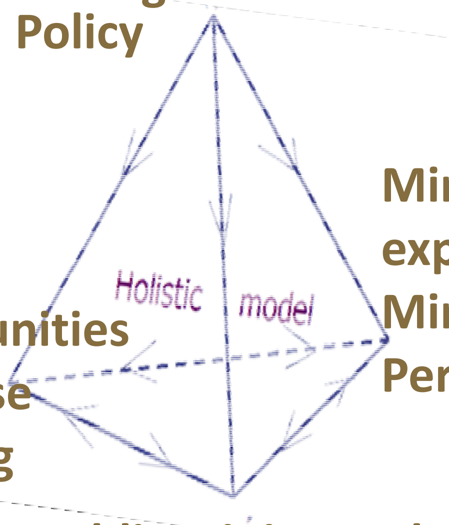

Mineral exploration
Mining
Permitting

Communities
Land use
Training

Public mining and mineral sciences

- Geometallurgy
- Tailing remediation
- Mine drainage

Geo-environmental ore deposit model modified from J. Kwong et al. presentation

- A new deposit type including the 1st U, 3rd Au and 5th Cu world resources in a single deposit (10,400 MT resources = 1054 billion CAD$)
- 80 Mt resources known in Canada
- IOCG and affiliated deposits are THE RESOURCES FOR FUTURE GENERATIONS!
- New IOCG mines (100-400 Mt resources) open nearly yearly since 2000 but none in Canada!
- High level of expertise on ore systems required for informed planning and decisions by industry and governments
- GEM and TGI outcomes applicable broadly; can fill the major knowledge gaps through short courses and special sessions at meetings, etc.

IOCG: Opportunity and challenges in Canada

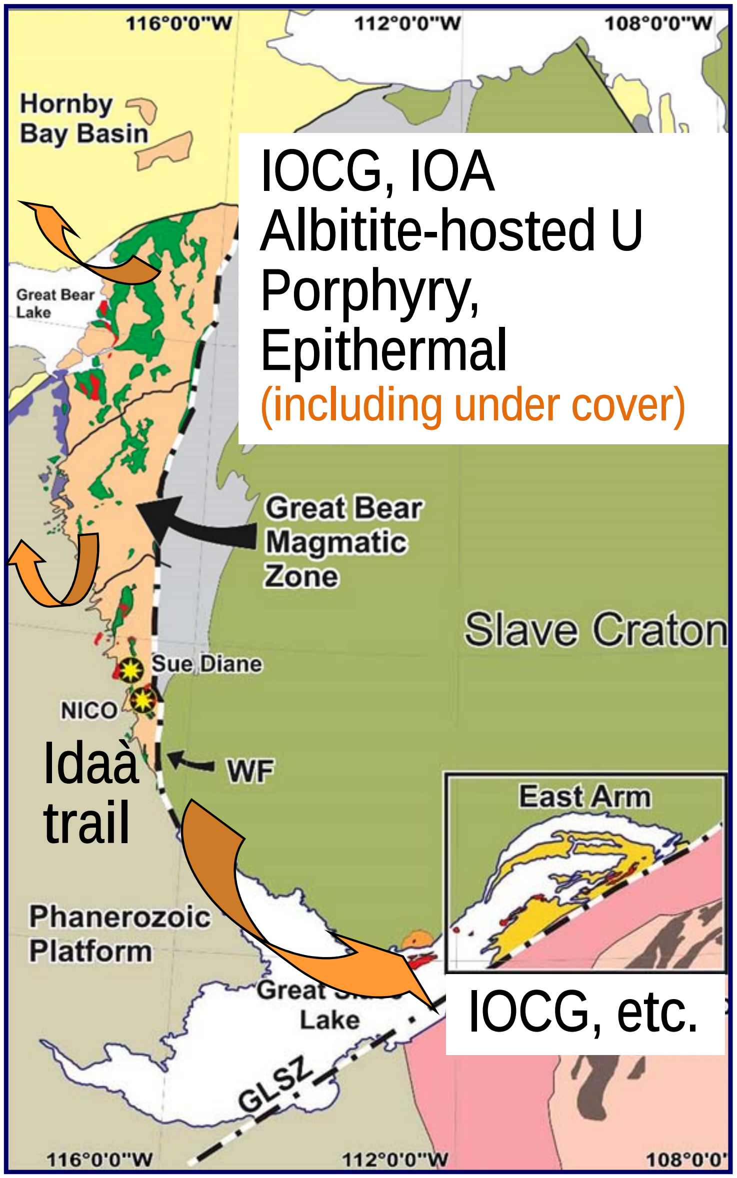

- Resources: highly prospective and UNTAPPED!
- Geoscience framework and mineral exploration too immature for sound mineral potential assessment across Canada
- Potential resources highly UNDER VALUED
- Spectacular physiography and high biodiversity (a consequence of IOCG atypical geology!) targeted for conservation areas and national parks
- Withdrawing IOCG settings from exploration could significantly impact the renewal of mineral resources for future generations in Canada
- Increasing geoscience information, including baseline knowledge of environmental footprint, is needed for informed decision on land used planning, environmental assessment, mine planning, government and industry project implementation and planning, policy, etc.

Great Bear IOAA footprints
Vectors to IOCG and affiliated deposits

- Superb 3D exposures of iron oxide and alkali-calcic alteration ore systems from 3-10 km depth to epithermal caps
- Alteration mapping genetically links IOCG, IOA, skarn, albitite-hosted U and mantos mineralisation types
- Alteration facies prograde to distinct metal associations (base, precious, specialised metals including for nuclear energy, green energy technology and geothermal energy)
- No subsequent orogenesis = very limited remobilisation (restricted to batholith emplacement, mafic dykes haloes and transcurrent faults)
- New geological and geophysical exploration criteria, technologies, methodologies and case studies
- Ore deposit model, mapping and exploration tools

Hildebrand 1986; Mumin et al. 2007, 2010; Corriveau et al. 2010a,b, 2011, 2016, 2017, in press a-h; Montreuil et al. 2013, 2015, 2016a,b,c; Potter et al. 2013, 2017; Hayward et al. 2016; Enkin et al. 2016

GEM

TGI Ore Systems

Celebrating 175 yrs

Thanks to all participants, collaborators, managers, and administration and laboratories personal involved in

Geological Survey of Canada (Natural Resources Canada)

Geo-mapping for Energy and Minerals – IOCG-Great Bear project participants

Targeted Geoscience Initiative – Uranium in Canada participants

GEM and TGI program managers, division directors and other GSC projects

Northwest Territories Geoscience Office

South Wopmay Bedrock Mapping project participants and managers

First Nations communities and governments, in particular the Community Government of Gamètì

Fortune Minerals, Alberta Star, Diamonds North, Honey Badger Exploration, Energizers, Aurora Geosciences

Academia (including BSc, MSc and PhD students) and other contributors

Aurora Research Institute, Research Licence No. 14844, No. 14639 and No.14548

Land Use Permit Class A No. W2010J0004 (GEM) and W2009C0001 (Fortune Minerals Limited)

Archaeological sites database agreements No. DR2010-390, No DR2009-335

Polar Continental Shelf Program projects 010009, 50709 and 00410

Task-sharing agreements: NRCan-Fortune Minerals, NRCan-Honey Badger Exploration-Energizer Resources, NRCan-Community Government of Gamètì

Geological Association of Canada Short Course Notes 20

Exploring for Iron Oxide Copper-Gold Deposits Canada and Global Analogues

Chapter 1 - Exploring for iron oxide copper-gold (Ag-Bi-Co-U) deposits – the need for case studies, classifications and exploration vectors
Louise Corriveau, Hamid Mumin

Chapter 2 - Classifying IOCG deposits
Patrick J. Williams

Chapter 3 - "Magnetite-group" IOCGs with special reference to Cloncurry and Northern Sweden: settings, alteration, deposit characteristics, fluid sources, and their relationship to apatite-rich iron ores
Patrick J. Williams

Chapter 4 - "Hematite-group" IOCG±U ore systems: tectonic settings, hydrothermal characteristics, and Cu-Au and U mineralising processes
Roger Skirrow

Chapter 5 - The IOCG-porphyry-epithermal continuum of deposits types in the Great Bear Magmatic Zone, Northwest Territories, Canada
Hamid Mumin, A.K. Somarin, B. Jones, L. Corriveau, L. Ootes, J. Camier

GAC Short Course Notes 20

Chapter 6 - Use of breccias in IOCG(U) exploration
Michel Jébrak

Chapter 7 - Alteration Vectors to IOCG mineralization – from uncharted terranes to deposits
Louise Corriveau, Patrick Williams, Hamid Mumin

Chapter 8 - Iron oxides trace element fingerprinting of mineral deposit type
Georges Beaudoin, Céline Dupuis

Chapter 9 - Alterations in IOCG-type and related deposits in the Manitou Lake area, eastern Grenville Province, Québec
Tom Clark, André Gobeil, Serge Chevé

Chapter 10 - Lower Cambrian iron oxide-apatite-REE (U) deposits of the Bafq District, east-central Iran
Farahnaz Daliran, Heinz-Günther Stosch, Patrick Williams

Chapter 11 - Iron oxide-copper-gold mineralization in the Greater Lufilian Arc, Africa
Alberto Lobo-Guerrero S.

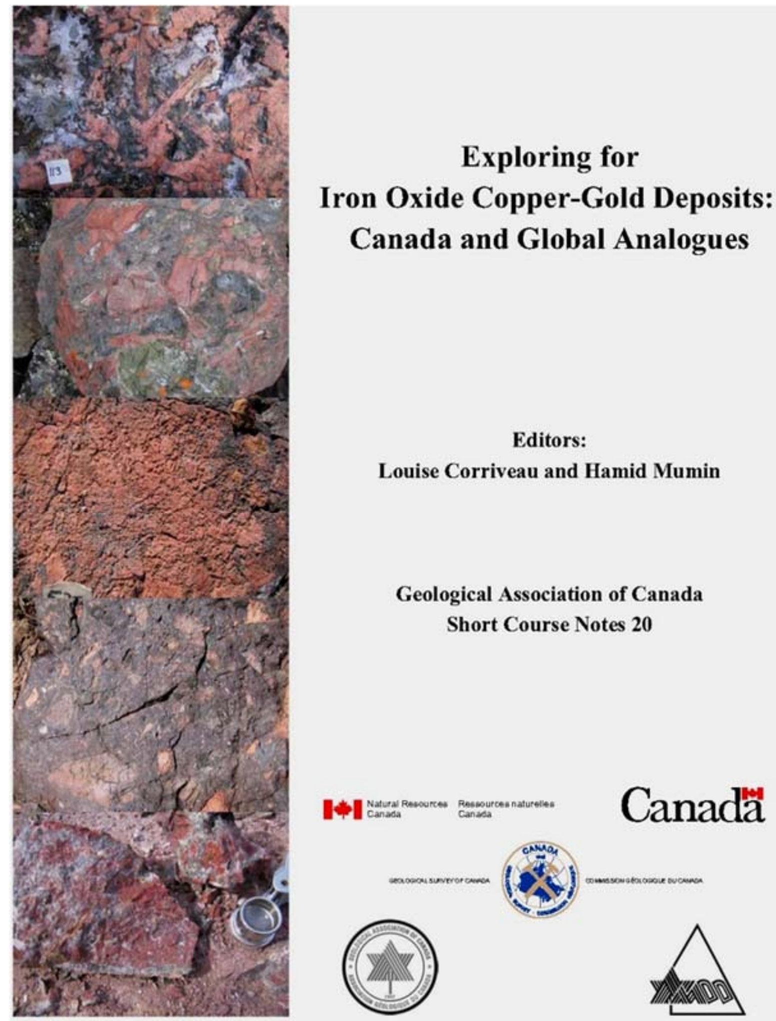

Chapter 12 - Alteration processes and impacts on regional-scale element mobility and geochronology, Tamlalt-Menhouhou deposit, Morocco
Ewan Pelleter, Dominique Gasquet, Alain Cheilletz, Abdellah Mouttaqi

Canada

Celebrating 175 yrs

Reference list

References

Acosta-Góngora, G.P., Gleeson, S.A., Samson, I., Ootes, L., Corriveau, L., 2015a, Gold refining by bismuth melts in the iron oxide-dominated NICO Au-Co-Bi (±Cu±W) deposit, NWT, Canada: Economic Geology, v. 110, p. 291–314.

Acosta-Góngora, P., Gleeson, S., Samson, I., Corriveau, L., Ootes, L., Taylor, B.E., Creaser, R.A., Muehlenbachs, K., 2015b, Genesis of the Paleoproterozoic NICO iron-oxide-cobalt-gold-bismuth deposit, Northwest Territories, Canada: Evidence from isotope geochemistry and fluid inclusions: Precambrian Research, v. 268, p. 168–193.

Aleinikoff, J.N., Selby, D., Slack, J.F., Day, W.C., Pillers, R.M., Cosca, M.A., Seeger, C.M., Fanning, C.M., Samson, I.M., 2016, U-Pb, Re-Os, and Ar/Ar geochronology of REE-rich breccia pipes and associated host rocks from the Mesoproterozoic Pea Ridge Fe-REE-Au deposit, St. Francois Mountains, Missouri: Economic Geology, v. 111, p. 1883–1914.

Allen, S.R., McPhie, J., 2002, The Eucarro Rhyolite, Gawler Range Volcanics, South Australia; a >675 km^3 compositionally zoned lava of Mesoproterozoic age: Geological Society of America, Bulletin, v. 114, p. 1592–1609.

Babo, J., Spandler, C., Oliver, N., Brown, M., Rubenach, M., Creaser, R.A., 2017, The high-grade Mo-Re Merlin deposit, Cloncurry District, Australia: Paragenesis and geochronology of hydrothermal alteration and ore formation: Economic Geology, v. 112, p. 397–422.

Badham, J.P.N., Morton, R.D., 1976, Magnetite–apatite intrusions and calc-alkaline magmatism, Camsell River, N.W.T: Canadian Journal of Earth Sciences, v. 13, p. 348–354.

Baker, H., Pattinson, D., Reardon, C., 2011, Technical review of the Kaunisvaara iron project, Sweden: SRK Consulting, National Instrument 43-101 Technical Report, available at www.sedar.com.

Baker, H., MacDougall, C., Pattinson, D., 2014, Technical review of the Hannukainen iron-copper-gold project, Kolari District, Finland: SRK Consulting, National Instrument 43-101 Technical Report, available at www.sedar.com.

Bardina, N.Y., Popov, V.S., 1992, Classification of metasomatic rocks and facies of shallow metasomatism: International Geology Review, v. 34, p. 187–196.

Barton, M.D., 2014, Iron oxide(–Cu–Au–REE–P–Ag–U–Co) systems, in Holland, H.D. and Turekian, K.K., eds., Treatise on geochemistry, Second Edition, volume 13: Elsevier, p. 515–541.

Bastrakov, E.N., Skirrow, R.G., 2007, Fluid evolution and origins of iron oxide–Cu–Au prospects in the Olympic Dam district, Gawler Craton, South Australia: Economic Geology, v. 102, p. 1415–1440.

Belperio, A., Flint, R., Freeman, H., 2007, Prominent Hill: A hematite-dominated, iron oxide copper-gold system: Economic Geology, v. 102, p. 1499–1510.

Benavides, J., Kyser, T.K., Clark, A.H., 2007, The Mantoverde iron oxide-copper-gold district, III región, Chile: The role of regionally derived, nonmagmatic fluids in chalcopyrite mineralization: Economic Geology, v. 102, p. 415–440.

Benavides, J., Kyser, T.K., Clark, A.C., Stanley, C., Oates, C., 2008a, Application of molar element ratio analysis of lag talus composite sample to the exploration for iron oxide-copper-gold mineralization: Mantoverde area, northern Chile: Geochemistry: Exploration, Environment Analysis, v. 8, p. 369–380.

Benavides, J., Kyser, T.K., Clark, A.C., Stanley, C., Oates, C., 2008b, Exploration guidelines for copper-rich iron oxide-copper-gold deposits in the Mantoverde area, northern Chile: The integration of host-rock molar element ratios and oxygen isotope compositions: Geochemistry: Exploration, Environment, Analysis, v. 8, p. 343–367.

References

Betts, P.G., Giles, D., 2006, The 1800-1100 Ma tectonic evolution of Australia: Precambrian Research, v. 144, p. 92–125.

Betts, P.G., Giles, D., Foden, J., Schaefer, B.F., Mark, G., Pankhurst, M.J., Forbes, C.J., Williams, H.A., Chalmers, N.C., Hills, Q., 2009, Mesoproterozoic plume-modified orogenesis in eastern Precambrian Australia: Tectonics, v. 28, TC3006, doi:10.1029/2008TC002325.

Béziat, D., Dubois, M., Debat, P., Nikiéma, S., Salvi, S., Tollon, F., 2008, Gold metallogeny in the Birimian craton of Burkina Faso (West Africa): Journal of African Earth Sciences, v. 50, p. 215–233.

BHP Billiton, 2015, http://www.bhpbilliton.com/home/investors/annualreporting2015.pdf.

BHP, 2017, Annual report: https://www.bhp.com/-/media/documents/investors/annual-reports/2017/bhpannualreport2017.pdf

Bilenker, L.D., Simon, A.C., Reich, M., Lundstrom, C.C., Gajos, N., Bindeman, I., Barra, F., Munizaga, R., 2016, Fe–O stable isotope pairs elucidate a high-temperature origin of Chilean iron oxide-apatite deposits: Geochimica et Cosmochimica Acta, v. 177, p. 94–104.

Blein, O., Corriveau, L., 2017, Recognizing IOCG alteration facies at granulite facies in the Bondy Gneiss Complex of the Grenville Province: Proceedings of the 14th SGA Biennial Meeting, 20-23 August 2017, Québec City, p. 907–911.

Bonnet, A.-L., Corriveau, L., 2007, Atlas et outils de reconnaissance de systèmes hydrothermaux métamorphisés dans les terrains gneissiques, in Goodfellow, W.D., ed., Mineral deposits of Canada: A synthesis of major deposit-types, district metallogeny, the evolution of geological provinces, and exploration methods: Geological Association of Canada, Mineral Deposits Division, Special Publication 5, (DVD), 95 p.

Bryan, S.E., Ukstins-Peate, I., Peate, D.W., Self, S., Jerram, D.A., 2010, The largest volcanic eruptions on Earth: Earth-Science Reviews, v. 102, p. 207–229.

Burgess, H., Gowans, R.M., Hennessey, B.T., Lattanzi, C.R., Puritch, E., 2014, Technical report on the feasibility study for the NICO gold–cobalt–bismuth–copper deposit, Northwest Territories, Canada: Fortune Minerals Ltd., NI 43-101 Technical Report No. 1335, 385 p. Available at www.sedar.com

Camprubí, A., González-Partida, E., 2017, Mesozoic magmatic–hydrothermal iron oxide deposits (IOCG 'clan') in Mexico: A review: Ore Geology Reviews, v. 81, p. 1084–1095.

Cap, 2013, Annual operating summary: Available at http://eng.cap.cl/wp-content/uploads/2014/08/cap_annual_report_2013.pdf

Capstone Mining Corp, 2014, Santo Domingo project, Region III, Chile: NI 43-101 Technical Report on Feasibility Study, 394 p. Available at www.sedar.com

Carriedo, J., Tornos, F., 2010, The iron oxide copper-gold belt of the Ossa Morena Zone, Southwest Iberia: Implications for IOCG genetic models, in Porter, T.M., (ed.), Hydrothermal iron oxide copper-gold and related deposits: A global perspective, volume 4, - Advances in the understanding of IOCG deposits: Porter Geoscience Consultancy Publishing, Adelaide, p. 441–460.

Chen, H., 2013, External sulphur in IOCG mineralization: Implications on definition and classification of the IOCG clan: Ore Geology Reviews, v. 51, p. 74–78.

Chen, H., Clark, A.H, Kyser, T.K., Ullrich, T.D., Baxter, R., Chen, Y., Moody, T.C., 2010, Evolution of the giant Marcona-Mina Justa iron oxide-copper-gold district, south-central Peru: Economic Geology, v. 105, p. 155–185.

Chen, H., Kyser, T.K., Clark, A.H., 2011, Contrasting fluids and reservoirs in the contiguous Marcona and Mina Justa iron oxide–Cu(–Ag–Au) deposits, south-central Perú: Mineralium Deposita, v. 46, p. 677–706.

Chen, H., Cooke, D.R., Baker, M.J., 2013, Mesozoic iron oxide copper-gold mineralization in the Central Andes and the Gondwana supercontinent breakup: Economic Geology, v. 108, p. 37–44.

References

Chen, W.T., Zhou, M.-F., 2012, Paragenesis, stable isotopes, and molybdenite Re-Os isotope age of the Lala iron-copper deposit, southwest China: Economic Geology, v. 107, p. 459–480.
Cherry, A., Kamenetsky, V., McPhie, J., Kamenetsky, M., Ehrig, K., Keeling, J., 2017, Post-1590 Ma modification of the supergiant Olympic Dam deposit: Links with regional tectonothermal events: Proceedings of the 14th SGA Biennial Meeting, 20-23 August 2017, Québec City, p. 847–850.
Chinalco Yunnan Copper Resources, 2010, Inferred resource estimate – Elaine-Dorothy uranium – rare earth element (REE): ASX/Media Announcement 24 March 2010
Chinalco Yunnan Copper Resources, 2012a, 26.1Mt inferred jorc resource estimate Elaine 1 copper-gold deposit: ASX/Media Announcement 29 June 2012.
Chinalco Yunnan Copper Resources, 2012b, CYU and GSE update on high grade uranium in NW Queensland: ASX/Media Announcement 25 October 2012.
Chinova Resources, 2014, Merlin molybdenum / rhenium project, 2014: available at http://www.inovaresources.com/images/pdf/Merlin_Project_%20Brisb_Mining_Conv_2014_v9.pdf
Chinova Resources, 2017, Mount Elliott Swan Resource estimation update summary. Available at www.chinovaresources.com
Clark, T., Gobeil, A., David, J., 2005, Fe oxide-Cu-Au-type and related deposits in the Manitou Lake area, eastern Grenville Province, Quebec: Variations in setting, composition and style: Canadian Journal of Earth Sciences, v. 42, p. 1829–1847.
Clark, T., Gobeil, A., Chevé, S., 2010, Alterations in IOCG-type and related deposits in the Manitou Lake area, Eastern Grenville Province, Québec, in Corriveau, L. and Mumin, A.H., eds., Exploring for iron oxide copper–gold deposits: Canada and global analogues: Geological Association of Canada, Short Course Notes 20, p. 127–146.
Corona-Esquivel, R., Tritlla, J., Levresse, G., 2011, Formation ages of the two Phanerozoic IOCG belts in México: Society for Geology Applied to Mineral Deposits, 11th, Antofagasta, Chile, Extended Abstracts, p. 473–475.
Corriveau, L., 2007, Iron oxide copper–gold deposits: A Canadian perspective, in Goodfellow, W.D., ed., Mineral deposits of Canada: A synthesis of major deposit-types, district metallogeny, the evolution of geological provinces and exploration methods: Geological Association of Canada, Mineral Deposits Division, Special Publication, v. 5, p. 307–328.
Corriveau, L., 2013, Architecture de la ceinture métasédimentaire centrale au Québec, Province de Grenville : Un exemple de l'analyse de terrains de métamorphisme élevé: Geological Survey of Canada, Bulletin 586, 264 p., doi:10.4095/226449.
Corriveau, L., 2017a, Iron-oxide and alkali-calcic alteration ore systems and their polymetallic IOA, IOCG, skarn, albitite-hosted U±Au±Co, and affiliated deposits: A short course series. Part 1: Introduction: Geological Survey of Canada, Scientific Presentation 56, 1 ppt file. doi:10.4095/300241.
Corriveau, L., 2017b, Les systèmes minéralisateurs à oxydes de fer et altération à éléments alcalins (±calciques) et leurs gîtes IOA, IOCG, skarns, U±Au±Co (au sein d'albitites) et affiliés: Une série de cours intensifs. Partie 1: Introduction: Geological Survey of Canada, Scientific Presentation 57, doi:10.4095/300242.
Corriveau, L., Mumin, A.H., 2010, Exploring for iron oxide copper–gold deposits: The need for case studies, classifications and exploration vectors, in Corriveau, L. and Mumin, A.H., eds., Exploring for iron oxide copper-gold deposits: Canada and global analogues: Geological Association of Canada, Short Course Notes 20, p. 1–12.

References

Corriveau, L., Spry, P., 2014, Metamorphosed hydrothermal ore deposits, in Holland, H.D. and Turekian, K.K., eds., Treatise on Geochemistry, Second Edition: Elsevier, v. 13, p. 175–194.

Corriveau, L., Perreault, S., Davidson, A., 2007, Prospective metallogenic settings of the Grenville Province, in Goodfellow, W.D., ed., Mineral deposits of Canada: A synthesis of major deposit-types, district metallogeny, the evolution of geological provinces, and exploration methods: Geological Association of Canada, Mineral Deposits Division, Special Publication 5, p. 819–848.

Corriveau, L., Mumin, A.H., Setterfield, T., 2010a, IOCG environments in Canada: Characteristics, geological vectors to ore and challenges, in Porter, T.M., ed., Hydrothermal iron oxide copper-gold and related deposits: A global perspective, volume 4–advances in the understanding of IOCG deposits: Porter Geoscience Consultancy Publishing, Adelaide, p. 311–344.

Corriveau, L., Williams, P.J., Mumin, A.H., 2010b, Alteration vectors to IOCG mineralisation – from uncharted terranes to deposits, in Corriveau, L. and Mumin, A.H., eds., Exploring for iron oxide copper-gold deposits: Canada and global analogues: Geological Association of Canada, Short Course Notes 20, p. 89–110.

Corriveau, L., Mumin, A.H., Montreuil, J.-F., 2011, The Great Bear magmatic zone (Canada): The IOCG spectrum and related deposit types: Society for Geology Applied to Mineral Deposits, 11th, Antofagasta, Chile, Extended Abstracts, p. 524–526.

Corriveau, L., Nadeau, O., Montreuil, J.-F., Desrochers, J.-P., 2014, Report of activities for the Core Zone: Strategic geomapping and geoscience to assess the mineral potential of the Labrador Trough for multiple metals IOCG and affiliated deposits, Canada: Geological Survey of Canada, Open File 7714.

Corriveau, L., Lauzière, K., Montreuil, J.-F., Potter, E.G., Hanes, R., Prémont, S., 2015, Dataset of geochemical data from iron oxide alkali-altered mineralizing systems of the Great Bear magmatic zone (NWT): Geological Survey of Canada, Open File 7643, 19 p., 6 geochemical datasets.

Corriveau, L., Montreuil, J.-F., Potter, E.G., 2016, Alteration facies linkages among IOCG, IOA and affiliated deposits in the Great Bear magmatic zone, Canada, in Slack, J., Corriveau, L. and Hitzman, M., eds., Proterozoic iron oxide-apatite (± REE) and iron oxide-copper-gold and affiliated deposits of Southeast Missouri, USA, and the Great Bear magmatic zone, Northwest Territories, Canada: Economic Geology, v. 111, p. 2045–2072.

Corriveau, L., Potter, E.G., Acosta-Góngora, P., Blein, O., Montreuil, J.-F., De Toni, A.F., Day, W., Slack, J.F., Ayuso, R.A., Hanes, R., 2017, Petrological mapping and chemical discrimination of alteration facies as vectors to IOA, IOCG, and affiliated deposits within Laurentia and beyond: Proceedings of the 14th SGA Biennial Meeting, 20-23 August 2017, Québec City, p. 851–855.

Corriveau, L., Montreuil, J.F., Potter, E.G., DeToni, A.F., in press a, Iron-oxide and alkali-calcic alteration ore systems and their polymetallic IOA, IOCG, skarn, albitite-hosted U±Au±Co, and affiliated deposits: A short course series. Part 3: The Great Bear magmatic zone and other Canadian districts: Geological Survey of Canada, Scientific Presentation xx.

Corriveau, L., Montreuil, J.F., Potter, E.G., DeToni, A.F., in press b, Iron-oxide and alkali-calcic alteration ore systems and their polymetallic IOA, IOCG, skarn, albitite-hosted U±Au±Co, and affiliated deposits: A short course series. Part 4: Alteration facies, metasomatic reaction paths and ore genesis: Geological Survey of Canada, Scientific Presentation xx.

References

Corriveau, L., Montreuil, J.F., Potter, E.G., DeToni, A.F., in press c, Iron-oxide and alkali-calcic alteration ore systems and their polymetallic IOA, IOCG, skarn, albitite-hosted U±Au±Co, and affiliated deposits: A short course series. Part 5: Na to Na-Ca-Fe facies: Geological Survey of Canada, Scientific Presentation xx.

Corriveau, L., Montreuil, J.F., Potter, E.G., DeToni, A.F., in press d, Iron-oxide and alkali-calcic alteration ore systems and their polymetallic IOA, IOCG, skarn, albitite-hosted U±Au±Co, and affiliated deposits: A short course series. Part 6: Skarns, HT Ca-Fe facies and IOA (iron oxide-apatite) deposits: Geological Survey of Canada, Scientific Presentation xx.

Corriveau, L., Montreuil, J.F., Potter, E.G., DeToni, A.F., in press e, Iron-oxide and alkali-calcic alteration ore systems and their polymetallic IOA, IOCG, skarn, albitite-hosted U±Au±Co, and affiliated deposits: A short course series. Part 7: HT to LT K-Fe, IOCG (iron oxide copper-gold) deposits, Co-Bi and K-skarn variants, albitite-hosted U or Au-U-Co deposits: Geological Survey of Canada, Scientific Presentation xx.

Corriveau, L., Montreuil, J.F., Potter, E.G., DeToni, A.F., in press f, Iron-oxide and alkali-calcic alteration ore systems and their polymetallic IOA, IOCG, skarn, albitite-hosted U±Au±Co, and affiliated deposits: A short course series. Part 8: Breccias: Geological Survey of Canada, Scientific Presentation xx.

Corriveau, L., Montreuil, J.F., Potter, E.G., DeToni, A.F., in press g, Iron-oxide and alkali-calcic alteration ore systems and their polymetallic IOA, IOCG, skarn, albitite-hosted U±Au±Co, and affiliated deposits: a short course series. Part 10: Metasomatic facies as an exploration tool: The NICO deposit: Geological Survey of Canada, Scientific Presentation xx.

Corriveau, L., Montreuil, J.F., Potter, E.G., DeToni, A.F., in press h, Iron-oxide and alkali-calcic alteration ore systems and their polymetallic IOA, IOCG, skarn, albitite-hosted U±Au±Co, and affiliated deposits: A short course series. Part 11: Footprints at granulite facies in the Bondy gneiss complex: Geological Survey of Canada, Scientific Presentation xx.

Corriveau, L., Blein, O., Gervais, F., Trapy, P.H., De Souza, S., in press i, Iron oxide and alkali-calcic alteration, skarn and epithermal mineralising systems of the Grenville Province, Canada: The Bondy gneiss complex in the Central Metasedimentary Belt as a case example – 14th SGA Biennial Meeting, Excursion Guidebook FT-02: Geological Survey of Canada, Open File 8349, 110 p.

Couture, J.-F., Cole, G., Poxleitner, G., Nilsson, J., Dance, A., Scott, C.C., 2014, Technical report for the Candelaria and Ojos del Salado copper projects, Chile: SRK Consulting, National Instrument 43-101 Technical Report prepared for Lundin Mining Corporation, 134 p., available at www.sedar.com.

Creaser, R.A., 1996, Petrogenesis of a Mesoproterozoic quartz latite-granitoid suite from the Roxby Downs area, South Australia: Precambrian Research, v. 79, p. 371–394.

Cudeco, 2017, Annual Rocklands resource update – 2017: Market release 31 October 2017.

Cuney, M., Kyser, K., 2008, Deposits related to Na-metamorphism and high-grade metamorphism, in Cuney, M., Kyser, K., eds. Recent and not-so-recent developments in uranium deposits and implications for exploration: Mineralogical Association of Canada, Short Course Series, 39, p. 97–116.

Cuney, M., Emetz, A., Mercadier, J., Mykchaylov, V., Shunko, V., Yuslenko, A., 2012, Uranium deposits associated with Na-metasomatism from central Ukraine: A review of some of the major deposits and genetic constraints: Ore Geology Reviews, v. 44, p. 82–106.

References

Daliran, F., Stosch, H.-G., Williams, P.J., Jamali, H., Dorri, M.-B., 2010, Early Cambrian iron oxide-apatite-REE (U) deposits of the Bafq district, east-central Iran, in Corriveau, L. and Mumin, A.H., eds., Exploring for iron oxide copper–gold deposits: Canada and global analogues: Geological Association of Canada, Short Course Notes 20, p. 147–159.

Davidson, G.J., Paterson, H., Meffre, S., Berry, R.F., 2007, Characteristics and origin of the Oak Dam East breccia-hosted, iron oxide-Cu-U-(Au) deposit: Olympic Dam region, Gawler Craton, South Australia: Economic Geology, v. 102, p. 1471–1498.

Day, W.C., Slack, J.F., Ayuso, R.A., Seeger, C.M., 2016, Regional geologic and petrologic framework for iron oxide ± apatite ± rare earth element and iron oxide copper-gold deposits of the Mesoproterozoic St. Francois Mountains Terrane, Southeast Missouri, USA, in Slack, J., Corriveau, L. and Hitzman, M., eds., Proterozoic iron oxide-apatite (± REE) and iron oxide-copper-gold and affiliated deposits of Southeast Missouri, USA, and the Great Bear magmatic zone, Northwest Territories, Canada: Economic Geology, v. 111, p. 1825–1858.

Day, W.C., Aleinikoff, J.N., du Bray, E., Ayuso, R.A., 2017, Constraints on age of magmatism and iron oxide-apatite (IOA) and iron oxide copper-gold (IOCG) mineral deposit formation in the Mesoproterozoic St. Francois Mountains terrane of southeast Missouri, USA: Proceedings of the 14th SGA Biennial Meeting, 20-23 August 2017, Québec City, p. 855–857.

Decrée, S., Marignac, C., De Putter, T., Yans, J., Clauer, N., Dermech, M., Aloui,K., Baele, J.-M., 2013, The Oued Belif hematite-rich breccia: A Miocene iron oxide Cu-Au-(U-REE) deposit in the Nefza mining district, Tunisia: Economic Geology, v. 108, p. 1425–1457.

Desrochers, J.-P., 2014, Technical report on the Sagar property, Romanet Horst, Labrador Trough, Québec, Canada (latitude, 56°22'N and longitude 68°00'W; NTS Map sheets 24B/05 and 24C/08): National Instrument 43–101 Technical Report prepared for Honey Badger Exploration Inc., available at www.sedar.com.

De Toni, A.F., 2016, Les paragénèses à magnétite des altérations associées aux systèmes à oxydes de fer et altérations en éléments alcalins, zone magmatique du Grand lac de l'Ours: Unpublished M.Sc. thesis, Institut National de la Recherche Scientifique, Quebec, Canada, 529 p.

Doebrich, J.L., Al-Jehani, A.M., Siddiqui, A.A., Hayes, T.S., Wooden, J.L., Johnson, P.R., 2007, Geology and metallogeny of the Ar Rayn terrane, eastern Arabian shield: Evolution of a Neoproterozoic continental-margin arc during assembly of Gondwana within the East African orogeny: Precambrian Research, v. 158, p. 17–50.

Domingos, F., 2009, The structural setting of the Canaã dos Carajás region and Sossego-Sequeirinho deposits, Carajás, Brazil: Durham PhD theses, Durham University, 483 p. Available at Durham E-Theses Online: http://etheses.dur.ac.uk/144/

Dragon Mining, 2012, Resource update for the Hangaslampi deposit, Kuusamo gold project: ASX announcement June 2012.

Dragon Mining, 2014, Resource updates lift Kuusamo ounces: ASX announcement, March 2014.

Drummond, B., Lyons, P., Goleby, B., Jones, J., 2006, Constraining models of the tectonic setting of the giant Olympic Dam iron oxide–copper–gold deposit, South Australia, using deep seismic reflection data: Tectonophysics, v. 420, p. 91–103.

Duncan, R.J., Hitzman, M.W., Nelson, E.P., Togtokhbayar, O., 2014, Structural and lithological controls on iron oxide copper-gold deposits of the southern Selwyn-Mount Dore corridor, Eastern Fold Belt, Queensland, Australia: Economic Geology, v. 109, p. 419–456.

References

Ehrig, K., McPhie, J., Kamenetsky, V.S., 2012, Geology and mineralogical zonation of the Olympic Dam iron oxide Cu-U-Au-Ag deposit, South Australia, in Hedenquist, J.W., Harris, M., Camus, F., eds. Geology and genesis of major copper deposits and districts of the world: A tribute to Richard H. Sillitoe: Economic Geology Special Publication 16, p. 237–267.

Ehrig, K., Kamenetsky, V.S., McPhie, J., Apukhtina, O., Ciabanu, C.L., Cook, N., Kontonikas-Charos, A., Krneta, S., 2017, The IOCG-IOA Olympic Dam Cu-U-Au-Ag deposit and nearby prospects, South Australia: Proceedings of the 14th SGA Biennial Meeting, 20-23 August 2017, Québec City, p. 823–827.

Enkin, R., Corriveau, L., Hayward, N., 2016, Metasomatic alteration control of petrophysical properties in the Great Bear magmatic zone (Northwest Territories, Canada): Economic Geology, v. 111, p. 2073–2085.

Evans, L., 2014, Grängesberg iron ab - technical report on the Grängesberg iron mine resource estimate, Bergslagen, Sweden: NI 43-101 Report, 173 p.

Fan, H.R., Hu, F.F., Yang, K.F., Pirajno, F., Liu, X., Wang, K.Y., 2014, Integrated U-Pb and Sm-Nd geochronology for a REE-rich carbonatite dyke at the giant Bayan Obo REE deposit, Northern China: Ore Geology Reviews, v. 63, p. 510–519.

Fan, H.R., Yang, K.F., Hu, F.F., Liu, S., Wang, K.Y., 2015, The giant Bayan Obo REE-Nb-Fe deposit, China: Controversy and ore genesis: Geoscience Frontiers, doi:10.1016/j.gsf.2015.11.005

First Quantum Minerals, 2013, Guelb Moghrein mineral reserves: Available at: www.first-quantum.com/Our-Business/operating-mines/Guelb-Moghrein/Reserves--Resources/default.aspx

Forslund, N., 2012, Alteration and fluid characterization of the Hamlin Lake IOCG occurrence, Northwestern Ontario, Canada: Unpublished M.Sc. Thesis, Lakehead University, Thunder Bay, 285 p.

Gandhi, S.S., 1978, Geological setting and genetic aspects of uranium occurrences in the Kaipokok Bay-Big River area, Labrador: Economic Geology, v. 73, p. 1492–1522.

Gandhi, S.S., Mortensen, J.K., Prasad, N., van Breemen, O., 2001, Magmatic evolution of the southern Great Bear continental arc, northwestern Canadian Shield: Geochronological constraints: Canadian Journal of Earth Sciences, v. 38, p. 767–785.

Gauthier, M., Chartrand, F., Cayer, A., David, J., 2004, The Kwyjibo Cu-REE-U-Au-Mo-F property, Quebec: A Mesoproterozoic polymetallic iron oxide deposit in the Northeastern Grenville Province: Economic Geology, v. 99, p. 1177–1196.

Gelcich, S., Davis, D.W., Spooner, E.T.C., 2005, Testing the apatite-magnetite geochronometer: U-Pb and $^{40}Ar/^{39}Ar$ geochronology of plutonic rocks, massive magnetite-apatite tabular bodies, and IOCG mineralization in Northern Chile: Geochimica et Cosmochimica Acta, v. 69, p. 3367–3384.

Goad, R.E., Mumin, A.H., Duke, N.A., Neale, K.L., Mulligan, D.L., 2000, Geology of the Proterozoic iron oxide-hosted, NICO cobalt-gold-bismuth, and Sue Dianne copper-silver deposits, southern Great Bear magmatic zone, Northwest Territories, Canada, in Porter, T.M., ed., Hydrothermal iron oxide copper-gold and related deposits. A global perspective, volume 1: Porter Geoscience Consultancy Publishing, Adelaide, p. 249–267.

Graupner, T., Mühlbach, C., Schwarz-Schampera, U., Henjes-Kunst, F., Melcher, F., Terblanche, H., 2015, Mineralogy of high-field-strength elements (Y, Nb, REE) in the world-class Vergenoeg fluorite deposit, South Africa: Ore Geology Reviews, v. 64, p. 583–601.

Griffin, W.L., Begg, G.C., O'Reilly, S.Y., 2013, Continental-root control on the genesis of magmatic ore deposits: Nature Geoscience, v. 6, p. 905–910.

References

Groves, D.I., Bierlein, F.P., Meinert, L.D., Hitzman, M.W., 2010, Iron oxide copper-gold (IOCG) deposits through Earth history. Implications for origin, lithospheric setting, and distinction from other epigenetic iron oxide deposits: Economic Geology, v. 105, p. 641–654.

GTK, 2015, Hannukainen deposit: GTK (Geological Survey of Finland), Mineral Deposit Report, v. 462, p. 1.

Harlov, D.E., Andersson, U.B., Förster, H.-J., Nyström, J.O., Dulski, P., Broman, C., 2002, Apatite–monazite relations in the Kiirunavaara magnetite–apatite ore, northern Sweden: Chemical Geology, v. 191, p. 47–72.

Harlov, D.E., Meighan, C.J., Kerr, I.D., Samson, I.M., 2016, Mineralogy, chemistry, and fluid-aided evolution of the Pea Ridge Fe oxide- (Y + REE) deposit, southeast Missouri, USA: Economic Geology, v. 111, p. 1963–1984.

Haynes, D.W., Cross, K.C., Bills, R.T., Reed, M.H., 1995, Olympic Dam ore genesis: A fluid mixing model: Economic Geology, v. 90, p. 281–307.

Hayward, N., Enkin, R.J., Corriveau, L., Montreuil, J-F., Kerswill, J., 2013, The application of rapid potential field methods for the targeting of IOCG mineralisation based on physical property data, Great Bear Magmatic Zone, Canada: Journal of Applied Geophysics, v. 94, p. 42–58.

Hayward, N., Corriveau, L., Craven, J., Enkin, R., 2016, Geophysical signature of alteration and mineralisation envelope at the Au-Co-Bi-Cu NICO deposit, NT, Canada, in Slack, J., Corriveau, L. and Hitzman, M., eds., Proterozoic iron oxide-apatite (± REE) and iron oxide-copper-gold and affiliated deposits of Southeast Missouri, USA, and the Great Bear magmatic zone, Northwest Territories, Canada: Economic Geology, v. 111, p. 2087–2110.

Hennessey, B.T., Puritch, E., 2008, A technical report on a mineral resource estimate for the Sue-Dianne deposit, Mazenod Lake area, Northwest Territories, Canada: Fortune Minerals Limited, NI 43-101 Technical Report, 125 p. Available at www.sedar.com

Hildebrand, R.S., 1986, Kiruna-type deposits: Their origin and relationship to intermediate subvolcanic plutons in the Great Bear magmatic zone, Northwestern Canada: Economic Geology, v. 81, p. 640–659.

Hitzman, M.W., 2000, Iron oxide-Cu-Au deposits. What, where, when, and why?, in Porter, T.M., ed., Hydrothermal iron oxide copper-gold and related deposits. A global perspective, volume 1: Porter Geoscience Consultancy Publishing, Adelaide, p. 9–25.

Hitzman, M.W., Valenta, R.K., 2005, Uranium in iron oxide-copper-gold (IOCG) systems: Economic Geology, v. 100, p. 1657–1661.

Hitzman, M.W., Oreskes, N., Einaudi, M.T., 1992, Geological characteristics and tectonic setting of Proterozoic iron oxide (Cu-U-Au-REE) deposits: Precambrian Research, v. 58, p. 241–287.

Hofstra, A., Aleinikoff, J., Ayuso, R., Bennett, M., Day, W., du Bray, E., Johnson, C., McCafferty, A., Meighan, C., Mercer, C., Neymark, L., Slack, J., Watts, K., 2017, Magmatic-hydrothermal origin of the Mesoproterozoic Pea Ridge IOA-REE deposit, southeast Missouri, USA: Proceedings of the 14th SGA Biennial Meeting, 20-23 August 2017, Québec City, p. 863–866.

Huang, Q.-Y., Kamenetsky, V.S., Ehrig, K., McPhie, J., Maas, R., Kamenetsky, M.B., Apukhtina, O.B., Chambefort, I., 2016, Olivine-phyric basalt at the Olympic Dam Cu-U-Au-Ag deposit: Insights into the mantle source and petrogenesis of the Gawler silicic large igneous province, South Australia: Precambrian Research, v. 281, p. 185–199.

Huang, X.-W., Qi, L, Gao, J.-F., Zhou, M.-F., 2013, First reliable Re–Os ages of pyrite and stable isotope compositions of Fe(-Cu) deposits in the Hami region, Eastern Tianshan orogenic belt, NW China: Resource Geology, v. 63, p. 166–187.

Huston, D.L., Hussey, K., 2001. Regional geology and metallogeny of the eastern Arunta: 2004 Chief Government Geologists Conference field excursion guide: Geoscience Australia, Record 2004/07.

Intrepid Mines, 2014, Kitumba mineral resources update and ore reserve: Intrepid Mines website, available at intrepidmines.com.au

References

Ismail, R., Ciobanu, C.L., Cook, N.J., Giles, D., Schmidt-Mumm, A., Wade, B., 2014, Rare earths and other trace elements in minerals from skarn assemblages, Hillside iron oxide–copper–gold deposit, Yorke Peninsula, South Australia: Lithos, v. 184–187, p. 456–477.

Jones, J.K., 1974, Notes on the Boss copper deposit, Dent County, Missouri: Unpublished report for Essex International, Inc., 3 p. (in Day et al. 2016)

Kerr, A., Sparkes, G.W., 2009, Uranium: Mineral commodities of Newfoundland and Labrador, No 5.

Kish, L., Cuney, M., 1981, Uraninite–albite veins from the Mistamisk valley of the Labrador Trough, Québec: Mineralogical Magazine, v. 44, p. 471–483.

Knight, J., Joy, S., Cameron, J., Merrillees, J., Nag, S., Shah, N., Dua, G., Jhala, K., 2002, The Khetri copper belt, Rajasthan, in Porter, T.M., ed., Hydrothermal iron oxide copper-gold and related deposits. A global perspective, volume 2: Porter Geoscience Consultancy Publishing, Adelaide, p. 321–341.

Knipping, J.L., Bilenker, L.D., Simon, A.C., Reich, M., Barra, F., Deditius, A.P., Lundstrom, C., Bindeman, I., Munizaga, R., 2015, Giant Kiruna-type deposits form by efficient flotation of magmatic magnetite suspensions: Geology, v. 43, p. 591–594, doi: 10 .1130 /G36650 .1.

Kolb, J., Meyer, F.M., Vennemann, T., Sindern, S., Prantl, S., Böttcher, M.E., Sakellaris, G.A., 2010, Characterisation of the hydrothermal fluids of the Guelb Moghrein iron oxide-cu-au-co deposit, Mauritania: Ore mineral chemistry, fluid inclusions and isotope geochemistry, in Porter, T.M., ed., Hydrothermal iron oxide copper-gold and related deposits: A global perspective, volume 4–advances in the understanding of IOCG deposits: Porter Geoscience Consultancy Publishing, Adelaide, p. 553–572.

Kontonikas-Charos, K., Ciobanu, C.L., Cook, N.J., 2014, Albitization and redistribution of REE and Y in IOCG systems: Insights from Moonta-Wallaroo, Yorke Peninsula, South Australia: Lithos, v. 208–209, p. 178–201.

Kontonikas-Charos, K., Ciobanu, C.L., Cook, N.J., Ehrig, K., Krneta S., Kamenetsky, V.S., 2017, Feldspar evolution in the Roxby Downs Granite, host to Fe-oxide Cu-Au-(U) mineralisation at Olympic Dam, South Australia: Ore Geology Reviews, v. 80, p. 838–859.

Kositcin, N., 2010, Geodynamic synthesis of the Gawler Craton and Curnamona Province: Geoscience Australia, Record, 2010/27, 113 p.

Kreiner, D., Barton, M.D., 2011, High-level alteration in iron-oxide (-Cu–Au) (IOCG) vein systems, examples near Copiapó, Chile: Proceedings of the 11th Biennial SGA meeting, Antofagasta, Chile, p. 497–499.

Krneta, S., Cook, N.J., Ciobanu, C.L., Ehrig, K., Kontonikas-Charosa, A., 2017, The Wirrda Well and Acropolis prospects, Gawler Craton, South Australia: Insights into evolving fluid conditions through apatite chemistry: Journal of Geochemical Exploration, v. 181, p. 276–291.

Kuşcu, İ., Yılmazer, E., Demirela, G., Gençalioğlu-Kuşcu, G., Güleç, N., 2010, Iron oxide-(copper±gold) mineralisation in the Turkish Tethyan collage, in Porter, T.M., ed., hydrothermal iron oxide copper-gold and related deposits: A global perspective, volume 4 - Advances in the understanding of IOCG deposits: Porter Geoscience Consultancy Publishing, Adelaide, p. 573–600.

Li, W., Audétat, A., Zhang, J., 2015, The role of evaporites in the formation of magnetite–apatite deposits along the Middle and Lower Yangtze River, China: Evidence from LA-ICP-MS analysis of fluid inclusions: Ore Geology Reviews, v. 67, p. 264–278.

Li, X., Zhao, X., Zhou, M.-F., Chen, W. T., Chu, Z., 2015, Fluid inclusion and isotopic constraints on the origin of the Paleoproterozoic Yinachang Fe-Cu-(REE) deposit, southwest China: Economic Geology, v. 110, p. 1339–1369.

L.K.A.B., 2013, Annual report: Luleå, Sweden: Luleå Grafiska, 138 p.

References

Lobo-Guerrero, S.A., 2010, Iron oxide–copper–gold mineralization in the greater Lufilian arc, Africa , in Corriveau, L. and Mumin, A.H., eds., Exploring for iron oxide copper-gold deposits: Canada and global analogues: Geological Association of Canada, Short Course Notes 20, p. 161–175.

Lopez, G.P., Hitzman, M.W., Nelson, E.P., 2014, Alteration patterns and structural controls of the El Espino IOCG mining district, Chile: Mineralium Deposita, v. 49, p. 235–259.

Lyons, J.I., 1988, Volcanogenic iron-oxide deposits, Cerro de Mercado and vicinity, Durango, Mexico: Economic Geology, v. 83, p. 1886–1906.

Macmillan, E., Cook, N.J., Ehrig, K., Ciobanu, C.L., Pring, A., 2016, Uraninite from the Olympic Dam IOCG-U-Ag deposit: Linking textural and compositional variation to temporal evolution: American Mineralogist, v. 101, p. 1295–1320.

Madeisky, H.E., 1996, A lithogeochemical and radiometric study of hydrothermal alteration and metal zoning at the Cinola epithermal gold deposit, Queen Charlotte Islands, British Columbia, in Coyner, A.R. and Fahey, P.L., eds., Geology and ore deposits of the American Cordillera: Geological Society of Nevada, USA, v. 3, p. 1153–1185.

Mao, J., Xie, G., Duan, C., Pirajno, F., Ishiyama, D., Chen, Y., 2011, A tectono-genetic model for porphyry–skarn–stratabound Cu–Au–Mo–Fe and magnetite–apatite deposits along the Middle–Lower Yangtze River Valley, Eastern China: Ore Geology Reviews, v. 43, p. 294–314.

Mark, G., Oliver, N.H.S., Williams, P.J., Valenta, R.K., Crookes, R.A., 2000, The evolution of the Ernest Henry Fe-oxide-(Cu–Au) hydrothermal system, in Porter, T.M., ed., Hydrothermal iron oxide copper–gold and related deposits: A global perspective, volume 1: Porter Geosciences Consultancy Publishing, Adelaide, p. 123–136.

Mark, G., Oliver, N.H.S., Williams, P.J., 2006, Mineralogical and chemical evolution of the Ernest Henry Fe oxide-Cu-Au ore system, Cloncurry district, northwest Queensland, Australia: Mineralium Deposita, v. 40, p. 769–801.

Marschik, R., Fontboté, L., 2001, The Candelaria–Punta del Cobre iron oxide Cu–Au (–Zn–Ag) deposits, Chile: Economic Geology, v. 96, p. 1799–1826.

Marschik, R., Chiaradia, M., Fontboté, L., 2003, Implications of Pb isotope signatures of rocks and iron oxide Cu–Au ores in the Candelaria-Punta del Cobre district, Chile: Mineralium Deposita, v. 38, p. 900–912.

Martinsson, O., Billström, K., Broman, C., Weihed, P., Wanhainen, C., 2016, Metallogeny of the Northern Norrbotten Ore Province, northern Fennoscandian Shield with emphasis on IOCG and apatite-iron ore deposits: Ore Geology Reviews, v. 78, p. 447–492.

Mathur, R., Marschik, R., Ruiz, J., Munizaga, F., Leveille, R.A., Martin, W., 2002, Age of mineralization of the Candelaria Fe oxide Cu-Au deposit and the origin of the Chilean iron belt, based on Re-Os isotopes: Economic Geology, v. 97, p. 59–71.

McPhie, J. Orth, K. Kamenetsky, V., Kamenetskya, M., Ehrig, K., 2016, Characteristics, origin and significance of Mesoproterozoic beddedclastic facies at the Olympic Dam Cu–U–Au–Ag deposit, South Australia: Precambrian Research, v. 276, p. 85–100.

Metal X, 2016, https://www.metalsx.com.au/system/assets/89/original/Metals_X_2016_Annual_Report.pdf

Monteiro, L.V.S., Xavier, R.P., Carvalho, E.R., Hitzman, M.W., Johnson, C.A., Souza Filho, C.R., Torresi, I., 2008, Space and temporal zoning of hydrothermal alteration and mineralization in the Sossego iron oxide-copper-gold deposit, Carajás Mineral Province, Brazil: Paragenesis and stable isotope constraints: Mineralium Deposita, v. 43, p. 129–159.

References

Montreuil, J.-F., Corriveau, L., Grunsky, E.C., 2013, Compositional data analysis of IOCG systems, Great Bear magmatic zone, Canada: To each alteration types its own geochemical signature: Geochemistry: Exploration, Environment, Analysis, v. 13, p. 229–247.

Montreuil, J.-F., Corriveau, L., Potter, E.G., 2015, Formation of albitite-hosted uranium within IOCG systems: The Southern Breccia, Great Bear magmatic zone, Northwest Territories, Canada: Mineralium Deposita, v. 50, p. 293–325.

Montreuil, J.-F., Corriveau, L., Davis, W., 2016a, Tectonomagmatic evolution of the southern Great Bear magmatic zone (Northwest Territories, Canada) – Implications on the genesis of iron oxide alkali-altered hydrothermal systems, in Slack, J., Corriveau, L. and Hitzman, M., eds., Proterozoic iron oxide-apatite (± REE) and iron oxide-copper-gold and affiliated deposits of Southeast Missouri, USA, and the Great Bear magmatic zone, Northwest Territories, Canada: Economic Geology, v. 111, p. 2111–2138.

Montreuil, J.-F., Corriveau, L., Potter, E.G., De Toni, A.F., 2016b, On the relation between alteration facies and metal endowment of iron oxide–alkali –altered systems, southern Great Bear Magmatic Zone (Canada), in Slack, J., Corriveau, L. and Hitzman, M., eds., Proterozoic iron oxide-apatite (± REE) and iron oxide-copper-gold and affiliated deposits of Southeast Missouri, USA, and the Great Bear magmatic zone, Northwest Territories, Canada: Economic Geology, v. 111, p. 2139–2168.

Montreuil, J.-F., Potter, E., Corriveau, L., Davis, W.J., 2016c, Element mobility patterns in magnetite-group IOCG systems: The Fab IOCG system, Northwest Territories, Canada: Ore Geology Reviews, v. 72, p. 562–584.

Montreuil, J.F., Corriveau, L., Blein, O., Potter, E.G., DeToni, A.F., in press, Iron oxide and alkali-calcic alteration ore systems and their polymetallic IOA, IOCG, skarn, albitite-hosted U±Au±Co and affiliated deposits: A short course series. Part 9: Geochemical footprints and element mobility across ore environments: Geological Survey of Canada, Scientific Presentation xx.

Moreto, C.P.N., Monteiro, L.V.S., Xavier, R.P., Creaser, R.A., DuFrane, S.A., Melo, G.H.C., 2015, Timing of multiple hydrothermal events in the iron oxide–copper–gold deposits of the Southern Copper Belt, Carajás Province, Brazil: Mineralium Deposita, v. 50, p. 517–546.

Mumin, A.H., Corriveau, L., 2004, The Eden deformation corridor and polymetallic mineral belt: Trans Hudson Orogen, Leaf Rapids District, Manitoba: Manitoba Geological Survey, Report of Activities 2004, p. 69–91.

Mumin, A.H., Corriveau, L., Somarin, A.K., Ootes, L., 2007, Iron oxide copper-gold-type polymetallic mineralisation in the Contact Lake Belt, Great Bear Magmatic Zone, Northwest Territories, Canada: Exploration and Mining Geology, v. 16, p. 187–208.

Mumin, A.H., Somarin, A.K., Jones, B., Corriveau, L., Ootes, L., Camier. J., 2010, The IOCG-porphyry-epithermal continuum of deposits types in the Great Bear magmatic zone, Northwest Territories, Canada, in Corriveau, L. and Mumin, A.H., eds., Exploring for iron oxide copper-gold deposits: Canada and global analogues: Geological Association of Canada, Short Course Notes 20, p. 59–78.

N9GBYBGMR (No. 9 Geological Brigade of the Yunnan Bureau of Geology and Mineral Resources), 1983, Report of exploration and prospecting of the Dahongshan iron and copper deposits, Xinping County, Yunnan Province: Unpublished report, p. 377 (in Chinese cited by Zhao et al. 2017b).

Naranjo, J.A., Henríquez, F., Nyström, J.O., 2010, Subvolcanic contact metasomatism at El Laco Volcanic Complex, Central Andes: Andean Geology, v. 37, p. 110–120.

References

Neymark, L.A., Holm-Denoma, C.S., Pietruszka, A.J., Aleinikoff, J.N., Fanning, C.M., Pillers, R.M., Moscati, R.J., 2016, High spatial resolution U-Pb geochronology and Pb isotope geochemistry of magnetite-apatite ore from the Pea Ridge iron oxide-apatite deposit, St. Francois Mountains, southeast Missouri, USA: Economic Geology, v. 111, p. 1915–1933.

Nold, J.L., Davidson, P., Dudley, M.A., 2013, The Pilot Knob magnetite deposit in the Proterozoic St. Francois Mountains Terrane, southeast Missouri, USA: A magmatic and hydrothermal replacement iron deposit: Ore Geology Reviews, v. 53, p. 446–469.

Nold, J.L., Dudley, M.A., Davidson, P., 2014, The Southeast Missouri (USA) Proterozoic iron metallogenic province—Types of deposits and genetic relationships to magnetite–apatite and iron oxide–copper–gold deposits: Ore Geology Reviews, v. 57, p. 154–171.

Nyström, J.O., Henríquez, F., 1994, Magmatic features of iron ores of the Kiruna type in Chile and Sweden: Ore textures and magnetite geochemistry: Economic Geology, v. 89, p. 820–839.

Oliver, N.H.S., Bons, P.D., 2001, Mechanisms of fluid flow and fluid–rock interaction in fossil metamorphic hydrothermal systems inferred from vein–wallrock patterns, geometry and microstructure: Geofluids, v. 1, p. 137–162.

Oliver, N.H.S., Mark, G., Pollard, P.J., Rubenach, M.J., Bastrakov, E., Williams, P.J., Marshall, L.C., Baker, T., Nemchin, A.A., 2004, The role of sodic alteration in the genesis of iron oxide-copper–gold deposits: Geochemistry and geochemical modelling of fluid-rock interaction in the Cloncurry district, Australia: Economic Geology, v. 99, p. 1145–1176.

Oliver, N.H.S., Rubenach, M.J., Baker, B.F., Blenkinsop, T.G., Cleverley, J.S., Marshall, L.J., Ridd, P.J., 2006, Granite-related overpressure and volatile release in the mid crust: Fluidized breccias from the Cloncurry district, Australia: Geofluids, v. 6, p. 346–358.

Oliver, N.H.S., Rusk, B.G., Long, R., Zhang, D., 2009, Copper- and iron-oxide-Cu-Au deposits, and their associated alteration and brecciation, Mount Isa block: SGA post-conference trip field guide: Mt Isa Cu, IOCG and breccias. EGRU/JCU, 40 p.

Ootes, L., Snyder, D., Davis, W.J., Acosta-Góngora, P., Corriveau, L., Mumin, A.H., Montreuil, J.-F., Gleeson, S.A., Samson, I.A., Jackson, V.A., 2016, A Paleoproterozoic Andean-type iron oxide copper-gold environment, the Great Bear magmatic zone, Northwest Canada: Ore Geology Reviews, v. 81, p. 123–139.

Oyarzun, R., Oyarzún, J., Ménard, J.J., Lillo, J., 2003, The Cretaceous iron belt of northern Chile: Role of oceanic plates, a superplume event, and a major shear zone: Mineralium Deposita, v. 38, p. 640–646.

Oz Minerals, 2013, Annual Carrapateena Resource Update – 2013: ASX Release, 28 November 2013, 25 p.

Oz Minerals, 2014a, Initial 202 Mt at 0.6% copper resource for Khamsin: ASX Release 26 May 2014, 20 p.

Oz Minerals, 2014b, Annual resource and reserve update for Prominent Hill: ASX Release 20 November 2014, 50 p.

Oz Minerals, 2017, Carrapateena project mineral resource restatement and ore reserve statement: Available at: https://www.ozminerals.com/media/oz-minerals-carrapateena-mineral-resource-and-ore-reserve-statement/

Paladin Energy, 2015a, Michelin deposit, geology and resources: Accessed February 2015, http://www.paladinenergy.com.au/default.aspx?MenuID=197

Paladin Energy, 2015b, Valhalla uranium deposit, mineral resources: Accessed February 2015, http://www.paladinenergy.com.au/default.aspx?MenuID=35

References

Perreault, S., Lafrance, B., 2015, Kwyjibo, a REE-enriched iron oxides-copper-gold (IOCG) deposit, Grenville Province, Québec, in Simandl, G.J. and Neetz, M., eds., Symposium on strategic and critical materials proceedings, November 13-14, 2015, Victoria, British Columbia: British Columbia Ministry of Energy and Mines, British Columbia Geological Survey Paper 2015-3, p. 139–145.

Polito, P.A., Kyser, T.K., Stanley, C., 2009, The Proterozoic, albitite-hosted, Valhalla uranium deposit, Queensland, Australia: A description of the alteration assemblage associated with uranium mineralization in diamond drill hole V39: Mineralium Deposita, v. 44, p. 11–40.

Porter, T.M., 2000, Hydrothermal iron oxide copper-gold and related deposits. A global perspective, volume 1: Porter Geoscience Consultancy Publishing, Adelaide, 349 p.

Porter, T.M., 2002, Hydrothermal iron oxide copper-gold and related deposits. A global perspective, volume 2: Porter Geoscience Consultancy Publishing, Adelaide, 377 p.

Porter, T.M., 2010a, Current understanding of iron oxide associated-alkali altered mineralised systems. Part 1 - An overview, in Porter, T.M., ed., Hydrothermal iron oxide copper-gold and related deposits. A global perspective, volume 3: Porter Geoscience Consultancy Publishing, Adelaide, p. 5–32.

Porter, T.M., 2010b, The Carrapateena iron oxide copper-gold deposit, Gawler Craton, South Australia: A review, in Porter, T.M., ed., Hydrothermal iron oxide copper-gold and related deposits. A global perspective, volume 3: Porter Geoscience Consultancy Publishing, Adelaide, p. 191–200.

Porto da Silveira, C.L., Schorscher, H.D., Miekeley, N., 1991, The geochemistry of albitization and related uranium mineralization, Espinharas, Paraiba (PB), Brazil: Journal Geochemistry Exploration, v. 40, p. 329–347.

Potter, E.G., Corriveau, L., Kerswill, J.K., 2013, Potential for iron oxide-copper–gold and affiliated deposits in the proposed national park area of the East Arm, Northwest Territories: Insights from the Great Bear magmatic zone and global analogs, in Wright, D.F., Kjarsgaard, B.A., Ambrose, E.J., and Bonham-Carter, G.F., eds., Mineral and energy resource assessment for the proposed Thaidene Nene National Park reserve, East Arm of Great Slave Lake, Northwest Territories: Geological Survey of Canada, Open File 7196, Chapter 19, p. 477–493.

Puritch, E., Ewert, W., Armstrong, T., Brown, F., Orava, D., Pearson, J.L., Hayes, T., Duggan, T., Holmes, G., Uceda, D., Sumners, W., Mackie, D., Rougier, M., Bocking, K., Mezei, A., Horne, B., 2012a, Technical report and updated mineral reserve estimate and front-end engineering and design (FEED) study on the NICO gold–cobalt–bismuth–copper deposit, Mazenod Lake area, Northwest Territories, Canada: NI 43–101 Technical Report No. 247 prepared for Fortune Minerals Ltd., 307 p.

Puritch, E., Rodgers, K., Pearson, J.L., Burga, D., Orava, D., Hayden, A., 2012b, Technical report and preliminary economic assessment of the Upper Beaver gold-copper deposit, Kirkland Lake, Ontario, Canada: NI 43–101 Technical Report No. 239, 178 p.

Ray, G.E., Lefebure, D.V., 2000, A synopsis of iron oxide ± Cu ± Au ± P ± REE deposits of the Candelaria-Kiruna-Olympic Dam family: British Columbia Ministry of Energy and Mines, Geological Fieldwork 1999, Paper 2000-1, p. 267–272.

Reed, M., Rusk, R., Palandri, J., 2013, The Butte magmatic-hydrothermal system: One fluid yields all alteration and veins: Economic Geology, v. 108, p. 1379–1396.

References

Reeve, J.S., Cross, K.C., Smith, R.N., Oreskes, N., 1990, The Olympic Dam copper-uranium-gold-silver deposit, South Australia, in Hughes, F., ed., Geology of mineral deposits of Australia and Papua New Guinea: Australian Institute of Mining and Metallurgy Monograph 14, p. 1009–1035.

Reid, A.J., Fabris, A., 2015, Influence of preexisting low metamorphic grade sedimentary successions on the distribution of iron oxide copper-gold mineralization in the Olympic Cu-Au province, Gawler craton: Economic Geology, v. 110, p. 2147–2157.

Reid, A., Thiel, S., McAnaney, S., Wade, C., 2017, Evidence for a cryptic paleo-suture zone: Implications for IOCG mineralisation in the Gawler Craton: Proceedings of the 14th Biennal SGA meeting, p. 883–886.

Reischmann, T., 1995, Precise U/Th age determination with baddeleyite (ZrO_2), a case study from the Phalaborwa Igneous Complex, South Africa: South African Journal of Geology, v. 98, p. 1–4.

Requia, K., Stein, H., Fontboté, L., Chiaradia, M., 2003, Re–Os and Pb–Pb geochronology of the Archean Salobo iron oxide copper–gold deposit, Carajás mineral province, northern Brazil: Mineralium Deposita, v. 38, p. 727–738.

Rex Minerals Ltd., 2015, Hillside project, mineral resources and ore reserves: Accessed at www.rexminerals.com.au

Reynolds, L.J., 2000, Geology of the Olympic Dam Cu-U-Au-Ag-REE deposit, in Porter, T.M., ed., Hydrothermal iron oxide copper-gold and related deposits: A global perspective, volume 1: Porter Geoscience Consultancy Publishing, Adelaide, p. 93–104.

Richards, J.P., López, G.P., Zhu, J.-J., Creaser, R.A., Locock, A.J., Mumin, A.H., 2017, Contrasting tectonic settings and sulfur contents of magmas associated with cretaceous porphyry Cu ± Mo ± Au and intrusion-related iron oxide cu-au deposits in Northern Chile: Economic Geology, v. 112, p. 295–318.

Rieger, A.A., Marschik, R., Díaz, M., 2010, The Mantoverde district, northern Chile: An example of distal portions of zoned IOCG systems, in Porter, T.M., ed., Hydrothermal iron oxide copper-gold and related deposits: A global perspective, volume 3: Porter Geoscience Consultancy Publishing, Adelaide, Australia, p. 273–284.

Romer, R.L., Martinsson, O., Perdahl, J.-A., 1994, Geochronology of the Kiruna iron ores and hydrothermal alterations: Economic Geology, v. 89, p. 1249–1261.

Rubenach, M., 2012, Chapter 4 - Structural controls of metasomatism on a regional scale, in Harlov, D.E. and Austrheim, H., eds., Metasomatism and the chemical transformation of rock: Lecture Notes in Earth System Sciences, Springer, p. 93–140.

Rusk, B., Emsbo, P., Xavier, R.P., Corriveau, L., Oliver, N., Zhang, D., 2015, A comparison of fluid origins and compositions in iron oxide-copper-gold and porphyry-Cu (Mo-Au) deposits: Australasian Institute of Mining and Metallurgy, PACRIM 2015 Congress, Proceedings, p. 271–280.

Sangster, P.J., Le Baron, P.S., Charbonneau, S.J., Laidlaw, D.A., Wilson, A.C., Carter, T.R., Fortner, L. 2012, Report of activities 2011, resident geologist program, southern Ontario regional resident geologist report: Southeastern and Southwestern Ontario Districts and Petroleum Resources Centre, Ontario Geological Survey, Open File Report 6277, 72 p.

Schofield, A., 2012, An assessment of the uranium and geothermal prospectivity of the southern Northern Territory: Geoscience Australia, Record 2012/51, 214 p.

References

Selleck, B., McLelland, J., Hamilton, M.A., 2004, Magmatic-hydrothermal leaching and origin of late- to post-tectonic quartz-rich rocks, Adirondack Highlands, New York, in Tollo, R.P., Corriveau, L., McLelland, J., and Bartholomew, M, eds., Proterozoic tectonic evolution of the Grenville Orogen in North America: Geological Society of America Memoir, No 197, p. 379–390.

Seo, S., Choi, S.G., Kima, D.W., Park, J.W., Oh, C.W., 2015, A new genetic model for the Triassic Yangyang iron-oxide–apatite deposit, South Korea: Constraints from in situ U–Pb and trace element analyses of accessory minerals: Ore Geology Reviews, v. 70, p. 110–135.

Sidder, G.B., Day, W.C., Nuelle, L.M., Seeger, C.M., Kisvarsanyi, E.B., 1993, Mineralogic and fluid-inclusion studies of the Pea Ridge iron-rare-earth-element deposit, southeast Missouri: U.S. Geological Survey Bulletin 2039, p. 205–216.

Sillitoe, R.H., 2003, Iron oxide–copper–gold deposits: An Andean view: Mineralium Deposita, v. 38, p. 787–812.

Skirrow, R.G., 2000, Gold-copper-bismuth deposits of the Tennant Creek district, Australia: A reappraisal of diverse high-grade systems, in Porter, T.M., ed., Hydrothermal iron oxide copper-gold and related deposits: A global perspective, volume 1: Porter Geoscience Consultancy Publishing, Adelaide, p. 149–160.

Skirrow, R., 2010, "Hematite-group" IOCG±U ore systems. Tectonic settings, hydrothermal characteristics, and Cu-Au and U mineralizing processes, in Corriveau, L. and Mumin, A.H., eds., Exploring for iron oxide copper-gold deposits: Canada and global analogues: Geological Association of Canada, Short Course Notes 20, p. 39–58.

Skirrow, R.G., Jaireth, S., Huston, D.L., Bastrakov, E.N., Schofield, A., van der Wielen, S.E., Barnicoat, A.C., 2009, Uranium mineral systems: Processes, exploration criteria and a new deposit framework: Geoscience Australia Record 2009/20, 44 p.

Slack, J., 2013, Descriptive and geoenvironmental model for cobalt–copper–gold deposits in metasedimentary rocks: U.S. Geological Survey Scientific Investigations Report 2010–5070–G, 218 p.

Somarin, A.K., Mumin, A.H., 2014, P–T-composition and evolution of paleofluids in the Paleoproterozoic Mag Hill IOCG hydrothermal system, Contact Lake belt, Northwest Territories, Canada: Mineralium Deposita, v. 49, p. 199–215.

Sparkes, G.W., 2017, Uranium mineralization within the Central Mineral Belt of Labrador: A summary of the diverse styles, settings and timing of mineralization. Government of Newfoundland and Labrador: Department of Natural Resources, Geological Survey, St. John's, Open File LAB/1684, 198 p.

Spratt, J.E., Jones, A.G., Jackson, V.A., Collins, L., Avdeeva, A., 2009, Lithospheric geometry of the Wopmay orogen Orogen from a Slave craton to Bear Province magnetotelluric transect: Journal of Geophysical Research, v. 114, 18 p.

Stosch, H.G., Romer, R.L., Daliran, F., Rhede, D., 2011, Uranium–lead ages of apatite from iron oxide ores of the Bafq District, East-Central Iran: Mineralium Deposita, v. 46, p. 9–21.

Sun, W., Yuan, F., Jowitt, S.M., Zhou, T., Hollings, P., Liu, G., Li, X., 2017, Geochronology and geochemistry of the Fe ore-bearing Zhonggu intrusions of the Ningwu Basin: Implications for tectonic setting and contemporaneous Cu-Au mineralization in the Middle–Lower Yangzte Metallogenic Belt: Ore Geology Reviews, v. 84, p. 246–272.

References

Tallarico, F.H.B., McNaughton, N.J., Groves, D.I., Fletcher, I.R., Figueiredo, B.R., Carvolho, J.B., Rego, J.L., Nunes, A.R., 2004, Geological and SHRIMP II U–Pb constraints on the age and origin of the Breves Cu-Au-(W-Bi-Sn) deposit, Carajás, Brazil: Mineralium Deposita, v. 39, p. 68–86.

Thiel, S., Heinson, G., 2013, Electrical conductors in Archean mantle—Result of plume interaction? Geophysical Research Letters, v. 40, p. 2947–2952

Thiel, S., Heinson, G., Reid, A., Robertson, K., 2016, Insights into lithospheric architecture, fertilisation and fluid pathways from AusLAMP MT: ASEG Extended Abstracts 2016, p. 1–6.

Thorkelson, D.J., Mortensen, J.K., Creaser, R.A., Davidson, G.J., Abbott, J.G., 2001, Early Proterozoic magmatism in Yukon, Canada: Constraints on the evolution of northwestern Laurentia: Canadian Journal of Earth Sciences, v. 38, p. 1479–1494.

Torab, F.M., Lehmann, B., 2007, Magnetite-apatite deposits of the Bafq district, Central Iran: Apatite geochemistry and monazite geochronology: Mineralogical Magazine, v. 71 (3), p. 347–363.

Tornos, F., Velasco, F., Hanchar, J.M., 2016, Iron-rich melts, magmatic magnetite, and superheated hydrothermal systems: The El Laco deposit, Chile: Geology, v. 44 (6), p. 427–430.

Tornos, F., Velasco, F., Hanchar, J.M., Velasco, F., Muñizaga, R., Levresse, G., 2017, The Roots and tops of magnetite-apatite mineralization: Evolving magmatic-hydrothermal systems: Proceedings of the 14th Biennal SGA meeting, p. 831–835.

Turner, D., 2012, Independent technical report on the Kiyuk Lake property, Nunavut Territory, Canada: National Instrument 43-101 report available on www.sedar.com.

Valley, P.M., Hanchar, J.M., Whitehouse, M.J., 2009, Direct dating of Fe oxide-(Cu-Au) mineralization by U/Pb zircon geochronology: Geology, v. 37, p. 223–226, doi: 10.1130/G25439A.1.

Valley, P.M., Hanchar, J.M., Whitehouse, M.J., 2011, New insights on the evolution of the Lyon Mountain granite and associated Kiruna-type magnetite-apatite deposits, Adirondack Mountains, New York State: Geosphere, v. 7, p. 357–389, doi: 10.1130/GES00624.1.

Vanhanen, E., 2001, Geology, mineralogy and geochemistry of the Fe-Co-Au-(U) deposits in the Paleoproterozoic Kuusamo Schist Belt, northeastern Finland: Geological Survey of Finland Bulletin, v. 399, 229 p.

Verbaas, J., Thorkelson, D.J., Crowley, J., Davis, W.J., Foster, D.A., Gibson, H.D., Marshall, D.D., Milidragovic, D., 2018, A sedimentary overlap assemblage links Australia to northwestern Laurentia at 1.6 Ga: Precambrian research, v. 305, p. 19–39.

Veríssimo, C.U.V., Santos, R.V., Parente, C.V., de Oliveira, C.G., Cavalcanti, J.A.D., Neto, J.A.N., 2016,The Itataia phosphate-uranium deposit (Ceara, Brazil) new petrographic, geochemistry and isotope studies: Journal of South American Earth Sciences, v. 70, p. 115–144.

Wade, B.P., Barovich, K.M., Hand, M., Scrimgeour, I.R., Close, D.F., 2006, Evidence for early Mesoproterozoic arc magmatism in the Musgrave Block, central Australia: Implications for Proterozoic crustal growth and tectonic reconstructions of Australia: Journal of Geology, v. 114, p. 43–63.

Waller, C.G., Robertson, M.J., Witley, J.C., Carthew, G.H., Morgan, D.J.T., 2014, Kitumba copper project, optimised pre-feasibility study: NI 43-101 Technical Report, prepared for Intrepid Mines Limited by Lycopodium Minerals Pty Ltd, 279 p.

References

Wang, S., Williams, P.J., 2001, Geochemistry and origin of Proterozoic skarns at the Mount Elliott Cu-Au(-Co-Ni) deposit, Cloncurry district, NW Queensland, Australia: Mineralium Deposita, v. 36, p. 109–124.

Wanhainen, C., Broman, C., Martinsson, O., 2003, The Aitik Cu–Au–Ag deposit in northern Sweden: A product of high salinity fluids: Mineralium Deposita, v. 38, p. 715–726.

Whitney, D.L., Evans, B.W., 2010, Abbreviations for names of rock-forming minerals: American Mineralogist, v. 95, p. 185–187.

Wilde, A., 2013, Towards a model for albitite-type uranium: Minerals, v. 3, p. 36-48.

Williams, P.J., 2010a, Classifying IOCG deposits, in Corriveau, L. and Mumin, A.H., eds., Exploring for iron oxide copper-gold deposits: Canada and global analogues: Geological Association of Canada, Short Course Notes 20, p. 13–22.

Williams, P.J., 2010b, "Magnetite-group" IOCGs with special reference to Cloncurry (NW Queensland) and Northern Sweden. Settings, alteration, deposit characteristics, fluid sources, and their relationship to apatite-rich iron ores, in Corriveau, L. and Mumin, A.H., eds., Exploring for iron oxide copper-gold deposits: Canada and global analogues: Geological Association of Canada, Short Course Notes 20, p. 23–38.

Williams, P.J., Skirrow, R.G., 2000, Overview of IOCG deposits in the Curnamona Province and Cloncurry district (eastern Mount Isa block), Australia, in Porter, T.M., ed., Hydrothermal iron oxide copper-gold and related deposits: A global perspective: Adelaide, Australian Mineral Foundation, p. 105–122.

Williams, P.J., Barton, M.D., Johnson, D.A., Fontbote, L., de Haller, A., Mark, G., Oliver, N.H.S., Marschik, R., 2005, Iron oxide copper-gold deposits; geology, space-time distribution, and possible modes of origin: Economic Geology 100th Anniversary Volume, p. 371–406.

Williams, P.J., Kendrick, M., Xavier, R.P., 2010, Sources of ore fluid components in IOCG deposits, in Porter, T.M., ed., Hydrothermal iron oxide copper–gold and related deposits: A global perspective, volume 3–Advances in the understanding of IOCG deposits: Porter Geoscience Consultancy Publishing, Adelaide, p. 107–116.

Wise, T., Reid, A., Jakica, S., Fabris, A. van der Wielen, S., Ziramov, S., Pridmore, D., Heinson, G., Soeffky, P., 2016, Olympic Dam seismic revisited: Reprocessing of deep crustal seismic data using partially preserved amplitude processing: ASEG Extended Abstracts 2016, 25th International Geophysical Conference and Exhibition, p. 607–613.

Woolrych, T.R.H., Christensen, A.N., McGill, D.L., Whiting, T., 2015, Geophysical methods used in the discovery of the Kitumba iron oxide copper gold deposit: Interpretation, v. 3, p. SL15–SL25.

Wu, C., 2008, Bayan Obo controversy: Carbonatites versus iron oxide-Cu_Au(REE-U): Resources Geology, v. 58, p. 348–354.

Xavier, R.P., Monteiro, L.V.S., de Souza Filho, C.R., Torresi, I., de Resende Carvalho, E., Dreher, A.M., Wiedenbeck, M., Trumbull, R.B., Pestilho, A.L.S., Moreto, C.P.N., 2010, The iron oxide copper-gold deposits of the Carajás mineral province, Brazil: An updated and critical review, in Porter, T.M., ed., Hydrothermal iron oxide copper–gold and related deposits: A global perspective, volume 3–Advances in the understanding of IOCG deposits: Porter Geoscience Consultancy Publishing, Adelaide, p. 285–306.

Yılmazer, E., Güleç, N., Kuşcu, I., Lentz, D.R., 2014, Geology, geochemistry, and geochronology of Fe-oxide Cu (±Au) mineralization associated with Şamlı pluton, western Turkey: Ore Geology Reviews, v. 57, p. 191–215.

References

Yu, J., Chen, Y., Mao, J., Pirajno, F., Duan, C., 2011, Review of geology, alteration and origin of iron oxide–apatite deposits in the Cretaceous Ningwu basin, Lower Yangtze River Valley, eastern China: Implications for ore genesis and geodynamic setting: Ore Geology Reviews, v. 43, p. 170–181.

Zeng, L.-P., Zhao, X.-F., Li, X.-C., Hu, H., McFarlane, C., 2016, In situ elemental and isotopic analysis of fluorapatite from the Taocun magnetite-apatite deposit, Eastern China: Constraints on fluid metasomatism: American Mineralogist, v. 101, p. 2468–2483.

Zhao, X.-F., Zeng, L.-P., Hu, H., Li, X.-C., 2016, Iron-oxide apatite deposits in eastern China formed by accumulation of magmatic hydrosaline chloride liquids: 34th IGC abstract, Paper 2293, Cape Town

Zhao, X.-F., Su, Z.-K., Zeng, L.-P., 2017a, Genetic models of IOCG and IOA deposits from China: Implications for ore genesis and their possible links: Proceedings of the 14th SGA Biennial Meeting, 20-23 August 2017, Québec City, p. 835–839.

Zhao, X.-F., Zhou, M.-F., Su, Z.-K., Li, X.-C., Chen, W.-T., Li, J.-W., 2017b, Geology, geochronology, and geochemistry of the Dahongshan Fe-Cu-(Au-Ag) deposit, Southwest China: Implications for the formation of iron oxide copper-gold deposits in intracratonic rift settings: Economic Geology, v. 112, p. 603–628.

Zhou, T., Fan, Y., Yuan, F., Zhang, L., Qian, B., Ma, L., Yang, X., 2013, Geology and geochronology of magnetite–apatite deposits in the Ning-Wu volcanic basin, Eastern China: Journal of Asian Earth Sciences, v. 66, p. 90–107.

Zhu, Z., Tan, H., Liu, Y., Li, C., 2017, Multiple episodes of mineralization revealed by Re-Os molybdenite geochronology in the Lala Fe-Cu deposit, SW China: Mineralium Deposita, doi.org/10.1007/s00126-017-0740-x

Zulinski, N., Osmani, I.A., 2011, Assessment report on the 2010 exploration programs Coldstream property Burchell Lake area and Moss Township district of Thunder Bay, Northwestern Ontario, NTS Map Sheet 52B10: Foundation Resources Inc., Assessment report available at www.sedar.com.

For additional information

Louise Corriveau – Louise.Corriveau@canada.ca, Natural Resources Canada, Geological Survey of Canada
Eric Potter – Eric.Potter@canada.ca, Natural Resources Canada, Geological Survey of Canada
Philippe Normandeau – philippe_normandeau@gov.nt.ca, Northwest Territories Geological Survey